UNIVERSITÀ DEGLI STUDI DI PADOVA

UNIVERSITA' DEGLI STUDI DI PADOVA

Dipartimento di Ingegneria Industriale DII

Corso di Laurea Magistrale in Ingegneria Energetica

PV ARRAY PERFORMANCE IN A HYBRID POWER PLANT AND SHADOW EVOLUTION ASSESSMENT

Relatore: Prof. Nicola Trivellin

Correlatore: Dott. Noah Tormena

Alessandro Trinco 2019246

Anno Accademico 2022/2023

RIASSUNTO ESTESO IN ITALIANO

Un impianto di potenza ibrido consiste in un parco eolico con moduli fotovoltaici installati in prossimità, assieme a sistemi di stoccaggio capaci di mantenere l'output di potenza e tensione stabile. Siccome gli aerogeneratori hanno bisogno di trovarsi a sufficiente distanza tra di loro per evitare perturbazioni e turbolenze che possono ridurre la produzione elettrica complessiva, un parco eolico occupa ampi spazi di terreno. Questo terreno sotto le turbine o in loro vicinanza può essere utilizzato per l'agricoltura, per produrre ulteriore energia elettrica con impianti fotovoltaici (o anche entrambi gli scopi con l'agrifotovoltaico). Ad esempio l'installazione di pannelli fotovoltaici permetterebbe di diminuire i costi di investimento legati alla connessione alla rete e pure i tempi di attesa per l'acquisizione dei permessi e quindi della burocrazia, ottenendo in questo modo un minore LCOE. Si potrebbe perciò produrre elettricità ad un prezzo più competitivo confrontato con le fonti convenzionali. Tutti questi vantaggi hanno spinto l'interesse di molti politici e di società private su questo tipo di tecnologia. Il parco eolico considerato in questa relazione finale è formato da cinque aerogeneratori e si trova a Gravina in Puglia (provincia di Bari). STE ENERGY S.R.L., una società di ingegneria a Padova, sta pianificando la progettazione di un impianto fotovoltaico utility scale in questo parco eolico, rendendo gli impianti di potenza ibridi una realtà anche in Italia. Gli obiettivi di questa relazione finale sono la stima della possibile produttività di un tale impianto fotovoltaico e la valutazione dell'impatto che l'ombreggiamento delle turbine eoliche (in particolare delle pale del rotore) ha sulla resa annuale dei pannelli, cercando di capire il peso che queste perdite legate all'ombreggiamento hanno sulla produzione elettrica. Questi fini vengono raggiunti tramite l'utilizzo di due software: PVSYST e windPRO. I loro risultati vengono poi uniti per ottenere risultati più completi. Successivamente l'evoluzione in un giorno ed in intervalli di tempo più piccoli dell'ombra gettata da un singolo aerogeneratore viene modellata matematicamente mediante il software MATLAB. Lo scopo di ciò consiste nell'ottenere la massima ampiezza dell'area spazzata dall'ombra della turbina durante il giorno peggiore dell'anno (solstizio di inverno, 21 dicembre), e pure gli istanti di tempo in cui un singolo modulo e un semplice generatore fotovoltaico sono ombreggiati dalla torre e dalle pale. In aggiunta anche il fenomeno dello shadow flickering, che è essenziale nella consueta analisi di impatto ambientale, è valutato in modo da ottenere valori approssimati del numero di ore e giorni in un anno in cui l'ombra è presente sull'area intorno agli aerogeneratori. In conclusione, con il software SIMULINK viene modellato l'effetto dinamico che l'ombreggiamento intermittente delle pale rotanti ha sulle prestazioni (in termini di tensione, corrente e potenza in continua) di un semplice generatore fotovoltaico,

considerando anche un algoritmo MPPT. Tutto questo lavoro prova la fattibilità dell'installazione di un impianto fotovoltaico insieme agli aerogeneratori, siccome le perdite di energia connesse all'ombreggiamento sono relativamente basse e il problema relativo all'oscillazione dell'irradianza solare, e quindi alle fluttuazioni degli output della tecnologia fotovoltaica verso i convertitori, può essere risolto grazie all'utilizzo di un algoritmo MPPT e di un sistema di controllo. Se proprio si volesse evitare qualsiasi preoccupazione legata al fenomeno dello shadow flickering, i moduli potrebbero essere posizionati a distanze superiori rispetto all'andamento spaziale dell'ombra gettata dalla turbina durante il solstizio di inverno.

ABSTRACT

A hybrid power plant consists of an onshore wind farm with photovoltaic plants installed in the same location, along with storage systems able to maintain power and voltage output stable. Since aerogenerators need to be at enough distances from each other to avoid perturbations and turbulence that can decrease overall electricity production and efficiency, a wind park occupies a huge amount of land. To optimize terrain utilization, soil under turbines can be employed for agriculture, for producing more energy with PV plants or both with agriphotovoltaics. With PV plants for example the investments required for grid connection can be reduced while bureaucracy is less a burden, allowing to reach a lower LCOE and making produced electricity more competitive compared to conventional sources. All these advantages have driven a lot of interest towards hybrid power plants, with many private enterprises jumping into this new market. The wind farm that is considered in this thesis is composed of five aerogenerators located at Gravina in Puglia (Bari province, Italy). STE ENERGY S.R.L., an engineering company in Padua, is planning to design a large-scale PV plant at this wind park position, making hybrid power plants a reality also in Italy. The goal of this master's degree thesis is the assessment of wind turbine tower, nacelle, rotor and blades shadows influence on a possible PV plant's annual energy production, trying to understand the effect that losses related to shadings have on its total yield. This target is achieved by two software exploitation: PVSYST and windPRO. Their results are then merged, reaching higher accuracy on shading influence assessment on PV plant performance. Furthermore, wind turbine shadow evolutions over a single day and during smaller periods are mathematically modelled inside MATLAB software, to analyse its behaviour, to evaluate the dimensions of area affected by shadow and to see which instants of time a single module or a simple PV array is shaded. Moreover, the blade shadow flickering phenomenon, that is essential for every environmental impact analysis, will be evaluated to obtain approximated values of number of hours and days in a year when shadow is present around aerogenerators. In conclusion the dynamic effect that intermittent shading has on a small PV array performance (voltage, current, power output) with a MPPT algorithm will be described by SIMULINK and SIMSCAPE ELECTRICAL software models. All this work will prove the feasibility of PV plant existence together with aerogenerators, since shadow linked energy losses are not so high and the problem related to solar irradiance oscillation and then output fluctuations towards inverter can be solved with a MPPT algorithm and a control system. If designer's wish is to completely avoid any shadow flickering problem, modules can be placed at distances higher than spatial trend of shadow casted by wind turbine during Winter solstice.

INDEX

INTRODUCTION

Planet Earth's average surface temperature has increased by 1.1°C since 1880, with higher peaks in several regions (especially at the poles: +5°C in last century): the human involvement on this phenomenon is called "anthropic greenhouse effect".

This causes permanent glaciers to melt on mountains, ocean levels to rise, high intensity meteorological events, that occur more frequently worldwide, but that have a higher impact particularly in climatic zones of poor Countries (Africa, South Asia, Indonesia, …); consequently, migration is the remaining solution for local populations.

Acting now is necessary to mitigate planet heating, avoiding the worst environmental scenarios. With decisional immobility, Earth surface average temperature will be 3°C or 4°C higher by the end of 21st century compared to pre-industrial values. In particular, Countries of the "Organisation for Economic Co-operation and Development" (OECD), the first in history to have gone through the industrial development and that have produced the highest quantity of polluting emissions, must take the responsibility in developing new technologies and invest in a more nature focused energy transition.

During the last ten years the international community, mainly European states, set challenging targets; the commitment started with the "Paris Agreements" (21st Conference of Parties, December 2015), when 195 Countries decided to keep the average surface temperature increase under 2°C compared to pre-industrial level (and if possible under 1.5°C) [1].

In order to reach this purpose, European Commission has built up 2030 and 2050 pathways like "Sustainable Development Goals", "European Green Deal", "Net-Zero to 2050". European Commission intention is clear: achieving 55% greenhouse gases emission (GHG) reduction by 2030 and net zero GHG emission by 2050 with respect to 1990 values.

Italy, as a European member state, signed the Renewable Energy Directive II (RED II) in 2018, which milestones are [2]:

1) share of renewable energy sources in the European Union's final gross energy consumption by 2030 equal or higher than 32% (article 3, par.1, page 24), updated to 40% in 2022 [3];

2) share of renewable energy sources in European Union's final gross energy consumption in the transport sector by 2030 equal or higher than 14% (article 25, par.1, page 44);

3) annual increase of renewable energy sources share in the thermal and refrigeration sector until 2030 equal or higher than 1.3% every year (article 23, par.1, page 41);

4) each European Union state member have the obligation of writing down a national integrated plan, where they depict how they intend to reach their fixed goals by 2030.

RED II led to the creation of Italian "Piano Nazionale Integrato Energia e Clima" (PNIEC), where Italian 2030 goals are defined [4]:

1) share of renewable energy sources in the Italian final gross energy consumption by 2030 equal or higher than 30%;

2) share of renewable energy sources in the Italian final gross energy consumption in the transport sector by 2030 equal or higher than 22%;

3) annual increase in renewable energy sources share in the thermal and refrigeration sector until 2030 equal or higher than 1.3% every year;

4) 43% (ETS sector) and 33% (non ETS sectors) of Italian GHG emission reduction versus 2005 value and Italian total GHG emission decrease of 51% versus 1990.

These purposes were implemented into Italian law on 8th November 2021, with the Legislative Decree 199/2021 [5]. This decree defines energy from renewable sources as: "energy from renewable not fossil sources like wind energy, solar thermal and photovoltaic, geothermal, waves, hydraulic, biomass, flue gases" (article 2, comma 1).

The Italian "Piano Nazionale Ripresa e Resilienza" (PNRR) underlines investment amounts and how to reach PNIEC goals.

Inside PNRR Mission 2 "green revolution and ecologic transition", 59.46 billion euro investments are divided in [6]:

_ 5.27 B€ for sustainable agriculture and circular economy (1.5 B€ agriphotovoltaic, 1.04 MW new capacity taking 4.3 Mm^2 cultivated surface);

_ 23.78 B€ for renewable energy, hydrogen, electrical network and sustainable mobility;

_ 15.36 B€ for building energy efficiency;

_ 15.05 B€ for territory and hydraulic resource safeguard.

5.9 B€, of the 23.78 B€, will be used to increase the share of produced energy from renewables, planning the installation for example of 200 MW of innovative projects (like offshore wind turbines).

Everything mentioned represents a continuous evolution and turmoil in the renewable energy field. Italian Lgs. D. 199/2021 defines "suitable areas" for RES installation as: "huge potential areas where to install electricity production plant from renewable source" (article 2, comma 1). These sites, defined by the "Ecologic Transition Ministry" (today called "Environment and Energy Security Ministry"), are not so numerous in the Italian territory (compared to the high national electric energy demand), therefore optimization of investments and land use is fundamental.

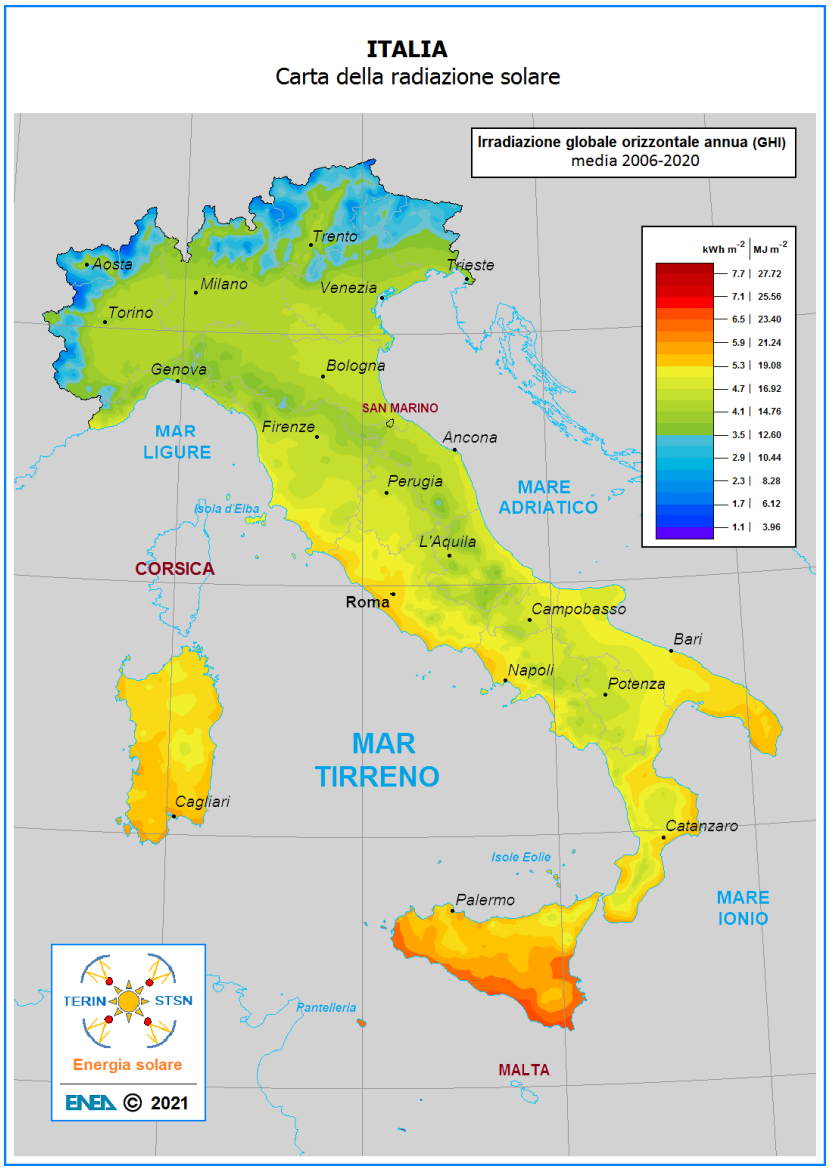

Figure 1. *Italian solar global irradiation on horizontal surface distribution, annual average values from 2006 to 2020. Source: http://www.solaritaly.enea.it/Radiazione/RadiazioneMappeIt.php.*

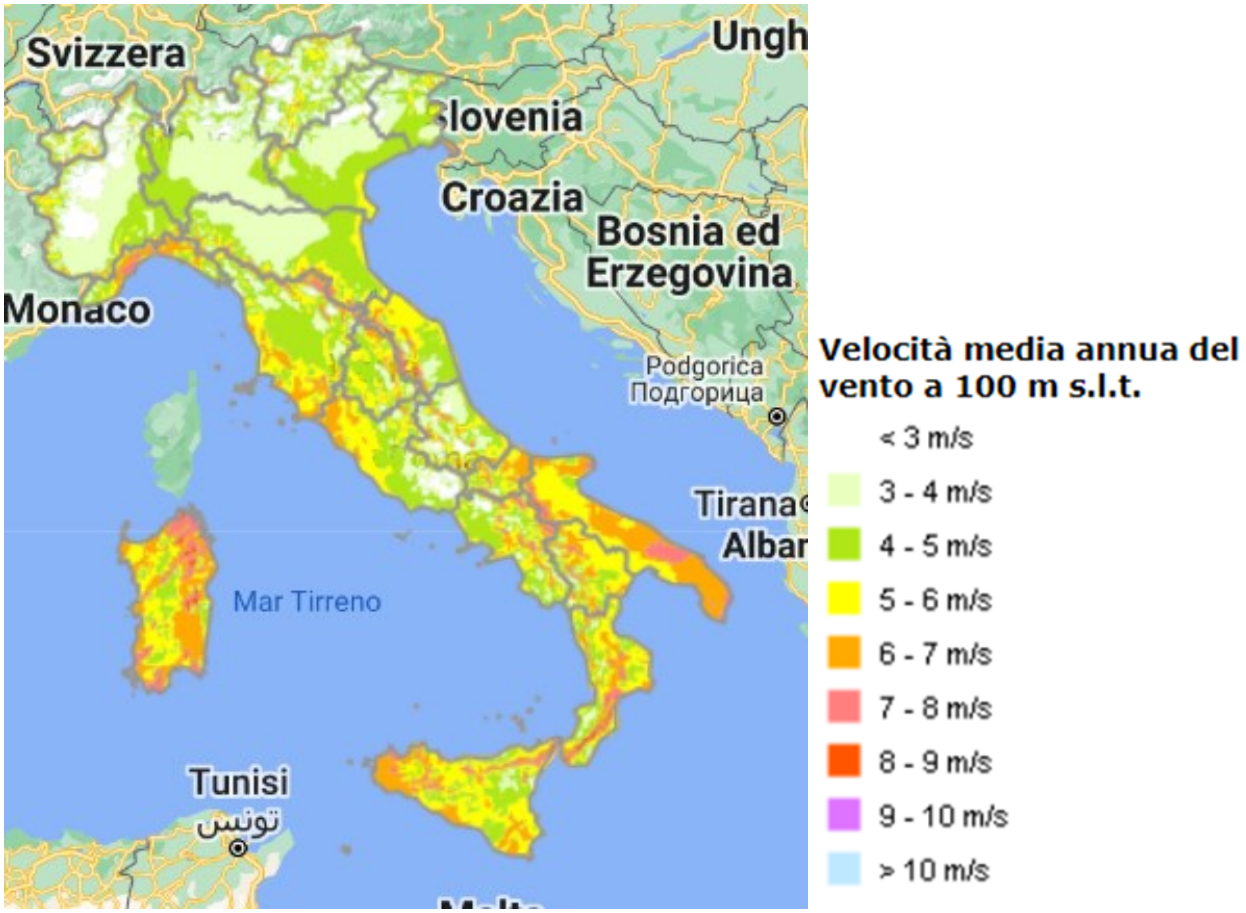

Figure 2. *Average annual wind speed onshore at 100m altitude in Italy. Source: New Eolic Atlas RSE, https://atlanteeolico.rse-web.it/start.phtml.*

This is the reason why nowadays "hybrid power plants" are receiving a lot of attention in Europe.

Hybrid power plants are based on large scale onshore wind farms with photovoltaic plants located at their base, along with storage systems (batteries) able to keep power and voltage output stable; indeed regulations on environmental impacts and the distance that wind farms must have from populated zones are really strict. In a wind farm aerogenerators need to be at certain distances from each other to avoid perturbations and turbulence that can decrease overall electricity production and efficiency, therefore a wind park occupies a huge land surface. To optimize terrain utilization, soil under turbines can be employed for agriculture, for producing more energy with PV plants or both with agriphotovoltaics. In this way investments required for grids, connection stations, site evaluation and bureaucracy are reduced. All these advantages have driven a lot of interest towards hybrid plants, with many investors jumping into this new market.

STE ENERGY S.R.L., the engineering company that supervised this master's degree thesis, designed near Gravina in Puglia (Bari province) a five-aerogenerator wind farm in the last years and

now the company is planning to install under the wind turbines a large-scale PV plant, making hybrid power plants a reality also in Italy.

This master's degree thesis wants to evaluate the influence that wind turbine tower, nacelle, rotor and blade shadows have on the annual energy production of a possible PV plant, trying to understand the effect that these shadings have on the overall energetic yield. Furthermore, WTG shadow evolution over a single day will be mathematically modelled in order to analyse its behaviour and impact area dimensions. Shading will not only be assessed during a whole day but also in shorter periods, to observe instants of time when a single PV module or a small array is shadowed. To achieve these goals, entire wind turbine and blades-only shadow evolution over time MATLAB models will be created. Also the blade shadow flickering phenomenon, essential for the environmental impact analysis, will be studied; it gives the total number of hours and days in a year when shadow is present on receptors. In the end the dynamic effect that intermittent blades shading has on a simple PV array performance (voltage, current, power output) with a MPPT algorithm will be described by SIMULINK block diagram models (SIMULINK is a MATLAB software module) and by a SIMSCAPE ELECTRICAL model.

CHAPTER 1

HISTORY OF PHOTOVOLTAIC TECHNOLOGY

The history of solar energy conversion into electricity started in 1839 when Alexandre Edmond Becquerel (Paris 1820 - Paris 1891), a French physicist, was the first scientist to describe the photovoltaic effect: an electrolytic cell, composed by two metallic electrodes submerged in a conducting liquid solution, undergoes an increase of generated electricity once it is shined by solar radiation [7]. He generated electricity by exposing one of the two electrodes to sunlight. He observed that with blue (380 nm) and ultraviolet radiations, the electricity created is higher [8].

Thirty-four years later, in 1873, Willoughby Smith, an English electrical engineer (Great Yarmouth, Norfolk 1828 – Eastbourne, Sussex 1891) discovered the photoconductivity of Selenium (Se), while in 1876 William Grylls Adams (Laneast 1836 - Broadstone 1915) and his student Richard Evans Day observed that selenium, when exposed to solar radiations, produces electric energy [7]. This was the first demonstration of the photovoltaic effect in a completely solid-state system [8]. Unfortunately, they failed to power devices using electricity from selenium.

But just in 1883 Charles Fritts (Boston 1850 - 1903) built the first “thin film solar cell” using selenium wafer [7]. He compressed molten selenium between two different metal plates; the Se film touched one of the two plates, whereas a gold leaf was located between the selenium layer and the other one [8]. In this way he proved that these devices could also have a lower cost too.

In 1905, Albert Einstein (Ulma 1879 – Princeton 1955) theoretically modelized the photoelectric effect, then Robert Millikan (Morrison 1868 - San Marino, California, 1953) experimentally proved it in 1916 [7]. Photoelectric effect consists of electrons emission from a metal surface when illuminated by light.

In 1918, Polish chemist Jan Czochralski (Kcynia 1885 – Poznań 1953) developed the “CZ method” for producing solid circular cross-section bars of monocrystalline silicon [7]. During the CZ process a crystal seed is immersed and slowly rotated in a crucible containing molten silicon (Si); the seed is afterwards raised from the crucible and melted silicon solidification happens, resulting in a monocrystalline silicon bar [9].

In 1954, Daryl Chapin (Ellensburg 1906 – Naples, Florida 1995), Calvin Fuller (Chicago 1902 – Vero Beach 1994) and Gerald Pearson (Salem 1905 – 1987) invented the first modern crystalline silicon PV cell, which had a solar energy conversion efficiency of 6%, at AT&T Bell Telephone Laboratories [8]; it could transform enough solar energy into electricity to power an electrical device. Today all these scientists are in the American "National Inventors Hall of Fame" NIHF.

In October 1955, a BELL LAB PV monocrystalline silicon module was installed on a pole as a solar battery for a telephone system in Americus (Georgia) to supply electricity [10].

Figure 1.1. *Photograph of original Bell Solar Battery installation in 1955. Source: https://www.bellsystemmemorial.com/belllabs_photovoltaics.html.*

From this moment, PV technology has been considered even for space applications: in 1958 Vanguard One satellite radios were fuelled by a less than one watt PV generator, followed by other satellites like Explorer Three, Vanguard Two and Sputnik Three [7].

Large scale fabrication and commercialization began in these years: from 1957 to 1960 Hoffman Electronics developed silicon solar cells with increasing efficiencies from 8% to 14% [7].

In 1976, inside RCA Laboratories, David Carlson (Weymouth 1942 - 2019) and Christopher Wronski (Warsaw 1939 - 2017) developed the first amorphous silicon PV cell [7]; they also demonstrated that hydrogenated amorphous silicon can be p-type or n-type doped, forming a pn-junction [11].

In 1982, ARCO SOLAR built the first 1 MW peak power PV plant in Hisperia, California; its modules had dual-axis tracking systems. Later, ARCO SOLAR also fabricated and commercialized in 1986, the first thin-film module, the G-4000 [7].

In 1985, South Wales University produced silicon cells with 20% energy conversion efficiency with $1\ \frac{kW}{m^2}$ solar irradiance [7].

In 1992, another University, this time South Florida, was able to create a thin film CdTe cell with 15.9% efficiency.

In 1999, SPECTROLAB Inc and the National Renewable Energy Laboratory (NREL) obtained a 32.3% conversion efficiency by means of a tandem solar cell with sunlight concentrated by lenses [7].

In the same year, the NREL set a new record for thin-film PV cells, 18.8% efficiency, and the worldwide PV cumulated installed capacity reached 1'000 MW.

In 2000, 32'800 PV cells were installed on the International Space Station (ISS) wings and Sandia National Laboratories developed the first solar inverter [7].

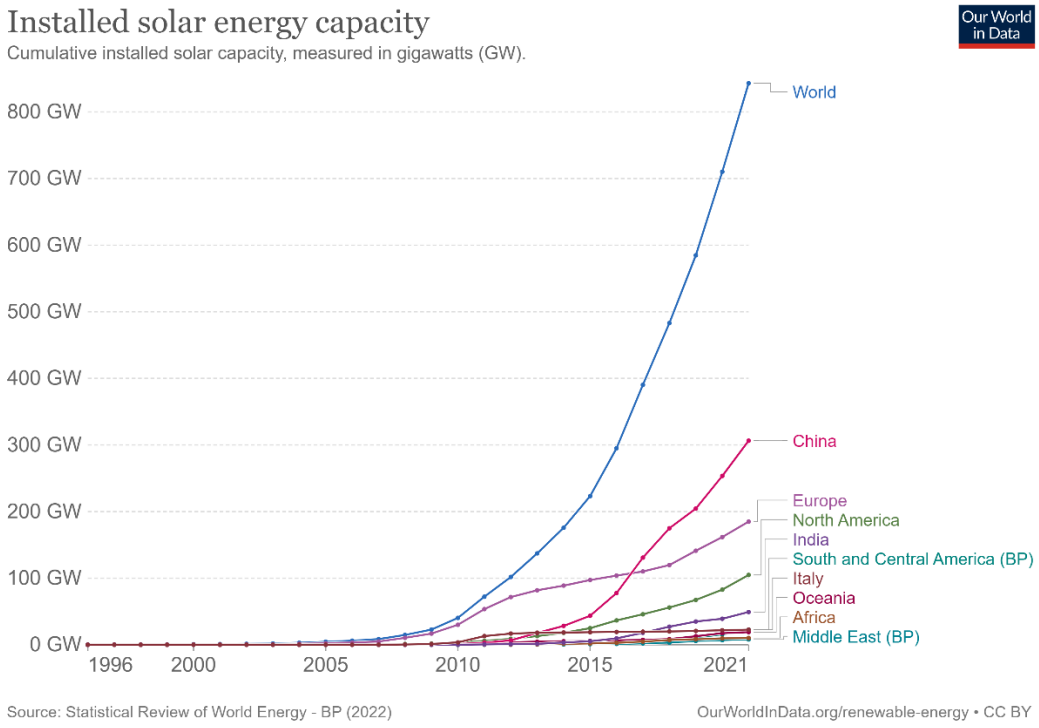

Figure 1.2. *From 1996 to 2021 total installed solar energy capacities, in the whole world and by regions. Data published by BP, data publisher's source: "Statistical Review of World Energy", https://www.bp.com/en/global/corporate/energy-economics/statistical-review-of-world-energy.html.*

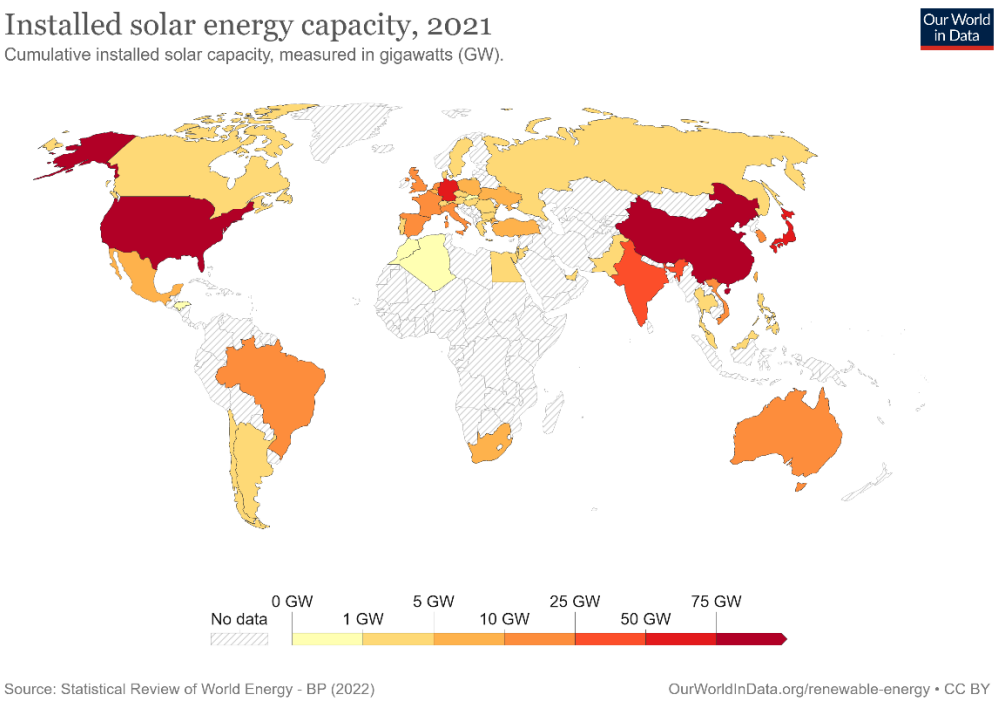

Figure 1.3. *Total installed solar energy capacity distribution in 2021. Data published by BP, data publisher's source: "Statistical Review of World Energy", https://www.bp.com/en/global/corporate/energy-economics/statistical-review-of-world-energy.html.*

The pictures above show the continuous expansion that solar technology has been undergoing worldwide. In the table below is reported solar capacity data of 1996 and 2021 for different geographical regions and some specific Countries.

Table 1.1. *Solar capacity data from "Statistical Review of World Energy", https://www.bp.com/en/global/corporate/energy-economics/statistical-review-of-world-energy.html.*

	1996	2021
Africa	0.00 GW	10.30 GW
Asia	0.06 GW	501.58 GW
Europe	0.07 GW	184.95 GW
Middle East	0.00 GW	7.97 GW
North America	0.03 GW	104.88 GW
Oceania	0.02 GW	19.07 GW
South and Central America	0.00 GW	22.82 GW
China	0.00 GW	306.40 GW
Italy	0.02 GW	22.69 GW
India	0.00 GW	49.34 GW
United States	0.01 GW	93.71 GW
High-income countries	0.15 GW	395.41 GW
Upper-middle-income countries	0.01 GW	351.69 GW
Lower-middle-income countries	0.00 GW	79.34 GW
World	0.17 GW	843.09 GW

Nowadays PV cell efficiencies have reached new records and are continuously growing over time. For example, monocrystalline silicon has reached an efficiency of 26.1%, multicrystalline silicon 23.3%, CdTe 22.1%, hydrogenated amorphous silicon 14%, CIGS 23.4%, while the highest value is 47.1% and it has been achieved by a four-junction tandem cell with solar concentrator [12].

However new promising technologies, such as organic solar cells, perovskite cells and quantum-dot cells are being demonstrated the market with interesting yields.

Moreover, the initial investment cost (CAPEX) related to PV plant installation is decreasing non-stop, making the levelized cost of electricity (LCOE) of PV technology (cost of 1 kWh generated) competitive with conventional and more polluting power production systems.

CHAPTER 2

PV TECHNOLOGY: AN OVERVIEW

2.1 SOLAR RADIATION

The Sun and its energy have been present throughout the history of humankind. It is a yellow dwarf star, mainly constituted made by hydrogen isotopes (about 75% of its mass) and helium (almost 25% of its mass), followed by other elements; these gases are kept together by an intense gravitational force. In fact, the Sun can be seen as a gravitational confinement nuclear fusion reactor, where in its core the reaction occurs: hydrogen H, deuterium D and tritium T nuclei are closer to each other because of gravitational forces and thus they fuse, partially converting the mass of the nuclei into energy following Einstein's formula (energy E, mass variation Δm, speed of light in vacuum c = $3 \cdot 10^8$m/s):

$$E = \Delta m \cdot c^2 \, . \quad (2.1)$$

The sum of the reactant's masses is lower than the overall initial mass of the products; this means that mass is converted into energy. One of these nuclear fusion reactions is the following:

$$D + T \rightarrow He^4 + n + E \, , \quad (2.2)$$

with a kinetic release of E=17.6 MeV, obtained by the neutron n and the helium He^4 (also named alpha-particle): 3.5 MeV for He^4 and 14.1 MeV for n. Since the number of fusion reactions that happen in the Sun's core is very high, it can reach temperatures up to $15 \cdot 10^6$ K. Around the Sun's heart there are other different layers where the heat transfer mechanisms between gases are irradiation and convection. The last layer is the Photosphere that has a temperature of approximately 5'800 K.

Based on radiative heat transfer theory, all matter that has a temperature higher than absolute zero (T=0 K) is able to exchange energy by emitting radiation. The basis of radiative energy exchange is the "blackbody model". A blackbody (or black surface) does not exist in nature and is defined as a system capable of completely absorbing the intensity of all incident spectrum radiations: a + r + t = 1, a (absorptivity) = 1, r (reflectivity) = t (transmittivity) = 0 [13, page 418-425]. The emitted

irradiance of a black body I_{bb} (W/m^2) is given by the Stefan-Boltzmann law (Stefan-Boltzmann constant $\sigma = 5.67 \cdot 10^{-8} \frac{W}{m^2 \cdot K^4}$):

$$I_{bb} = \sigma \cdot T^4 . \quad (2.3)$$

The Sun's temperature, when considered as a blackbody, is 5'777 K [14, page 3]. Radiation released by the Sun is not simply electromagnetic waves (made by magnetic and electric fields that change over time and space), but it behaves like particles too: this is known as the particle-wave duality of light. An electromagnetic wave presents the following features:

1) a wavelength (distance between two consecutive wave peaks);

2) an amplitude (its intensity, "strength");

3) a direction and a speed of propagation.

In 1900, physicist Max Planck (Kiel 1858 - Gottinga 1947) made the hypothesis that a wave carries discrete amounts of energy (quanta), that Gilbert Lewis (Weymouth, Massachusetts, 1875 - Berkeley, California, 1946) named photons, which values of Eph (eV) depend on wave propagation velocity in the medium c and wavelength λ (Planck constant $h = 4.1357 \cdot 10^{-15}$ eVs):

$$E_{ph} = h \cdot \frac{c}{\lambda} . \quad (2.4)$$

This formula shows that photon energy is inversely proportional to its wavelength: so, photon radiation in the ultraviolet and visible range (380÷800 nm) have higher energy compared to infrared photon radiation. From this equation, photon energy in the visible range varies between 1.5÷3.5 eV. A particular fact about electromagnetic waves is that they do not require a medium to propagate, but they can move through space vacuum too. In summary, the Sun emits energy by radiation, that propagates through the void with a speed of $3 \cdot 10^8$ m/s until it reaches Earth's atmosphere, after an average journey of $150 \cdot 10^6$ km. Considering this mean distance between Sun and Earth, the irradiance of orthogonally incident solar spectrum radiation, per unit of surface, outside of the atmosphere is called solar constant G_{sc} and it is equal to 1'367 W/m^2 [14, page 6]. In reality, as Keplero's first law says [15, page 277], the "green planet" moves around Sun with an elliptical orbit, where the star occupies one of the two focuses. The position where the distance is the maximum ($152 \cdot 10^6$ km) is called Aphelion, whereas the one where it is minimum ($147 \cdot 10^6$ km) Perihelion; this is the reason why the solar constant is only an average. A more precise value of the solar irradiance outside of the atmosphere $G_{0,d}$ (W/m^2) during a given day (d) of the year can be calculated by [14, page 9]:

$$G_{0,d} = G_{sc} \cdot \left(1 + 0.033 \cdot \cos\left(\frac{360 \cdot d}{365}\right)\right). \quad (2.5)$$

Knowing solar angles and Sun coordinates is fundamental for obtaining solar irradiance information. These are [14, pages 9÷18]:

- DECLINATION ANGLE δ (°): due to the inclination of Earth's rotational axis by 23.45°, it is the angle between the propagation direction of solar rays and the equator parallel,

  $$\delta = 23.45° \cdot \sin\left(\frac{360}{365} \cdot (d - 1)\right) = 23.45° \cdot \sin\left(\frac{360}{365} \cdot (284 + d)\right) \quad (2.6)$$

  with d being the number of the day of the year.

  Particular values:

  winter solstice (21st December) → δ = -23.45°

  spring equinox (21st March) → $\delta = 0°$

  summer solstice (21st June) → $\delta = 23.45°$

  autumn equinox (23rd September) → $\delta = 0°$
- SOLAR ELEVATION ANGLE α (°): angle between the propagation direction of solar beam and the horizontal surface; values needed include the location of interest latitude φ (°), the declination angle δ of the day, the hour angle ω (°) related to the time considered:

  $$\sin(\alpha) = \cos(\delta) \cdot \cos(\varphi) \cdot \cos(\omega) + \sin(\delta) \cdot \sin(\varphi) \quad (2.7)$$
- HOUR ANGLE ω (°): it is the angle between the meridian crossing the position of interest on Earth's surface and the meridian where the Sun is at zenith (ω = 0° at solar noon, ω < 0° in the morning, ω > 0° in the afternoon):

  $$\omega = 15 \cdot (TST - 12) \quad (2.8)$$

  with true solar time TST (h) calculated knowing the legal time LT (h), longitude ψ (°) of the location, time difference ΔTz (h) of the position's time zone compared to Greenwich mean time GMT, equation of time ET (h), summer time difference ΔTs (-1 h in summer, 0 h in winter):

  $$TST = LT + \Delta\text{Tz} - \frac{\psi}{15°} + \text{ET} + \Delta\text{Ts}. \quad (2.9)$$

  In this equation, East to Greenwich longitudes are considered negative.
- SOLAR AZIMUTH γs (°): according to ENEA (Ente per le Nuove tecnologie, l'Energia e l'Ambiente) reference, it is the angle between the solar ray propagation direction projection on the horizontal surface and the South direction (positive if the projection is eastward, negative if it is westward):

  $$\sin(\gamma s) = \frac{\cos(\delta) \cdot \sin(\omega)}{\cos(\alpha)}. \quad (2.10)$$

Solar position is unequivocally described by solar elevation α and solar azimuth γs. These angles are necessary to calculate solar irradiance reaching a plane on Earth's surface. The total incident radiation is given by the sum of three different components:

1) DIRECT RADIATION: it is the radiation fraction that does not change its propagation direction while it is moving through the atmosphere. Its irradiance Id (W/m^2) is:

$$Id = Ior \cdot \frac{\sin(\alpha+\beta)}{\sin(\alpha)} = Ior \cdot \frac{\cos(i)}{\sin(\alpha)} \quad (2.11)$$

where α is the solar height angle, β (°) is the plane inclination angle related to horizontal surface, i (°) is the incident angle, Ior (W/m^2) is the measured value of direct irradiance on a horinzontal plane (measured by a pyrheliometer).

Incidence angle i is the angle between the normal direction to plane and the solar beam propagation direction. The general equation for the incidence angle is:

$$\cos(i) = \sin(\delta) \cdot \sin(\varphi) \cdot \cos(\beta) - \sin(\delta) \cdot \cos(\varphi) \cdot \sin(\beta) \cdot \cos(\gamma s) + \cos(\delta) \cdot \cos(\varphi) \cdot \cos(\beta) \cdot \cos(\omega) + \cos(\delta) \cdot \sin(\varphi) \cdot \sin(\beta) \cdot \cos(\gamma s) \cdot \cos(\omega) + \cos(\delta) \cdot \sin(\beta) \cdot \sin(\gamma s) \cdot \sin(\omega) \quad (2.12)$$

2) DIFFUSED RADIATION: it is the radiation fraction that, because of multiple interactions with particles, dust and clouds inside the atmosphere, undergoes several alterations of propagation direction (for instance Rayleigh scattering is one of the phenomena occurring) before reaching the ground. It depends a lot on weather conditions and it is stronger than direct radiation when it is foggy or the sky is totally covered by clouds. Considering an isotropic model of radiation diffusion, which considers equal diffusion from all directions, the formula that allows to calculate its value Dd (W/m^2) is:

$$Dd = Dor \cdot \frac{1+\cos(\beta)}{2} \quad (2.13)$$

where Dor (W/m^2) is the diffused irradiance incident on a horizontal plane measured with a pyranometer equipped with a shadow ring/sphere, to avoid the measurement of total irradiance, and β is the tilt angle.

3) REFLECTED RADIATION: it is the radiation fraction that is reflected by soil, or any other reflective surface, before reaching the inclined surface of interest whose material has a certain albedo ρa (-), that is defined as the fraction of total irradiance hitting the ground that is reflected. After measuring the overall irradiance incident on the ground Gor (W/m^2) by means of a pyranometer, the reflected irradiance Rr (W/m^2) on a tilted surface is:

$$Rr = Gor \cdot \rho a \cdot \frac{1-\cos(\beta)}{2}. \quad (2.14)$$

Finally, the total irradiance G (W/m^2) reaching an inclined plane is the sum of these three components:

$$G = Id + Dd + Rr\ . \quad (2.15)$$

Instead, solar irradiation, that is the solar energy reaching a unitary surface during a certain period of time, is obtained by integrating this total irradiance over that same time range.

To understand how much the solar rays's potential is weakened during their journey through atmosphere, the Air Mass AM concept (-) is used [14, page 9]. By definition it is the ratio between the actual path length travelled by light inside atmosphere and the minimum one that takes place only when the Sun's position is at zenith:

$$AM = \frac{1}{\cos(\theta)} \quad (2.16)$$

where ϑ is the zenith angle (°). The most important value is AM1.5 (α ≅ 42° at a middle latitude), utilized in the Standard Test Conditions STC to evaluate and compare solar cell performance. Due to the presence of different gas molecules in the atmosphere like carbon dioxide CO_2, ozone O_3, water vapor H_2O, solar spectrum intensity decreases:

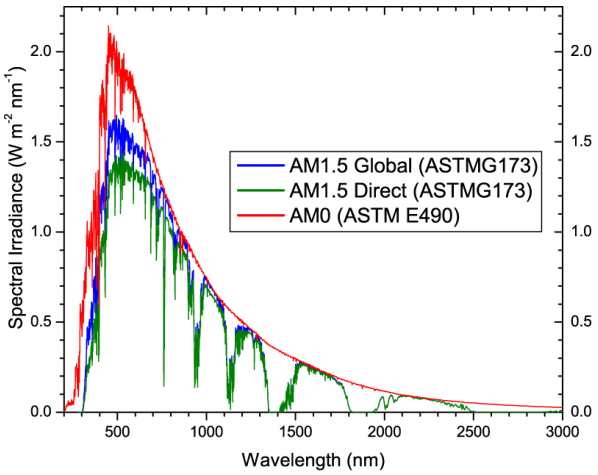

Figure 2.1. *Intensity of solar radiation reaching the ground at different air masses. Source: PVeducation, https://www.pveducation.org/pvcdrom/appendices/standard-solar-spectra.*

2.2 PHOTOVOLTAIC EFFECT

The electrons in a semiconductor atom occupy with a certain probability orbitals with discrete, non-continuous energy levels. Since in a pure material the number of atoms is really enormous, energy bands exist and they represent all the possible energy levels of electrons; the last two of these

energy bands are valence band, filled by low energy and strongly bonded to nuclei electrons, and conduction band, with higher energy electrons. These two bands are separated by an energy bandgap Eg (eV), a range of forbidden energy levels, which magnitude is different for each material (for example silicon has Eg=1.12 eV) [16, pages 40÷44]. Eg is the minimum amount of energy needed for to promote an electron from the valence band to the conduction band. A sufficient mean thermal kinetic energy E_k (J) of the electrons $E_k = \frac{3}{2} \cdot k \cdot T$ (2.17) [17, pages 75-81], related to absolute temperature T (K) by the Boltzmann constant k ($\frac{eV}{K}$), can promote one electron from the valence band to the conduction band and simultaneously create a hole (positive unitary charge): this is called thermal electron-hole pair (ehp) generation.

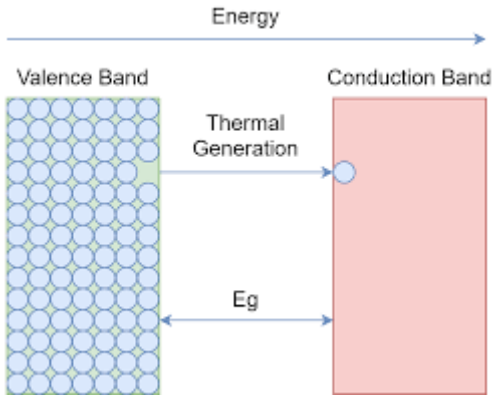

Figure 2.2. *Electron promotion by thermal generation. Source: "Semiconductor theory", Muhammad Shahid, https://www.electronics-lab.com/article/semiconductor-theory.*

At thermal equilibrium, therefore at constant temperature, together with thermal generation (absorption of a phonon that produces an ehp) also thermal recombination takes place (recombination of ehp, electron returns to its previous energy level by emitting a phonon) and electron (n_0) and hole (p_0) thermal concentrations remain constant. If a semiconductor is shined, radiations having energy $E_{ph} = h \cdot \frac{c}{\lambda} \geq Eg$ (2.18) can create electrons and holes [18, *Absorption of Light*]. When both thermal and photonic ehp generation occur, total electron n and hole p concentrations (cm^{-3}) are given by the sum of thermal density n_0, p_0 and photon density n', p':

$$n = n_0 + n' \qquad p = p_0 + p' \,. \quad (2.19)$$

If suddenly the solar spectrum vanishes, photonic generated ehp quickly recombine, thus conducting electrons return in the valence band.

Semiconductors can be divided into two families [16, page 46]:

1) DIRECT BANDGAP SEMICONDUCTORS

They are semiconductors whose lowest conduction band and highest valence band energy levels have equal momentum. Only $E \geq Eg$ is sufficient to produce an ehp, so these are semiconductors used for thin film technologies (in the order of tenths of micron).

2) INDIRECT BANDGAP SEMICONDUCTORS

They are semiconductors whose lowest conduction band and highest valence band energy levels have not equal momentum. $E \geq Eg$ is not enough to produce an ehp, but an increase in carrier momentum is required too. These are semiconductors used for thick PV cells, for instance silicon ones (about 200 μm thickness).

2.3 PHOTOVOLTAIC CELL

A photovoltaic cell is a device based on several material layers one on top of the other. Starting from the one that faces solar radiation, they are ordered in the following way:

- front surface electrical contacts;
- anti reflection coating (ARC);
- n-type semiconductor layer (emitter);
- pn-junction (space charge or depletion region);
- p-type semiconductor layer (base);
- back surface field (BSF);
- back surface electrical contacts.

But how does a PV cell work?

1) LIGHT MANAGEMENT

One of the primary aspects of a photovoltaic device is “light management”. Indeed, its performance (conversion efficiency and peak power) is strictly dependent on how much the solar cell is able to minimise light reflection and thus maximise the total amount of absorbed photons. A material, when hit by radiations, can reflect them at the interface of two different propagation mediums, absorb them while they are moving through its thickness and transmit them out of the other side. Obviously just the absorbed fraction of the incident spectrum is actually employed to generate electron-hole pairs. Summarising, PV cell front surface material must increase and decrease as much as possible solar spectrum absorption and reflection respectively. The equation below depicts the intensity decay of a monochromatic radiation during its travel through a medium [18, *Generation Rate*] :

$$I(x,\lambda) = I_0 \cdot e^{-\alpha(\lambda)\cdot x}\,, \quad (2.20)$$

where $I(x,\lambda)$ is the intensity of a monochromatic radiation ($\frac{\mathrm{W}}{\mathrm{m}^2\cdot\mu\mathrm{m}}$) at a certain position x in the material, I_0 is its initial intensity, $\alpha(\lambda)$ is the medium absorption coefficient for that specific wavelength λ. As a matter of fact, $\alpha(\lambda)$ changes with the wavelength and the type of semiconductor. Lower wavelength radiations have higher $\alpha(\lambda)$ values than higher ones, so the latter penetrate deeper inside the material and more thickness is needed.

Semiconductors can be classified into two big groups: direct bandgap semiconductors (for example GaAs, CdTe) and indirect bandgap semiconductors (for instance mono- and poly-crystalline Si). The distinction between these classes has been written in the previous paragraph. Since it is easier to create free carriers inside a direct bandgap type, it has higher values of $\alpha(\lambda)$ than the second type: this is the reason why direct bandgap semiconductors are known as thin film technologies (few microns thickness versus hundreds of microns for traditional thick film Si cells).

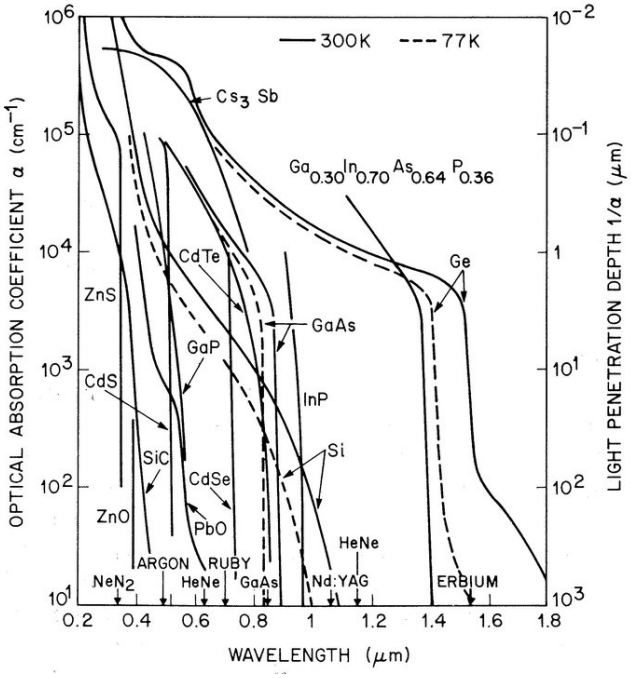

Figure 2.3. *Absorption coefficient variation with radiation wavelength. Source: researchgate.net, https://www.researchgate.net/figure/Absorption-coefficient-of-semiconductor-materials-at-300-K-and-77-K-6_fig2_343736867.*

In general, two methods for increasing light absorption probability are commonly performed: texturization and anti-reflection coating. Texturization consists of producing pyramidal roughness on the front and back PV cell surfaces; this causes on the front surface a greater number of

consecutive reflections and longer paths inside thickness because of Snell law, while on the back surface total internal reflection (TIR) happens. Snell's law is

$$n_1 \cdot \sin(\theta_1) = n_2 \cdot \sin(\theta_2) , \quad (2.21)$$

being n_1, n_2 the refractive index real components (-) of the entering and exiting mediums, θ_1, θ_2 incident angles (°) that the radiation propagation direction creates with interface normal.

ARC is a particular material sheet capable of causing a disruptive interference on reflected radiations. This is especially true for the wavelength λ which ARC sizing is based: thickness must be $t = \frac{\lambda}{4 \cdot n}$ (2.22), with n being the ARC refractive index. Usually silicon nitride Si_3N_4 is the adopted solution. ARC has electrical advantages too; in fact, it can passivate dangling unsaturated chemical bonds that are present on the PV front surface, reducing recombination centres density and improving device light conversion efficiency [18, *Anti-Reflection Coatings*].

Texturization on the PV cell rear side is made on p-type semiconductor surface and on aluminium Al or silver Ag metal back contacts, gaining in this way TIR and passivation [18, *Surface Texturing*]. Furthermore, Al or Ag atoms are diffused into the p-type semiconductor by firing, achieving a higher acceptor doping that generates a new junction, preventing diffusion motion in the base of lost and not collected by pn-junction minority electrons. This is called back surface field (BSF).

2) METALLIC CONTACTS

Front surface metallic contacts are generally composed by two or three Ag busbars connected by thinner Ag fingers, decreasing as much as possible their shading effect and so cell performance loss. Other materials are also exploited; an example are transparent conducting oxides (TCO) that are both conductive and transparent, improving light absorption efficiency. Under contacts semiconductors can have greater doped regions, diminishing contact resistance and increasing semiconductor carriers tunnelling probability. The same concepts can be applied to back surface contacts. If only front surface light is used to produce electricity, back contact will be a uniform Al layer; but if there is the necessity to capture solar rays from the back face too, then Ag busbars and fingers are preferred (bifacial PV cell).

3) PN-JUNCTION

There are several kinds of PV devices: the more traditional thick film solar cells (monocrystalline silicon and polycrystalline silicon) and the thin film ones (amorphous silicon, composite semiconductors like CdTe, GaAs, CIS, CIGS, …). Regarding crystalline silicon cells, the reaction

starts from pn-junction. A pn-junction is achieved when two diversely doped sheets of Si are put in contact, a n-type Si semiconductor and a p-type one (or by differently doping the two silicon sides):

N-TYPE SILICON SEMICONDUCTOR → Silicon is a fourth group element in the periodic table, its atomic number is 14 and it has 4 valence electrons in its most external orbital shell. This means that it can make a maximum of 4 covalent bonds to complete its 4 sp3 hybrid molecular orbitals (they are organised to form a tetrahedral shape) by sharing its valence electrons with surrounding Si atoms, generating one or more crystals that repeat themselves throughout the lattice. By means of the doping process, silicon atoms can be substituted with other element atoms, called dopants; these are of different groups and thus with diverse numbers of valence electrons. The difference between n-type Si and p-type Si is related to the elements chosen in the doping process. Indeed, a n-type Si is obtained by substituting Si atoms with fifth group element atoms like phosphorus P, arsenic As and antimony Sb, that each leaves an uncoupled electron, increasing global electron concentration n. Dopants in this case are named "donors", since they behave as positively charged ions giving away an electron.

P-TYPE SILICON SEMICONDUCTOR → differently from n-type, a p-type silicon is originated by doping with third group element atoms like boron B, aluminium Al, gallium Ga and indium In. They are named "acceptors" since they behave as negatively charged ions taking an electron from Si atoms.

PN-JUNCTION → the creation of the depletion (or space charge) region happens because of the spatial concentration gradient of electrons and holes inside n-type and p-type semiconductors respectively, near their junction. The gradients cause two diffusion motions, one of electrons (from n-type to p-type), the other of holes (from p-type to n-type), with an overall diffusion current density

$$J_n = J_{n,diff} + J_{p,diff} \quad (2.23)$$

$$J_{n,diff} = q \cdot Dn \cdot \frac{dn}{dx} \qquad J_{p,diff} = -q \cdot Dp \cdot \frac{dp}{dx} \quad (2.24)$$

where $J_{n,diff}$, $J_{p,diff}$ are the electron and hole diffusion current densities, q is the fundamental electric charge ($1.6 \cdot 10^{-19}$C), $\frac{dn}{dx}$ and $\frac{dp}{dx}$ are the electron and hole concentration gradients ($\frac{\text{cm}^{-3}}{\text{cm}}$), Dn and Dp are the electron and hole diffusion coefficients ($\frac{\text{cm}^2}{\text{s}}$). Electrons move further than holes, since their diffusion length L (cm) is greater because of a better mobility given by a lower effective mass, therefore a higher diffusion coefficient (considering equal recombination lifetime τ):

$$L_n = \sqrt{D_n \cdot \tau} > \sqrt{D_p \cdot \tau} = L_p \quad (2.25)$$

During these diffusion movements, electron-hole recombination processes occur; thanks to this phenomenon, a depletion region without carriers appears but in reality there are negatively charged acceptors and positively charged donors into it. These ions generate an internal electric field that counteracts the diffusion motions, making the overall current null. When a solar ray hits with its spectrum a PV cell emitter or base face, radiations are absorbed and they generate electron-hole pairs along the whole device thickness depending on its wavelength (remember that absorption coefficient of a material depends on material nature itself and on radiation wavelength). Created carriers inside pn-junction are separated by the internal electric field, while majority and minority free-moving charges in the emitter and in the base move by diffusion inside the junction (because of a concentration gradient, since the depletion region has nearly zero carrier density); then electrons and holes are separated by the electric field. Minority electrons in the base move towards the n-type silicon, whereas majority electrons inside the emitter are repelled; minority holes in the emitter spread towards p-type silicon, while majority holes inside base are bounced back. Collection probability CP (-) of carriers, i.e. the possibility that they diffuse into the SCR and they are separated, depends on the position where they are generated by light in the device. If they are inside their diffusion length, they will be separated before recombining and vice versa. The final result is a diffusion current from n-type to p-type called light generated current I_L (A):

$$J_L = \frac{I_L}{A} = \int_0^{Xdevice} [\int_{\lambda_1}^{\lambda_2} \alpha(\lambda) \cdot f(\lambda) \cdot e^{-\alpha(\lambda) \cdot x} \cdot d\lambda] \cdot CP(x) \cdot dx \quad (2.26)$$

where J_L is the light generated current density ($\frac{\mathrm{A}}{\mathrm{cm}^2}$), A is the front and/or back PV cell surface (cm^2), x is the position along device thickness (cm), α is the absorption coefficient (cm^{-1}), f is the incident photon flux ($\mathrm{cm}^{-1} \cdot \mathrm{s}^{-1}$), CP is the collection probability (-), λ_1 and λ_2 are minimum and maximum solar spectrum wavelengths (nm). This current has opposite verse compared to the forward diode current I_D (A), so the net PV cell current is:

$$I = I_L - I_D = I_L - I_0 \cdot (e^{\frac{qV}{nkT_c}} - 1) \ , \quad (2.27)$$

with I_0 being the reverse saturation current (A), V the applied voltage (V), $\mathrm{k} = 8.62 \cdot 10^{-5}$eV/K Boltzmann constant, Tc the absolute cell temperature (K), n the "non-ideality factor" (-). From this equation the PV cell I-V characteristic is built [18, *P-n Junctions*].

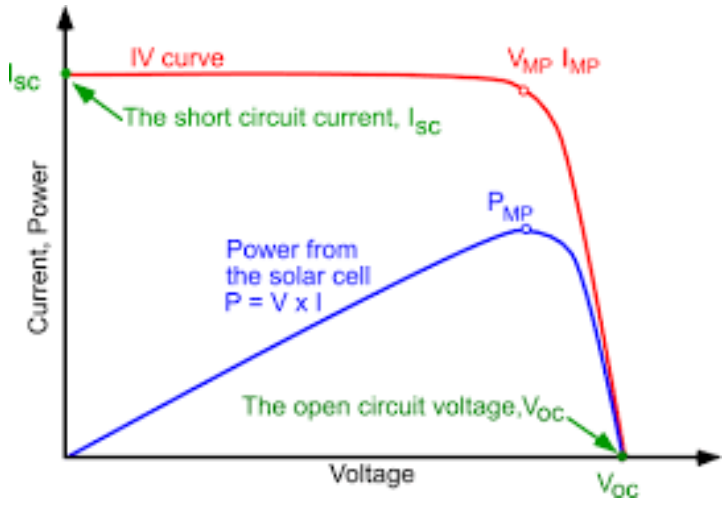

Figure 2.4. *Solar cell I-V and P-V curves. Source: PVeducation, https://www.pveducation.org/pvcdrom/solar-cell-operation/iv-curve.*

The graph reports the main PV cell electrical parameters in STC operating conditions, therefore total irradiance G = 1 $\frac{kW}{m^2}$, AM1.5, cell temperature Tc = 25°C:

SHORT-CIRCUIT CURRENT Isc (A) → light generated current I_L = Isc, maximum current that the cell can emit;

OPEN-CIRCUIT VOLTAGE Voc (V) → maximum cell voltage, when $I_D = I_L$ = Isc;

MAXIMUM POWER POINT CURRENT Imp (A) → maximum power current generated by cell;

MAXIMUM POWER POINT VOLTAGE Vmp (V) → maximum power voltage generated by cell.

Cell temperature Tc (°C), in alternative conditions to STC, can be calculated by the equation:

$$Tc = T_{env} + G \cdot \left(\frac{NOCT - 20°C}{G_{NOTC}}\right), \quad (2.28)$$

with T_{env} being the actual environmental temperature (°C), G the real total irradiance ($\frac{W}{m^2}$), NOTC the nominal operating cell temperature (°C) and G_{NOTC} the total irradiance in NOCT conditions ($\frac{W}{m^2}$). NOCT conditions are: $T_{env} = 20°C$, $G_{NOTC} = 800 \frac{W}{m^2}$, air speed equal to 1 $\frac{m}{s}$.

Isc, Voc, Imp, Vmp and peak power Pmp change with cell temperature Tc and total irradiance G:

$$Isc = Isc(STC) \cdot \frac{G}{G(STC)} \cdot (1 + \alpha \cdot (Tc - 25°C)) \quad (2.29)$$

$$Voc = Voc(STC) \cdot \left(1 + \beta \cdot (Tc - 25°C)\right) + A \cdot \ln\left(\frac{G}{G(STC)}\right) \quad (2.30)$$

$$Pmp = Pmp(STC) \cdot \frac{G}{G(STC)} \cdot \left(1 + \gamma \cdot (Tc - 25°C)\right) \quad (2.31)$$

$$A = \frac{n \cdot k \cdot Tc}{q} \quad (2.32)$$

where n is the "non-ideality factor", k is the Boltzmann constant, α, β, γ are the temperature variation coefficients of current, voltage and power (%/°C) respectively. Vmp and Imp temperature variation coefficients lay inside β and γ range. Solar energy conversion efficiency in datasheets is always expressed in STC conditions with the formula:

$$\eta = \frac{Pmp}{G \cdot A} = \frac{Vmp \cdot Imp}{G \cdot A} = \frac{Voc \cdot Isc \cdot FF}{G \cdot A} \quad (2.33)$$

with cell fill factor $FF = \frac{Vmp \cdot Imp}{Voc \cdot Isc}$ (-) (2.34) and cell area A (cm^2) [16, page 58÷59].

The equivalent electrical circuit of a PV cell is:

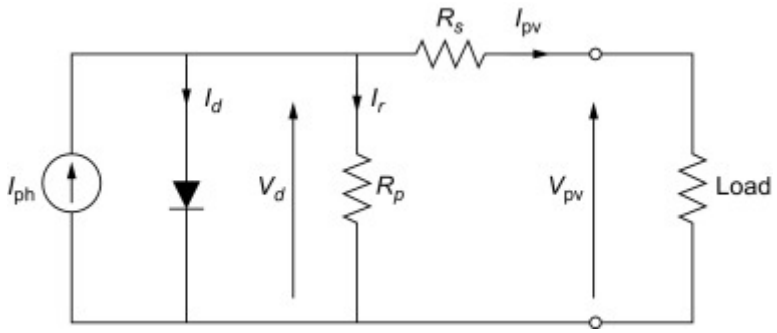

Figure 2.5. *Single diode equivalent circuit of a solar cell. Source: "Submerged and Floating Photovoltaic Systems Modelling, Design and Case Studies", Marco Rosa-Clot, Giuseppe Marco Tina, 2018, chapter 3, paragraph 4.*

where Rs is the series resistance (Ω) encountered by carriers through their travel toward contacts, Rp is the shunt resistance (Ω) related to the inversion of carriers movement due to the presence of defects inside the cell.

2.4 PHOTOVOLTAIC MODULE

A single PV cell is not capable of producing enough DC power to satisfy user requirements, because of its relatively low DC current and especially its very low DC voltage output. This is the reason why more cells, with the same I-V characteristic (to avoid mismatch losses), are connected in series (and eventually in parallel): this allows the increase of the series (string) equivalent voltage, that is equal to the sum of all unitary device voltages, while the total current is equal to the sum of all the currents of cells/strings connected in parallel. The module I-V characteristic results

from these voltage and current operations. Therefore, the way cells are connected is the basis of a PV module. Cell connections are performed by means of two or three conducting copper ribbons linking the same number of busbars on a cell emitter front surface with the base contacts of the subsequent one. This process is done for all the cells of the string.

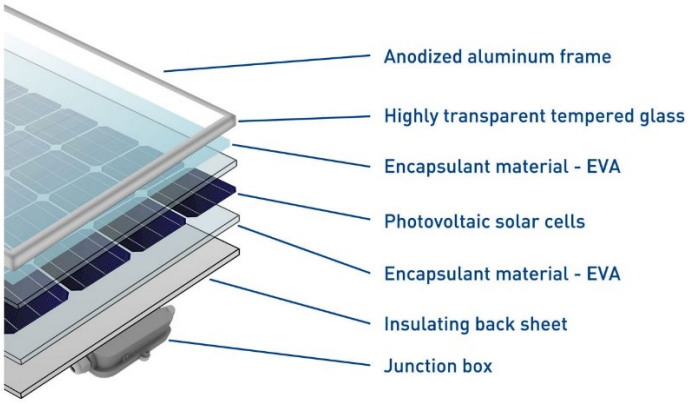

Figure 2.6. *PV module layers. Source: ECOPROGETTI SRL, https://ecoprogetti.com/the-structure-of-photovoltaic-module.*

The primary components of a PV module are [18, *Module Materials*]:

1) TEMPERED LOW IRON CONTENT GLASS

It is fundamental to protect solar cells from weather agents like rain, hail (strong impacts) and wind. Glass must be as transparent as possible, while an ARC on it improves optical efficiency of the whole device.

2) ETHYLENE VINYL ACETATE (EVA) LAYER

Material that melts at 140÷150 °C; it is spread on solar cells to gain electrical isolation, impermeability and, because of its flexibility, mechanical protection from glass. From a chemical point of view, EVA is stable in contact with silicon.

3) SOLAR CELLS CONNECTED IN SERIES

4) ANOTHER EVA LAYER

5) TEDLAR BACKSHEET

Tedlar (PVF) is an artificial material historically created and produced worldwide by DuPont. "DuPont Tedlar is a highly versatile, polyvinyl fluoride film that provides a long-lasting finish to a wide variety of surfaces exposed to harsh environments while its inert, non-stick properties make it an excellent release film for parts processed under high temperature and pressure" [19]. So, PVF

grants safety to solar cells from mechanical impacts and weather agents. In addition, it has high electrical resistivity (a PV module is a second class insulation equipment) and it also has good reflectivity that increases the path of escaped radiations inside solar cells and thus the absorption yield. It is also used as backsheet in the module.

6) ANODIZED METALLIC (ALUMINUM) FRAME

The frame provides mechanical rigidity to the set of layers, ensuring protection from lateral impingements.

7) JUNCTION BOX

It is pasted on the tedlar plate, where the module positive and negative connections are placed together with bypass diodes.

8) BYPASS DIODES

Consequence of one or more cells partially or completely shadowed in a module is a performance loss, that means reduction of power output and other electrical parameters. This phenomenon is known as mismatch loss. Furthermore, fully shaded cells are not generators but diodes, dissipating part of the remaining shined cells generated power into heat by Joule effect due to current flowing. If this situation is not solved in time, high temperature hot spots (up to 150°C) due to Joule effect could irreparably damage both EVA and glass layers. Bypass diodes, antiparallelly connected to a certain number of cells in series, are the solution. In this way a very small current flows through series connected cells, preventing hot spots and mitigating power and energy production loss.

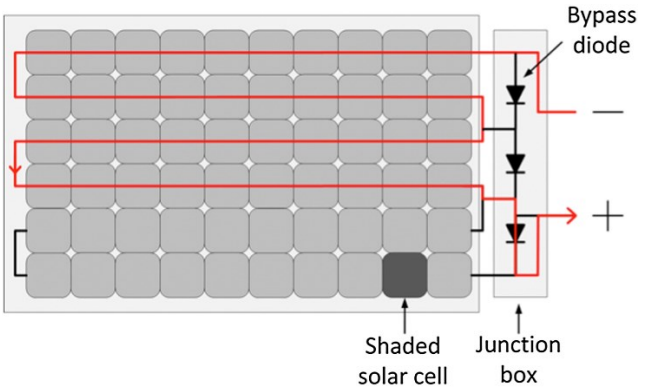

Figure 2.7. *Solar cells and bypass diodes in a PV module. Source: "Photovoltaics in the shade: one bypass diode per solar cell revisited", from "Progress in photovoltaics" book, pages 836-849, October 2017, Boudewijn B. Pannebakker, Arjen C. de Waal, Wilfried G.J.H.M. van Sark, Wiley Online Library.*

2.5 PHOTOVOLTAIC PLANT

Two PV plant configurations currently exist:

- STAND ALONE SYSTEM (OFF-GRID)

Plant for users that are too difficult or expensive to be connected to the electrical grid, so in this case the energy produced is self-consumed or stored by electrochemical batteries.

- GRID CONNECTED SYSTEM

Plant where users are also connected to the grid, being capable of self-consuming produced energy and transmitting it to the national low or medium voltage distribution network.

The main components of a PV plant are [14, pages 760÷778]:

1) PV GENERATOR/ARRAY

A string is made by series connected modules in order to reach the required voltage value. These strings can be linked in parallel, increasing current output. Generator rated DC power P_0 (W) is given by multiplying single module STC peak power $P_{mod,STC}$ and number of same I-V characteristic modules N:

$$P_0 = \mathrm{N} \cdot P_{mod,STC} \,. \quad (2.35)$$

If the goal is maximising efficiency and production of each single module, it is necessary to keep them at their best inclination and orientation angle, avoiding both internal (related to PV plant components and modules themselves) and external shading (related to external natural and artificial objects).

2) INVERTER AND MPPT

An inverter is a device composed of one or more DC/DC converters (able to modify the DC generated voltage magnitude), one or more maximum power point trackers and a DC/AC converter (to convert DC voltage into AC voltage, with frequency equal to 50 Hz in Italy). The MPPT is a device that follows in each instant of time the maximum power point of a PV generator I-V characteristic, since its performance changes with irradiance, temperature and solar spectrum. Inverter choice must be done by accounting for PV generator electrical properties variations with environmental conditions and solar spectrum features, especially in the so called “worst conditions”.

3) BATTERY

An electrochemical DC power storage device can be directly connected to the PV generator through a DC/DC converter capable of modulating voltage magnitude into the one required by the battery. Otherwise, it can be linked to the inverter AC side with an AC/DC converter.

4) MONODIRECTIONAL AND BIDIRECTIONAL COUNTERS

Important for measuring energy produced by the generator, energy transmission to electrical grid and self-consumed energy fraction. They are the keys for incentive calculations.

5) SOLAR CABLES

Solar module connections require cables that can withstand high temperatures and strongly energetic UV radiations, with good flexibility. Common cables can be used for other plant sections only if they are still protected from UV radiations; this can be done by placing them inside special pipes or underground. Cable sizing is related to the number of modules connected in series and in parallel, considering their currents and voltages during the worst operating conditions, trying to decrease as much as possible the power losses along conductors too.

6) SAFETY DEVICES

Safety devices that are always installed in a PV plant are blocking diodes, fuses, circuit breakers and surge protectors. In general blocking diodes and fuses are series connected to each string of the PV array, preventing current inversion and over-current in case of failure. Fuses must be chosen considering the highest possible short circuit current in the worst operating conditions, as fuses must not melt during normal operation. Circuit breakers protect from over-currents in case of short circuit faults, while surge protectors from over-voltages.

CHAPTER 3

HYBRID POWER PLANTS

3.1 HYBRID POWER PLANT GENERALITIES

Hybrid power plants are systems made of wind turbines, photovoltaic array, batteries for storage and control devices (inverters). This type of plants has specific advantages: since both technologies depend on the presence of natural resources and since solar energy together with wind intensity are not continuous during a day, a hybrid plant is able to produce power for more hours per year than either technology working alone; this feature decreases the probability of not generating power, reducing in this way the levelized cost of electricity (LCOE), i.e. the time needed for returning the investment, and thus the financial risk [20]. A more constant and stable power production allows to export energy with better quality to transmission or distribution networks, thanks also to the energy accumulated in the batteries when generation and demand are not simultaneous (keeping as constant as possible the voltage and the frequency at the grid connection). Moreover, a hybrid plant is suitable to strongly decrease the overall CAPEX investments for cables, connections, transformers, stations, roads, and to also reduce the time required for municipalities and public administrations to approve construction permits; indeed, the latter is one of the worst problems when talking about renewables in Italy [21]. As a matter of fact, “multi-technology parks are more than just a market trend: hybrid parks can sometimes even be a condition for obtaining a permit” [21]. The presence of a photovoltaic array also allows for the use of pieces of land at the turbines base, that would remain unused because of health and environmental limitations, which can be significant in case of scarce terrain availability. An example of hybrid plant in Europe is the first one built by Vattenfall company in South-West Netherlands, called “Haringvliet Zuid Energy Park” and inaugurated on 22nd March 2022. Vattenfall decided to integrate a photovoltaic system (115'000 panels, 38 MWp DC peak power) plus battery storage (12 sea containers with 288 “BMW i3” batteries, for a total of 12 MW) into its Haringvliet onshore wind farm project (6 wind turbines, 22 MW nominal power). The quantity of electricity that this park has generated is equal to the annual consumption of 39'000 households (solar panels alone will produce enough to supply 12’000 households) [22]. The energy storage system is designed to keep the electricity grid in balance and can be exploited in future as storage for renewable power [22]. Total investment is about 35 million euro [20].

Figure 3.1. *Haringvliet Zuid Energy Park by VATTENFALL. Source: https://group.vattenfall.com/press-and-media/newsroom/2020/vattenfalls-largest-hybrid-energy-park-is-taking-shape-in-the-netherlands.*

Ross Williams, construction project manager at Haringvliet Zuid Energy Park, said: "wind and solar complement each other very well in terms electricity production. Wind has its higher producing months during the darker, winter months, when solar is less productive, and solar has its optimal months when wind is less productive during summer. This means that, by sharing a single grid connection, we can optimise the use of the full grid connection capacity more often throughout the year, increasing the overall production of the hybrid park for roughly the same investment in the grid connection. The battery facility then provides the additional service of maintaining a balance on the system when it comes to operating frequency and storage of excess electricity" [22].

3.2 GRAVINA IN PUGLIA HYBRID POWER PLANT

Referring to the project described in this thesis, STE ENERGY S.R.L. designed a wind farm composed of five General Electric GE 6.1-158 Cypress 6.1 MW nominal power aerogenerators, with 30.5 MW total power, in the municipal territory of Gravina in Puglia (Bari province). The park is located 13 km North-West from Gravina urban centre; site access is possible from provincial road SP26. The wind farm high voltage line connection point, at the standard voltage of 36 kV, is the TERNA electric station named "Gravina Centrale" [23].

Figure 3.2. *Wind turbine positions in Gravina in Puglia municipality. Source: Google Earth software.*

In picture above the five wind turbines can be seen, called WTG01, WTG02, WTG03, WTG04 and WTG05. The main characteristics of a GE 6.1-158 Cypress three bladed aerogenerator are: tubular steel tower with hub height from ground of 120.9 m, rotor diameter of 158 m, active yaw control (designed to steer the wind turbine with respect to wind direction), active pitch control (to regulate turbine rotor speed) with full blade pitch angle range of approximately 90 degrees (zero degree position corresponds to the blade being flat in relation to the prevailing wind), a variable speed generator (doubly-fed induction generator) with a power electronic converter system (it consists of a converter on the rotor side, a DC intermediate circuit and a power inverter on the grid side), a three-windings dry-type transformer located at the rear of the nacelle (medium voltage range of 10÷33 kV), nacelle length of 12.8 m and height of 4.3 m [24]. The wind farm aerogenerators geographical coordinates at Gravina in Puglia site are in the table below:

Table 3.1. *Wind turbines position in Gravina in Puglia site.*

WTG	Longitude	Latitude	Altitude [m]
WTG01	16°15'17,51" E	40°50'49,07" N	381,1
WTG02	16°15'43,18" E	40°50'31,57" N	396,3
WTG03	16°16'09,63" E	40°50'23,75" N	375,4
WTG04	16°16'32,40" E	40°50'25,91" N	378,5
WTG05	16°16'54,11" E	40°50'21,49" N	390,8

Nowadays, STE ENERGY S.R.L. desires to integrate in the same Gravina wind park location a PV plant of supposed overall 49.607 MWp DC peak power and 41.5 MW AC power, with batteries for storage of 25 MW injection power. The bifacial PV modules that will be implemented are the

TRINASOLAR VERTEX 670 Wp model (monocrystalline silicon cells), placed with North-South horizontal monoaxial trackers at three meters of height from ground. The model of inverters will be the SUNGROW SG350HX, to convert DC power produced by photovoltaic array into AC power with voltage level and frequency required by TERNA transmission network. Cables and power lines can be shared with the wind farm. Grid connection to the national transmission network is planned to be located at the "Pellicciari" electric station at 36 kV [25]. A possible PV plant layout is the following:

Figure 3.3. *A possible PV plant layout in Gravina wind farm. Source: "Impianto Fotovoltaico Gravina in Puglia (BA), Relazione tecnico-informativa". Ing. Alberto Voltolina.*

The datasheets of the TRINASOLAR VERTEX 670 Wp PV module [26] and the SUNGROW SG350HX inverter [27] are available in APPENDIX A. To develop this new hybrid power system and to investigate its performance, modelling and mathematical calculations must be done by means of specific software. All work performed in relation to these targets is going to be explained in the next chapters.

CHAPTER 4

WTG SHADOW FLICKERING

4.1 SHADOW FLICKERING DEFINITION

One of the main environmental problems related to aerogenerators in wind farms is the “shadow flickering” phenomenon; in other words, it is the periodic oscillation of direct solar radiation shading due to the rotating blades that “interrupt” light propagation. This only happens when the sky is clear of clouds and wind intensity in site is higher than the aerogenerator cut-in speed, which is necessary for keeping the rotor in motion.

Figure 4.1. *Drawing of shadow flickering phenomenon. Source: https://cleantechnica.com/2022/03/30/living-in-wind-energys-shadow/.*

This phenomenon has an effect on both people and PV module performance. In fact, the assessment of shadow flickering is one of the key parts of wind turbine environmental impact reports. Shadow flickering intensity is defined as the difference of radiation strength (in a given position) in presence or absence of blade obstruction. This rapid and oscillating variation of light intensity on a given area may have negative consequences on photosensitive people; currently, there are not international regulations and limitations regarding shadow flickering. However, a standard based on scientific evidence was introduced in 1984 in Germany by Verkuijlen and Westra: in their paper they highlighted that the light intensity oscillation frequency that can produce a sense of unease to human individuals is between 2.5 Hz and 20 Hz [28]. Another important study on this topic is the one argued by Graham Harding and Pamela Harding [29].

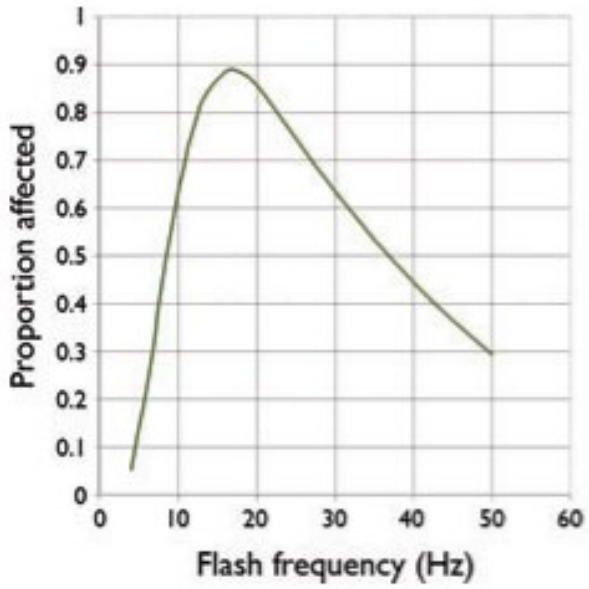

Figure 4.2. *Proportion of patients with photosensitive epilepsy sensitive to flicker as a function of the frequency. Source: graph from [8], obtained by elaboration of data from Binnie et al. (2002).*

Since the proportion of photosensitive patients affected by shadow flickering from wind turbines does not decrease much with the distance from the turbine tower axis (significant reduction occurs at distances farther than one-hundred times the aerogenerator hub height), to safeguard human health the critical maximum permitted flashing frequency must be 3 Hz, i.e. a rotational speed of a three bladed wind rotor equal to 60 rpm. Therefore, conventional limits are frequency lower than 2.5÷3Hz, and maximum rotational speed within 50÷60 rpm. Recent three bladed aerogenerators operate at constant rotational speeds lower than 60 rpm; this way, human related problems are controlled. Since (as written in Chapter 2) DC voltage, current and power output from a solar cell, and thus from a module, depend on the solar irradiance reaching the sensible surfaces, shadow flickering generates rapid DC voltage, current and power variations at the inverter input that can cause problems for power quality and grid stability in the PV plant network connection point. Shadow flickering presence and duration is strongly connected to wind intensity and direction, cloud coverage percentage of the sky, sun position coordinates (day, time, location on Earth's surface). Then two different conditions for shadow flickering impact analysis can be defined: worst-case and real-case.

- **WORST-CASE HYPOTHESIS**

Worst-case shadow flickering is the most penalizing ideal situation (maximum duration of the phenomenon), when there is clear sky condition from sunrise to sunset, continuous rotation of the blades, rotor plane always perpendicular to propagation direction of direct radiation from the Sun to

the receptor, absence of any anthropic or natural obstacles between wind turbines and receptors (except for site terrain orography). Results obtained by this calculation are extremely cautionary.

- **REAL-CASE HYPOTHESIS**

Real-case shadow flickering is a more realistic situation that can be studied considering the real local sunshine duration over a year (real number of sunlight hours or sky without clouds in a year) and the actual yearly operational hours of wind turbines, because the latter depends on the statistical wind features of the considered site (wind speed may be lower than the cut-in value). Nevertheless, real-case is cautionary in turn, since for instance the rotor plane is considered orthogonal to the direct radiation and there is still an absence of light propagation, anthropic and natural obstacles.

The shadow flickering analysis, for both worst and real situation, for the Gravina in Puglia site was executed by means of "SHADOW (FLICKER) MODULE" of windPRO software. Instead, the PV plant AEP (Annual Energy Production) evaluation was obtained with windPRO "PV SOLAR MODULE" and PVSYST software.

4.2 WORST-CASE SHADOW FLICKERING ANALYSIS

WindPRO SHADOW (FLICKER) MODULE allows to compute how many hours per year, days per year and maximum minutes per day shadow flickering phenomenon occurs in the area around the wind turbines, giving an idea of the eventual environmental impact. Moreover, a calendar of shadowing periods during all days of a year can be generated, showing when and how much time receptors are not shined. Calculations can be made for the worst-case scenario and for a more real-case scenario (referring to the different hypothesis described before). The worst-case depicts the maximum potential risk of shadow flickering environmental impact. For extra context, the shadow impact limits (related to physiological response, photosensitivity) for receptors near a wind farm are (from German guidelines) [30]:

1) maximum 30 hours per year of worst-case shadow flickering;

2) maximum 30 minutes per day of worst-case shadow flickering.

In Sweden and Denmark, for practical purposes, 10 hours (Denmark) and 8 hours (Sweden) per year for real-case shadow flickering are used respectively as limits [31, page 83].

The calculation of potential shading effects on a receptor is carried out by simulating and computing the Sun position related to the wind turbine rotor position and its resulting shadow for

every one minute time step in a full year. If the rotor shadow shades a receptor at a given time instant, that outcome is registered as one minute of potential shadow impact.

It is possible to choose two types of shadow flickering impact computations: “shadow flicker map” and “shadow flicker at receptors”, both can be made for worst- and real-case. In these calculations, in the advanced settings, no limit was given to the shadow flickering maximum observation distance and the lower angle limit of the Sun above the horizon was set to 0° (shadow is never ignored for Sun elevation α lower than a certain angle).

- **WORST-CASE SHADOW FLICKER MAP**

After inputting in the software the geographical location of the Gravina in Puglia site (latitude = 40.837°, longitude = 16.272°, the ones of WTG04), the digital terrain model (DTM) of the location with ground elevation data, ground height contours, positions of the wind farm five aerogenerators, wind turbine data such as hub height and rotor diameter, the position, size and orientation (tilt angle and azimuth) of receptors (in this case, of the PV plant modules); in shadow map calculations, receptors are grid points around the WTG areas. The default receivers are horizontal 1x1 square meters at elevation given by DTM. All five wind turbine shadows are considered in the worst-case analysis. The shadow flicker map is useful because it allows to observe the approximated extent of the shadow flickering impact on the wind farm surroundings. Obtained worst-case shadow flickering maps are:

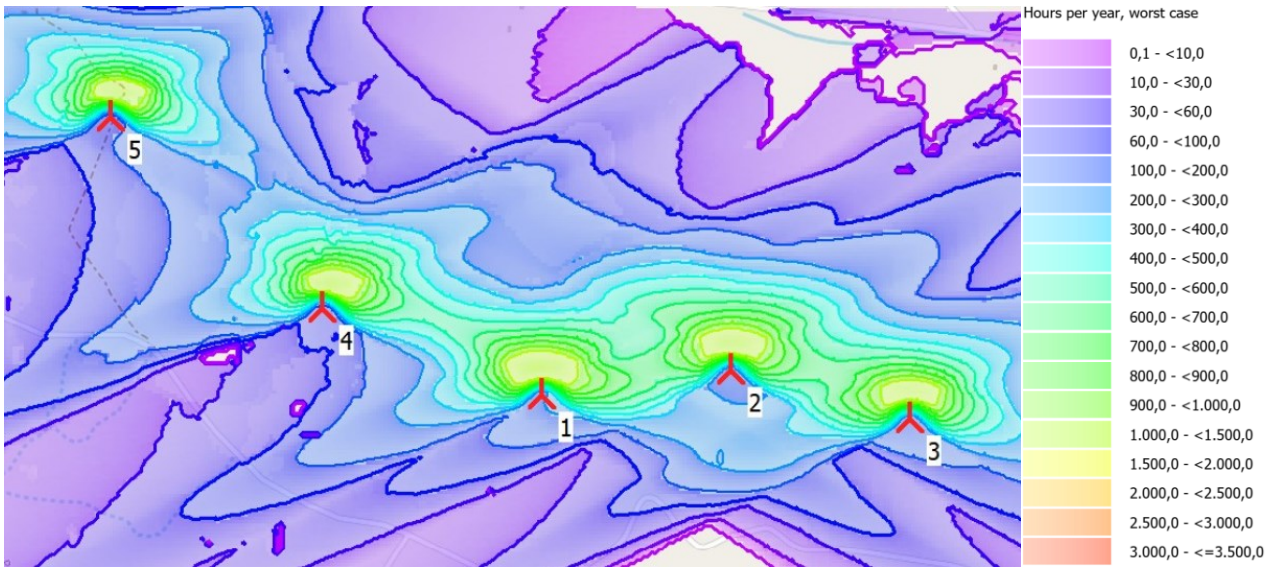

Figure 4.3. *Worst-case shadow hours per year map at the Gravina in Puglia wind farm.*

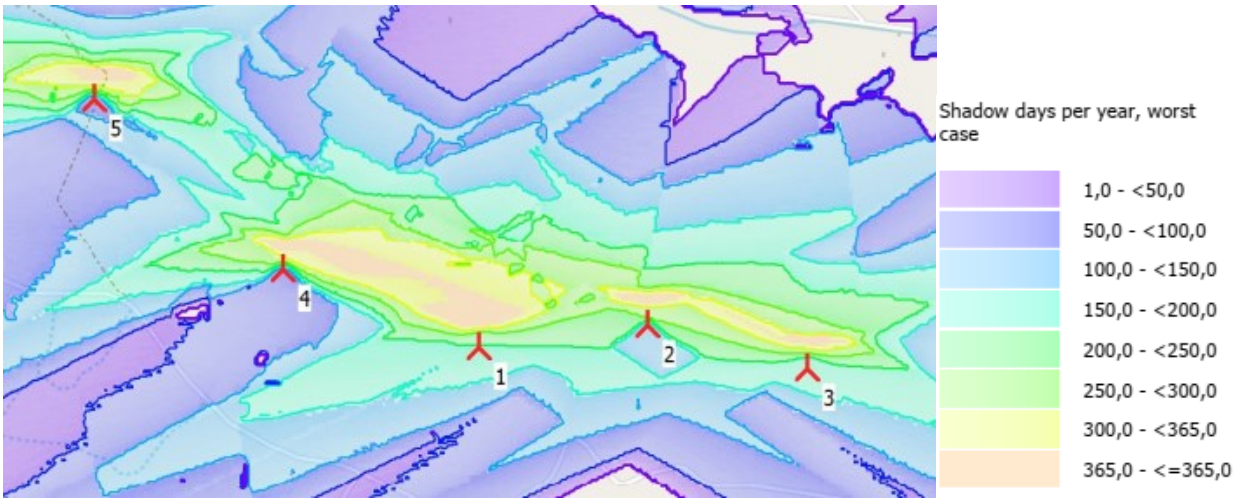

Figure 4.4. *Worst-case shadow days per year map at the Gravina in Puglia wind farm.*

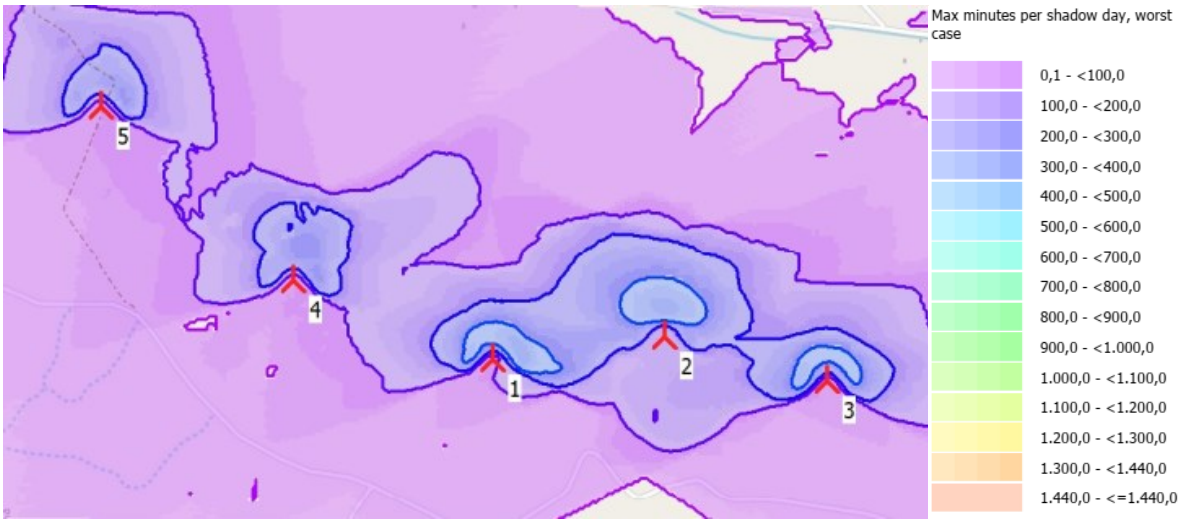

Figure 4.5. *Worst-case max shadow minutes per day map at the Gravina in Puglia wind farm.*

APPENDIX B contains the worst-case shadow flickering maps for only WTG04 and WTG05, the two nearest turbines to the PV plant location that cause more troubles. These maps show that areas near the WTGs are the most affected by the shadow flickering phenomena, so PV module strings in those positions are going to undergo power variations (voltage and current flickering), an outcome that influences the overall PV plant performance and stresses the MPPTs and inverters to which they are connected. From Figure 4.4, zones with shadow flickering occurrence throughout the year, so each day, can be seen in light blue.

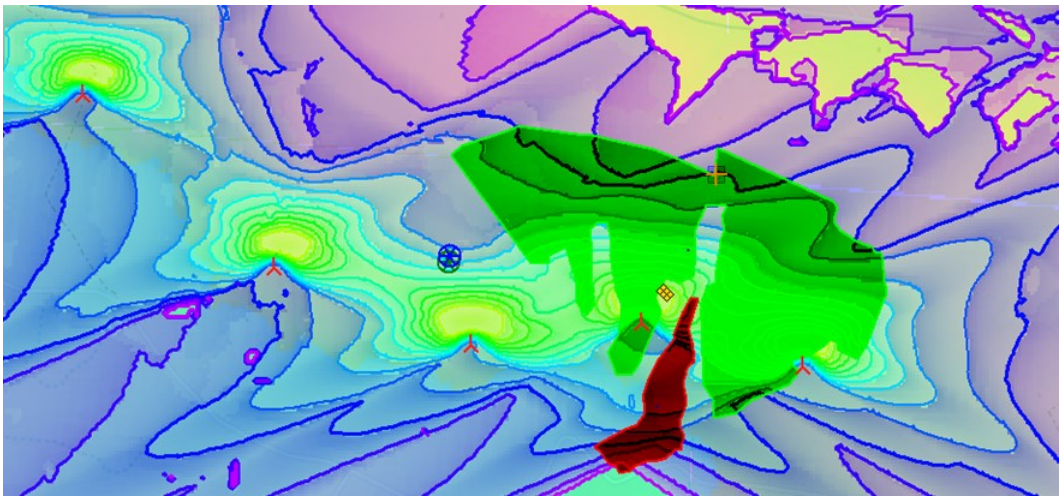

Figure 4.6. *Worst-case shadow hours per year map, with PV plant areas in red and dark green.*

To slightly reduce this problem, PV module strings must be installed at a certain distance outside the zones with the highest number of shadow hours per year (at least outside a semi-circular area with a 100 m radius towards North with the turbines as centres, distance measured manually by means of Google Earth software tool).

4.3 REAL-CASE SHADOW FLICKERING ANALYSIS

As written before, worst-case shadow flickering analysis is a very ideal situation and its results are extremely cautionary. Having a more precise and realistic study can give better information on possible effects of shadow flickering around wind turbines. Real-case analysis in windPRO performs it, starting from the location meteorological and wind statistics. Indeed, real-case assessment takes worst-case results and applies reduction factors on them, taking into account the probability of having clear sky conditions on that site (the sunshine duration, "eliofania" in Italian, i.e. the actual illumination duration without cloud covering in a given period of time, generally expressed in hours [32]) and the effective hours per year of aerogenerator operation (when wind intensity is higher than turbine cut-in speed). Specifically, three reduction factors are used [31]:

1) operation time reduction factor, calculated as the ratio between the total operational hours and the total number of hours in a year (8760 h). This factor is constant within the year and for all turbines.

2) Wind direction reduction factor, calculated for each receptor-turbine pair. It consists in the ratio between the area of the projected rotor disk onto a plane at a given direction and the full rotor disk. This ratio is therefore weighted by the frequency of operation at the given direction. If there are

several turbines that are casting their shadows simultaneously on a given receptor, a weighted average will be calculated between the wind direction reduction factor of each one.

The operational hours statistics, that is the number of hours that the WTG will be in operation in the different wind direction sectors during the year, is used to calculate both operational time and wind direction reduction factors. This statistical data is taken from the on-site measurements database nearest to Gravina in Puglia made available on-line by windPRO and EMD INTERNATIONAL.

3) Sun reduction factor, calculated for each month as the ratio between average daily Sun hours and mean total daily hours. Monthly sunshine probabilities are the percentages of daytime hours with Sun for every month, given as the ratio between actual Sun hours and possible Sun hours in a day or as the number of average sunshine hours per day. In this real case analysis, values are taken from internal windPRO databases (data from existing meteorological stations worldwide), in particular the average daily sunshine hours per month in Amendola (Foggia province, latitude = 41.53°, longitude = 15.72°) employed for Sun reduction factor calculations are depicted in the diagram below:

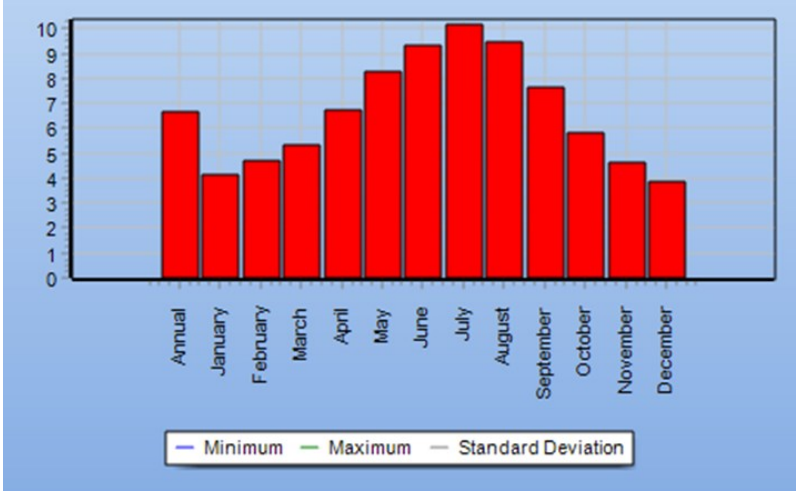

Figure 4.7. *Average daily sunshine hours per month in Amendola, 1969-1993. Source: windPRO.*

The number of shadow flickering hours per year, days per year and maximum minutes per day for real-case analysis is then calculated from the worst-case values by multiplying them by these three reduction factors. The next figures are the same maps seen in the worst-case conditions, but showing real-case situation results:

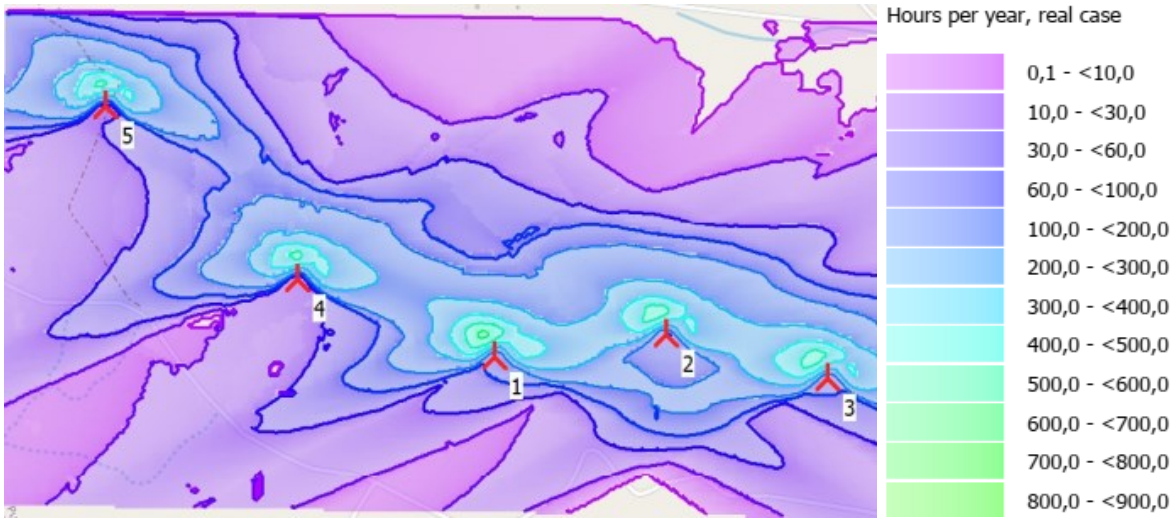

Figure 4.8. *Real-case shadow hours per year map at the Gravina in Puglia wind farm.*

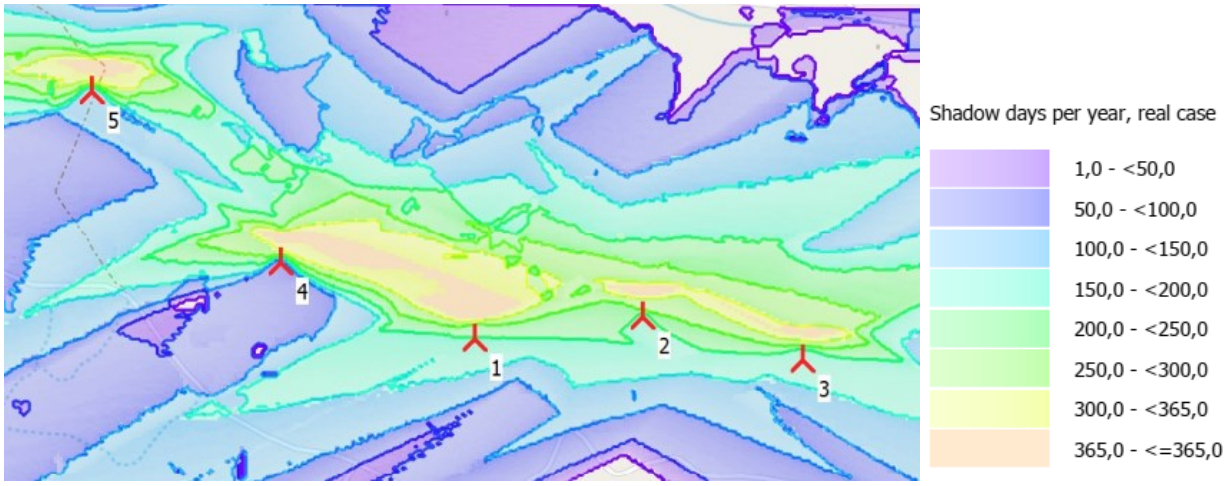

Figure 4.9. *Real-case shadow days per year map at the Gravina in Puglia wind farm.*

Figure 4.10. *Real-case max shadow minutes per day map at the Gravina in Puglia wind farm.*

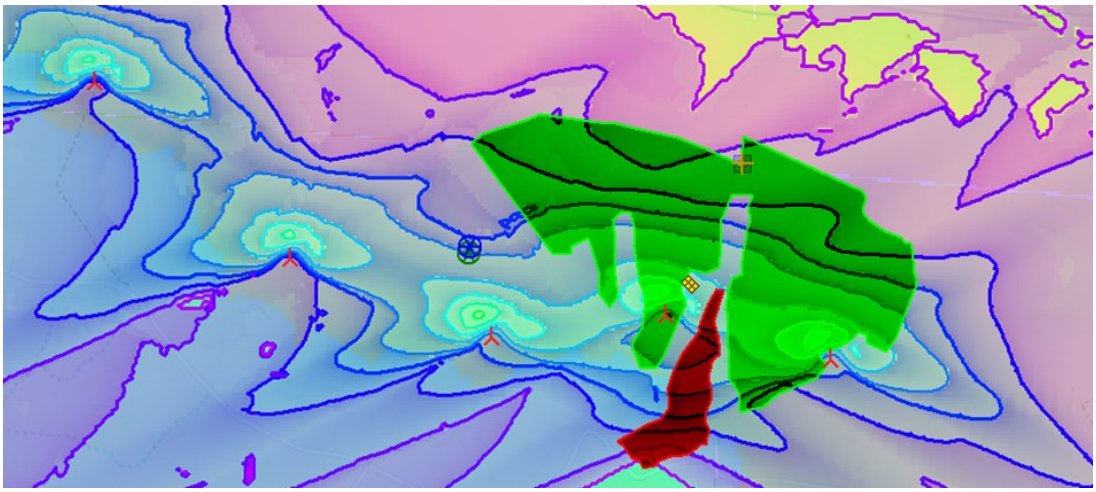

Figure 4.11. *Real-case shadow hours per year map, with PV plant areas in red and dark green.*

From real-case maps, the areas around wind turbines are more than 50% less affected by shadow flickering phenomena, making it easier to manage voltage, current and power output oscillations (flickers) from PV module strings into inverters. Also, the distance of the panels installation location from the aerogenerators can be lower than 100 m, thus increasing overall DC and AC PV plant production.

CHAPTER 5

PERFORMANCE OF A HYBRID PLANT PV ARRAY

To evaluate the PV array of a hybrid power plant AEP (Annual Energy Production), installed on the ground under the aerogenerators, it is fundamental to consider not only the power output losses due to mutual shading between modules of adjacent strings (even if back-tracking allows to reduce them as much as possible), but also losses due to wind turbine tower and rotor shadows. As described in Chapter 4, all areas around the aerogenerators are affected by shadow flickering related to blades rotation, thus the overall annual energy production will be lower than in the case without turbines.

The software utilized for the assessment of the PV plant performance were "PVSYST-GRID CONNECTED MODULE" and "windPRO-SOLAR PV MODULE". With the first software, yearly energy production is estimated without considering turbine blades in motion (they are kept still) but taking into account mutual and topographic shading; whereas the second, because of RAM limitations and a high computational burden, calculates annual energy yield regarding all components of wind turbine shadows (tower, nacelle, rotor and blades) and blades rotation effect on shadowing is considered too. Then, results will be updated based on different shadow power loss shares on energy generation.

5.1 PV ARRAY AEP WITH PVSYST

PVSYST is a software able to evaluate the AEP of a PV plant in a given site starting from certain irradiation data. The module used in this thesis is "Grid-connected PV". During the first step of the model construction, site position in geographical coordinates is defined (WTG04 coordinates, see Table 3.1), along with site meteorological data like monthly solar irradiation and local environmental temperature. Geographical location determines the path of the Sun over the year. Since meteorological data is the starting point of AEP evaluation, but on-site measurements were not available from STE ENERGY S.R.L., information was imported from an on-line open database: PVGIS-SARAH average values from 1st January 2005 to 31st December 2016. The most important data given by that database is monthly average global irradiation on a horizontal plane, monthly

average diffused irradiation on a horizontal plane and monthly average local environmental temperature, average values for years from 2005 to 2016.

Table 5.1. *Meteorological data for Gravina in Puglia from PVGIS-SARAH database.*

Month	Glob.Irr.Horiz.	Diff.Irr.Horiz.	Temp.
	kWh/m^2	kWh/m^2	°C
January	61	27.9	6.5
February	74.9	35.1	6.7
March	117.6	51.4	9.4
April	154.8	64.4	13
May	199.2	75.7	17.5
June	208.7	74.5	22.3
July	227.3	66.7	25.8
August	201.8	62.1	25.6
September	140.3	54.1	20.9
October	101.9	42.5	15.9
November	67.1	29.5	11.4
December	55.4	25	7.3
Year	1610	608.9	15.2

After these inputs, PVSYST gives as outputs also the solar diagrams or Sun paths. However, PVSYST simulation is not carried out with these monthly values, but by hourly steps over an entire year. Therefore it was necessary to artificially generate related hourly values of global irradiation, diffuse irradiation and temperature starting from the PVGIS-SARAH monthly values. PVSYST uses special algorithms to generate the hourly values. All these preliminary steps are performed inside "PVSYST-DATABASES MODULE": "geographical sites" tab for location definition, "known format" tab for data import from open sources and "synthetic data generation" tab for mean hourly values creation.

The PV array is composed by module strings having a North-South horizontal axis tracker, with West-East inclination angles between -60° and +60°. In regard to orientation, panels are all horizontal to the ground (0°) and their azimuth is towards South (0°). As previously written, back-tracking is present to reduce mutual shadowing. In fact, array layout should be carefully optimized against mutual shadings: a significant fraction of the yield may be lost by the effect of panel presence, even when the Sun is very low on the horizon. Today, the back-tracking strategy is widely employed for mitigating this phenomenon: when mutual shading begins, the tracking angle does not follow the Sun anymore, but it changes so that shadowing does not occur. This is possible because of a control system. Since PV array modules are installed three metres above a generally grassy ground, an albedo equal to 20% was considered. From historical temperature measurements in the PVGIS tool of the European Union's joint-research-centre, the minimum location environmental

temperature was set to -5°C, which is important for defining the number of modules per string connected to the inverter input and the upper constraint for the open-circuit voltage Voc. Regarding other temperatures, default values were kept: Winter operational temperature for maximum Vmpp equal to 20°C, Summer operational temperature for minimum Vmpp equal to 60°C, usual operational temperature under STC irradiance equal to 50°C. For modelling daylight availability and irradiance components, the default Perez-Ineichen transposition model was set. The PV module chosen is TRINASOLAR VERTEX 670 Wp, while the inverter is SUNGROW SG350HX; see APPENDIX A for their datasheets. PV module vertical spacing in the same string is 20 cm and distance between N-S horizontal contiguous trackers is 6 m. Height from the ground of the horizontal South facing portrait layout PV modules is 3 m again. Portrait panel orientation means that its long side (2.384 m) is vertical, while its short side (1.303 m) is horizontal. Because the minimum site temperature set was -5°C, the number of series connected modules forming a string was 29, since the maximum inverter PV input voltage is 1500 V and total string Voc voltage at -5°C temperature is 1450 V; in reality, using equation (2.30), single-module open circuit voltage at lowest temperature Voc(-5°C) is 49.56 V, while single-string value is equal to 1437 V ($29 \cdot 49.56\ V = 1437\ V$). With 29 modules in series there are not problems even at -10°C too, since single-module Voc(-10°C) is 50.13 V and Voc_string(-10°C) is 1454 V ($29 \cdot 50.13\ V = 1454\ V$), lower than the 1500 V inverter input upper limit, thus allowing for a safe behaviour also in case of colder Winter periods.

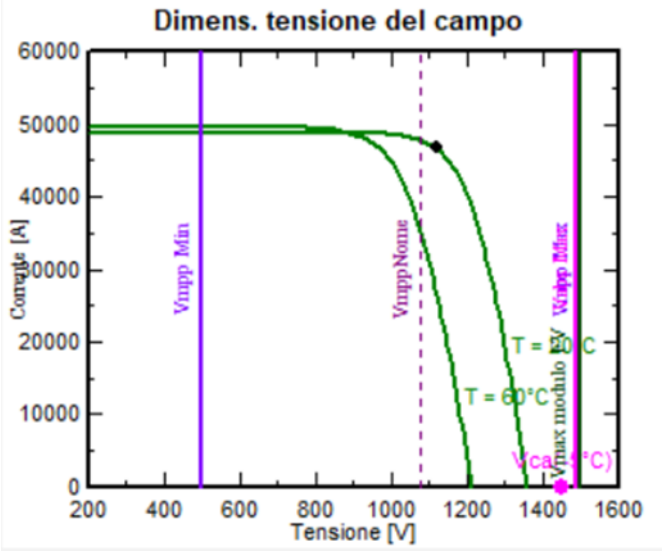

Figure 5.1. *Sizing voltages and currents of the PV plant. Source: PVSYST.*

Maximum and minimum Vmpp values of the string are inside the inverter MPPT voltage range (500 V ÷ 1500 V): Vmpp(20°C) is equal to 1119 V and Vmpp(60°C) to 967 V. Impp in STC of a string is 17.39 A, while at 60°C with the same global irradiance it is 17.63 A, which is lower than

the maximum PV input current for a single MPPT (40 A). Thus, for each MPPT the limit number of strings connected in parallel is two. The estimated total number of strings, that is 2639, was obtained during "near shadings" 3D model construction: it is the number of strings resulting from PVSYST calculations starting from all the PV array physical features described before. In total there are 76'531 modules. The number of inverters is 125. The PV plant DC nominal power at STC is 51.276 MW, while at 1 kW/m^2 irradiance and 50°C operating temperature it is 47.052 MW; the PV plant AC nominal power at STC is 40 MW and therefore the DC/AC nominal ratio is 1.282. The overload loss of inverters is equal to 0.3%.

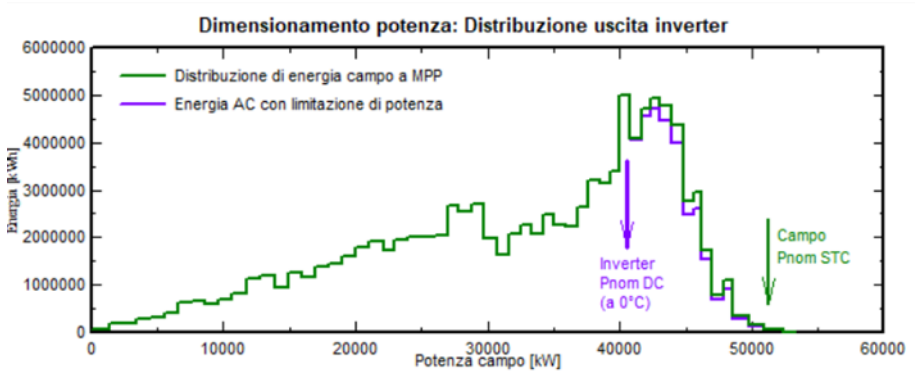

Figure 5.2. *DC and AC energy distribution with PV plant output power. Source: PVSYST.*

The near shadings 3D scene was built by using an orthophoto of the Gravina in Puglia site taken from Google Earth software and the digital terrain model (DTM) of that location, while the PV plant borderlines were drawn on DTM following the picture. Afterwards a construction input in that zone was given to PVSYST: the software, as previously explained, gave 2639 strings.

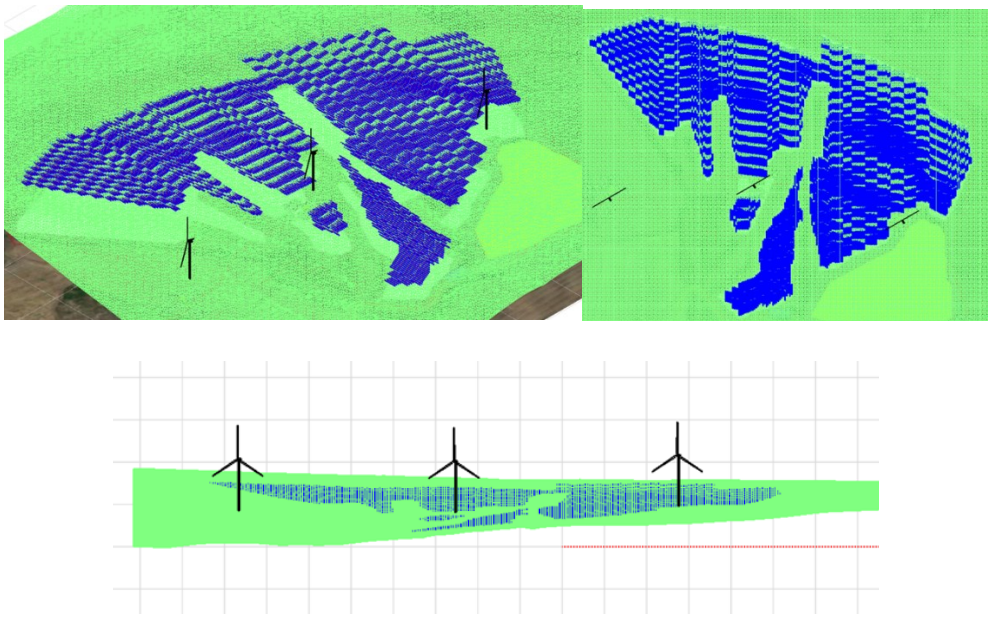

Figure 5.3. *Near shadings 3D scene from different views. Source: PVSYST.*

In the end, the aerogenerators 3D objects were created and placed in the right position and orientation. Since rotating blade shadow losses are not accounted for in PVSYST, just the aerogenerators nearest to the PV plant were considered: WTG03, WTG04 and WTG05 (see Table 3.1 for geographical coordinates). They are directed towards North-North-West (see wind roses in Figure 6.4).

After the 3D model construction for the near shadings estimate, PVSYST computes the shading factors (shaded fraction of the sensitive area, 0 if not shaded, 1 if fully shaded), for all positions on the sky hemisphere "seen" by the PV plane. They allow the calculation of the shading factor for both diffused and albedo radiation components. For each hourly value, the simulation process will interpolate this table according to the position of Sun to evaluate the effective shading factor of the direct component [33, page 25].

Table 5.2. *Shading factor table. Source: PVSYST.*

Tabella fattore d'ombra (lineare), per la componente diretta, Orient. #1

Azimut / Altezza	-180°	-160°	-140°	-120°	-100°	-80°	-60°	-40°	-20°	0°	20°	40°	60°	80°	100°	120°	140°	160°	180°
90°	0.000	0.000	0.000	0.000	0.000	0.000	0.000	0.000	0.000	0.000	0.000	0.000	0.000	0.000	0.000	0.000	0.000	0.000	0.000
80°	0.005	0.004	0.001	0.000	0.000	0.000	0.000	0.000	0.000	0.000	0.000	0.000	0.000	0.000	0.000	0.000	0.001	0.004	0.005
70°	0.023	0.016	0.008	0.002	0.000	0.000	0.000	0.001	0.001	0.001	0.000	0.000	0.000	0.000	0.000	0.002	0.007	0.016	0.023
60°	0.043	0.025	0.009	0.002	0.001	0.001	0.001	0.001	0.002	0.001	0.001	0.000	0.000	0.000	0.000	0.002	0.009	0.024	0.043
50°	0.068	0.029	0.007	0.006	0.006	0.003	0.001	0.002	0.002	0.002	0.002	0.001	0.000	0.001	0.002	0.003	0.006	0.028	0.068
40°	0.101	0.025	0.018	0.032	0.026	0.015	0.007	0.002	0.003	0.003	0.003	0.001	0.003	0.009	0.015	0.020	0.011	0.026	0.101
30°	0.151	0.020	0.076	0.085	0.073	0.051	0.027	0.008	0.005	0.005	0.004	0.004	0.019	0.037	0.051	0.065	0.058	0.018	0.151
20°	0.248	0.107	0.199	0.254	0.213	0.172	0.134	0.038	0.007	0.007	0.006	0.025	0.077	0.101	0.127	0.167	0.152	0.083	0.248
10°	0.519	0.499	0.525	0.460	0.375	0.294	0.231	0.159	0.033	0.013	0.023	0.083	0.117	0.152	0.198	0.273	0.361	0.405	0.519
2°	0.028	0.233	0.346	0.374	0.451	0.462	0.323	0.268	0.166	0.009	0.067	0.081	0.134	0.211	0.296	0.478	0.395	0.223	0.028

Fattore d'ombra per il diffuso: 0.088 e per l'albedo: 0.372

This also enables the building of the iso-shading graphs, which give a synthetic view of when and where the shadowing is particularly problematic [33, page 25]. For the iso-shading graphs and the other detailed losses considered inside PVSYST PV array project see APPENDIX C (some data like solar cables and other connections size were not available, so default values were adopted).

For extra context, and to see what the maximum shading effect produced by rotating blades could be in PVSYST, also an extreme 3D near shadings case was built. In this scene, blades were considered to be so fast in their rotation that in their place circular solid areas were located instead, with the same N-N-W orientation where wind has the highest frequency and intensity; radius is always 79 m. Furthermore, tubular steel towers were designed by using a cylinder with 4.3 m diameter and 120.9 m height. These composed objects substituted the previously created models of wind turbines WTG03, WTG04 and WTG05, at the same positions given by table 3.1.

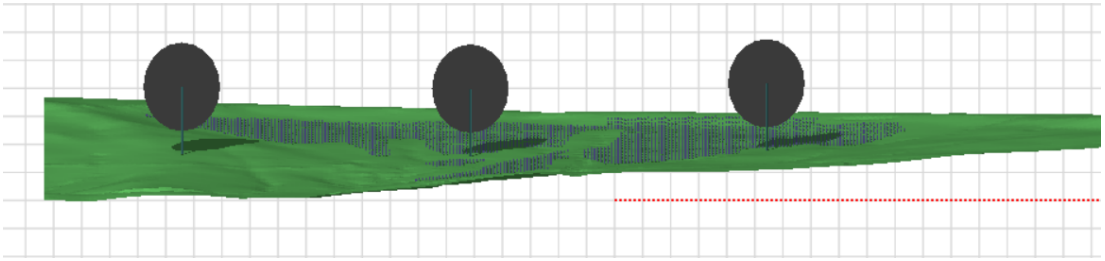

Figure 5.4. *Near shadings 3D construction of extreme case. Source: PVSYST.*

Table 5.3. *Shading factor table of extreme case. Source: PVSYST.*

Tabella fattore d'ombra (lineare), per la componente diretta, Orient. #1

Azimut / Altezza	-180°	-160°	-140°	-120°	-100°	-80°	-60°	-40°	-20°	0°	20°	40°	60°	80°	100°	120°	140°	160°	180°
90°	0.000	0.000	0.000	0.000	0.000	0.000	0.000	0.000	0.000	0.000	0.000	0.000	0.000	0.000	0.000	0.000	0.000	0.000	0.000
80°	0.008	0.005	0.002	0.000	0.000	0.001	0.002	0.002	0.002	0.001	0.000	0.000	0.000	0.000	0.000	0.001	0.003	0.006	0.008
70°	0.029	0.021	0.010	0.002	0.002	0.004	0.009	0.012	0.013	0.011	0.005	0.001	0.000	0.000	0.001	0.004	0.012	0.021	0.029
60°	0.052	0.033	0.013	0.002	0.004	0.010	0.018	0.023	0.026	0.023	0.014	0.004	0.000	0.001	0.001	0.005	0.013	0.031	0.052
50°	0.076	0.040	0.012	0.006	0.013	0.019	0.028	0.034	0.039	0.038	0.025	0.008	0.000	0.004	0.005	0.010	0.016	0.036	0.076
40°	0.108	0.034	0.023	0.032	0.038	0.040	0.045	0.050	0.055	0.056	0.040	0.014	0.002	0.014	0.023	0.034	0.031	0.044	0.108
30°	0.171	0.025	0.078	0.085	0.087	0.084	0.080	0.077	0.075	0.080	0.058	0.025	0.019	0.047	0.071	0.093	0.085	0.055	0.171
20°	0.273	0.108	0.199	0.198	0.173	0.152	0.140	0.134	0.118	0.118	0.096	0.059	0.057	0.101	0.150	0.183	0.174	0.120	0.273
10°	0.519	0.500	0.479	0.415	0.330	0.256	0.271	0.291	0.211	0.172	0.144	0.124	0.097	0.183	0.253	0.281	0.323	0.406	0.519
2°	0.028	0.202	0.314	0.341	0.417	0.430	0.358	0.349	0.215	0.087	0.111	0.098	0.121	0.228	0.271	0.445	0.358	0.199	0.028

Fattore d'ombra per il diffuso: 0.063 e per l'albedo: 0.250

Regarding all the other PV plant features, such as the type of module and inverter, the number of panels, strings and inverters, detailed losses, yearly environmental conditions (total irradiation and temperature), N-S horizontal axis tracking, backtracking and albedo, these were kept the same as the original case. PVSYST simulation results for both cases are available in APPENDIX C.

5.1.1 PVSYST RESULTS

- **PVSYST 3D MODEL WITH THREE-BLADED AEROGENERATORS**

Total DC power = 51.276 MWp

Total AC power = 40 MWac

DC/AC power ratio = 1.282

Annual DC nominal energy production (before losses) = 102’806 MWh/year

Annual AC energy production exported to the grid = 92’648 MWh/year

Energy loss = Annual DC energy production - Annual AC energy production = 10'158 MWh/year

Specific DC energy production per module = 1’807 kWh/kWp/year

Average annual Performance Ratio PR = 84.80 %

Yearly global irradiation → $H_{PVSYST} = \frac{\left(1\frac{kW}{m^2}\cdot 92648000\frac{kWh}{yr}\right)}{51276\ kWp\cdot 0.848} = 2'130.718\frac{kWh}{m^2\cdot yr}$

DETAILED LOSSES

Mutual panel shading loss was obtained by making the same simulation in PVSYST, but with a 3D near shadings model without turbines, with just PV modules and DTM (see APPENDIX C). Therefore, the shading loss due to the aerogenerators was calculated by subtracting the mutual panel shading loss (4.89 %) to the total near shading loss (5.04 %) taken from the PVSYST simulation reports, obtaining the estimated turbines shading loss (0.15%).

Total near shading loss = 5.04 %

Mutual panel shading loss = 4.89 %

Turbines shading loss = 5.04 % - 4.89 % = 0.15 %

Losses due to IAM (incidence angle modifier) = 0.23 %

Soiling loss factor = 1.00 %

PV loss due to temperature = 4.10 %

LID - Light induced PV performance degradation = 2.00 %

Mismatch loss (modules and strings) = 2.10 %

Ohmic DC wiring loss = 1.03 %

Inverter Loss during operation = 1.39 %

Inverter Loss over nominal inv. Power = 0.05 %

AC ohmic wiring loss = 0.62 %

Sum of all considered losses = 17.56 % (12.67 % without mutual panel shading)

- **PVSYST EXTREME CASE 3D MODEL**

Total DC power = 51.276 MWp

Total AC power = 40 MWac

DC/AC power ratio = 1.282

Annual DC nominal energy production (before losses) = 100’985 MWh/year

Annual AC energy production exported to the grid = 91’110 MWh/year

Energy loss = Annual DC energy production - Annual AC energy production = 9’875 MWh/year

Specific DC energy production per module = 1’777 kWh/kWp/year

Average annual Performance Ratio PR = 83.39 %

Yearly global irradiation → $H_{PVSYST} = \frac{\left(1\frac{kW}{m^2}\cdot 91110000\frac{kWh}{yr}\right)}{51276\ kWp\cdot 0.8339} = 2'130.777\ \frac{kWh}{m^2\cdot yr}$

DETAILED LOSSES

The shading loss due to the aerogenerators was calculated by subtracting the same mutual panel shading loss (4.89 %) to the total near shading loss (6.73 %) taken from the extreme case PVSYST simulation report, obtaining the estimated turbines shading loss (1.84%). The latter is the maximum shading loss by wind turbine obtainable in PVSYST.

Total near shading loss = 6.73 %

Mutual panel shading loss = 4.89 %

Turbines shading loss = 6.73 % - 4.89 % = 1.84 %

Losses due to IAM = 0.22 %

Soiling loss factor = 1.00 %

PV loss due to temperature = 4.03 %

LID - Light induced PV performance degradation = 2.00 %

Mismatch loss (modules and strings) = 2.10 %

Ohmic DC wiring loss = 1.02 %

Inverter Loss during operation = 1.39 %

Inverter Loss over nominal inv. Power = 0.03 %

AC ohmic wiring loss = 0.61 %

Sum of all considered losses = 19.13 % (14.24 % without mutual panel shading)

It must be remembered that a PVSYST problem is that aerogenerator rotors are kept stationary over time during the simulation, so rotor shading is evaluated with stationary blades. Since PVSYST is not able to consider blade rotation in shading analysis, the annual energy production analysis AEP was executed also with another software able to consider blade rotation shading too. This software is windPRO (SOLAR PV MODULE). The main problem related to windPRO usage is the very huge computational burden related to the PV plant AEP simulation, which is stressful even for a personal computer with 8 Gb of RAM. This is the reason why the windPRO AEP evaluation was made considering only the turbine tower and rotor shadows.

5.2 PV ARRAY AEP WITH WINDPRO SOLAR PV MODULE

The "windPRO-SOLAR PV MODULE" allows users to design wind parks and photovoltaic plants, computing their energy yields [34, page 3].
Before designing the hybrid power plant and performing AEP evaluation, it was fundamental to define the background maps of the Gravina in Puglia site, the elevation data by height contour lines (or elevation grid data), the meteorological data like solar irradiation components and local environmental temperature (with meteo object tool). All necessary maps and elevation data were given by STE ENERGY S.R.L. colleagues, while meteorological data was downloaded from online open-source databases. Because of difficulties in carrying out calculations with a laptop having 8 Gb of RAM, the ERA5 (Gaussian grid) database for irradiance and environmental temperature was considered, since it contains hourly measurements (not half-hourly data like Heliosat-SARAH), reducing in this way the overall calculation burden. For meteorological data, only the year 2021 (from 1st January 2021 to 1st January 2022) was considered, with the purpose of decreasing laptop performance problems again. Year 2021 global irradiance and environmental temperature, both measured by technical instruments at 2 m height from ground, are displayed in the following charts.

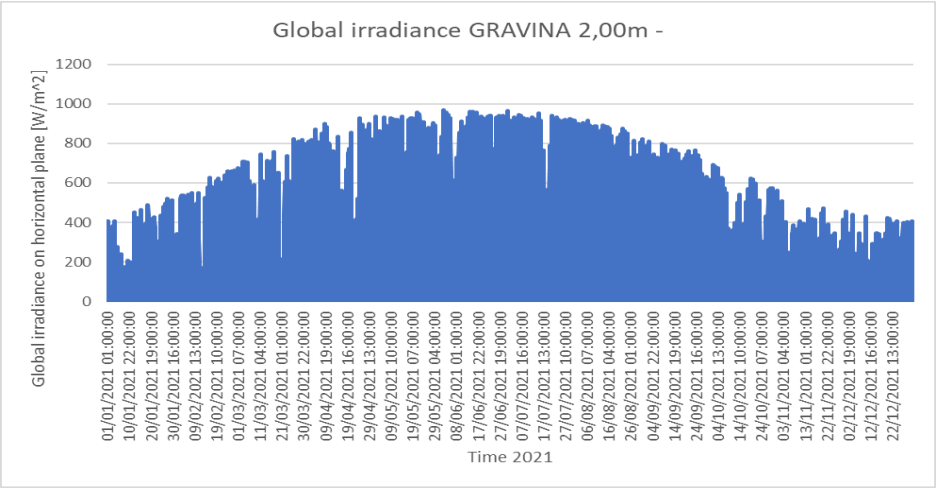

Figure 5.5. *Global irradiance on Gravina in Puglia during 2021. Source: ERA5 (Gaussian grid).*

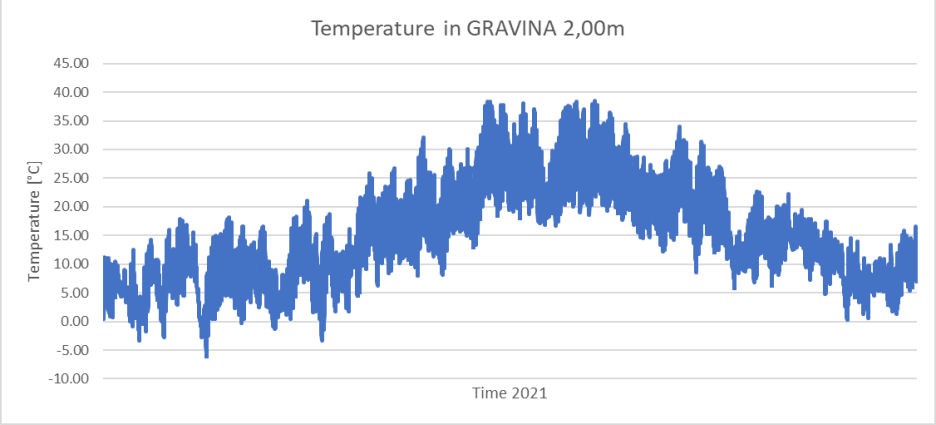

Figure 5.6. *Environmental temperature at Gravina in Puglia during 2021. Source: ERA5 (Gaussian grid).*

ERA5 (Gaussian grid) was also preferred to ERA5-T database since meteorological stations of the first one are closer than the second one to Gravina in Puglia location. For the calculation of diffused radiation component, the default Erbs model was employed, whereas for transferring irradiation values from the horizontal to the inclined plane the default Perez model was considered.

The PV plant design step required the creation of a solar PV object. To generate the PV plant borderlines, QGIS software was used along with Google Earth. In fact, polyline shape-files representing two separated parts of the overall plant were drawn “by hand” on QGIS interface following the orthophoto of Gravina in Puglia possible plant area (see Figure 3.2 and 3.3). Then, these two shape-files were imported into windPRO, making the definition of boundaries for the PV plant design easier. The total area available for the PV plant is 66.6 ha. Afterwards, all module and inverter characteristics were inputted into solar PV object. Also, in this assessment the vertical spacing between panels in the same string is 20 cm, the distance between N-S horizontal contiguous trackers is 6 m and the height from ground of the horizontal South facing portrait layout bifacial

modules is 3 m. The horizontal trackers tilt angle limits are -60° and 60° again; back-tracking was taken into account too. Albedo was 20 % (grass terrain). For the inverter: 0.85 AC/DC power ratio (for bifacial panels it should be between 0.8 and 0.9) [34, page 7], 320 kWac size. Since the AEP calculation related to the overall PV plant area and the total number of modules was not possible because of a very large amount of time required for calculation and the lack of enough laptop RAM, the PV plant surface was divided into three zones:

1) area around WTG04, considering shadows of all wind turbines;

2) area around WTG05, considering shadows of all wind turbines;

3) remaining area without any wind turbine shadows.

Losses considered in the plant (values given by STE ENERGY S.R.L. colleagues) can be divided into two groups:

BEFORE INVERTER

DC wiring (% at max power) 1.5 %, degradation per year 2 %, soiling 1 %, constant loss (mismatch etc.) 2.1 %, other 0 %.

AFTER INVERTER

Availability 1 %, substation 0 %, grid external 0.9 %, grid curtailment 0 %.

Shading losses considered for AEP calculations were just related to WTG tower-nacelle and WTG rotor, to reduce in this way the computational load, thus obtaining faster results (not topography shading, panel mutual shading and other obstacles). Reduced rotor area and bifacial reduction factor default values were used, 50 % (rotor area can be reduced in the calculation to compensate for the rotor disk not being a solid structure [34, page 48]) and 0.75 respectively.

To decrease the computational burden again, chosen calculation resolution for shading cover were month (date) and ten minutes (time). In this way calculations per panel are only 864 and RAM capacity is sufficient. It is important to remember that, in the results, gross includes the reduction due to incidence angle modifier, loss percentages are all related to gross production (shading losses per area, % of gross), performance ratio is calculated net (except after inverter loss) relative to the irradiance on the inclined plane multiplied by the panel efficiency at STC. After running windPRO-SOLAR PV MODULE for each of these three cases, the global plant results are obtained by summing the results of every single zone and computing average values. APPENDIX D contains more information about the three windPRO cases results.

5.2.1 AREA AROUND WTG04: RESULTS

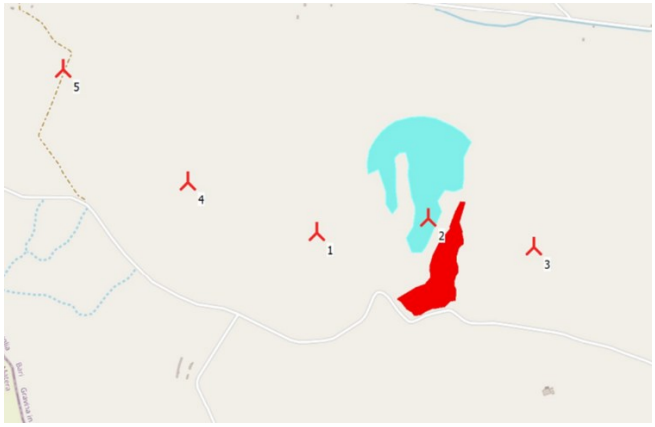

Figure 5.7. *Area around WTG04 for AEP evaluation.*

Design area = 22.72 ha

Number of PV panels = 24’718

Number of inverters = 45

Rated DC power = 16'561.1 kWp

Rated AC power = 14'400 kW

Average rated power AC/DC ratio = 0.87

Average rated power DC/AC ratio = 1.15

- **FIRST OPERATION YEAR LOSSES**

WTGs tower-nacelle shading loss = 0.32 %

WTGs rotor shading loss = 1.03 %

Combined WTGs shading energy loss = 1.26 %

Actual WTGs tower-nacelle shading loss is lower than 0.32 % since blades cover, during their rotation, part of tower and nacelle shadows over time. This is the reason why, in the combined WTGs shading energy loss, total loss is lower than the effective sum (1.35 %). WTGs tower-nacelle shading loss considered by windPRO is $1.26\ \% - 1.03\ \% = 0.23\ \%$.

Before inverter loss = 5.92 %

Inverter clipping loss = 0.53 %

Inverter DC/AC conversion loss = 1.18 %

After inverter loss = 1.72 %

All loss (sum of all losses from PV to grid) = 1.26% + 5.92% + 0.53% + 1.18% + 1.72% = 10.61 %

- **FIRST OPERATION YEAR PRODUCTION**

Performance ratio, yearly average PR = 79.3 %

Gross DC energy production = 36'287.8 MWh/yr

PV plant energy losses = 0.1061 · 36'287.8 MWh/yr = 3’850.13 MWh/yr

Net AC energy exported to the grid = 36'287.8 MWh/yr · (1-0.1061) = 32'437.66 MWh/yr

Capacity factor = 25.7 % → 2’251 h/yr

5.2.2 AREA AROUND WTG05: RESULTS

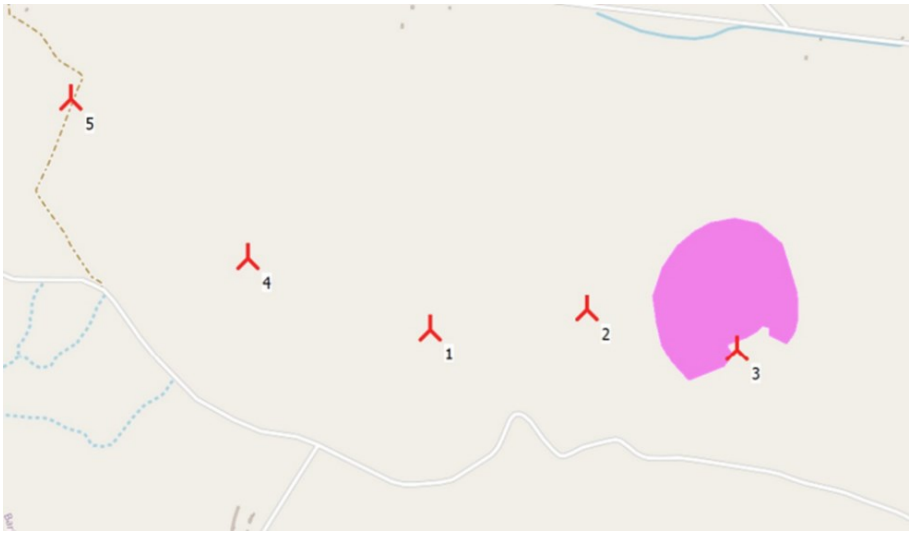

Figure 5.8. *Area around WTG05 for AEP evaluation.*

Design area = 18.49 ha

Number of PV panels = 20’342

Number of inverters = 37

Rated DC power = 13'629.1 kWp

Rated AC power = 11'840 kW

Average rated power AC/DC ratio = 0.87

Average rated power DC/AC ratio = 1.151

- **FIRST OPERATION YEAR LOSSES**

WTGs tower-nacelle shading loss = 0.30 %

WTGs rotors shading loss = 1.68 %

Combined WTGs shading energy loss = 1.82 %

Actual WTGs tower-nacelles shading loss is lower than 0.30 % since blades cover during their rotation part of tower and nacelle shadows over time. This is the reason why, in the combined WTGs shading energy loss, total loss is lower than the effective sum (1.98 %). WTGs tower-nacelle shading loss considered by windPRO is $1.82\ \% - 1.68\ \% = 0.14\ \%$.

Before inverter loss = 5.89 %

Inverter clipping loss = 0.49 %

Inverter DC/AC conversion loss = 1.17 %

After inverter loss = 1.71 %

All loss (sum of all losses from PV to grid) = 1.82% + 5.89% + 0.49% + 1.17% + 1.71% = 11.08 %

- **FIRST OPERATION YEAR PRODUCTION**

Performance ratio, yearly average PR = 78.7 %

Gross DC energy production = 30'027.3 MWh/yr

PV plant energy losses = 0.1108 · 30'027.3 MWh/yr = 3’327.025 MWh/yr

Net AC energy exported to the grid = 30'027.3 MWh/yr · (1-0.1108) = 26’700.27 MWh/yr

Capacity factor = 25.7 % → 2251 h/yr

5.2.3 REMAINING AREA: RESULTS

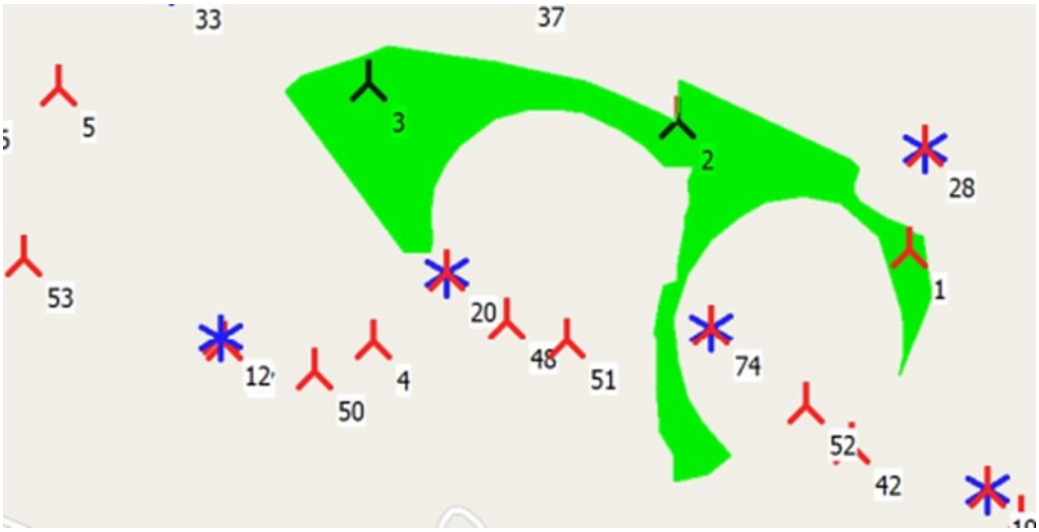

Figure 5.9. *Remaining area for AEP evaluation, without WTG shadows.*

Design area = 25.45 ha

Number of PV panels = 27’649

Number of inverters = 50

Rated DC power = 18'524.8 kWp

Rated AC power = 16’000 kW

Average rated power AC/DC ratio = 0.86

Average rated power DC/AC ratio = 1.1578

- **FIRST OPERATION YEAR LOSSES**

WTG tower-nacelle shading loss = 0 %

WTG rotors shading loss = 0 %

Before inverter loss = 5.88 %

Inverter clipping loss = 0.75 %

Inverter DC/AC conversion loss = 1.19 %

After inverter loss = 1.74 %

All loss (sum of all losses from PV to grid) = 5.88% + 0.75% + 1.19% + 1.74% = 9.56 %

- **FIRST OPERATION YEAR PRODUCTION**

Performance ratio, yearly average PR = 80.3 %

Gross DC energy production = 41'228.7 MWh/yr

PV plant energy losses = 0.0956 · 41'228.7 MWh/yr = 3'941.464 MWh/yr

Net AC energy exported to the grid = 41'228.7 MWh/yr · (1-0.0956) = 37'287.236 MWh/yr

Capacity factor = 26.6 % → 2330 h/yr

5.2.4 TOTAL PV PLANT AEP IN WINDPRO

Total design area = 22.72 ha + 18.49 ha + 25.45 ha = 66.66 ha

Total number of PV panels = 24'718 + 20'342 + 27’649 = 72’709

Total number of inverters = 45 + 37 + 50 = 132

Total rated DC power = 16'561.1 kWp + 13'629.1 kWp + 18'524.8 kWp = 48’715 kWp

Total rated AC power = 14'400 kW + 11'840 kW + 16'000 kW = 42’240 kW

Average rated power AC/DC ratio = 0.867

Average rated power DC/AC ratio = 1.153

- **FIRST OPERATION YEAR LOSSES**

Average WTGs tower-nacelle shading loss = (0.31% + 0.3%)/2 = 0.305 %

Average effective WTGs tower-nacelle shading loss = 0.23 % + 0.14 % = 0.185 %

Average WTGs rotor shading loss = (1.03% + 1.68%)/2 = 1.355 %

Total WTG shading loss = 0.305 % + 1.355 % = 1.66 % < 1.84 %

Total combined WTG shading loss = 0.185 % + 1.355 % = 1.54 % < 1.84 %

Since upper limit for wind turbines shading loss is 1.84 %, from the value obtained in the extreme case PVSYST simulation (see page 61), the average value of 1.54 % for the total WTG combined shading loss is correct.

Following losses are obtained from windPRO performance simulation of total PV plant area without shadings:

Before inverter loss = 5.94 % (average value of the three cases before 5.897 %)

Inverter clipping loss = 0.85 % (average value of the three cases before 0.547 %)

Inverter DC/AC conversion loss = 1.19 % (average value of the three cases before 1.18 %)

After inverter loss = 1.74 % (average value of the three cases before 1.725 %)

Total loss (all losses from PV to grid) = 1.54% + 5.94% + 0.85% + 1.19% + 1.74% = 11.26 %

- **FIRST OPERATION YEAR TOTAL PRODUCTION**

Total gross DC energy production = 107'543.8 MWh/yr

Total PV plant energy losses = 0.1126 · 107’543.8 MWh/yr = 12'109.432 MWh/yr

Total net AC energy exported to the grid = 107'543.8 MWh/yr · (1-0.1126) = 95'434.368 MWh/yr

- **PERFORMANCE RATIO CALCULATION**

$$PR = \frac{(STC\ irradiance)\cdot Eac}{(DC\ power)\cdot H}\text{, performance ratio} \quad (5.1)$$

$$H = \frac{(STC\ irradiance)\cdot Eac}{(DC\ power)\cdot PR}\text{, yearly global irradiation} \quad (5.2)$$

$$H_{WTG04} = \frac{\left(1\frac{kW}{m^2}\cdot 32'437'660\ \frac{kWh}{yr}\right)}{16'561.1\ kWp\cdot 0.793} = 2'469.944\frac{kWh}{m^2\cdot yr}$$

$$H_{WTG05} = \frac{\left(1\frac{kW}{m^2}\cdot\ 26'700'270\ \frac{kWh}{yr}\right)}{13'629.1\ kWp\cdot 0.787} = 2'489.28\frac{kWh}{m^2\cdot yr}$$

$$H_{remaining} = \frac{\left(1\frac{kW}{m^2}\cdot 37'287'236\ \ \frac{kWh}{yr}\right)}{18'524.8\ kWp\cdot 0.803} = 2'506.635\frac{kWh}{m^2\cdot yr}$$

$$H_{mean} = \frac{2'469.944\frac{kWh}{m^2\cdot yr} + 2'489.28\frac{kWh}{m^2\cdot yr} + 2'506.635\frac{kWh}{m^2\cdot yr}}{3} = 2'488.62\frac{kWh}{m^2\cdot yr}$$

$$PR_{tot} = \frac{\left(1\frac{kW}{m^2}\cdot 95'434'368\ \frac{kWh}{yr}\right)}{48'715\ kWp\cdot 2'488.62\frac{kWh}{m^2\cdot yr}} = 0.7872 = 78.72\ \%$$

5.3 POSSIBLE PV PLANT AEP WITH WINDPRO AND PVSYST: RESULTS

Now the previous results obtained with PVSYST (from the first case, not the extreme one) and windPRO will be used to obtain better values of shading losses, considering WTG tower-nacelle, WTG rotor and mutual panel shadings. In this way, better results could be gained since the outcomes from a single software do not consider all type of possible shadow losses.

- **SHADING LOSSES**

Average combined WTGs rotors + towers-nacelle shading loss = 1.54 % → datum from windPRO

Mutual panels shading loss = 4.89 % → datum from PVSYST

Total shading losses due to WTGs + panels = 1.54 % + 4.89 % = 6.43 %

5.3.1 WINDPRO PV PLANT AEP WITH NEW TOTAL SHADING LOSSES

Shading loss difference = 6.43 % - 1.54 % = 4.89 %

Indeed, mutual panel shading loss 4.89% is not considered into windPRO AEP evaluation.

- **FIRST OPERATION YEAR LOSSES**

Total shading loss (WTGs + panels) = 6.43 %

Before inverter loss = 5.94 %

Inverter clipping loss = 0.85 %

Inverter DC/AC conversion loss = 1.19 %

After inverter loss = 1.74 %

All loss (sum of all losses from PV to grid) = 6.43% + 5.94% + 0.85% + 1.19% + 1.74% = 16.15 %

- **FIRST OPERATION YEAR NEW TOTAL PRODUCTION**

Gross DC energy production = 107'543.8 MWh/yr

PV plant energy losses = 0.1615 · 107'543.8 MWh/yr = 17'368.324 MWh/yr

Net AC energy exported to the grid = 107'543.8 MWh/yr · (1-0.1615) = 90'175.476 MWh/yr

$$PR_{tot} = \frac{\left(1\frac{kW}{m^2} \cdot 90'175'476\frac{kWh}{yr}\right)}{48'715\ kWp \cdot 2'488.62\frac{kWh}{m^2 \cdot yr}} = 0.7438 = 74.38\ \%$$

5.3.2 PVSYST PV PLANT AEP WITH NEW TOTAL SHADING LOSSES

Shading loss difference = 6.43 % - 5.04 % = 1.54 % - 0.15 % = 1.39 %

The share 1.39% is the shading loss increase due to the blades rotation.

- **FIRST OPERATION YEAR LOSSES**

Total shading loss (WTGs + panels) = 6.43 %

Losses due to IAM = 0.23 %

Soiling loss factor = 1.00 %

PV loss due to temperature = 4.10 %

LID - Light induced PV performance degradation = 2.00 %

Mismatch loss (modules and strings) = 2.10 %

Ohmic DC wiring loss = 1.03 %

Inverter Loss during operation = 1.39 %

Inverter Loss over nominal inv. Power = 0.05 %

AC ohmic wiring loss = 0.62 %

All loss (sum of all losses from PV array to grid) = 18.95 %

- **FIRST OPERATION YEAR TOTAL PRODUCTION**

Annual DC energy production (before losses) = 102’806 MWh/year

Total annual AC energy produced = 92’648 MWh/year · (1-0.0139) = 91’360.193 MWh/year

$$PR_{PVSYST} = \frac{\left(1\frac{kW}{m^2} \cdot 91'360'193\frac{kWh}{yr}\right)}{51'276\ kWp \cdot 2'130.718\frac{kWh}{m^2 \cdot yr}} = 0.8362 = 83.62\ \%$$

In the end, these numbers show that shading losses due to WTGs and panels are the highest energy losses inside the PV plant AEP estimation, but in reality WTG shadow loss is lower than mutual shading. In fact, the maximum value for the first one is 1.84 %, while the second one maximum value is 4.89 %. This little increase of shading losses due to turbines presence demonstrates the feasibility, in terms of energy yield, of module installation under wind farms for energy production, so the possibility of integrating aerogenerators with PV modules and then creating hybrid power plants. The only problem could be the effect that discontinuous shadows due to rotating blades can have on inverters and their MPPT, since both voltage and current, therefore power, change with a given frequency.

CHAPTER 6

WTG SHADOW EVOLUTION MODEL

6.1 WTG SHADOW MODEL AND SHADED AREA

One of the goals set in this thesis is the analysis of the shadow evolution of a wind turbine on a single module and on a simple PV array installed at its base, creating a model able to depict it. First, a MATLAB script for the estimation of how much land is occupied by the shadow casted by the WTG on a (X,Y) plane (a flat terrain is the hypothesis) in a given day of the year is reported. To generate the overall MATLAB code, the shadow model of the tower and three rotating blades are separately created, then they will be combined to develop the overall effect.

- **TOWER SHADOW MODEL**

The basis of the tower shadow assessment is focused on the calculation of x and y coordinates of its different altitude points on a (X,Y) plane having origin at the WTG tower axis. Each of these points is considered as a bar of a certain elevation that produces a shadow length (Lshad). Considering tower diameter too, for each altitude three points are taken into account: axis, western and eastern tower points. Data such as geographical location (latitude and longitude of Gravina in Puglia WTG04, 40.837° and 16.272° respectively), PV module dimensions, angular speed of a single blade $\omega = \frac{82\frac{\mathrm{m}}{\mathrm{s}}}{79\ \mathrm{m}} = 1.038\frac{\mathrm{rad}}{\mathrm{s}}$ (maximum blade tip speed equal to 82 m/s, rotor radius 79 m [24]), the distance between PV module centre of gravity and tower axis, the distance between N-S axis tracker and tower axis, the number of day for which all computations are done, are inserted as inputs. Then, by mean of equations (2.6), (2.7), (2.8), (2.9), (2.10), the position of the Sun is obtained, that is fundamental for calculating all coordinates. The period of time in a day considered in the script is between 8:00 am and 16:00 pm: in every minute Sun and shadow positions will be evaluated. Using two "for-cycles", the code calculates, for each elevation from 1 m to 121 m, the x and y shadow coordinates of the axis, the western and eastern points for each minute from 8:00 am to 16:00 pm; estimation is done for each minute, from minute 480 (equal to 8:00 am) to minute 960 (equal to 16:00 pm), when in a day there are 1440 minutes in total. The x and y coordinates on the (X,Y) plane are computed starting from the axis point shadow length calculation $Lshad$ =z/tg(α) (6.1), where z is the specific altitude of the tower elevation point in metres, and then:

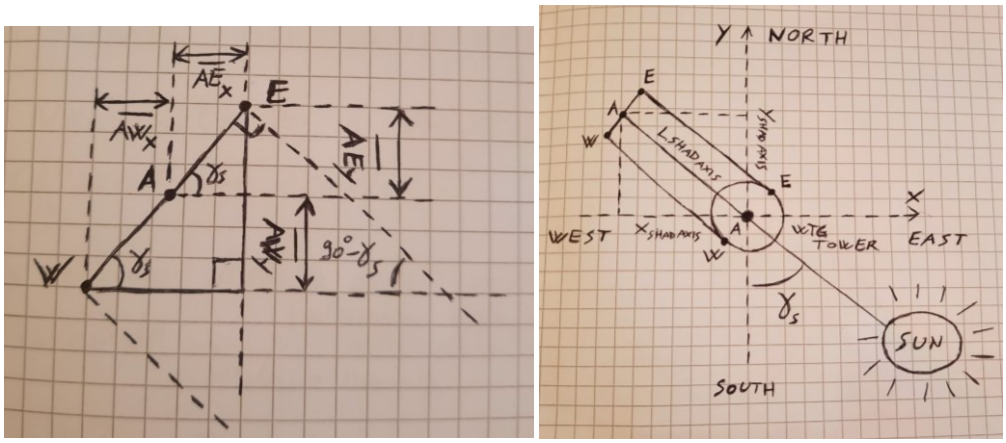

Figure 6.1. *Drawings of axis, western and eastern points shadow coordinates on a (X,Y) plane.*

For the axis point

$$xshad_{axis} = Lshad \cdot \sin(\gamma s) = \frac{z}{t(\alpha)} \cdot \sin(\gamma s) \quad [m] \qquad (6.2)$$

$$yshad_{axis} = Lshad \cdot \cos(\gamma s) = \frac{z}{t(\alpha)} \cdot \cos(\gamma s) \quad [m] \qquad (6.3)$$

For the western point

$$xshad_w = xshad_{axis} - \overline{AW_x} = \frac{z}{t(\alpha)} \cdot \sin(\gamma s) - \frac{diam(z)}{2} \cdot \cos(\gamma s) \quad [m] \qquad (6.4)$$

$$yshad_w = yshad_{axis} + \overline{AW_y} = \frac{z}{t(\alpha)} \cdot \cos(\gamma s) + \frac{diam(z)}{2} \cdot \sin(\gamma s) \quad [m] \qquad (6.5)$$

For the eastern point

$$xshad_e = xshad_{axis} + \overline{AE_x} = \frac{z}{t(\alpha)} \cdot \sin(\gamma s) + \frac{diam(z)}{2} \cdot \cos(\gamma s) \quad [m] \qquad (6.6)$$

$$yshad_e = yshad_{axis} - \overline{AE_y} = \frac{z}{t(\alpha)} \cdot \cos(\gamma s) - \frac{diam(z)}{2} \cdot \sin(\gamma s) \quad [m] \qquad (6.7)$$

where diam(z) [m] is the tower external diameter (it is made of tubular steel) at height z.

In the model, x and y coordinates on the PV module surface are derived from tower points shadow coordinates. By inputting N-S distance between the tower axis and the PV module centre of gravity (named $TAPVA_{distance}$ in the code) and W-E distance between the tower axis and the horizontal string tracker axis (called $TANSTA_{distance}$ in the script), x and y shadow coordinates on the PV panel surface of each tower altitude can be computed with:

$$0\,m \le yshadmod_{axis,e,w} = yshad_{axis,e,w} - dpvy \le 2.384\,m = Hmod \quad [m] \qquad (6.8)$$

$$dpvy = TAPVA_{distance} - \frac{Hmod}{2} \quad [m] \qquad (6.9)$$

$$0\ m \leq xshadmod_{axis,e.w} = xshad_{axis,e,w} - dpvx \leq 1{,}303\ m = Wmod \quad [m] \qquad (6.10)$$

$$dpvx = TANSTA_{distance} - \frac{Wmod}{2} \quad [m] \qquad (6.11)$$

Where the (X,Y) Cartesian system origin is placed on the bottom-left PV module corner: x is positive towards East, while y towards North. It must be remembered that the panel is in its portrait layout, as it can be noticed from the equations above. Moreover, "dpvy" is the distance along the y axis between the tower axis and the southern horizontal module side, while "dpvx" is the distance along the x axis between the tower axis and the western vertical module side. Hmod and Wmod are the height and width of the panel [m]. A really coarse approximation of the "shading loss" at every minute between 8:00 am and 16:00 pm during a day, considered as the share of sensitive PV module surface that is covered by the shadow casted by each tower altitude, is achieved by considering West, East and axis shadow points on the panel area as forming a rectangular trapezium shading shape (see the figure below to have a better idea of the approximation just described).

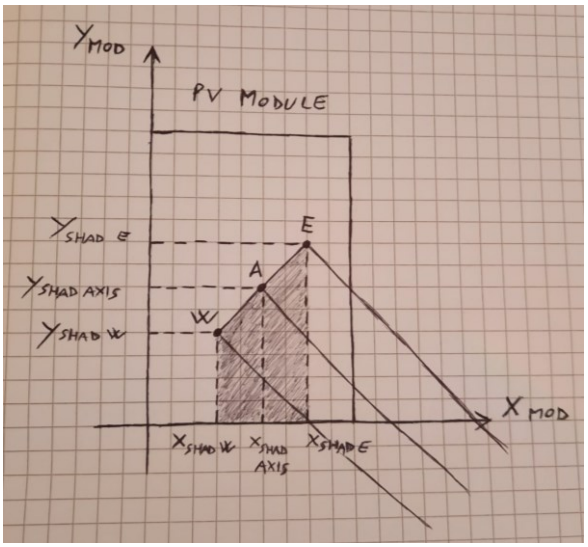

Figure 6.2. *Drawing of the shadow loss coarse approximation idea.*

- **THREE ROTATING BLADES SHADOW MODEL**

To model the three rotating blade shapes on a (X,Z) rotor plane, leading edges were considered as a straight line for simplicity, while trailing edges were divided into three parts with different profiles and thus equations. The rotor hub was not considered in the model. From the GE Cypress dimensions datasheet [35], chord length at 90%·Rtip (Rtip is blade radius, equal to 79 m by assumption) is equal to 1.3 m, while a maximum chord length of 4 m is supposed to be at 30%·Rtip (23.7 m) and at blade root a 2 m chord length is assumed. From 0%·Rtip to 30%·Rtip a cosine

function, from 30%·Rtip to 90%·Rtip (71.1 m) a linear function and from 90%·Rtip to Rtip a parabolic function: this is the thought trailing edge profile.

BLADE TRAILING EDGES SHAPE FUNCTIONS

$$z(R) = 3 - \cos\left(\frac{R}{7.543944303}\right) \ [m] \ \rightarrow \ if \ 0\,m \leq R < 23.7\,m \quad (6.12)$$

$$z(R) = 5.349999993 - (0.056962025 \cdot R) \ [m] \ \rightarrow \ if \ 23.7\,m \leq R < 71.1\,m \quad (6.13)$$

$$z(R) = 6.842105264 - \left(\frac{R^2}{912.1461538}\right) \ [m] \rightarrow \ if \ 71.1\,m \leq R \leq 79\,m \quad (6.14)$$

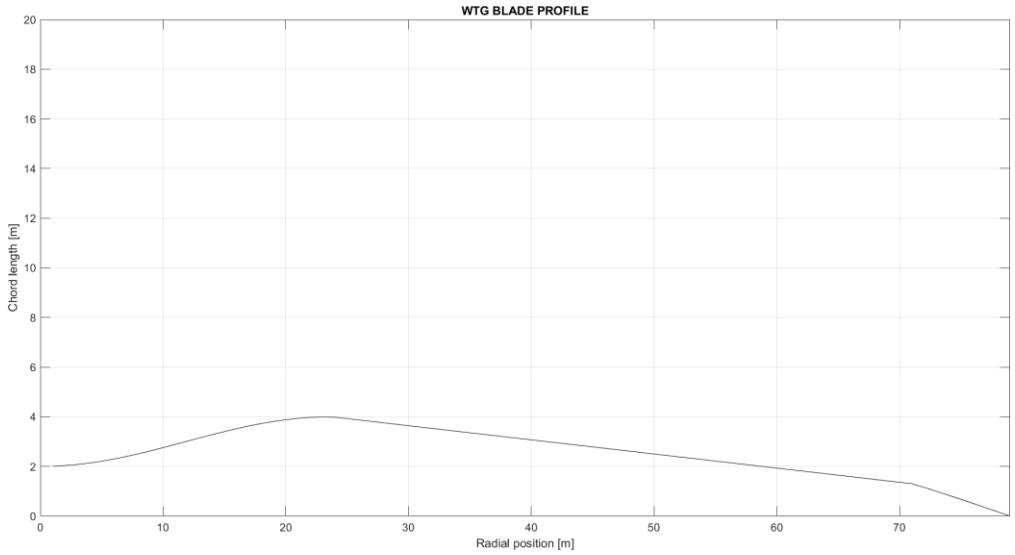

Figure 6.3. *Blade profile from MATLAB chart.*

Three rotating blades leading edge (LE) and trailing edge (TE) points x and z coordinates are modelled by polar coordinates (ρ,ϑ), taking into account their rotation too. As written before, blade angular speed is $\omega = 1.038\,\frac{\text{rad}}{\text{s}}$. The minus signs in the next equations are related to the fact that the direction of rotation is clockwise [24], while the blades are separated by an angle of 120° ($\frac{2}{3}\cdot\pi$ rad). Polar coordinates for the leading-edge points of the three blades are obtained with the following equations (t stands for time):

$$\vartheta_{le1}(t) = -\omega \cdot t \ \ [rad] \quad (6.15)$$

$$\vartheta_{le2}(t) = -\omega \cdot t + \frac{2}{3}\cdot\pi \ \ [rad] \quad (6.16)$$

$$\vartheta_{le3}(t) = -\omega \cdot t - \frac{2}{3}\cdot\pi \ \ [rad] \quad (6.17)$$

$$0 \leq \rho_{le1} = \rho_{le2} = \rho_{le3} = R \leq R_{tip} \ \ [m] \quad (6.18)$$

Instead, polar coordinates for the trailing-edge points:

$$\theta_{te1}(t) = \vartheta_{le1}(t) + arctg\left(\frac{z(R)}{R}\right) \quad [rad] \quad (6.19)$$

$$\theta_{te2}(t) = \vartheta_{le2}(t) + arctg\left(\frac{z(R)}{R}\right) \quad [rad] \quad (6.20)$$

$$\theta_{te3}(t) = \vartheta_{le3}(t) + arctg\left(\frac{z(R)}{R}\right) \quad [rad] \quad (6.21)$$

$$\rho_{te1} = \rho_{te2} = \rho_{te3} = \sqrt{R^2 + z(R)^2} \quad [\mathrm{m}] \quad (6.22)$$

where z(R) [m] is the blade chord length at radial position R [m].

The projections on the x (West-East) and z (elevation) axes, with origin centre at the "virtual hub axis", of LE and TE points of the blades are (120.9 m is the rotor hub axis height):

$$\rho_{xle1} = \rho_{xle2} = \rho_{xle3} = \rho_{xle} = \rho_{le} \cdot \cos\left(\theta_{le}(t)\right) \quad [m] \quad (6.23)$$

$$\rho_{zle1} = \rho_{zle2} = \rho_{zle3} = \rho_{zle} = \rho_{le} \cdot \sin\left(\vartheta_{le}(t)\right) + 120.9 \quad [m] \quad (6.24)$$

$$\rho_{xte1} = \rho_{xte2} = \rho_{xte3} = \rho_{xte} = \rho_{te} \cdot \cos\left(\theta_{te}(t)\right) \quad [m] \quad (6.25)$$

$$\rho_{zte1} = \rho_{zte2} = \rho_{zte3} = \rho_{zte} = \rho_{te} \cdot \sin\left(\vartheta_{te}(t)\right) + 120.9 \quad [m] \quad (6.26)$$

All these points cast a shadow on the previously described (X,Y) plane with the WTG tower axis as the centre. In fact, LE and TE blade points are in this case considered as vertical bars too, just as for the tower points. By hypothesis, the rotor plane (X,Z) is always oriented towards the North-North-West direction, since from wind rose depictions it is possible to observe that the highest wind intensity and frequency is along that direction (30° = 0.5236 rad).

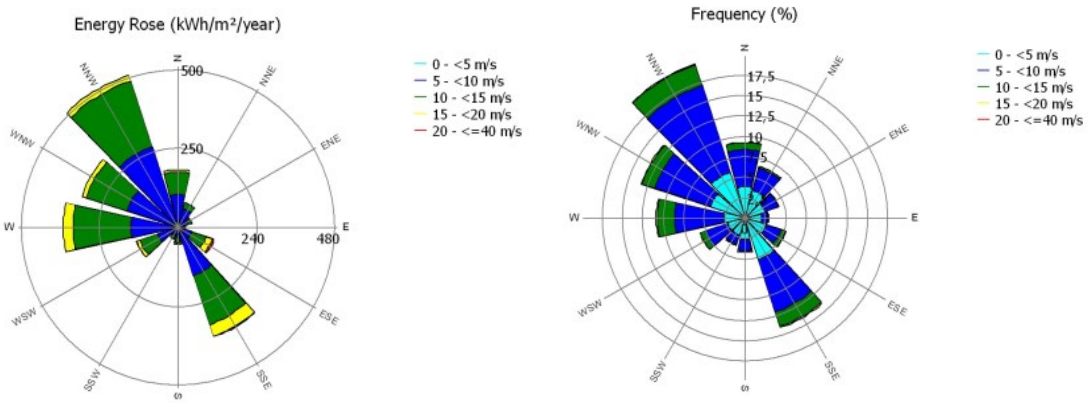

Figure 6.4. *Energy and frequency wind roses of the Gravina in Puglia hybrid power plant site, from windPRO.*

$$Lshad_{le1,2,3} = Lshad_{le} = \frac{\rho_{zle}(t)}{tg(\alpha)} \quad [m] \quad (6.27)$$

$$xshad_{le1,2,3} = xshad_{le} = Lshad_{le} \cdot \sin(\gamma s) + (\rho_{xle}(t) \cdot \cos(0.5236)) \quad [m] \quad (6.27)$$

$$yshad_{le1,2,3} = yshad_{le} = Lshad_{le} \cdot \cos(\gamma s) - (\rho_{xle}(t) \cdot \sin(0.5236)) \quad [m] \quad (6.28)$$

$$Lshad_{te1,2,3} = Lshad_{te} = \frac{\rho_{zte}(t)}{tg(\alpha)} \quad [m] \quad (6.29)$$

$$xshad_{te1,2,3} = xshad_{te} = Lshad_{te} \cdot \sin(\gamma s) + (\rho_{xte}(t) \cdot \cos(0.5236)) \quad [m] \quad (6.30)$$

$$yshad_{te1,2,3} = yshad_{te} = Lshad_{te} \cdot \cos(\gamma s) - (\rho_{xte}(t) \cdot \sin(0.5236)) \quad [m] \quad (6.31)$$

For simplicity, the rotor plane can always be considered perpendicular to the direct radiation projection on the (X,Y) plane too; in this way the only changes in the previous equations are:

$$xshad_{le1,2,3} = xshad_{le} = Lshad_{le} \cdot \sin(\gamma s) + (\rho_{xle}(t) \cdot \cos(\gamma s)) \quad [m] \quad (6.32)$$

$$yshad_{le1,2,3} = yshad_{le} = Lshad_{le} \cdot \cos(\gamma s) - (\rho_{xle}(t) \cdot \sin(\gamma s)) \quad [m] \quad (6.33)$$

$$xshad_{te1,2,3} = xshad_{te} = Lshad_{te} \cdot \sin(\gamma s) + (\rho_{xte}(t) \cdot \cos(\gamma s)) \quad [m] \quad (6.34)$$

$$yshad_{te1,2,3} = yshad_{te} = Lshad_{te} \cdot \cos(\gamma s) - (\rho_{xte}(t) \cdot \sin(\gamma s)) \quad [m] \quad (6.35)$$

The x and y shading coordinates on the PV module surface, derived from LE and TE points shadow coordinates, are achieved with the same process seen before for the tower:

$$0\ m \leq yshadmodblade_{le,te} = yshad_{le,te} - dpvy \leq 2.384\ m = Hmod \quad [m] \quad (6.36)$$

$$0\ m \leq xshadmodblade_{le,te} = xshad_{le,te} - dpvx \leq 1{,}303\ m = Wmod \quad [m]. \quad (6.37)$$

For each blade, the very broad approximation of shadow loss is obtained in the same way as seen for the tower case.

- **OVERALL WTG SHADOW MODEL**

The complete MATLAB script related to this topic, given by the sum of tower and blade shading evolution models, is reported in APPENDIX E(1); other useful graphs can be replicated by running the script, like shadow coordinates on the PV panel surface. The following resulting figures are obtained for the 21st of December (Winter solstice, day n° 355) and for a module positioned at whatever $TAPVA_{distance}$ and $TANSTA_{distance}$ at the Gravina in Puglia site. The 21st of December was chosen because it is the day when solar elevation α is at its annual minimum and therefore the shadow casted by the WTG components are the longest during the year. So, these pictures represent

the widest area that the shadow of a WTG (the same of the project) can cover around it: it is the extreme condition. It is important to remember that the WTG rotor is fixed with normal direction towards North-North-West (see Figure 6.4).

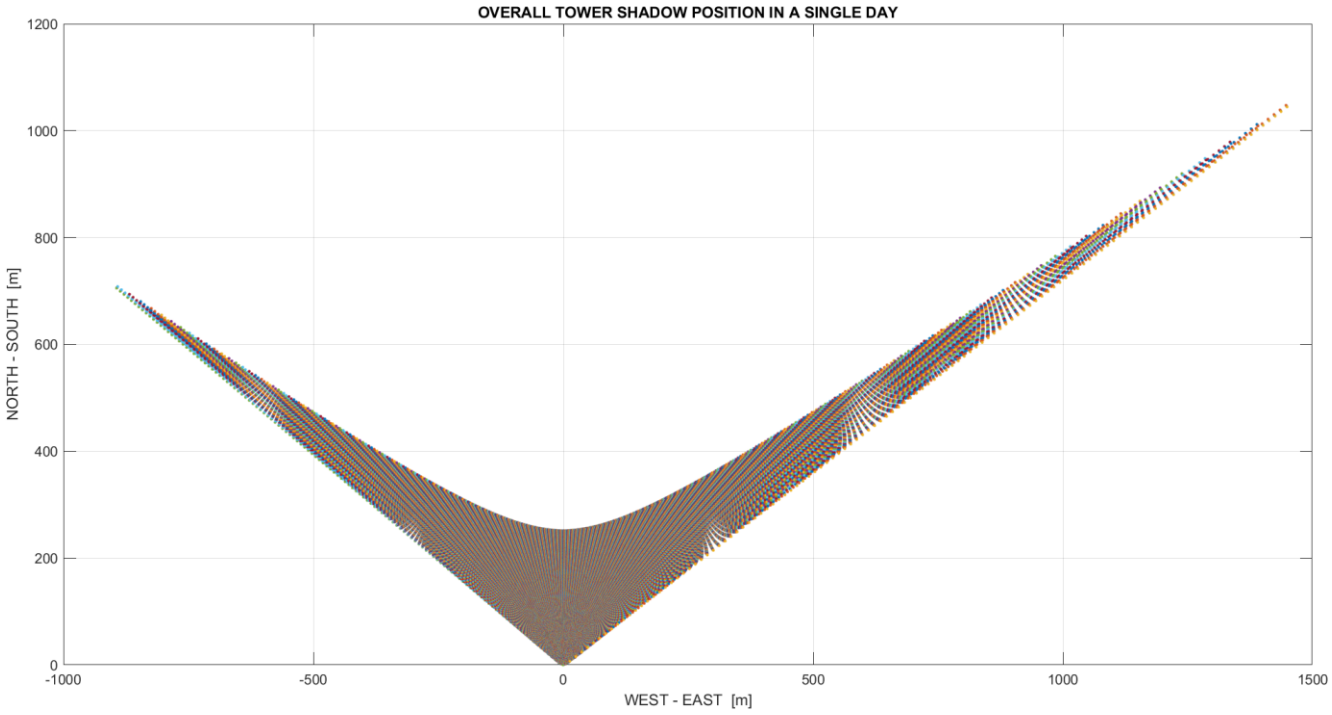

Figure 6.5. *Maximum shaded area by the WTG tower during a single day (21st of December).*

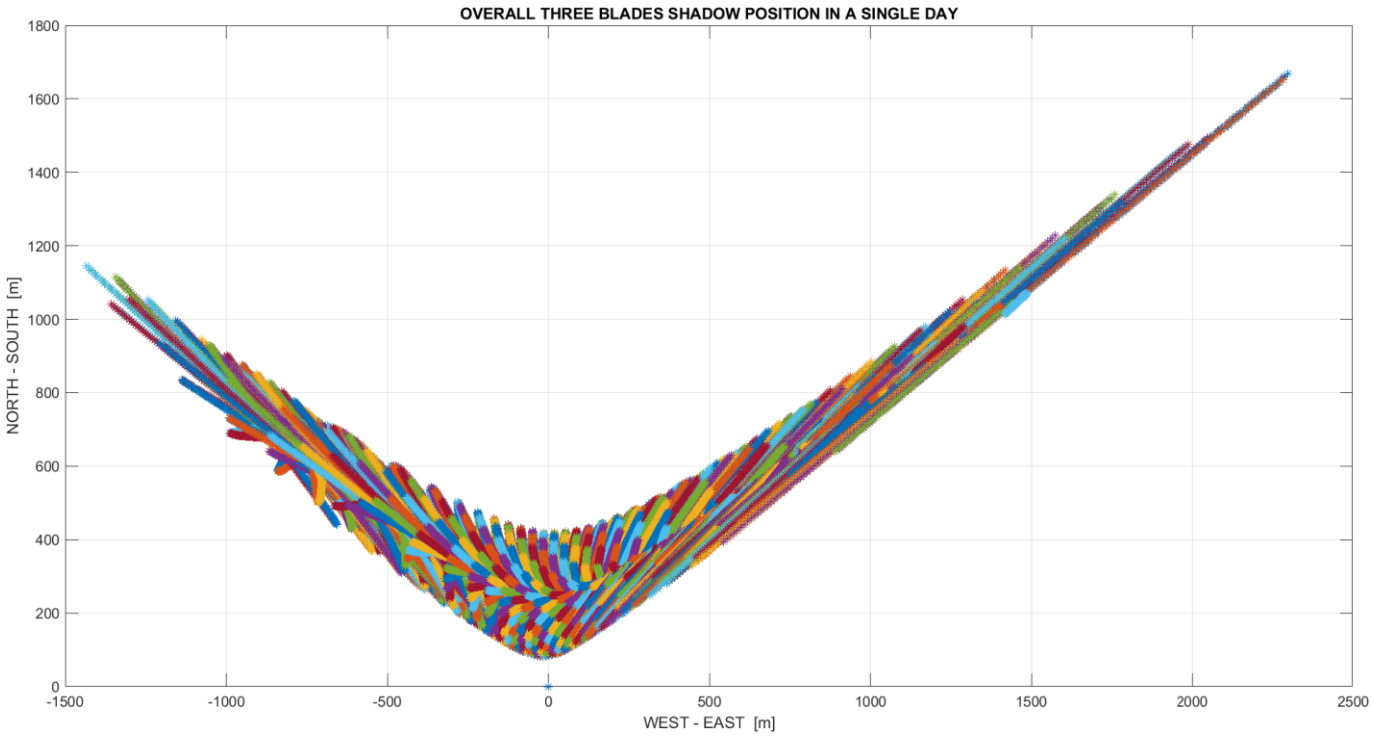

Figure 6.6. *Maximum shaded area by the WTG rotating blades during a single day (21st of December).*

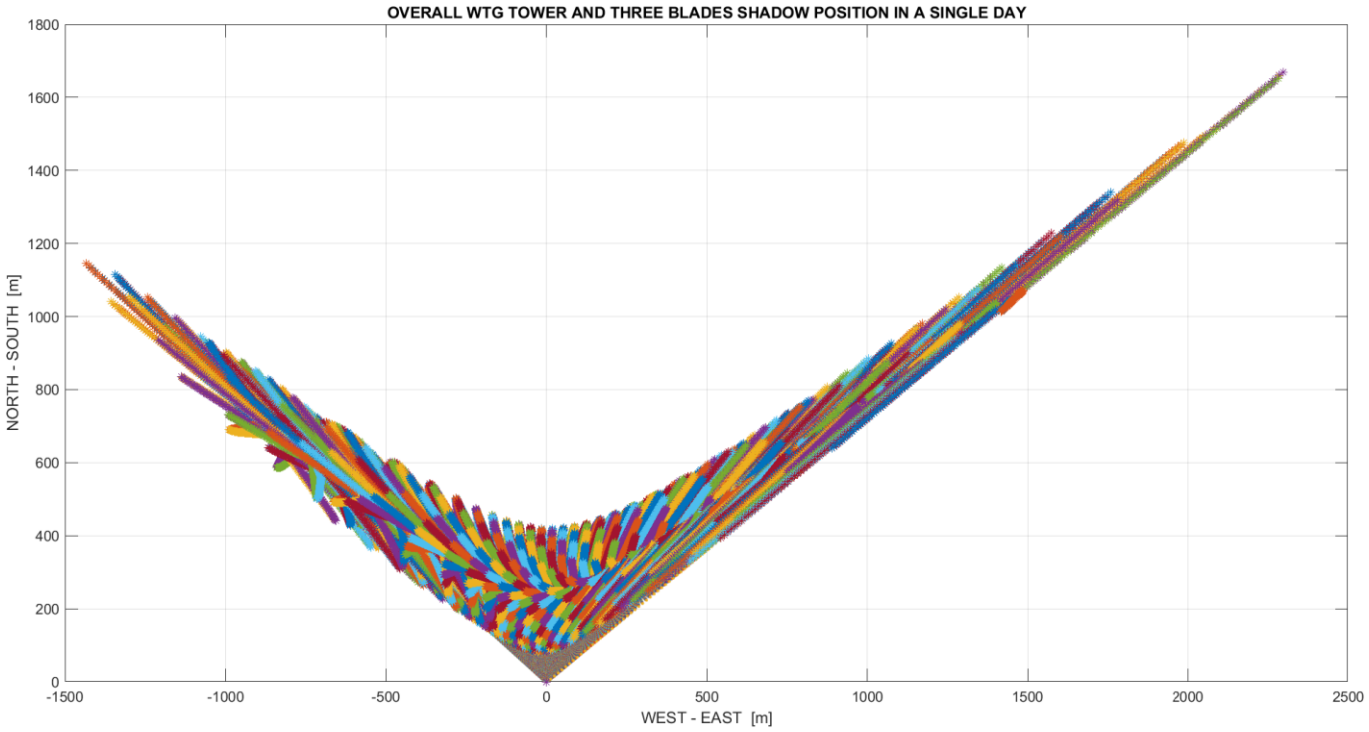

Figure 6.7. *Maximum shaded area by the entire WTG during a single day (21st of December).*

For extra context, in the following image the shape of entire WTG shadow casted on the (X,Y) plane, i.e. the ground, on the 21st of December (day number 355) and at 12:00 o'clock legal time (minute 720) is shown.

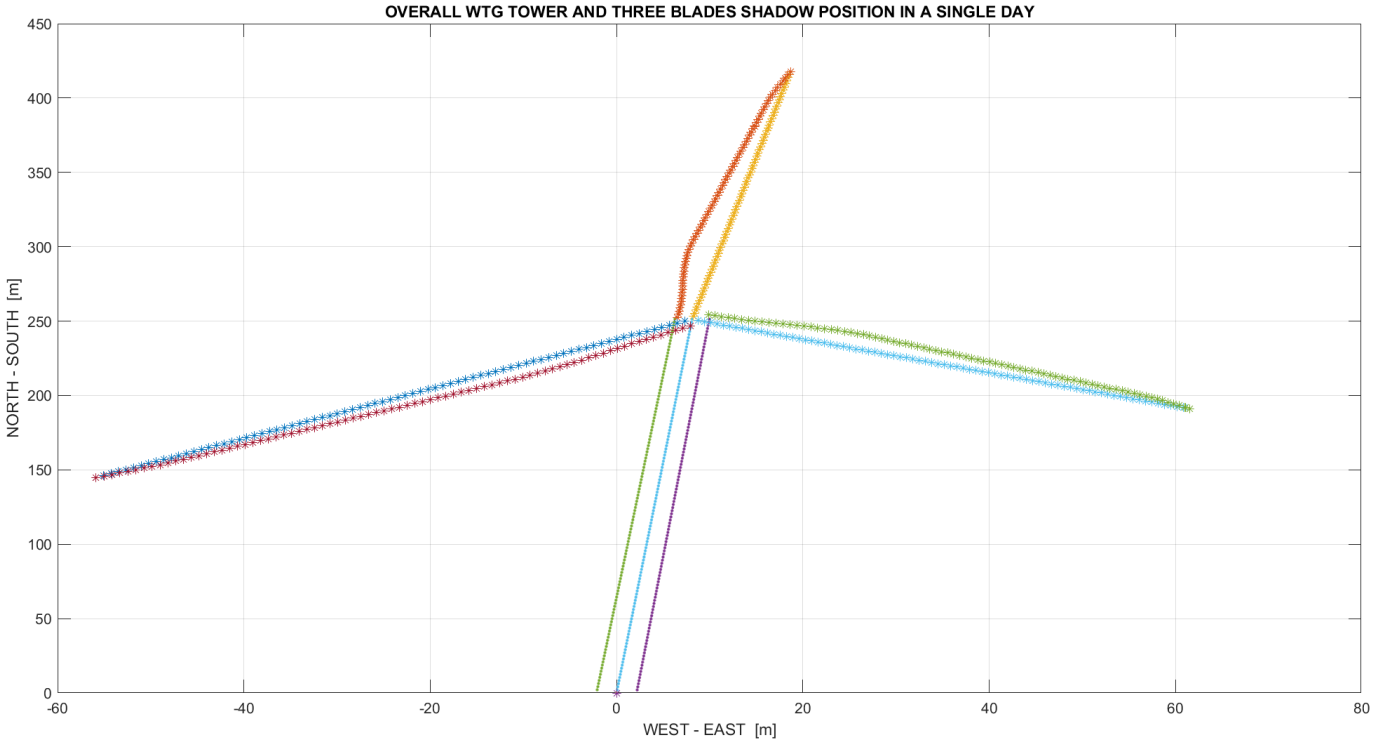

Figure 6.8. *Shape of the entire WTG shadow casted on ground on 21st of December and 12:00 legal time.*

6.2 TIME SERIES OF ENTIRE WTG SHADOW ON A SINGLE PV MODULE

It could be really interesting to see when a certain PV module on the (X,Y) plane (origin at the WTG tower axis location) is shadowed and when it is not. For this purpose, a new MATLAB script was written. Differently from before, the time period between 8:00 am and 16:00 pm in a day is defined in seconds and not in minutes ($2.88 \cdot 10^4$s is equivalent of 8:00 am, $5.76 \cdot 10^4$s is equivalent of 16:00 pm); this means that for every second the presence of shading on the sensible surface will be verified. After starting the running of the code, the North-South and the West-East centre of gravity positions of the panel can be inputted from the MATLAB Command Window, along with the number of the day (from 1 to 365) required for the analysis. For each minute of the previously described time range, x and y shadow coordinates of every tower and blade points are calculated again. If one of these points is inside the PV module surface on the (X,Y) plane, the panel is considered shaded and at that time instant shading is equal to "one". Conversely, shading is "zero" and module is fully illuminated by the Sun. Indeed, "zero" means that in that particular instant the PV panel is not shaded, whereas "one" means that the module is shaded. After all calculations, the final result will be a time series vector, the elements of which are only zeros and ones for every second in the analysis. For simplicity, the following approximation was made: "one" does not consider if the panel is only partially or completely shaded, but by hypothesis when "one" appears in the time series vector it means that the module is considered completely shaded, even if in reality it is partially shaded. These vectors are separately created both for the WTG tower and blades, making two shadow time series to show in different figures when the panel is separately shaded by the tower and by the blades. Finally, a unique zero-one vector is made taking into account the whole wind turbine and the related time series graph is generated, displaying the total outcome: tower and blades results are united.

In the pictures below, the outputs of this MATLAB script for a PV module located at the North-South barycentre position ($TAPVA_{distance}$) equal to 240 m and the West-East one ($TANSTA_{distance}$) equal to 0 m on Winter solstice (on the 21st of December, day number 355) are shown. It is possible to observe the periods of time when the panel is shaded constantly by the tower and when it is shadowed periodically by the three blades. Shading by the tower starts from second $4.2621 \cdot 10^4$ (11:50 am) and finishes at second $4{,}2907 \cdot 10^4$ (11:55 am), while periodic shading by the blades starts from second $3.8558 \cdot 10^4$ (10:42 am) and finishes at second $4.7325 \cdot 10^4$ (13:08 pm).

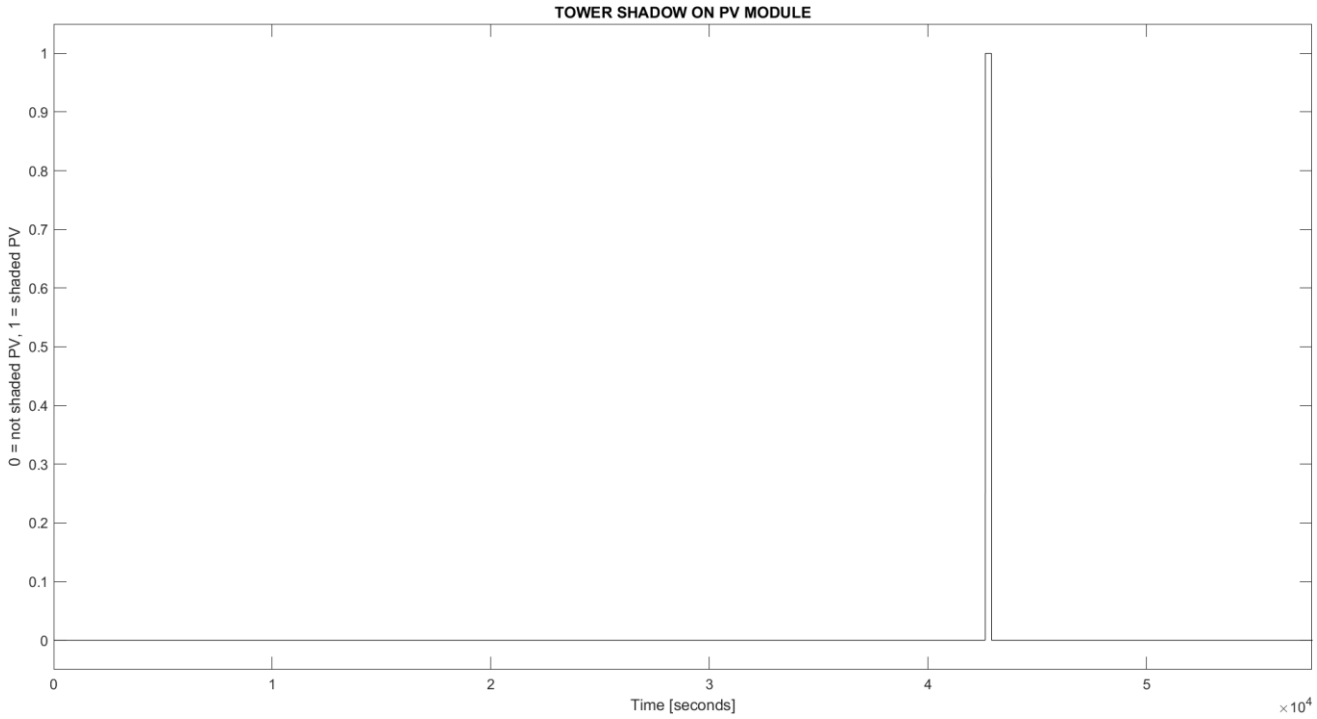

Figure 6.9. *WTG tower shading time series on single PV panel.*

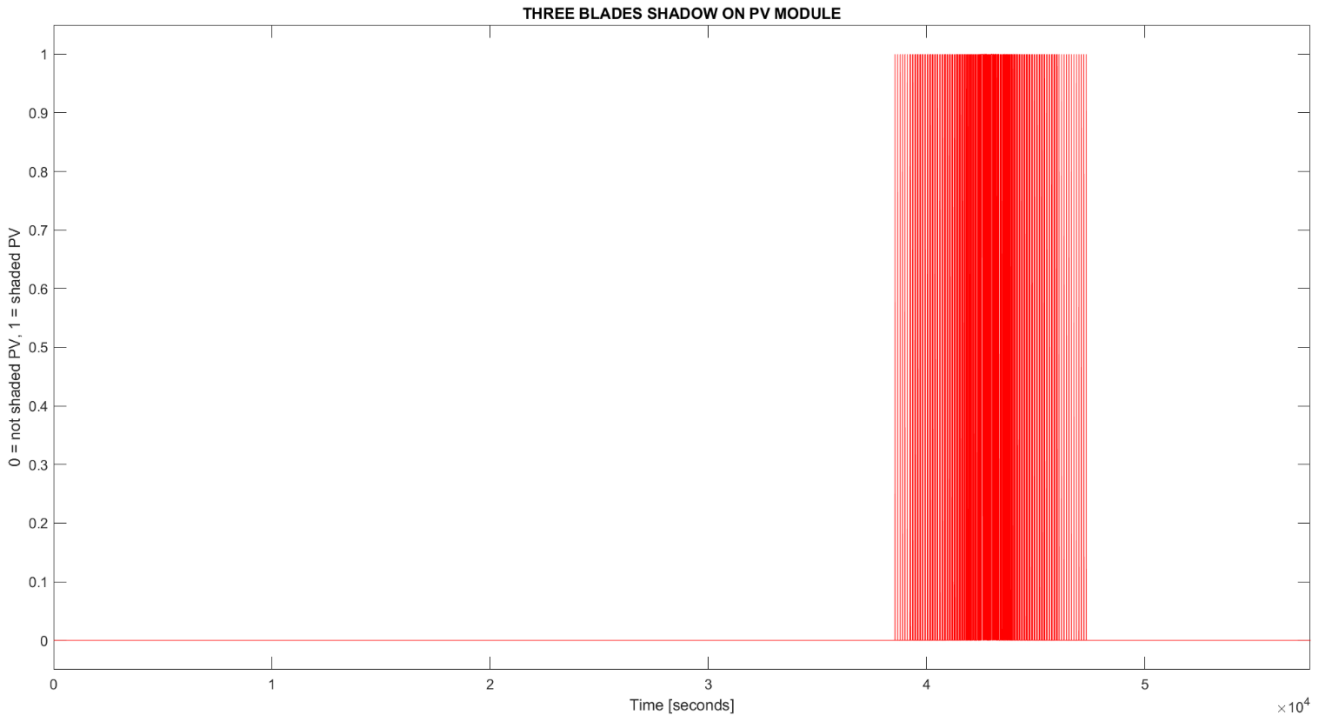

Figure 6.10. *WTG blades shading time series on single PV panel.*

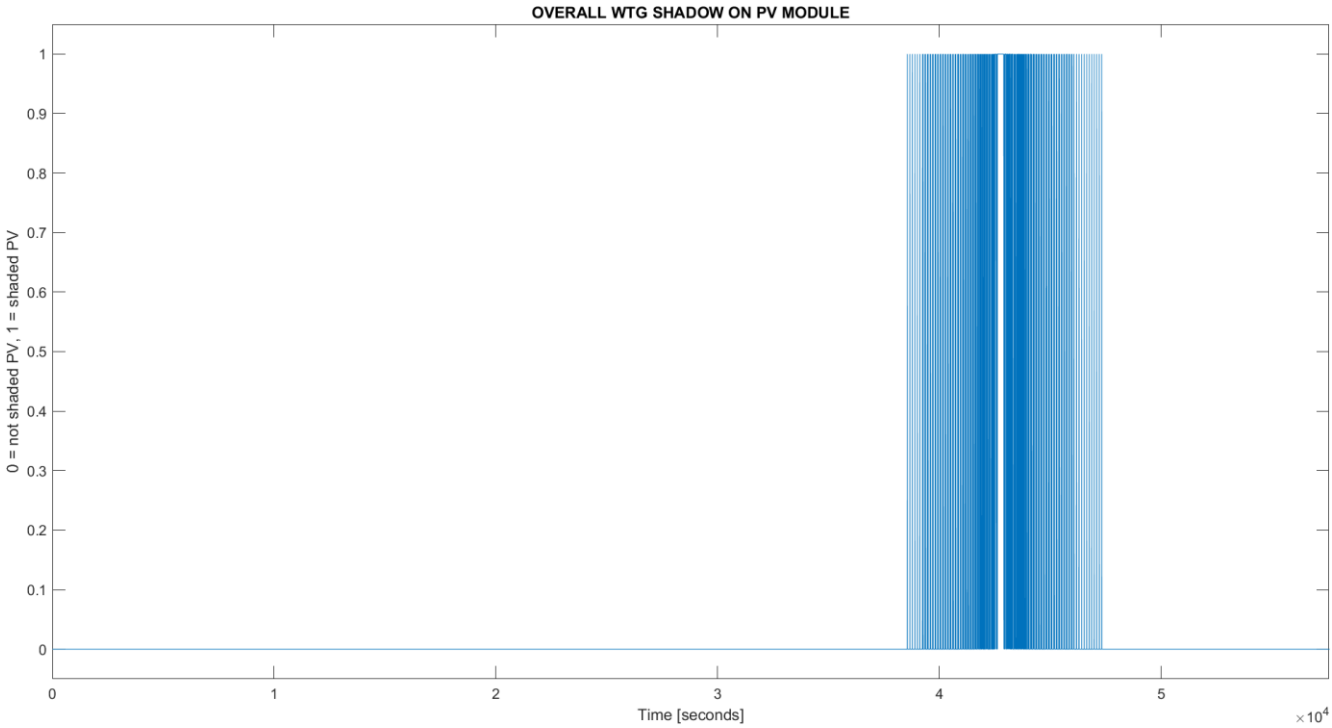

Figure 6.11. *Entire WTG shading time series on single PV panel.*

The MATLAB code described in this paragraph is fully detailed in APPENDIX E(2), and other charts can be replicated by running it.

Shadow fluctuations on a single panel can be seen in a much smaller period, not considering seconds but tenths of second. The MATLAB script is the same as before, yet with some modifications. In this case, the time range is 30 minutes, from 11:35 am to 12:05 pm (in total, a range of $18 \cdot 10^4$ tenths of second). The following figures depict the shadow time series, as explained before, for a unique PV module at the North-South barycentre position ($TAPVA_{distance}$) equal to 240 m and the West-East one ($TANSTA_{distance}$) equal to 0 m at Winter solstice (on the 21st of December, day number 355) again. Tower and blade shading starting and ending instants are the same as for the 8:00 am to 16:00 pm time range. In the figures, continuous tower shading and fluctuating blade shading can be clearly seen. Refer to APPENDIX E(3) for the complete code, from which other interesting graphs can be replicated by running it.

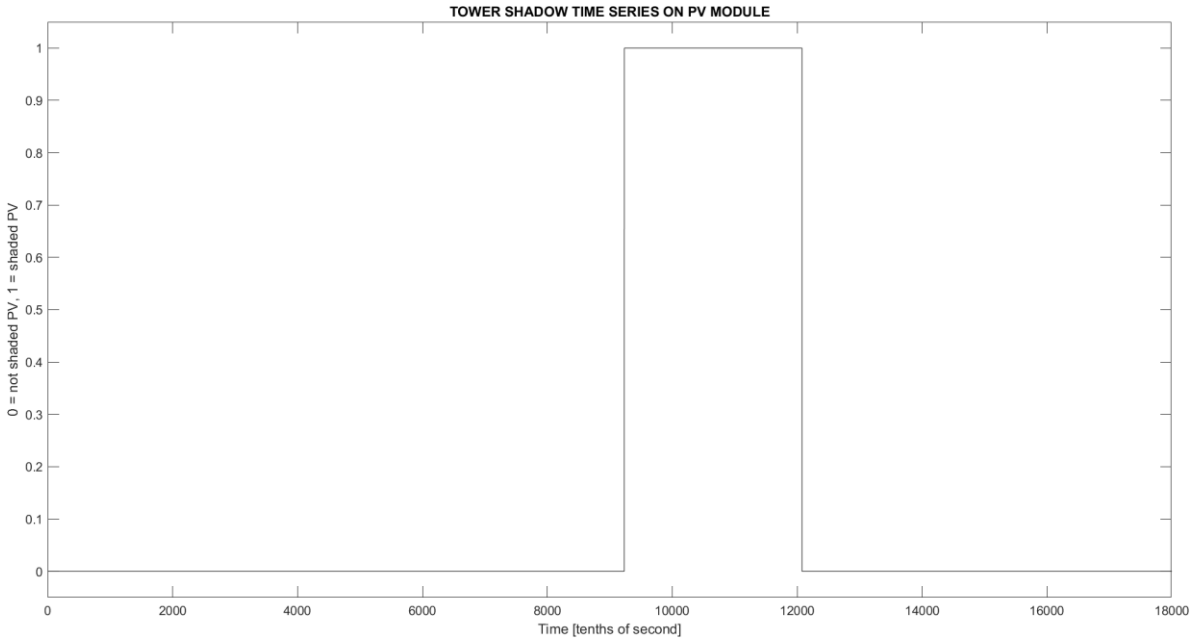

Figure 6.12. *WTG tower shading during a shorter time series on a single PV panel.*

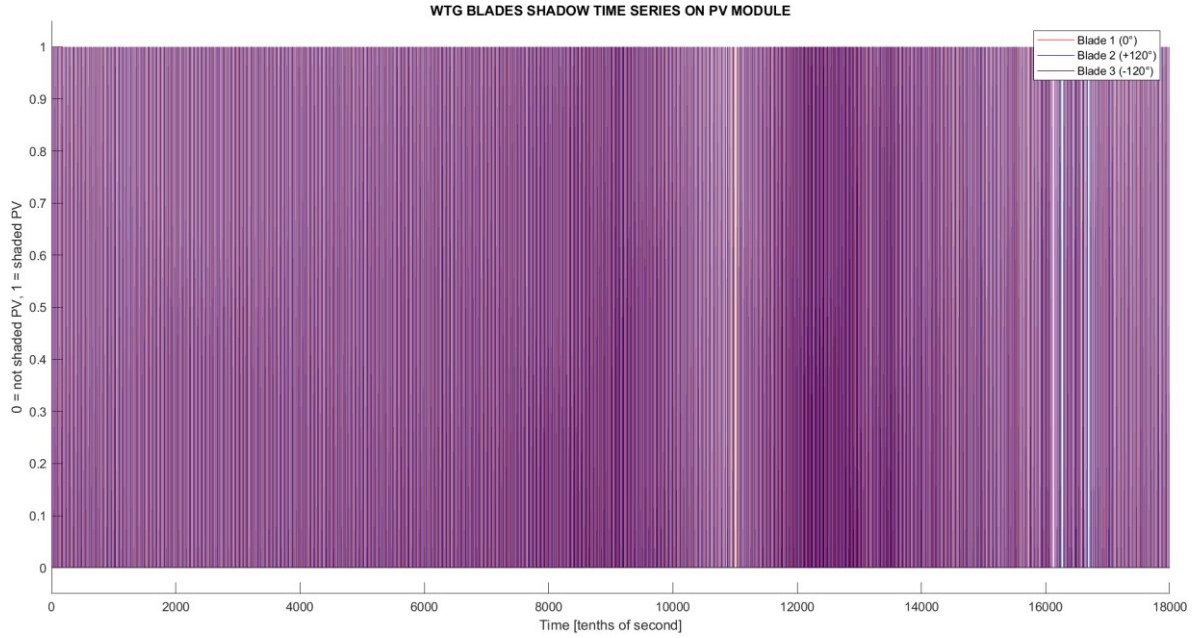

Figure 6.13. *WTG blades shading during a shorter time series on a single PV panel.*

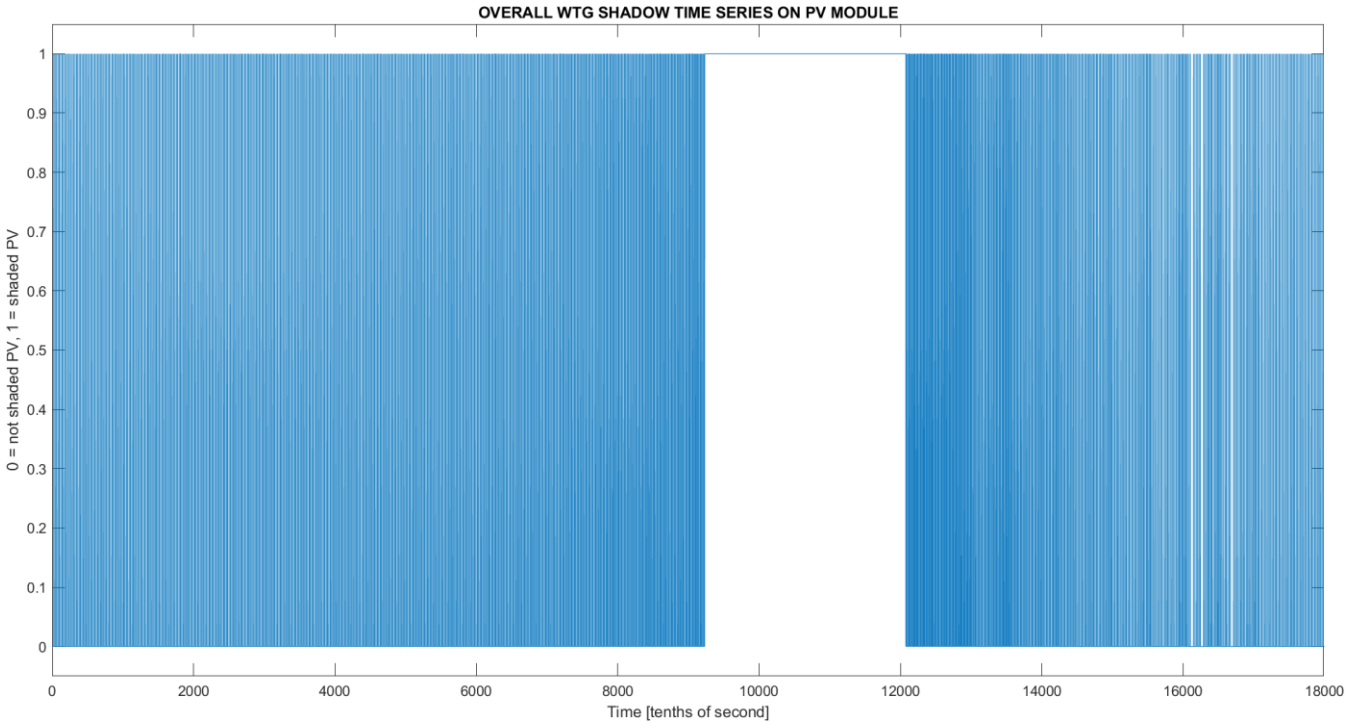

Figure 6.14. *Entire WTG shading during a shorter time series on a single PV panel.*

6.3 ONE MINUTE TIME SERIES OF BLADE SHADOWS ON A PV PANEL

A more precise description of when and how much time a single PV panel on the (X,Y) plane is shaded simply by the WTG blades (now the tower is not considered) was obtained considering a much smaller time range of one minute. This minute is divided into hundredths of second, so that in a minute there are $6 \cdot 10^3$ hundredths of second; in this way the blades and their shadow movements can be temporally followed with better accuracy, catching the exact instant when the module is partially or completely shaded. The same approximation used for partial and total shading seen in the previous paragraph is still valid. The following figures represent the one-minute blade shadow time series, as explained before, for a PV module at the North-South barycentre position ($TAPVA_{distance}$) equal to 300 m, West-East one ($TANSTA_{distance}$) equal to 0 m, at Winter solstice (on the 21st of December, day number 355) and at 11:45 am (inputs are: hour = 11 and minutes = 45). The geographical position taken into account for the coordinates of the Sun calculation is always the one of WTG04 at the Gravina in Puglia site (latitude = 40.837°, longitude = 16.272°). Rotational speed is the same, 1.038 rad/s, calculated from the wind turbine datasheet [24]. The panel is portrait oriented: the shortest side is horizontal (1.303 m), the longest side is vertical (2.384 m).

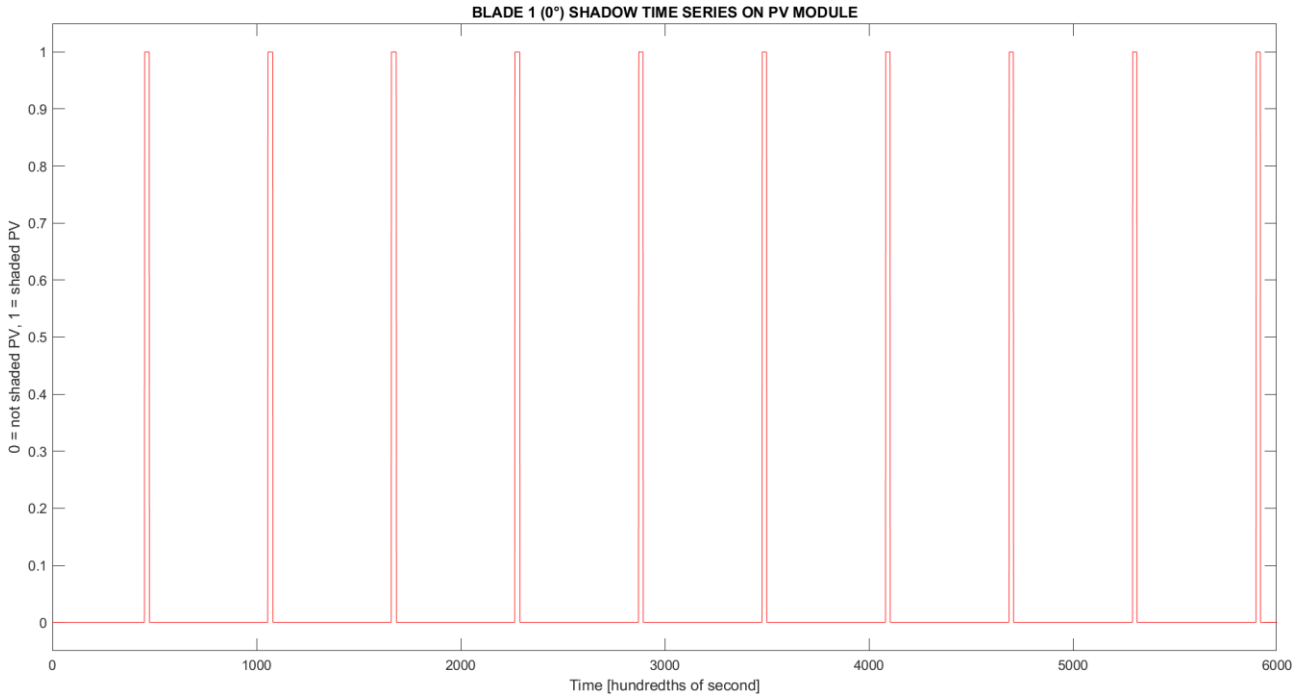

Figure 6.15. *Blade 1 (0°) shading during the one-minute time series on a single PV panel.*

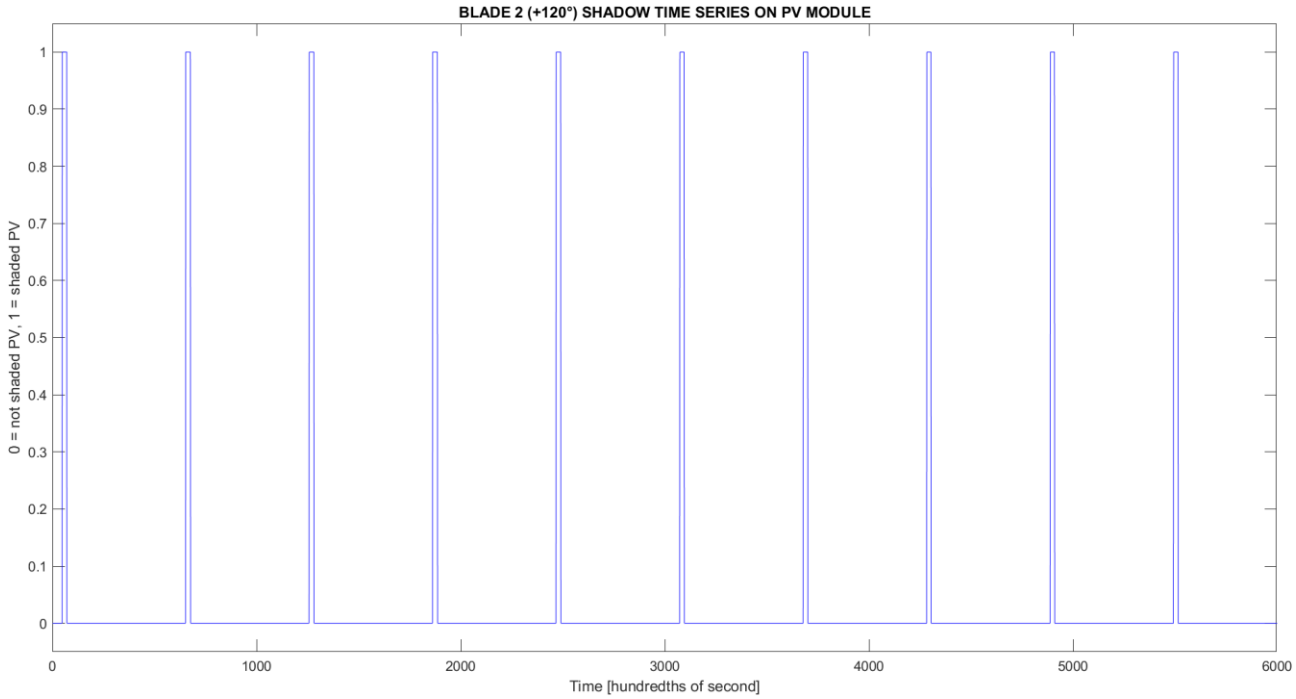

Figure 6.16. *Blade 2 (+120°) shading during the one-minute time series on a single PV panel.*

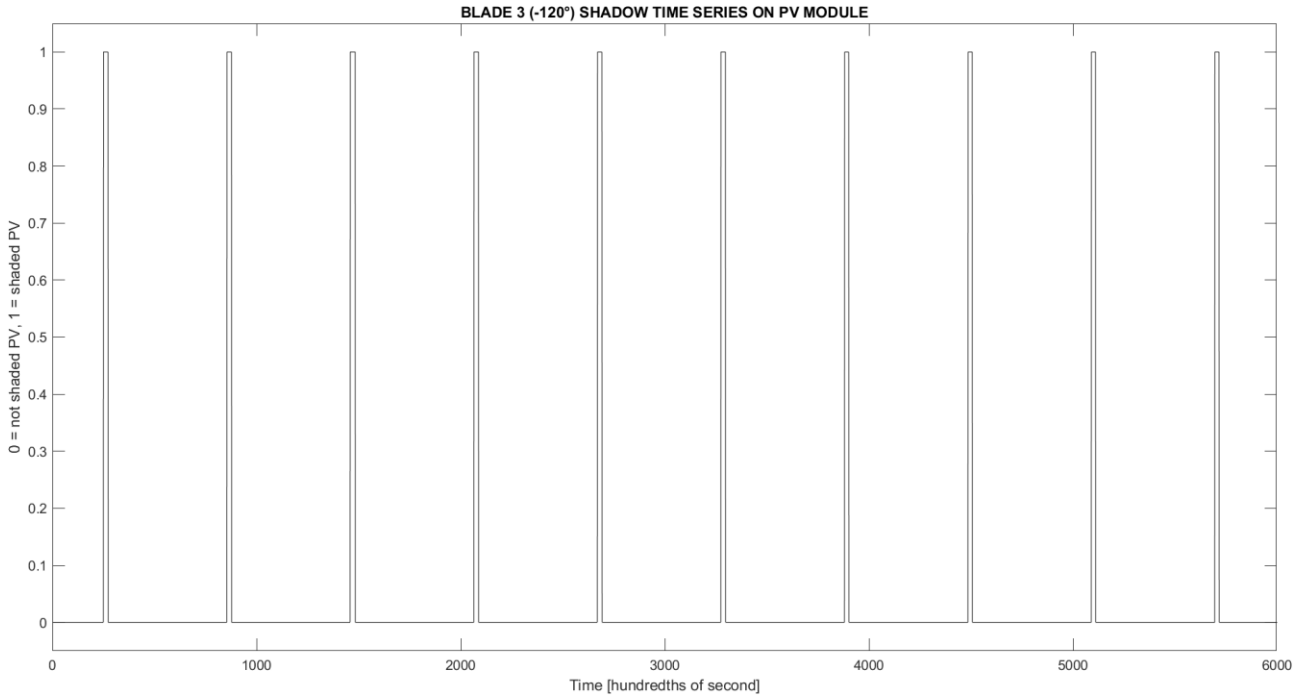

Figure 6.17. *Blade 3 (-120°) shading during the one-minute time series on a single PV panel.*

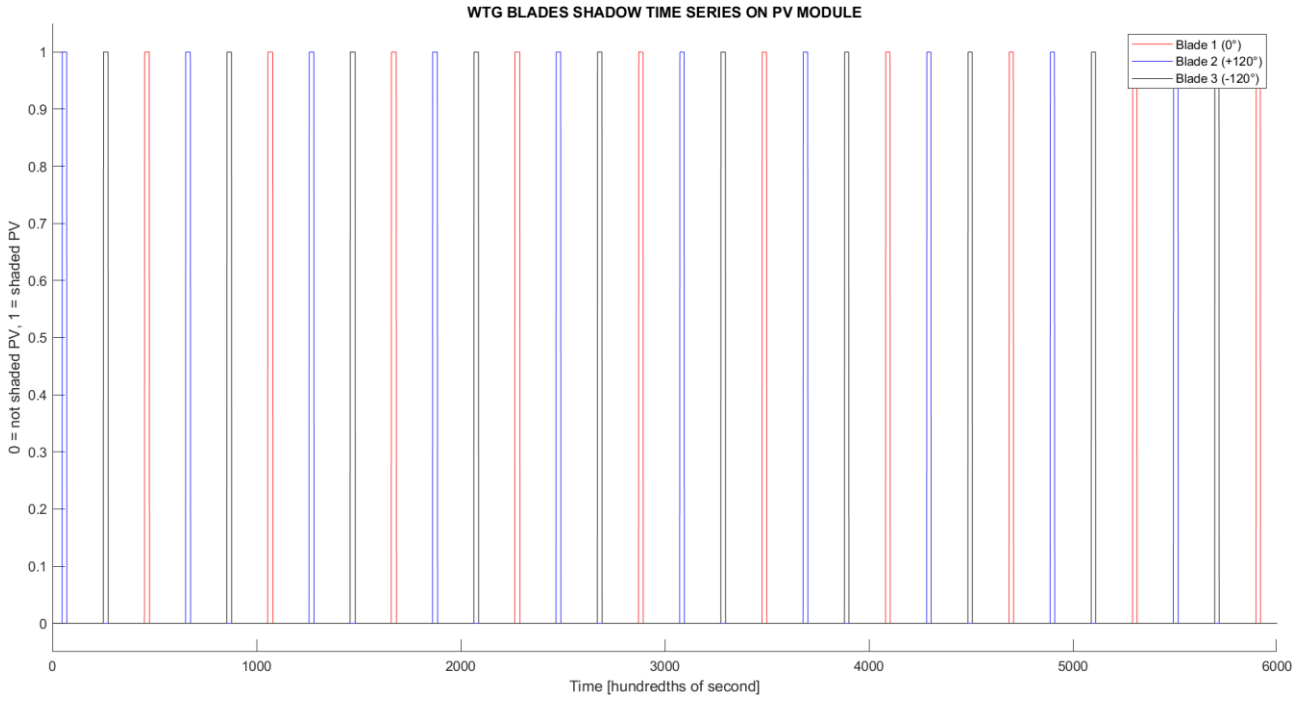

Figure 6.18. *One-minute blades shadow time series on a single PV panel, as sum of the previous charts.*

In this case, the average shading time of the three blades is about 23 hundredths of second (2.3 tenths of second, 0.23 seconds), while the mean time between two consecutive shadings is about 179 hundredths of second (17.9 tenths of second, 1.79 seconds). The mean time between two consecutive shadings of the same blade is about 581 hundredths of second (58.1 tenths of second, 5.81 seconds). These values were obtained by a graphical analysis of Figure 6.18.

Refer to APPENDIX E(4) for the complete script, from which other interesting graphs can be replicated by running it.

6.4 ONE MINUTE TIME SERIES OF BLADE SHADOWS ON A PV ARRAY

The analysis of blade shadow evolution over the one-minute time range in hundredths of second ($6 \cdot 10^3$ hundredths of second in one minute) was extended also to the situation of a simple small PV array, made by two North-South axis strings each one with two panels connected in series. The distance between strings is the one of the Gravina in Puglia PV plant, i.e. 6 m. The same for the vertical distance between two modules in the string, that is 20 cm. All panels are portrait oriented (shortest side horizontal 1.303 m, longest side vertical 2.384 m). Modules are numerated from one to two ("one" is the southern one, "two" is the northern one) depending on their string: "string one" is the western one, while "string two" is the eastern one. In summary, "module1-string1" is positioned South-West, "module2-string1" is positioned North-West, "module1-string2" is positioned South-East and "module2-string2" is positioned North-East. Blade angular speed is 1.038 rad/s, calculated from the wind turbine datasheet again [24]. Geographical position for the coordinates of the Sun calculation is always the one of WTG04 at the Gravina in Puglia site (latitude 40.837°, longitude 16.272°).

The following figures represent the one-minute blade shadow time series for the small PV array described before. Inputs to the script from MATLAB Command Window are the North-South barycentre position of module1-string1 ($TAPVA_{distance}$) equal to 300 m, and the West-East one ($TANSTA_{distance}$) equal to 0 m, at Winter solstice (on the 21st of December, day number 355) and at 11:45 am (hour = 11 and minutes = 45).

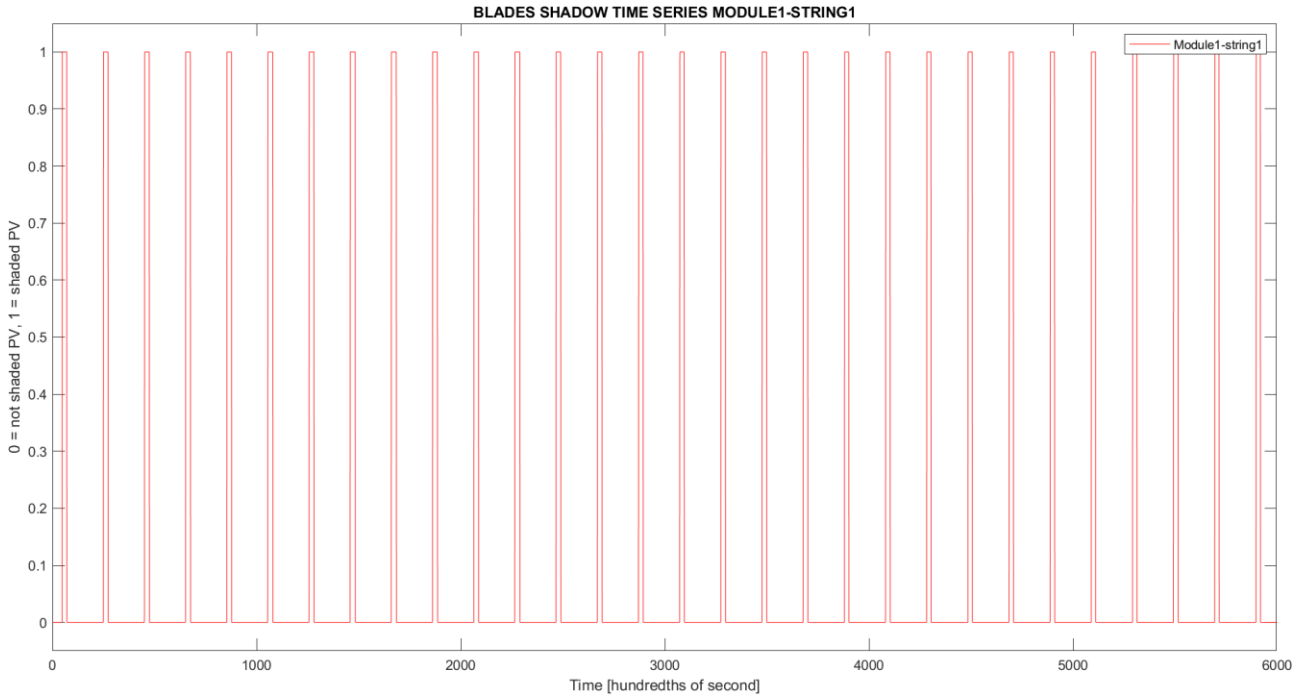

Figure 6.19. *One-minute blades shadow time series on module1-string1.*

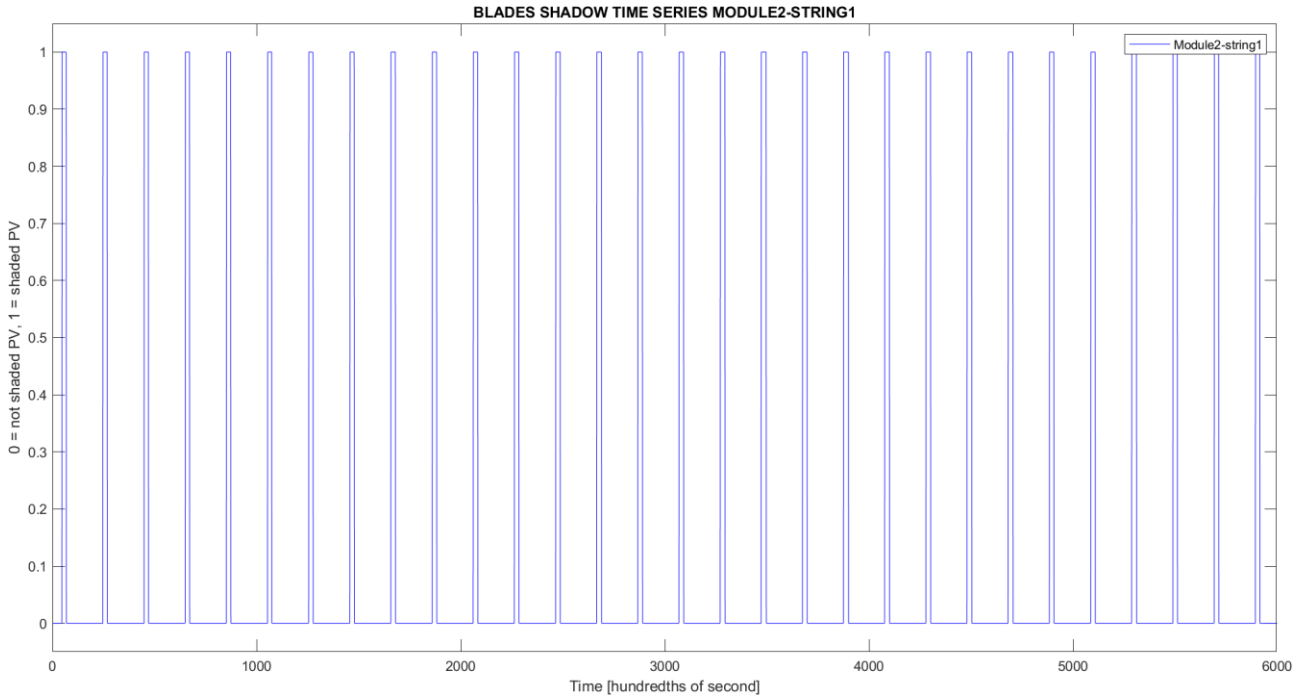

Figure 6.20. *One-minute blades shadow time series on module2-string1.*

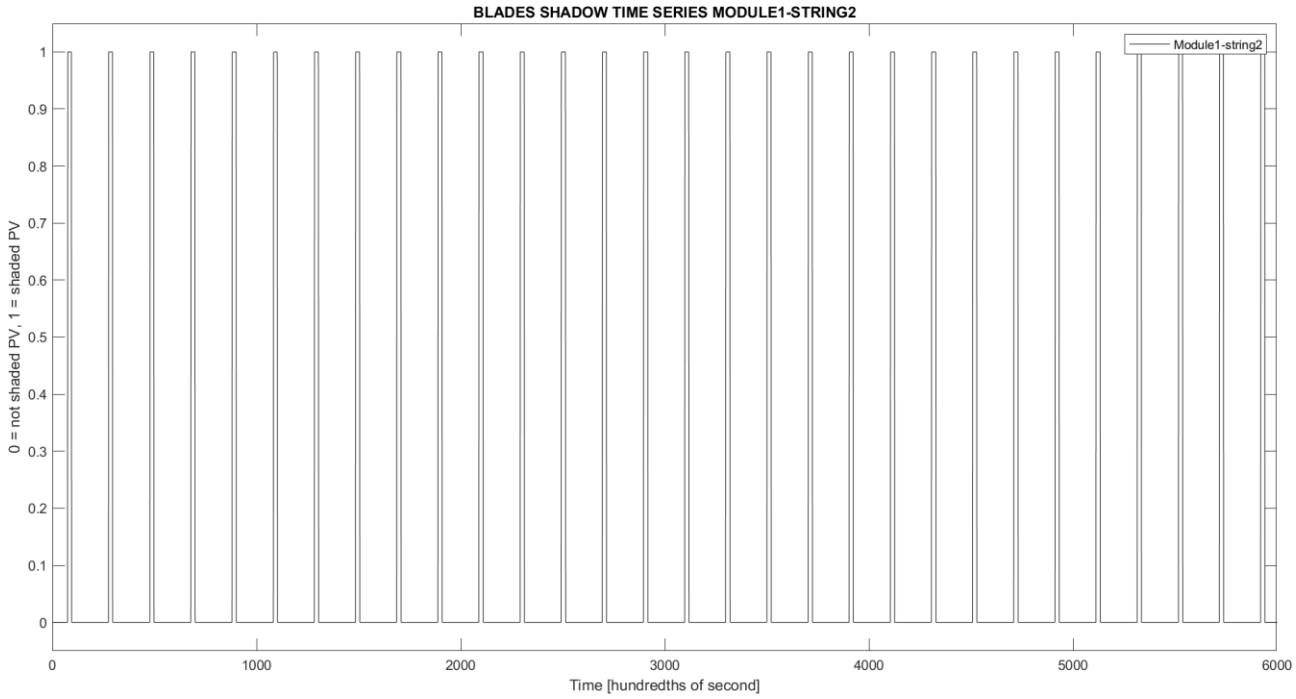

Figure 6.21. *One-minute blades shadow time series on module1-string2.*

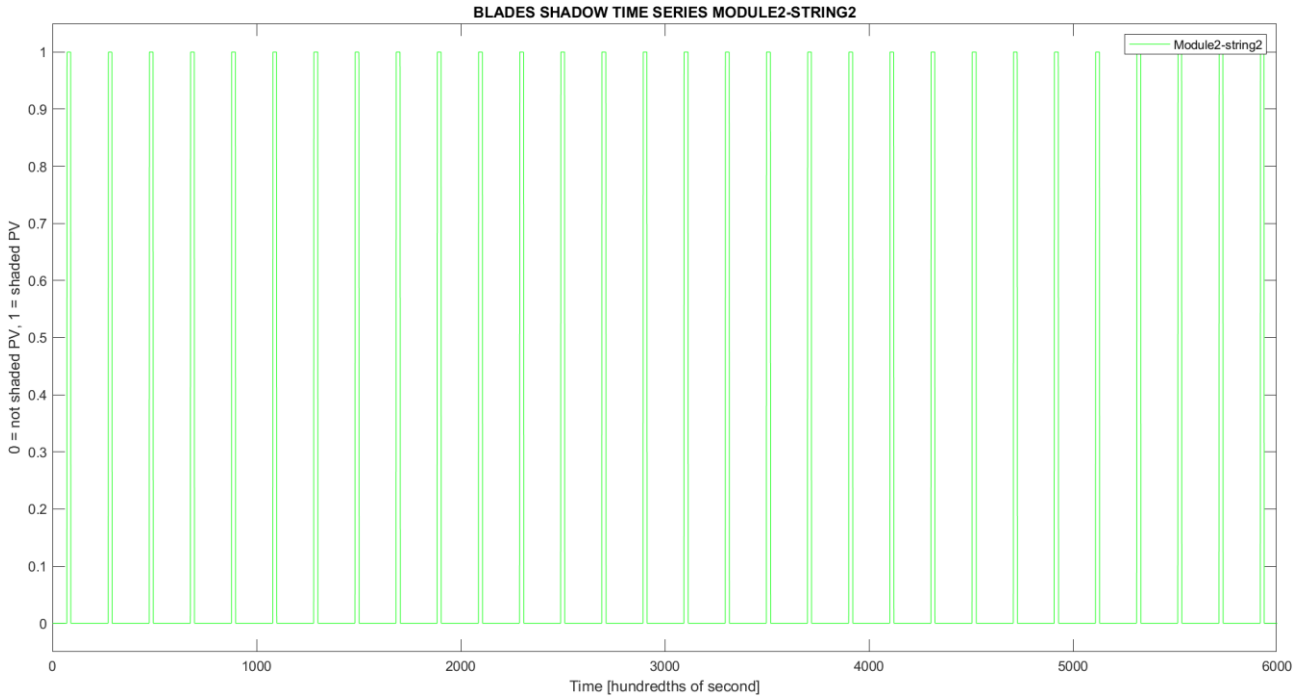

Figure 6.22. *One-minute blades shadow time series on module2-string2.*

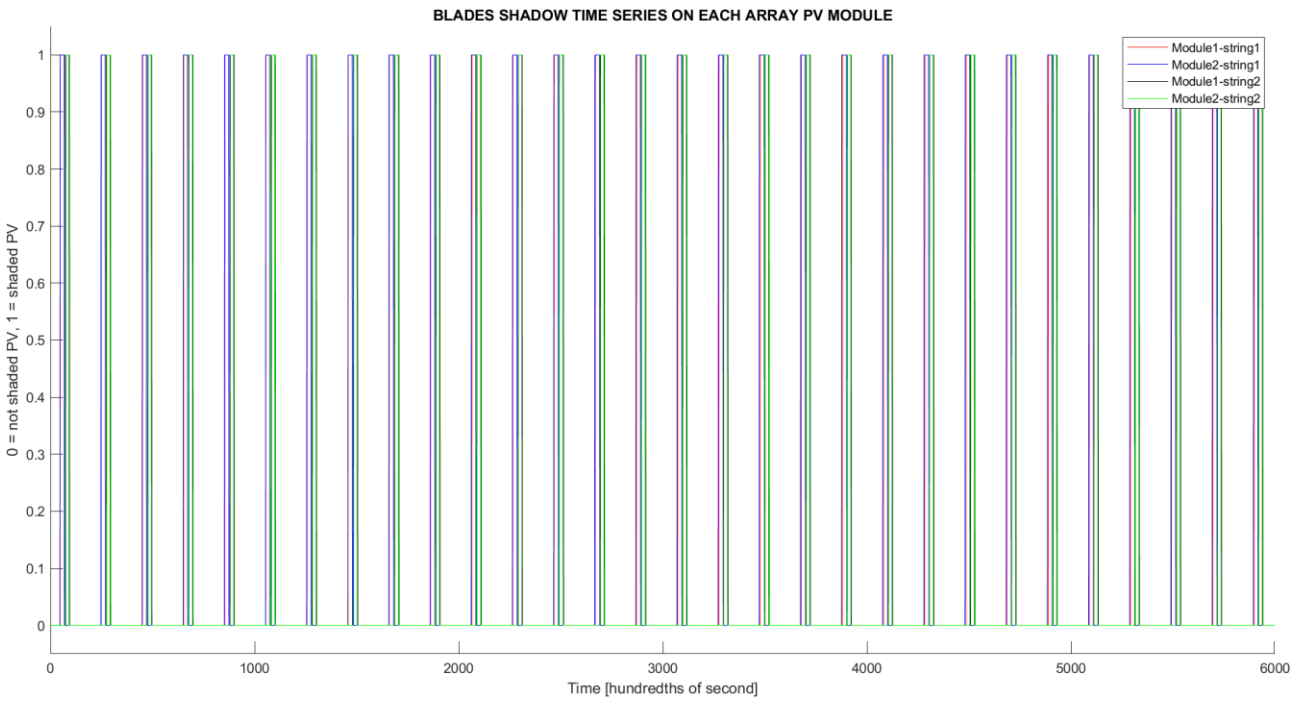

Figure 6.23. *One-minute blades shadow time series on the entire PV array, as the sum of previous charts.*

From these results, it can be noticed that shadings of the four modules overlap. In this case the average shading time of the first-string panels (module1-string1, module2-string1) is about 23 hundredths of second for module1-string1 and 24 hundredths of second for module2-string1 (27 hundredths of second for the global string), while the average time between two consecutive shadings is about 179 hundredths of second for module1-string1 and 178 hundredths of second for module2-string1 (175 hundredths of second for entire first string). For the second-string panels (module1-string2, module2-string2), the average shading time is about 22 hundredths of second for module1-string2 and 20 hundredths of second for module2-string2 (24 hundredths of second for the whole second string), while the average time between two consecutive shadings is about 180 hundredths of second for module1-string2 and 181 hundredths of second for module2-string2 (177 hundredths of second for entire second string). The average time between the start of module1-string1 shading and the start of module1-string2 shading is about 24 hundredths of second; whereas the average time between the start of module2-string1 shading and the start of module2-string2 shading is about 25 hundredths of second. Instead, the average time between the start of module2-string1 shading and the start of module1-string1 shading is about 4 hundredths of second; whereas the average time between the start of module2-string2 shading and the start of module1-string2 shading is about 3 hundredths of second. All these values were taken from a graphical analysis of Figure 6.23. Refer to APPENDIX E(5) for the complete script, from which other interesting graphs can be replicated by running it.

CHAPTER 7

DYNAMIC ANALYSIS OF A SIMPLE PV ARRAY OUTPUT

In the previous chapter, the shadow evolution of a three-bladed turbine over an entire day and shading instants over smaller periods on a single PV module surface and on a simple array were analysed. Now the target is showing what happens to the same small array made by two strings with two modules in series in terms of performance, so how DC voltage, current and power change over one minute (with the same shading evolution seen in paragraph 6.4). In other words, its dynamic behaviour will be assessed by a MATLAB related software package: SIMULINK. "SIMULINK is a block diagram environment for multidomain simulation and Model-Based Design. It supports system-level design, simulation, automatic code generation, and continuous test and verification of embedded systems. SIMULINK provides a graphical editor, customizable block libraries, and solvers for modelling and simulating dynamic systems" [36]. Therefore, SIMULINK is a graphical environment that can be used for modelling and simulating dynamic systems; it is capable of analysing a model behaviour for a certain time period by a continuous or discrete way. In fact, for each instant of interest (which is indicated into model settings, where assessment time and variable or fixed time step analysis, along with the equation solver, can be chosen) it makes all calculations and gives results. It is possible to create block diagrams, where each block represents or describes a part of the system like a physical component, a subsystem or a function. A block is completely defined by a mathematical or logical relationship between its input and output signals (SIMULINK gives libraries of blocks, ordered depending on their functionality). A SIMULINK model can be organized in hierarchical systems, from the higher to lower ones, depending on detail level, making the understanding of a model and its simulation easier. Then, a single system can be composed by many subsystems, connected by their input-output signals. Signals are depicted by lines in SIMULINK and they show the data transfer from different blocks; they can be a matrix, a vector, a scalar, with different type of precision (double, single, …). Each block or subsystem has one or more input and output ports (created by inport and outport blocks), where the data exchange from a lower level to the higher ones occur. A complex and an easier model, composed only by

SIMULINK blocks and signals (SIMSCAMPE libraries are not considered now), are going to be presented with their structures and outcomes.

- **COMPLEX PV ARRAY SIMULINK MODEL**

The PV array block diagram model was created starting from the division of all its components into different levels and subsystems. In the top level just the starting inputs from constant blocks, the MATLAB function blocks describing shading, the PV array subsystem block and the scope blocks for graphical visualisation over time of results are present. The inputs, that can be decided by user, are always the same ones seen inside previous MATLAB models: the North-South barycentre position ($TAPVA_{distance}$ [m]), the West-East one ($TANSTA_{distance}$ [m]), the day number [-], the hour [h] and minute [min]. As introduced before, the constant blocks from "sources library" are employed to generate the starting scalar signals. Since a continuous dynamic study is made for every hundredth of second in one minute, the time instant during a simulation is considered by a clock block (sources library again) but multiplied by one hundred by a gain block (math operations library), since the clock block output unit is second and the MATLAB function blocks need hundredth of second to do all calculations. Inside model settings window, the start simulation time is set to 0 s and the stop time to 60 s, with a fixed time step equal to 0.01 s; the solver is automatically selected by software (automatic solver selection). In this way SIMULINK will do all computations and block diagram model simulations for each hundredth of second over one minute. The scope blocks show PV array DC voltage (V), current (A) and power (W) evolution. A mux block (signal routing library) is used to create a single vectorial signal from the scalar input signals produced by constant blocks. Then, this vectorial signal enters four MATLAB function blocks, that are used to understand if at a certain instant each panel is shaded or not. The output scalar signals from these blocks can be zero, if panel is shined, or one, if it is completely shaded by WTG blades (only the blade shadows are taken into account, since they are responsible for array performance fluctuations); complete module shading is considered for simplicity, partial shading is not evaluated. The MATLAB code inside these function blocks can be seen inside APPENDIX F.

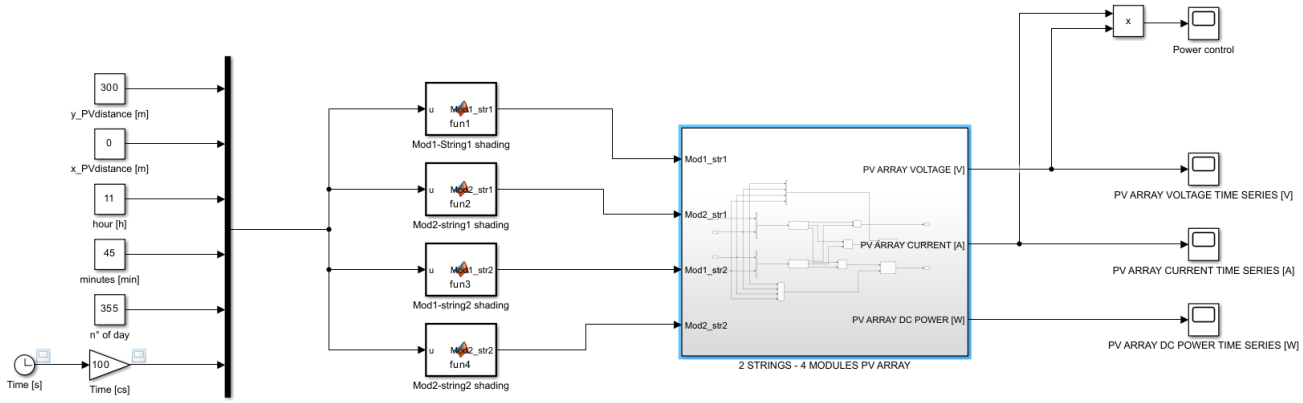

Figure 7.1. *Top level PV array block diagram.*

These one and zero outputs are the next subsystem inputs, that is the PV array subsystem, and then its two strings. The two strings signal connections are highlighted by one minmax and two add blocks (math operations library). The max block is used for calculating PV array voltage, taking the maximum voltage between the two strings at each time step, while current and power are calculated by adding string1 and string2 output values. Afterwards, two MATLAB function blocks are introduced: they point out the effect and behaviour of the two blocking diodes that are series connected to each string. Their aim is to avoid the reversal of the current flowing inside a string, due to the voltage difference between the two strings in parallel because of different shading; indeed, varying the irradiance reaching sensible surfaces, modules are not more generators but loads. The presence of bypass diodes, antiparallel connected to series of cells, avoids hot spots formation and panel degradation, but a voltage difference between strings occurs. For simplicity, the blocking diode model is the ideal switch one (ideal circuit breaker), assuming that its voltage drop is negligible. When two strings with different voltages are parallel linked, blocking diode avoids this situation by “opening” the string electrical circuit having the lower voltage, because it is reverse biased. Thus, the PV array current and power outcomes depend on blocking diodes behaviour: for example when a string is completely shined but the other one has one of the two modules shaded, the blocking diode “opens” the circuit (when a diode is reverse biased, its flowing current is very small) and approximately current and power outputs are merely the ones of the fully shined string (considering the voltage drop along bypass diodes negligible again). An add block is used to calculate the number of panels that are shadowed; its output scalar signal is one of the inputs of the MATLAB function block for blocking diodes power behaviour. The blocking diodes current and power MATLAB scripts are present inside APPENDIX F.

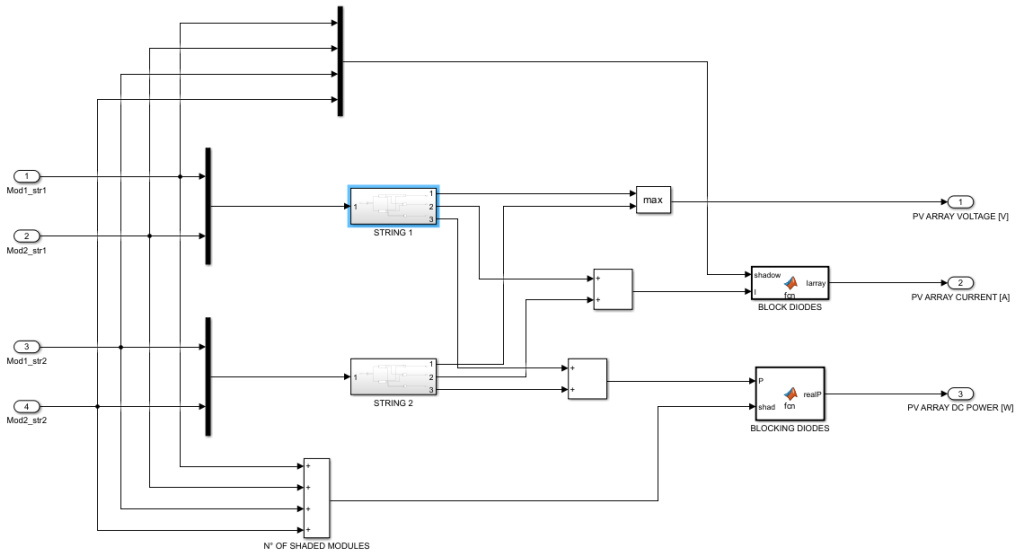

Figure 7.2. *PV array subsystem block diagram.*

Subsequently, inside both string levels, there are two panel subsystems that are series connected. Their inputs are still the one or zero scalar from the top-level shading MATLAB function blocks, while their outputs are MPP voltage, MPP current and peak power. For the sake of simplicity, it was considered that each PV array panel is equipped with a MPPT algorithm and a control system, that are able to instantly pursue the maximum power point of module I-V electrical curve when irradiance condition change (even if this is obviously not true, since such a configuration is highly expensive and mostly used MPPT algorithms, as "perturb and observe" and "incremental conductance", need time to find the right MPP). This is the reason why, in this model, it is supposed that the modules always generate in each instant their MPP current and have their MPP voltage at poles.

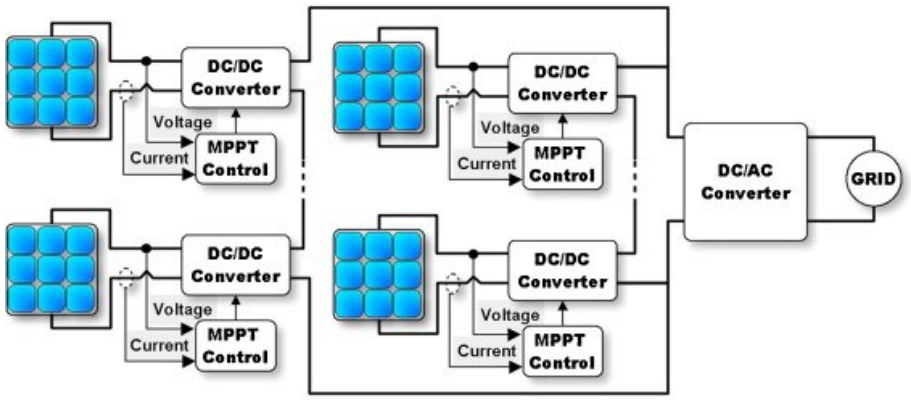

Figure 7.3. *Drawing of assumed PV array structure. Source: "modeling of photovoltaic fields in mismatched conditions for energy yield evaluations". G.Petrone, C.A. Ramos-Paja.*

There are the add and minmax blocks again, for computing string total voltage, power and current respectively. Another assumption is that even the bypass diodes of modules are considered as their ideal switch model, with negligible voltage drop and their flowing current equal to the one generated by shined module in the string, when their panel is shaded.

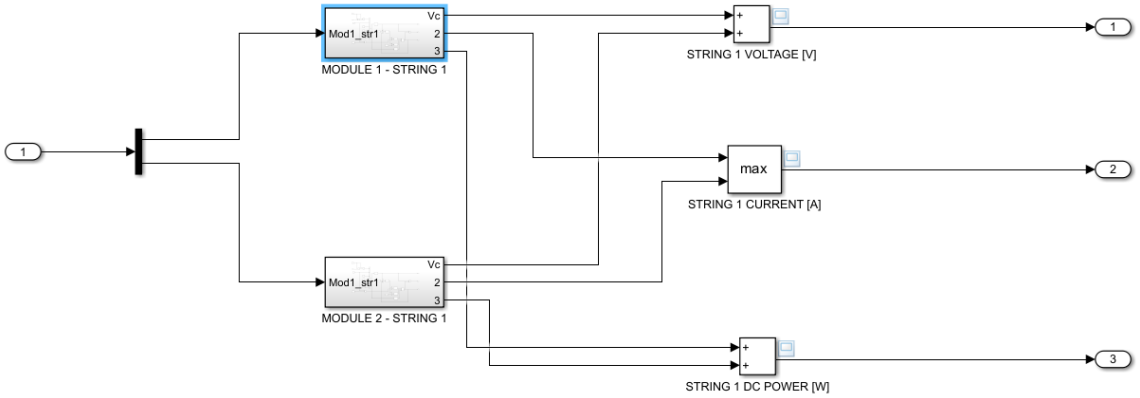

Figure 7.4. *PV string subsystem block diagram.*

The PV module subsystems are the last levels. Here the input signals are the solar irradiance G value ($\frac{\mathrm{kW}}{\mathrm{m^2}}$), the module operating temperature T_{mod}, the STC short-circuit current (18.5 A), the STC MPP voltage (38.3 V), Isc (α = 0.0004 $°C^{-1}$) and Vmpp (γ = -0.0034 $°C^{-1}$) temperature variation coefficients of the TRINASOLAR VERTEX panel, taken from its catalogue (APPENDIX A). The solar irradiance and blades shading effect on modules is computed by using a product and a subtract block, to obtain the desired G value depending on the fact that, in that instant, shading occurs. The module block diagram was built considering its electrical single diode equivalent circuit, the same of a single cell. Its parameters were obtained by the usage of a SIMSCAPE ELECTRICAL block, the PV array block, after inserting all panel data from datasheet. The parameters are achieved by an optimization function fitting module data: the diode saturation current Io at STC temperature (25°C) equal to $6.494 \cdot 10^{-12}$ A, the diode quality factor n that is about one, the series resistance equal to 0.156 Ω and the parallel resistance equal to 92.3 Ω. The block diagram layout of a panel is generated starting from a PV module single diode equivalent circuit (see figure 2.5). All electrical quantities are obtained by MATLAB function blocks. As written before, the voltage (V) applied at module poles is Vmpp (because of MPPT presence), calculated by equation

$$V_{mod} = V_{mpp}(STC) \cdot \left(1 + \gamma \cdot (T_{mod} - 25°C)\right) + \left(A \cdot \ln\left(\frac{G}{\frac{1kW}{m^2}}\right)\right) \quad (7.1)$$

and A is equal to

$$A = \frac{M \cdot n \cdot k \cdot T}{q}, \quad (7.2)$$

with $M = \frac{132}{2} = 66$ being the number of series connected cells in the module (132 is the total number of cells in a module, 2 is the number of strings in parallel since panel is bifacial), n the "non-ideality factor", k the Boltzmann constant, T the panel working temperature in Kelvin and q the unitary charge. The actual panel short-circuit current Isc (A) is computed by equation (2.29). The diode voltage instead by function

$$V_d = V_{mod} + (R_s \cdot I_{mod}) \quad (7.3)$$

where Rs is the module series resistance and I_{mod} is the real current emitted by module (A), calculated inside one of the subsequent MATLAB function blocks (iterations logically happen for diode voltage evaluation). The diode current (A) is computed from equation

$$I_d = I_0 \cdot (e^{\frac{q \cdot Vd}{66 \cdot n \cdot k \cdot T_{mod}}} - 1) \quad (7.4)$$

where q is the elementary charge (C), V_d is the diode voltage (V), n is the "non-ideality factor", k is the Boltzmann constant (J/K), T_{mod} is the panel working temperature (K) and 66 is the number of series connected cells. To account for diode saturation current temperature dependence, an equation considered inside the solar cell block (SIMSCAPE ELECTRICAL library) is exploited:

$$Isat = Io \cdot \left(\frac{Tmod}{298.15\ K}\right)^{\frac{TXIS}{n}} \cdot e^{\left(\frac{Eg \cdot \left(\frac{Tmod}{298.15} - 1\right)}{n \cdot Vt}\right)} \quad (7.5)$$

where Io is the diode saturation current at measured temperature (analysis made at STC, 298.15 K), Tmod is the module temperature, TXIS is the temperature exponent of Isat, n is the diode quality factor, Eg is the energy bandgap (for silicon is 1.12 eV) and $Vt = \frac{k \cdot Tmod}{q}$ (7.6) is the thermal voltage. The shunt resistance Rp current loss is

$$I_{loss} = \frac{V_d}{R_p} = \frac{V_{mod} + (R_s \cdot I_{mod})}{R_p}. \quad (7.7)$$

The current I_{mod} (A) produced by the module is given by an add block

$$I_{mod} = I_{sc} - I_d - I_{loss} \quad (7.8)$$

that will be used in another iteration as input for diode voltage and current computations.

Finally, DC power Pmod (W) is

$$P_{mod} = V_{mod} \cdot I_{mod}, \quad (7.9)$$

output from a product block.

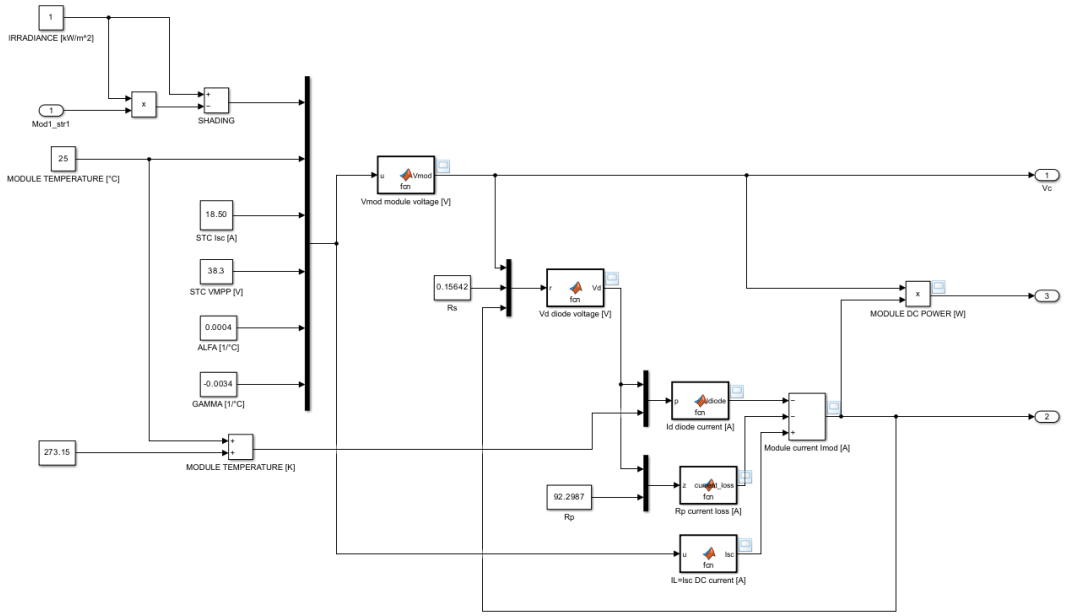

Figure 7.5. *PV panel subsystem block diagram.*

All the resulting outputs from every single module block diagram rise towards higher subsystem levels until the PV array one, giving in this way the overall outcomes to scope blocks, where results evolution over one minute can be displayed. The input data considered was the North-South barycentre position ($TAPVA_{distance}$) equal to 300 m, the West-East one ($TANSTA_{distance}$) equal to 0 m, at Winter solstice (on the 21st of December, day number 355) and time 11:45 am (hour = 11, minutes = 45). All modules were considered shined in STC: irradiance (1 $\frac{kW}{m^2}$) and working temperature of 25°C. The charts below are taken from module1-string1 block diagram.

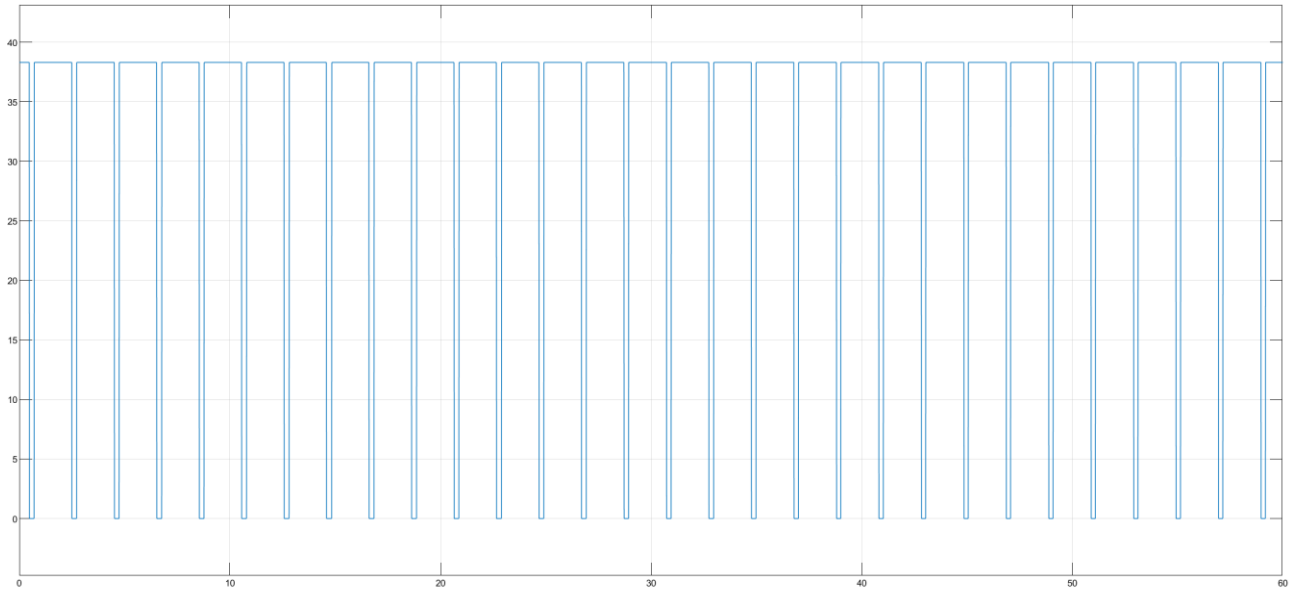

Figure 7.6. *Module1-string1 voltage Vmod (V).*

The module1-string1 voltage Vmod varies between 38.3 V when shined and 0 V when shaded.

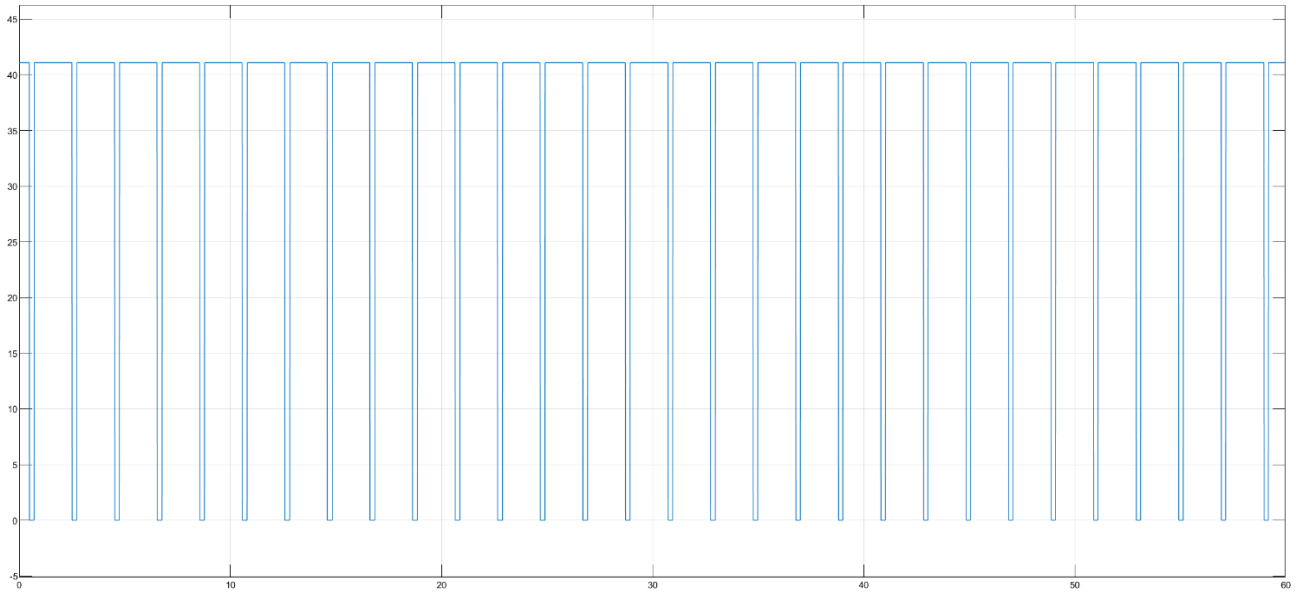

Figure 7.7. *Module1-string1 diode voltage Vd (V).*

The module1-string1 diode voltage Vd changes between 41.09 V when shined and 0 V when shaded.

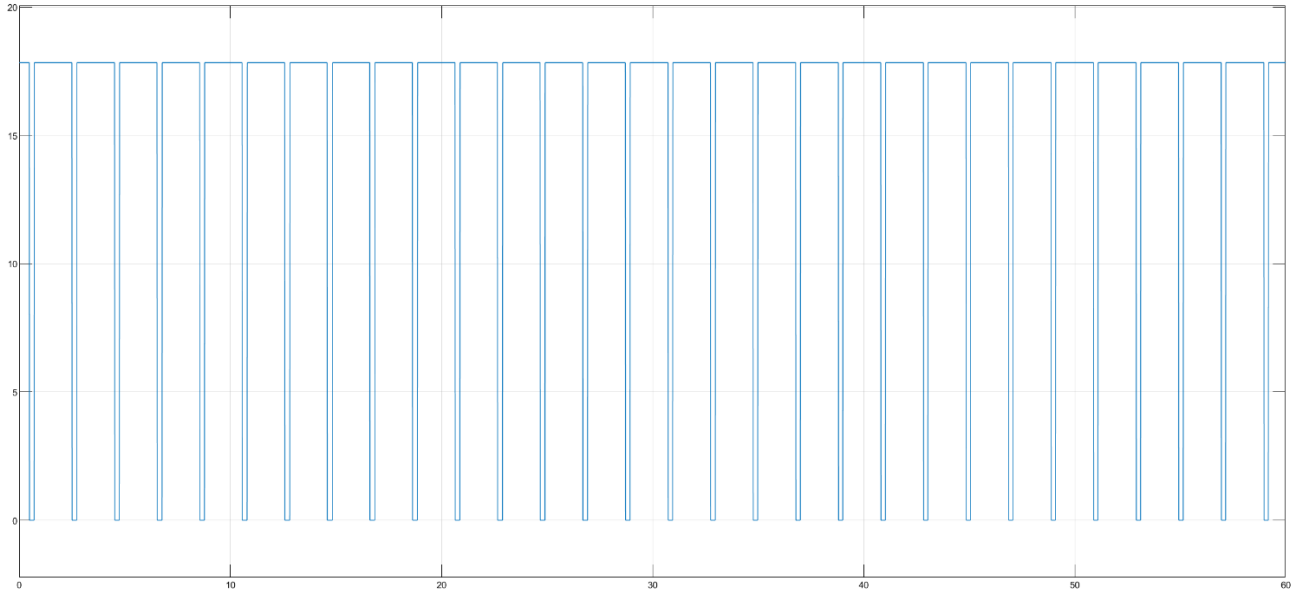

Figure 7.8. *Module1-string1 current Imod (A).*

The module1-string1 current Imod changes between 17.836 A when shined and 0 A when shaded.

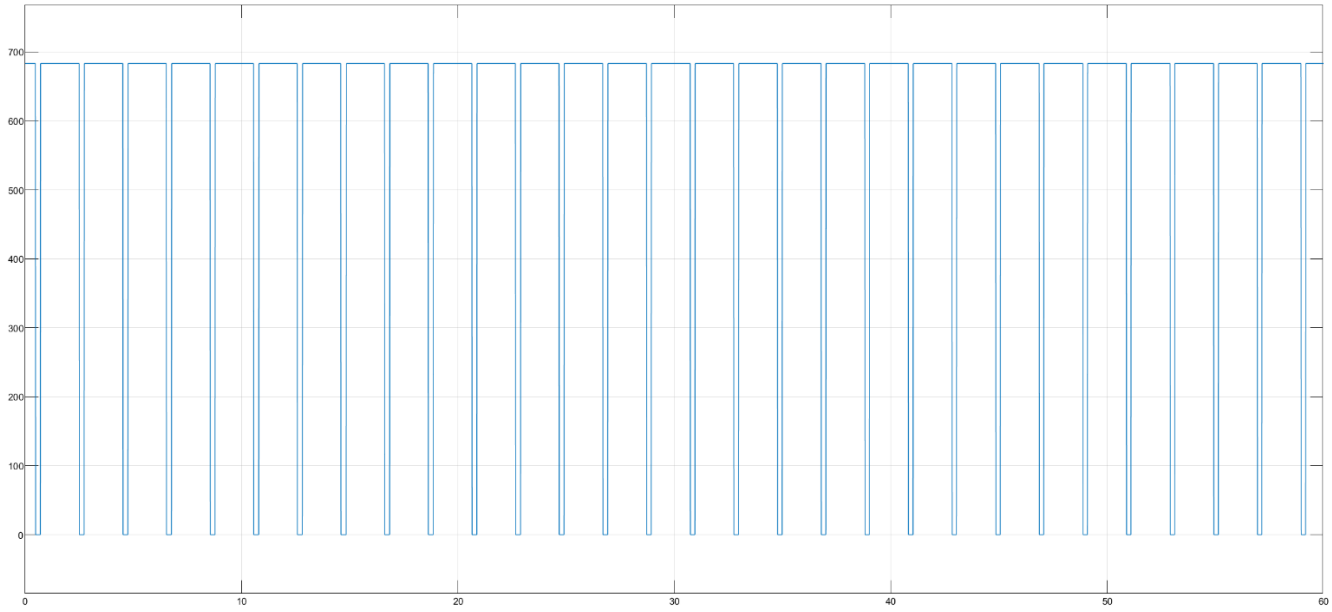

Figure 7.9. *Module1-string1 power Pmod (W).*

The module1-string1 power Pmod changes between 683.12 W when shined and 0 W when shaded.

The module1-string1 short-circuit current Isc, the maximum power point current Impp (current emitted by panel), the maximum power point voltage Vmpp (panel voltage at poles) and the peak power Pp values, calculated at different solar irradiances G and different module operating temperatures Tmod by this complex SIMULINK model, are inside following tables.

Table 7.1. *Module1-string1 outputs at various irradiances and constant working temperature (25°C).*

Gtot (kW/m^2)	Tmod (°C)	Isc_model (A)	Imod_model (A)	Vmod_model (V)	P_model (W)
1	25	18.5	17.836	38.3	683.12
0.9	25	16.65	16.043	38.121	611.58
0.8	25	14.8	14.239	37.922	539.984
0.7	25	12.95	12.427	37.695	468.462
0.6	25	11.1	10.609	37.434	397.141
0.5	25	9.25	8.785	37.125	326.16
0.4	25	7.4	6.958	36.747	255.684
0.3	25	5.55	5.128	36.259	185.942
0.2	25	3.7	3.298	35.572	117.3
0.1	25	1.85	1.47	34.397	50.564
0	25	0	0	0	0

Table 7.2. *Module1-string1 outputs at constant irradiance (1 kW/m^2) and various working temperatures.*

Gtot (kW/m^2)	Tmod (°C)	Isc_model (A)	Imod_model (A)	Vmod_model (V)	P_model (W)
1	-5	18.278	17.561	42.205	741.195
1	0	18.315	17.608	41.555	731.697
1	5	18.352	17.654	40.904	722.123
1	10	18.389	17.7	40.253	712.478
1	15	18.426	17.745	39.602	702.761
1	20	18.463	17.791	38.951	692.975
1	25	18.5	17.836	38.3	683.12
1	30	18.537	17.881	37.649	673.2
1	35	18.574	17.926	36.998	663.212
1	40	18.611	17.97	36.347	653.159

The subsequent graphs are instead taken from string1 block diagram.

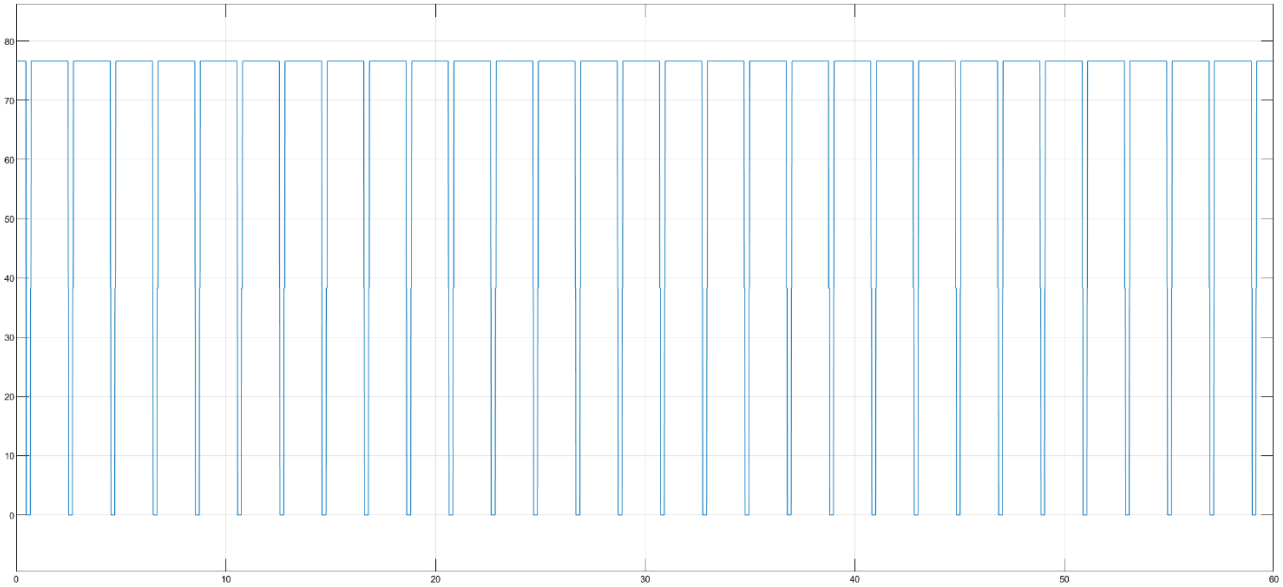

Figure 7.10. *String1 voltage (V).*

The string1 voltage varies between 76.6 V when all modules are shined and 0 V when all shaded. For some hundredths of second, the string voltage is equal to 38.3 V, i.e. when only one of the two modules is shaded.

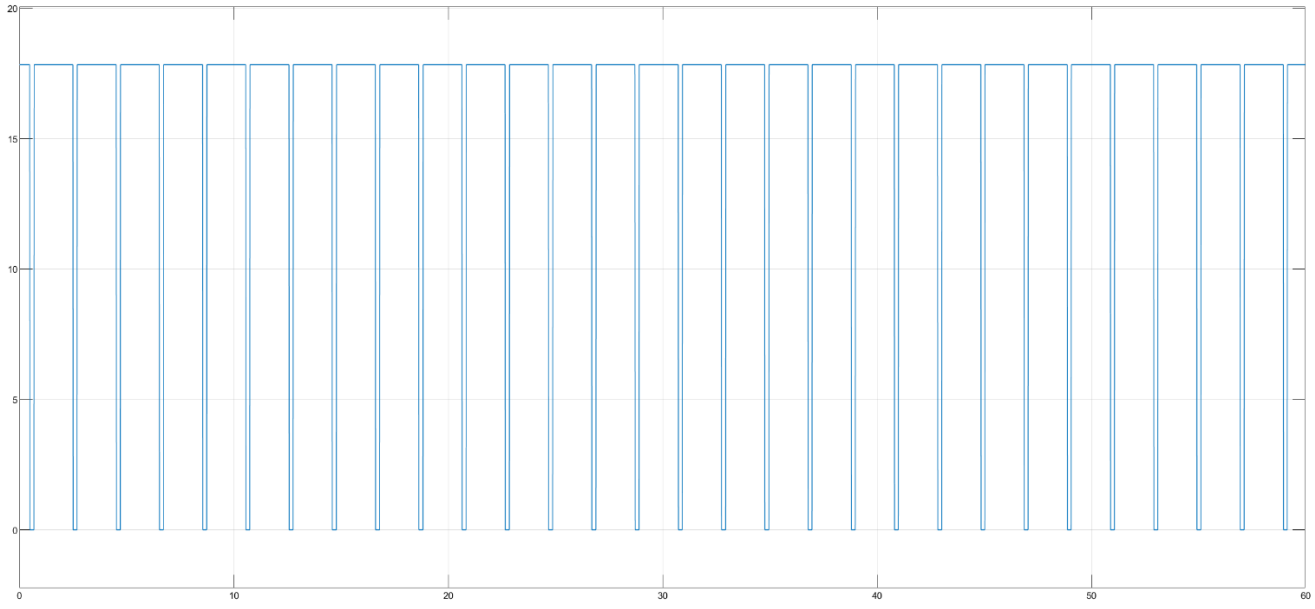

Figure 7.11. *String1 current (A).*

The string1 current varies between 17.836 A when all modules are shined (or only one) and 0 A when all shaded.

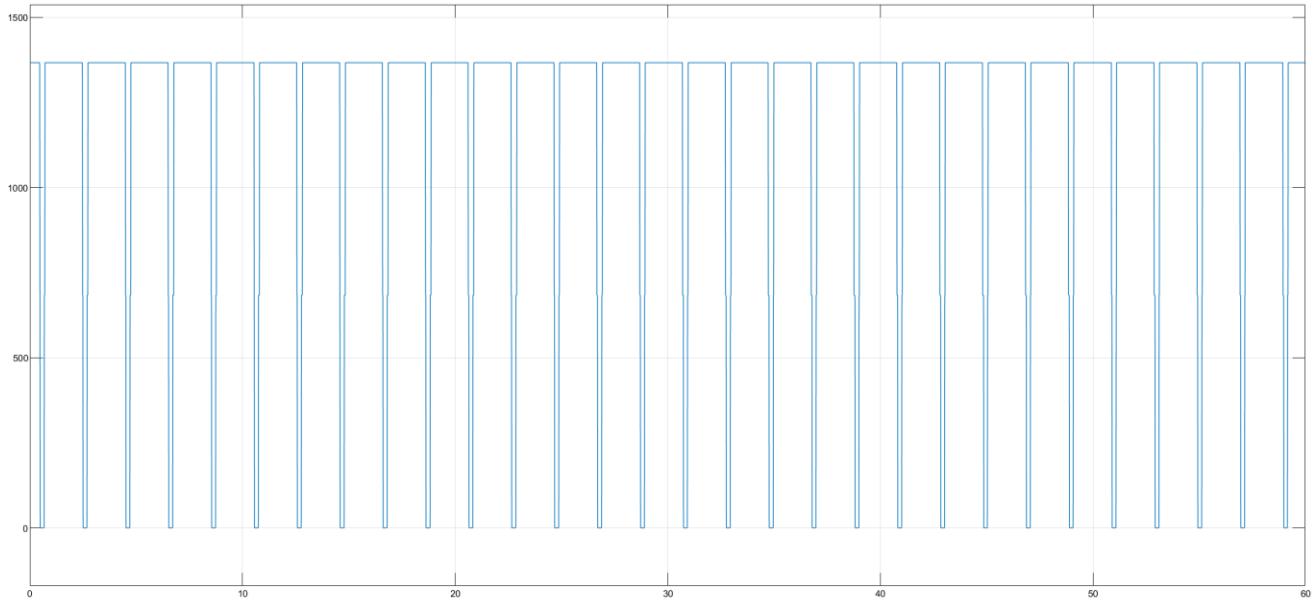

Figure 7.12. *String1 power (W).*

The string1 power varies between 1366.24 W when all modules are shined and 0 W when all shaded. For some hundredths of second, the string power is equal to 683.12 W, i.e. when only one of the two modules is shaded.

In the end, the following pictures are taken from overall PV array system scope blocks.

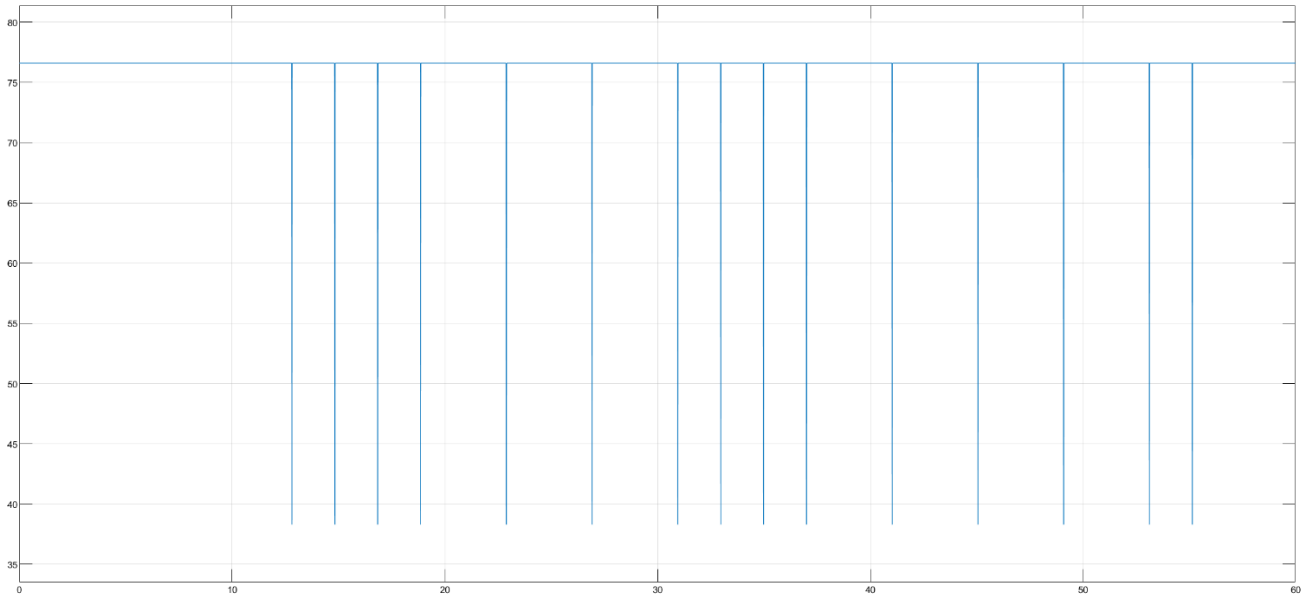

Figure 7.13. *PV array voltage (V).*

The PV array voltage varies between 76.6V, while for some hundredths of second is equal to 38.3V, with the effect of blocking diodes.

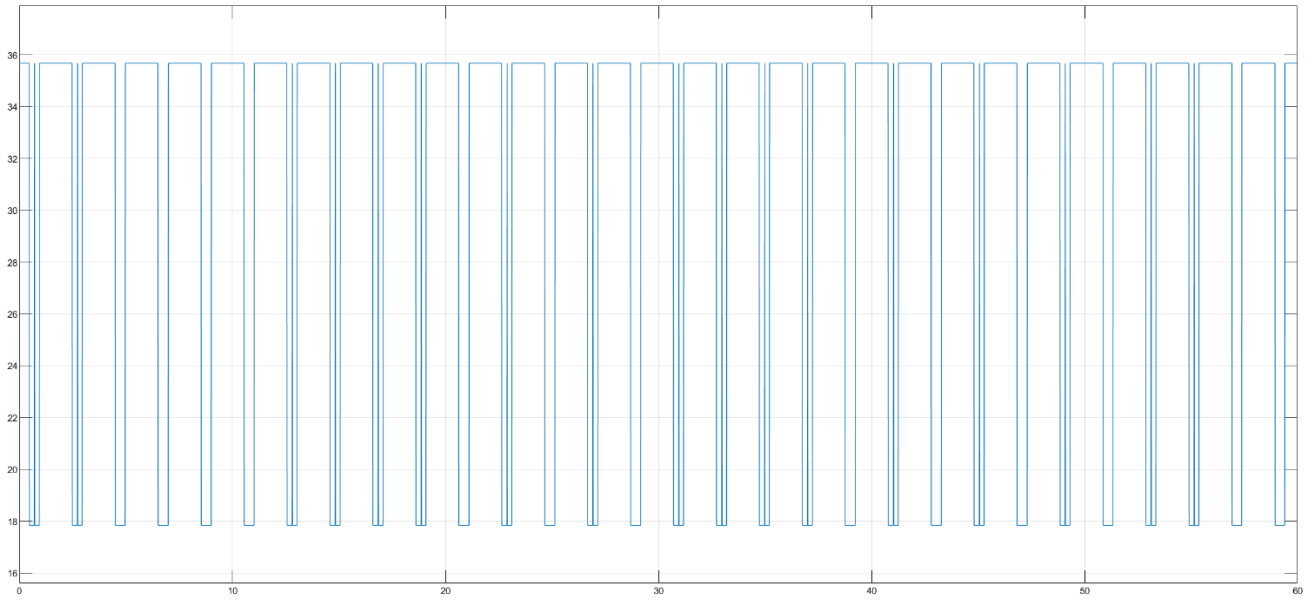

Figure 7.14. *PV array current (A).*

The PV array current varies between 35.672 A and 17.836 A, with the effect of blocking diodes.

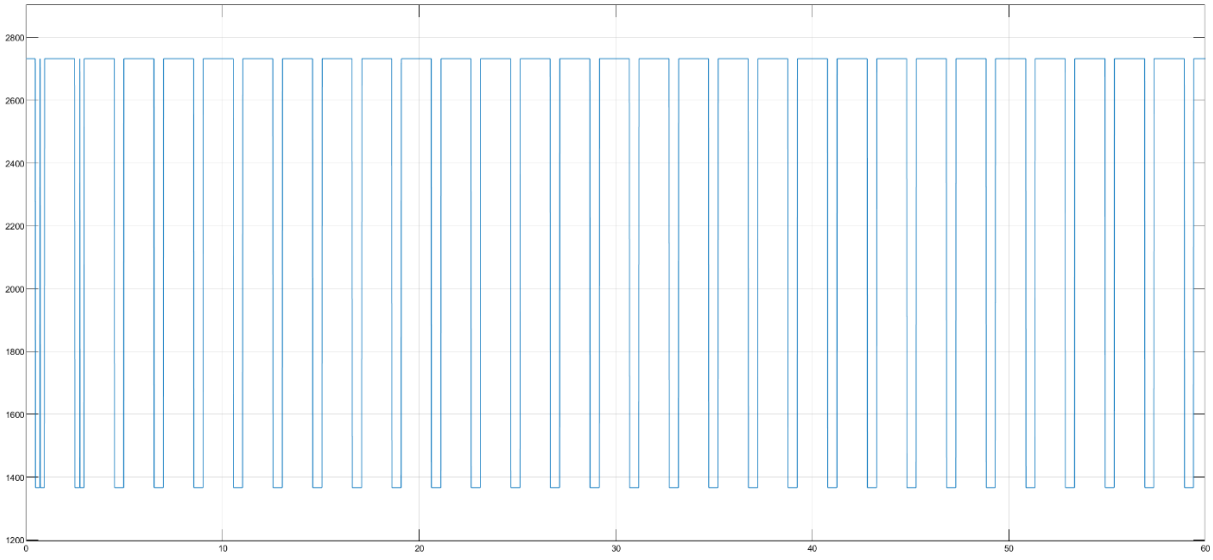

Figure 7.15. *PV array power (W).*

The PV array power varies between 2732.482 W (all modules are actually producing) and 1366.241 W (two modules are actually producing), with the effect of blocking diodes.

- **SIMPLER PV ARRAY SIMULINK MODEL**

A simpler PV array SIMULINK block diagram can be obtained with the same structure and assumptions of the previously defined model, both for signal connections and hierarchical levels, but instead using the equations (2.29), (2.30), (7.1), (2.34) and (7.8) for computing Isc, Voc, Vmod, FF and Imod. Indeed, by fill factor

$$FF = \frac{Vmpp \cdot Impp}{Voc \cdot Isc} = \frac{Pp}{Voc \cdot Isc} = 0.78 \text{ from the module datasheet,}$$

once Isc and Voc are calculated, the FF can be used to get DC power P of the module and then, from the ratio between P and Vmod, Imod is obtained. By hypothesis, the FF is considered constant at all conditions of irradiance and temperature.

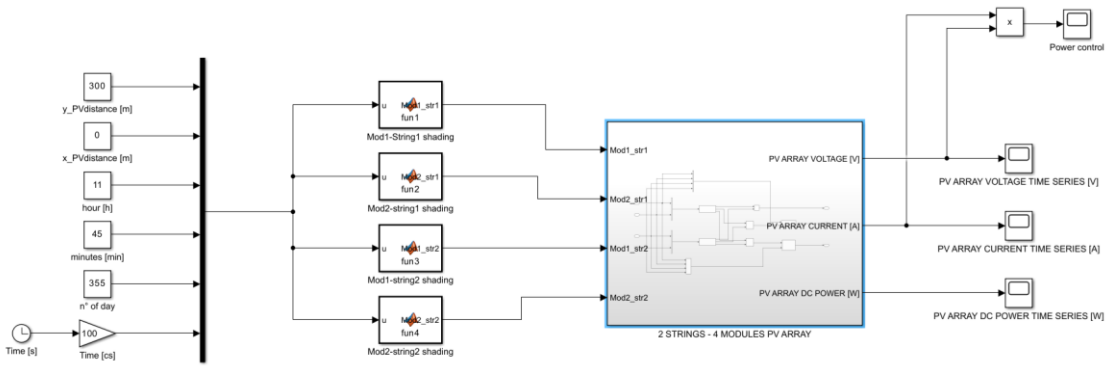

Figure 7.16. *Simpler model top level PV array block diagram.*

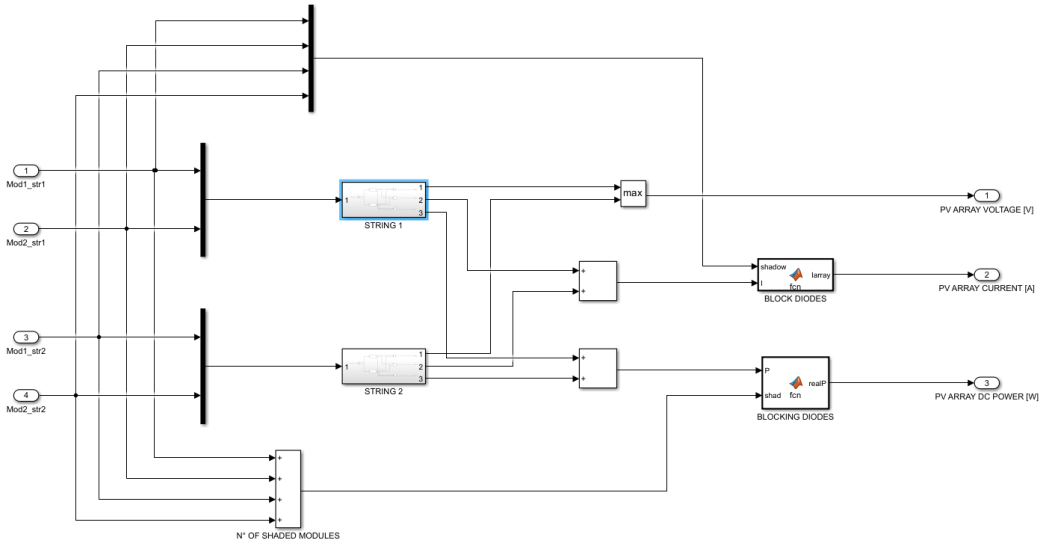

Figure 7.17. *Simpler model PV array subsystem block diagram.*

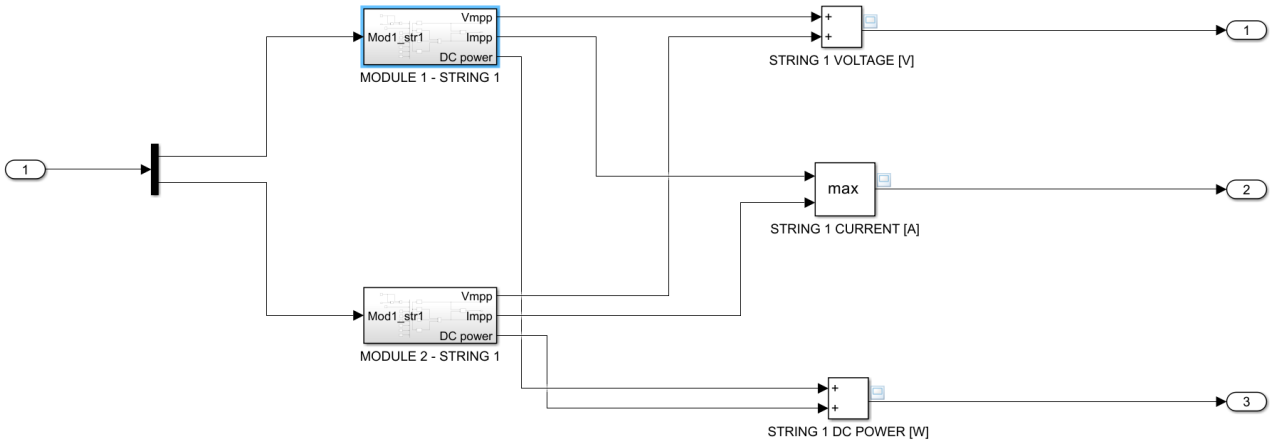

Figure 7.18. *Simpler model PV string subsystem block diagram.*

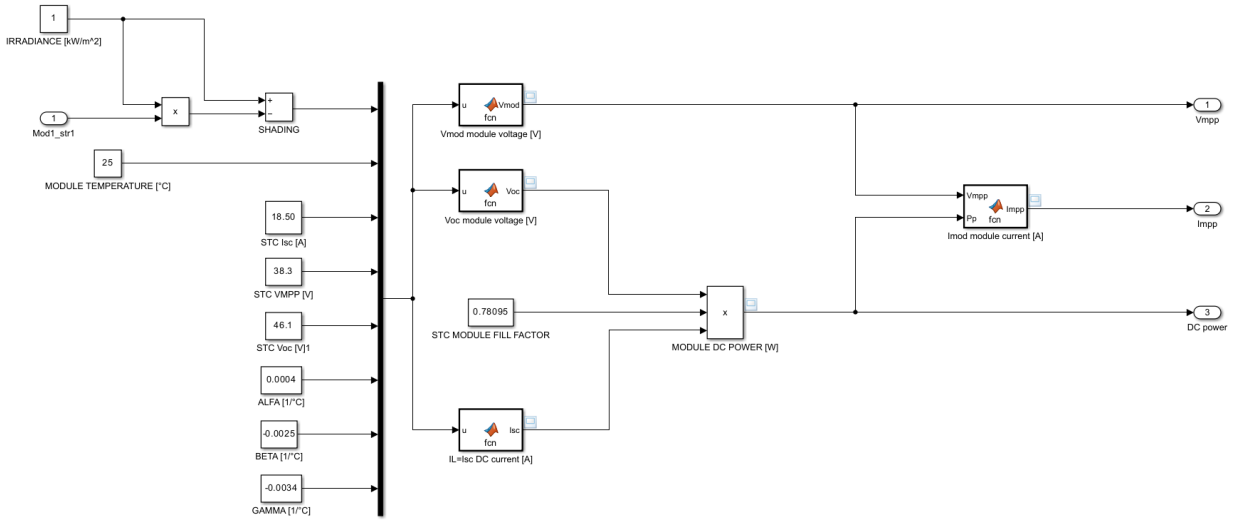

Figure 7.19. *Simpler model PV panel subsystem block diagram.*

The module1-string1 short-circuit current Isc, the current emitted by panel Imod, the voltage at module poles Vmod and the DC power P values, calculated at different solar irradiance G and different module operating temperature Tmod by this easier SIMULINK model, are inside the following tables.

Table 7.3. *Module1-string1 outputs at various irradiances and constant working temperature (25°C).*

Gtot (kW/m^2)	Tmod (°C)	Isc_model (A)	Voc_model (V)	Vmod_model (V)	Imod_model (A)	P_model (W)
1	25	18.5	46.1	38.3	17.39	666.033
0.9	25	16.65	45.921	38.121	15.663	597.108
0.8	25	14.8	45.722	37.922	13.935	528.455
0.7	25	12.95	45.495	37.695	12.206	460.109
0.6	25	11.1	45.234	37.434	10.475	392.114
0.5	25	9.25	44.925	37.125	8.741	324.529
0.4	25	7.4	44.547	36.747	7.006	257.437
0.3	25	5.55	44.059	36.259	5.267	190.964
0.2	25	3.7	43.372	35.572	3.523	125.324
0.1	25	1.85	42.197	34.397	1.772	60.964
0	25	0	0	0	0	0

Table 7.4. *Module1-string1 outputs at constant irradiance (1 kW/m^2) and various working temperatures.*

Gtot (kW/m^2)	Tmod (°C)	Isc_model (A)	Voc_model (V)	Vmod_model (V)	Imod_model (A)	P_model (W)
1	-5	18.278	49.557	42.207	16.76	707.394
1	0	18.315	48.981	41.555	16.859	700.584
1	5	18.352	48.405	40.904	16.96	693.74
1	10	18.389	47.829	40.253	17.064	686.863
1	15	18.426	47.252	39.602	17.17	679.953
1	20	18.463	46.676	38.951	17.278	673.01
1	25	18.5	46.1	38.3	17.39	666.033
1	30	18.537	45.524	37.649	17.504	659.023
1	35	18.574	44.947	36.998	17.622	651.98
1	40	18.611	44.371	36.347	17.743	644.903

Inside the subsequent tables, model 1 related values are the simpler block diagram results, while model 2 ones are the more complex SIMULINK model outcomes.

Table 7.5. *Differences between models at various irradiances and constant working temperature.*

Gtot (kW/m^2)	Tmod (°C)	Isc_model1 (A)	Isc_model2 (A)	Vmod_model1 (V)	Vmod_model2 (V)	Imod_model1 (A)	Imod_model2 (A)	P_model1 (W)	P_model2 (W)
1	25	18.5	18.5	38.3	38.3	17.39	17.836	666.033	683.12
0.9	25	16.65	16.65	38.121	38.121	15.663	16.043	597.108	611.58
0.8	25	14.8	14.8	37.922	37.922	13.935	14.239	528.455	539.984
0.7	25	12.95	12.95	37.695	37.695	12.206	12.427	460.109	468.462
0.6	25	11.1	11.1	37.434	37.434	10.475	10.609	392.114	397.141
0.5	25	9.25	9.25	37.125	37.125	8.741	8.785	324.529	326.16
0.4	25	7.4	7.4	36.747	36.747	7.006	6.958	257.437	255.684
0.3	25	5.55	5.55	36.259	36.259	5.267	5.128	190.964	185.942
0.2	25	3.7	3.7	35.572	35.572	3.523	3.298	125.324	117.3
0.1	25	1.85	1.85	34.397	34.397	1.772	1.47	60.964	50.564
0	25	0	0	0	0	0	0	0	0

Table 7.6. *Differences between models at constant irradiance and various working temperatures*.

Gtot (kW/m^2)	Tmod (°C)	Isc_model1 (A)	Isc_model2 (A)	Vmod_model1 (V)	Vmod_model2 (V)	Imod_model1 (A)	Imod_model2 (A)	P_model1 (W)	P_model2 (W)
1	-5	18.278	18.278	42.207	42.205	16.76	17.561	707.394	741.195
1	0	18.315	18.315	41.555	41.555	16.859	17.608	700.584	731.697
1	5	18.352	18.352	40.904	40.904	16.96	17.654	693.74	722.123
1	10	18.389	18.389	40.253	40.253	17.064	17.7	686.863	712.478
1	15	18.426	18.426	39.602	39.602	17.17	17.745	679.953	702.761
1	20	18.463	18.463	38.951	38.951	17.278	17.791	673.01	692.975
1	25	18.5	18.5	38.3	38.3	17.39	17.836	666.033	683.12
1	30	18.537	18.537	37.649	37.649	17.504	17.881	659.023	673.2
1	35	18.574	18.574	36.998	36.998	17.622	17.926	651.98	663.212
1	40	18.611	18.611	36.347	36.347	17.743	17.97	644.903	653.159

The two models are quite similar regarding their outcomes. In fact, the relative differences in percentage of the two models results, compared to the simpler model values, are present in the subsequent table.

Table 7.7. *Differences in percentage between the results of the two SIMULINK models*.

Gtot (kW/m^2)	Tmod (°C)	ΔIsc (%)	ΔVmod (%)	ΔImod (%)	ΔPmod (%)
1	-5	0	0.0047	4.7792	4.7782
1	0	0	0.0000	4.4427	4.4410
1	5	0	0.0000	4.0920	4.0913
1	10	0	0.0000	3.7271	3.7293
1	15	0	0.0000	3.3489	3.3543
1	20	0	0.0000	2.9691	2.9665
1	25	0	0.0000	2.5647	2.5655
1	30	0	0.0000	2.1538	2.1512
1	35	0	0.0000	1.7251	1.7228
1	40	0	0.0000	1.2794	1.2802

CHAPTER 8

SIMPLE PV ARRAY OUTPUT WITH MPPT

To analyse better the output produced by the simple PV array, an electrical circuit was built and a MPPT algorithm was integrated to show the dynamic of maximum power point pursuit of the whole PV generator. Two electrical circuits were made by using SIMSCAPE ELECTRICAL software, a branch of SIMULINK that contains new libraries of components for modelling and simulating electric and mechatronic systems [37]. The only difference between these two circuits is how the bypass diodes are modelled: the simpler case uses an ideal switch, the other a piecewise linear diode (unfortunately, an exponential model gave equation solution and convergence problems). The pictures below depict the SIMULINK-SIMSCAPE ELECTRICAL models created.

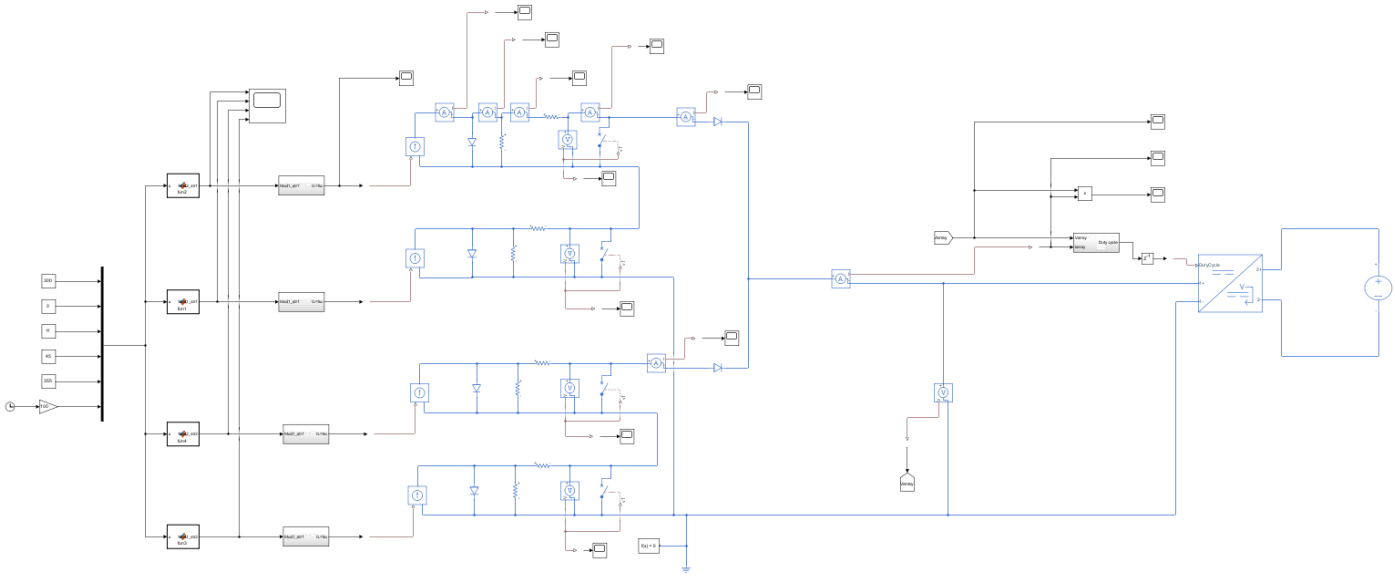

Figure 8.1. *Electrical circuit block diagram with the ideal switch bypass diodes model.*

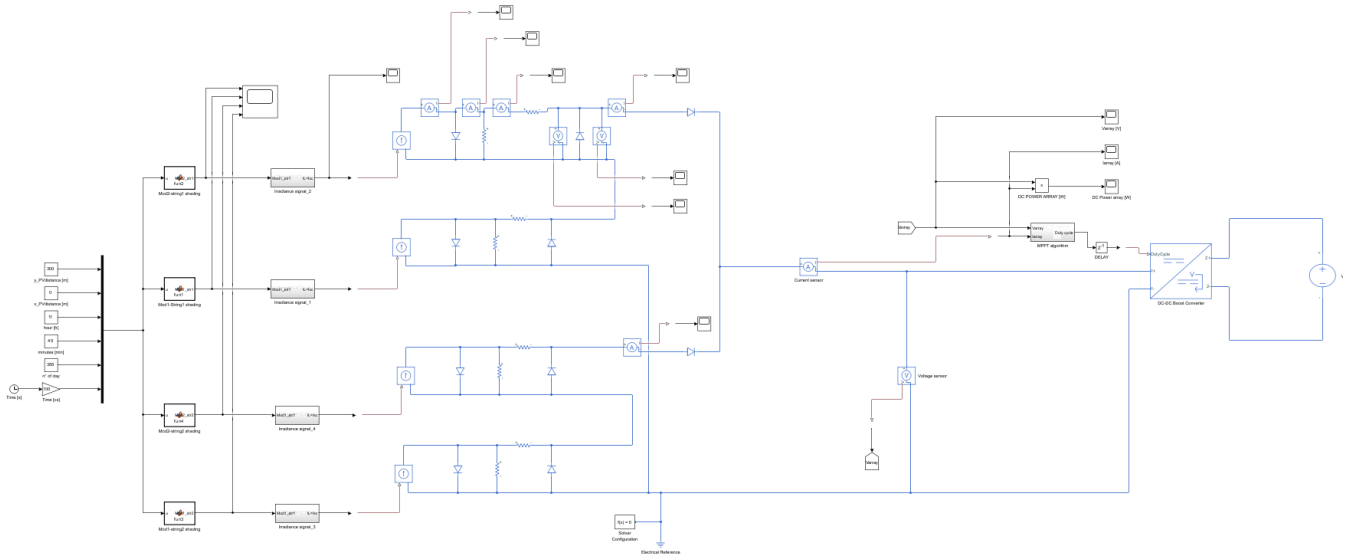

Figure 8.2. *Electrical circuit block diagram with the piecewise linear bypass diodes model.*

All blocks on the left side are the same ones seen in Chapter 7 SIMULINK models (shading on modules and overall PV generator trends are visible in the Figures 6.19, 6.20, 6.21, 6.22, 6.23). The differences with the previous diagrams start from the short-circuit current calculation subsystems (Isc=18.5 A), where it is calculated depending on module operating temperature and irradiance condition. The solar irradiance value changes from 1000 $\frac{W}{m^2}$ to 0 $\frac{W}{m^2}$ (complete shading) with the same evolution seen in previous chapters (rotating blades shadow). Afterwards, the simulink-ps converter blocks (SIMSCAPE utilities library) change the nature of those subsystem output signals from SIMULINK domain to physical one: physical signals are necessary for the usage of all SIMSCAPE blocks. To represent all four panels of the array, the single diode model is considered. It is made by a controlled current source block (electrical sources library), generating the photoelectric current depending on solar illumination, an exponential diode block (electrical elements library) and two resistance blocks for series and shunt. These single diode model parameters were obtained from a SIMSCAPE ELECTRICAL PV array block (specialized power systems, sources library) by inserting all module features from datasheet; the diode saturation current Isat is $6.494 \cdot 10^{-12}$ A, the quality factor n is 1, the series resistance Rs is 0.156 Ω and the shunt resistance is 92.3 Ω. The parameter computations are performed by an optimization function, implemented inside the PV array block, that determines these parameters to fit the module data. The following graphs are the I-V curves of a single panel and of the simple PV generator given by the PV array block.

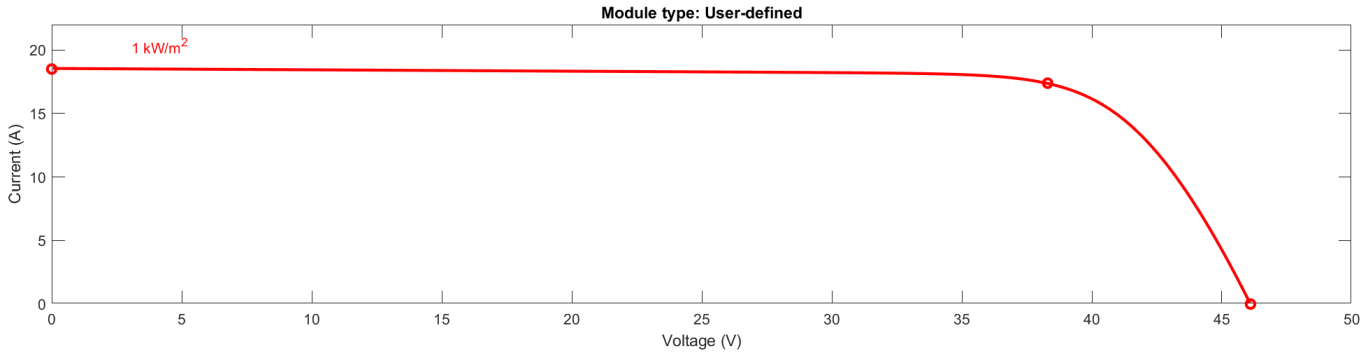

Figure 8.3. *Module I-V characteristic.*

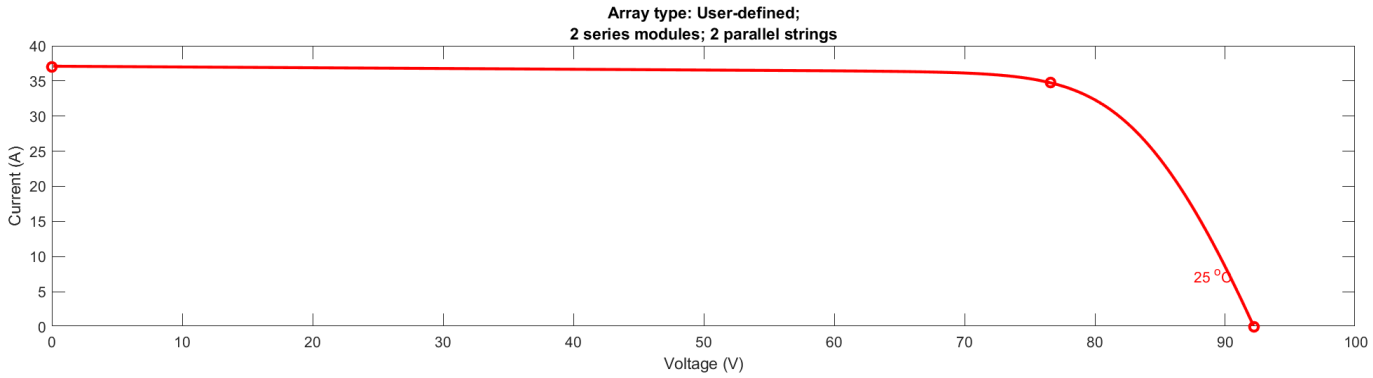

Figure 8.4. *Simple PV array I-V characteristic.*

In summary, these four single diode models approximate the four PV panels of the array, each one with different shading scenarios: module1-string1, module2-string1, module1-string2 and module2-string2. The irradiance used for measurements is 1000 $\frac{\mathrm{W}}{\mathrm{m}^2}$, while the operating temperature considered for simulation is set to 25°C (STC) and supposed constant throughout the minute period. These equivalent electrical circuits are series connected when they are in the same string, and afterwards the two strings are parallel connected: this is possible by linking the physical signals with the positive and negative outports of the blocks. The bypass diodes are connected in an antiparallel way to module equivalent circuits; they are modelled by switches with very small resistance or by piecewise linear model. In the first case the opening or closing of the switches are controlled by voltage sensor blocks, which measure the voltage at panel circuit poles that goes as a signal to switch block input. This measurement is then compared to chosen threshold voltage of the switch, i.e. 0 V: when the voltage of a panel, measured by a voltage sensor block, is higher than this threshold value (it is shined) the switch is open, otherwise it is closed (module is shaded). Indeed, when a panel is shaded, it behaves as a load and its voltage changes sign. This is the reason why threshold voltage was set to zero. In the second case, the panel protection is gained by piecewise linear model diodes with default parameters (forward voltage is 0.6 V) and infinite reverse breakdown voltage by hypothesis. Instead, the blocking diodes, that are series connected to strings,

are described by an exponential diode model; their parameters, as forward voltage, reverse breakdown voltage and reverse saturation current are the default ones. The current and voltage sensor blocks (SIMSCAPE sensors and transducers library), capable of measuring the current emitted by PV array and its voltage, produce two SIMULINK signals that are the inputs of MPPT subsystem. Besides, the PV array contacts are directly connected to a DC-DC boost converter that is controlled by a duty cycle, which is the output of the MPPT algorithm. The other side of the converter is linked to an ideal voltage generator block (SIMSCAPE sources library), able to keep a higher DC voltage than PV generator (for instance 120V).

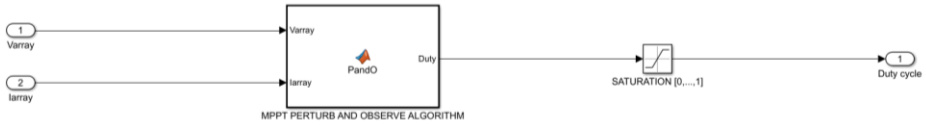

Figure 8.5. *MPPT algorithm subsystem.*

A MPPT is an algorithm that is implemented inside the solar inverter control systems and its usefulness consists of continuously adjusting the impedance seen by the PV array, allowing its operation at maximum power point when working conditions as temperature or irradiance are changing. The algorithm chosen for MPPT is “perturb and observe” (P&O), whose logic is depicted in the flowchart below [38].

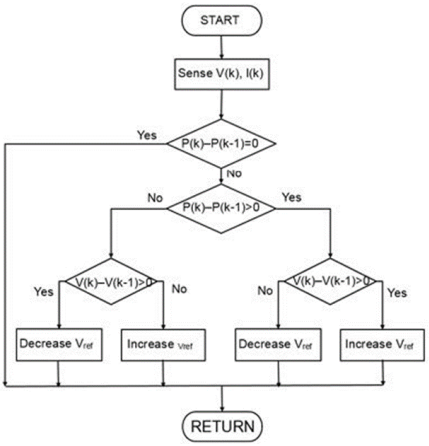

Figure 8.6. *Perturb and observe MPPT algorithm logical flowchart.*

The P&O algorithm perturbs PV array operating voltage by changing the impedance at its poles and then it calculates its power output by current and voltage measurements, comparing the new value with previous one. It continues its action until the array maximum power point is reached, even if current and voltage steadily oscillate around their MPP values. In the electrical circuit, the MPPT is implemented by a MATLAB function block, where the code describing its logical flowchart has got

a duty cycle value as output. The full MPPT script is written inside APPENDIX G (instructions for its construction are contained in a MATHWORKS video, which was followed step by step; all rights are reserved to MATHWORKS [38]). The same MPPT algorithm can be implemented in the circuit by a logical stateflow chart (APPENDIX G). The chosen duty cycle step (deltaDuty in the code) is 0.1% (acceptable since some papers performs the MPPT analysis with smaller values, like 0.05%), whereas the MPPT update rate is 100 Hz (the update frequency can be much higher than this value too, for example 500 Hz [39]); this means that a simulation and thus PV array current and voltage measurements occur every hundredth of second. This value was chosen to better follow all possible irradiance variations due to the blade shadow effect. A saturation block (SIMULINK discontinuities library) enables to keep duty cycle values in the range between zero and one, then it exits from the subsystem and, before reaching the DC-DC boost converter, it is held one iteration time step by a delay block (SIMULINK discrete library). A solver configuration block (SIMSCAPE utilities library), along with an electrical reference block (SIMSCAPE connectors & references library), must always be connected to a circuit and they are fundamental to start calculations. The period considered is one minute again, with one hundredth of second fixed time steps and solver automatically chosen by software. The next pictures show the evolution of PV array DC voltage, current and power with the operation of MPPT, having irradiance variations on panels, for the circuit having piecewise linear bypass diodes (results are like the ideal switch bypass diodes case).

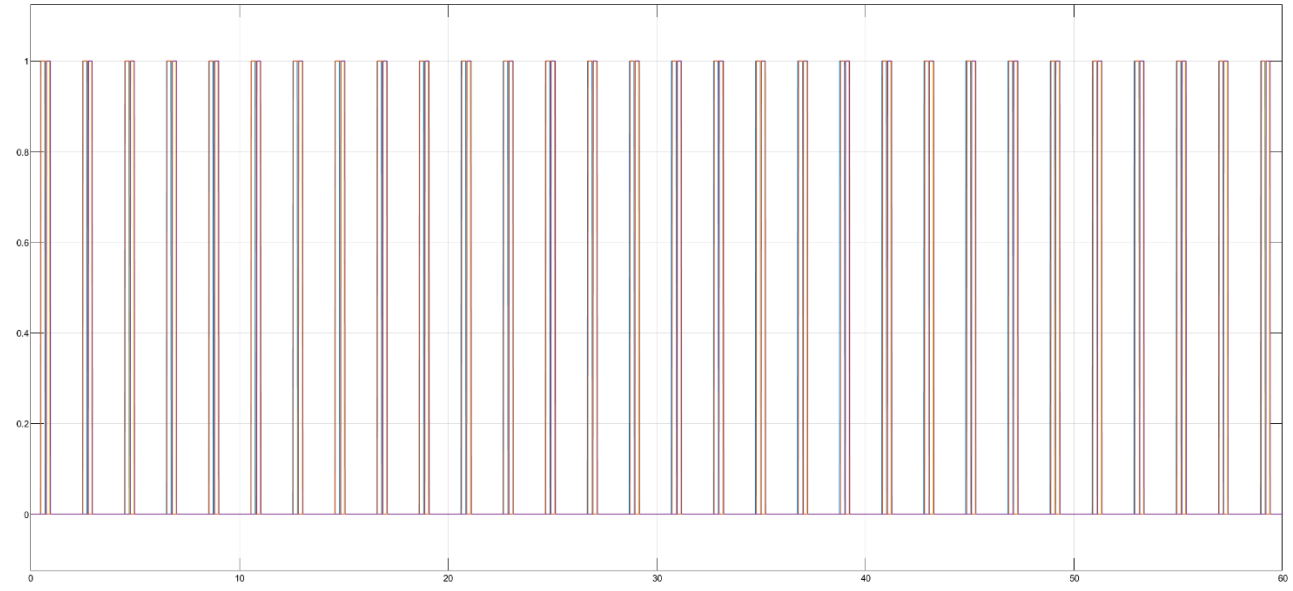

Figure 8.7. *PV array panels shadow evolution over one minute.*

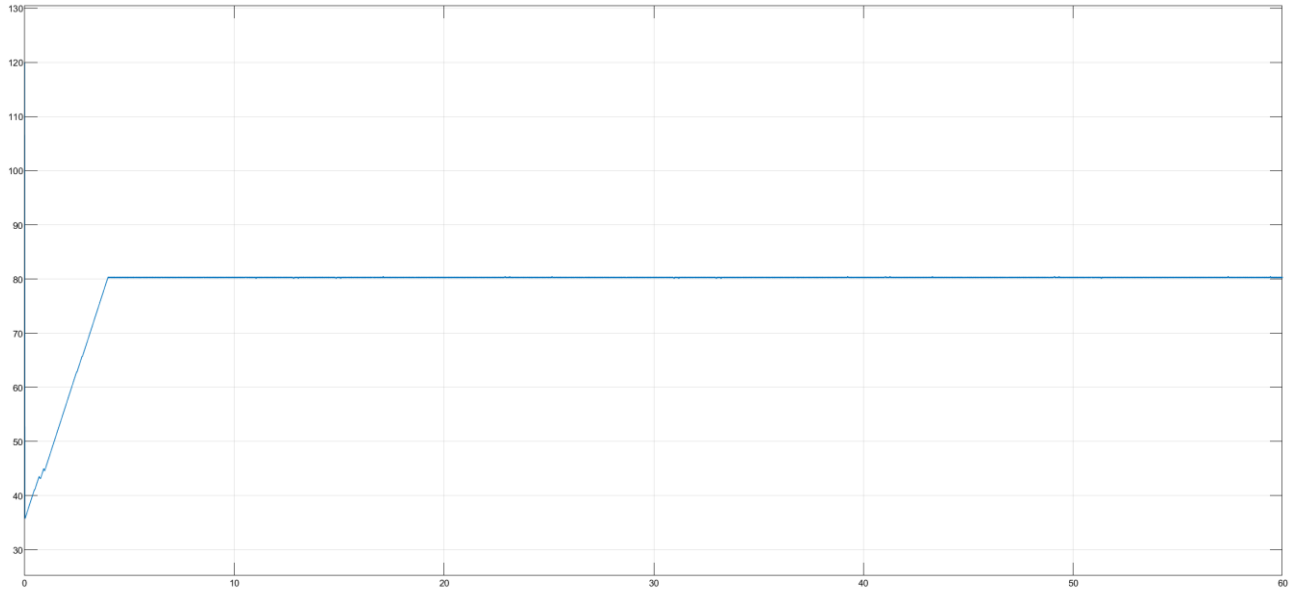

Figure 8.8. *PV array voltage evolution over one minute, controlled by MPPT.*

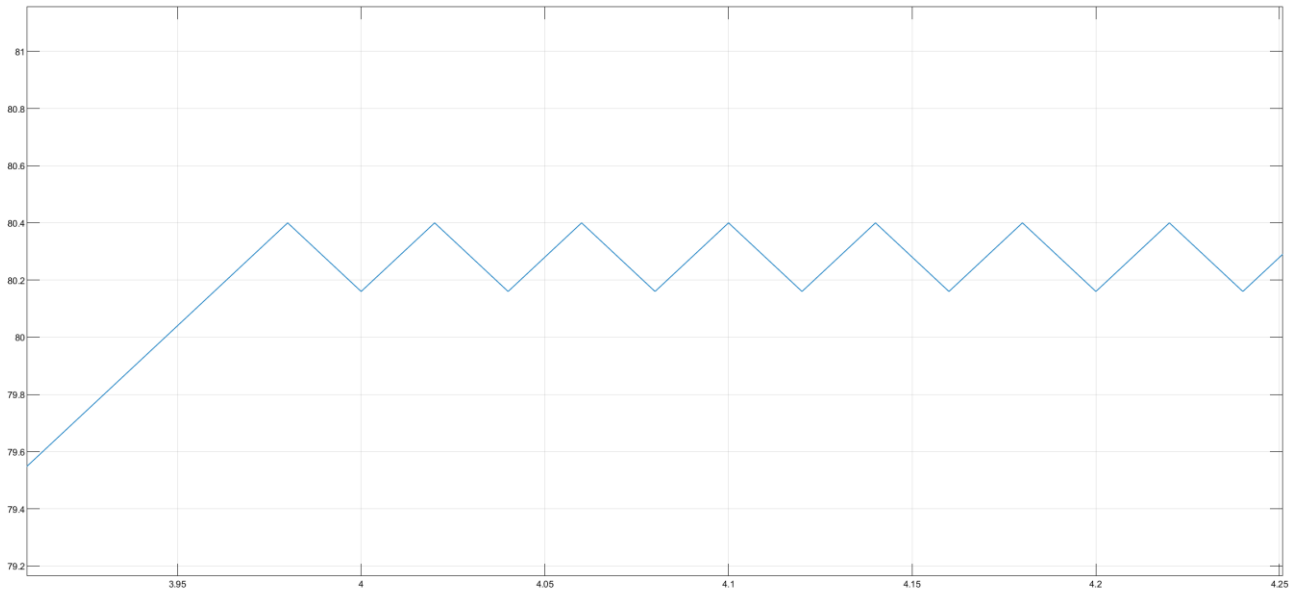

Figure 8.9. *MPPT operation on PV array voltage.*

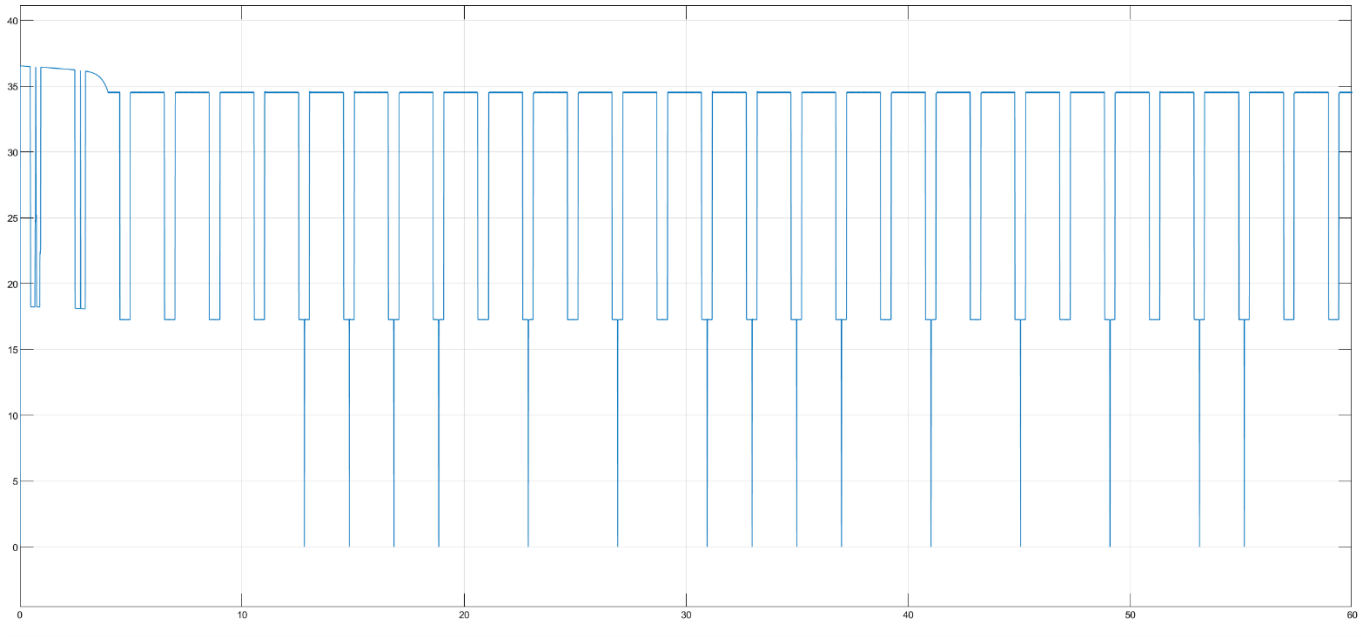

Figure 8.10. *PV array current evolution over one minute, controlled by MPPT.*

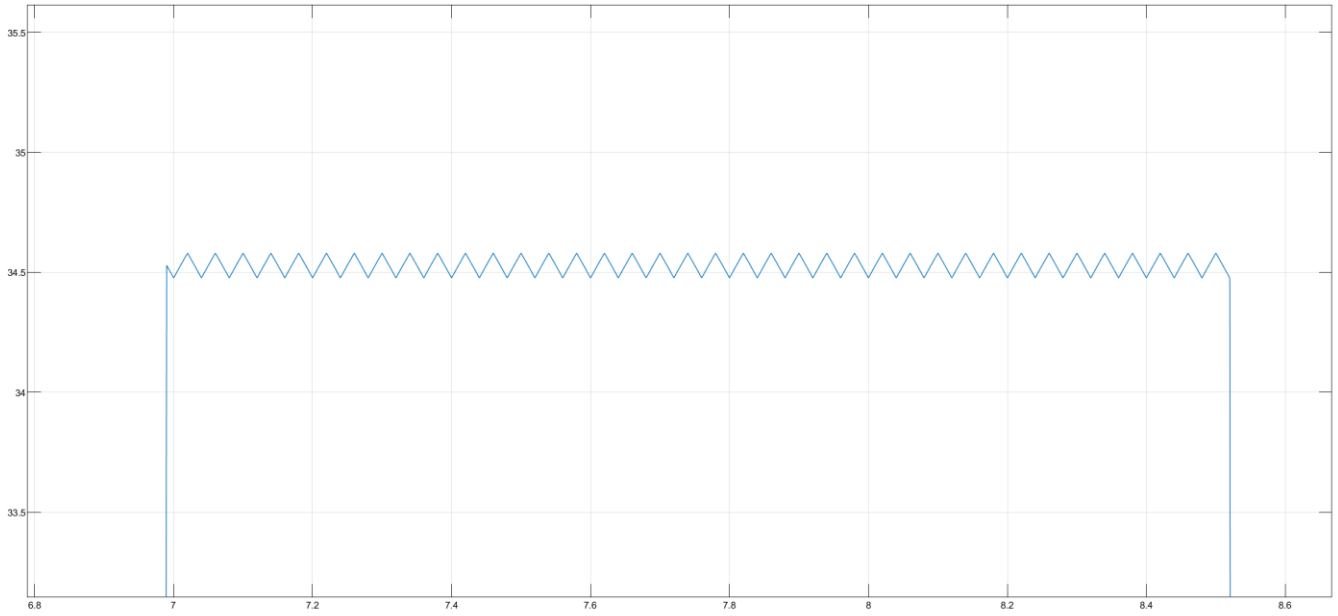

Figure 8.11. *MPPT operation on PV array current.*

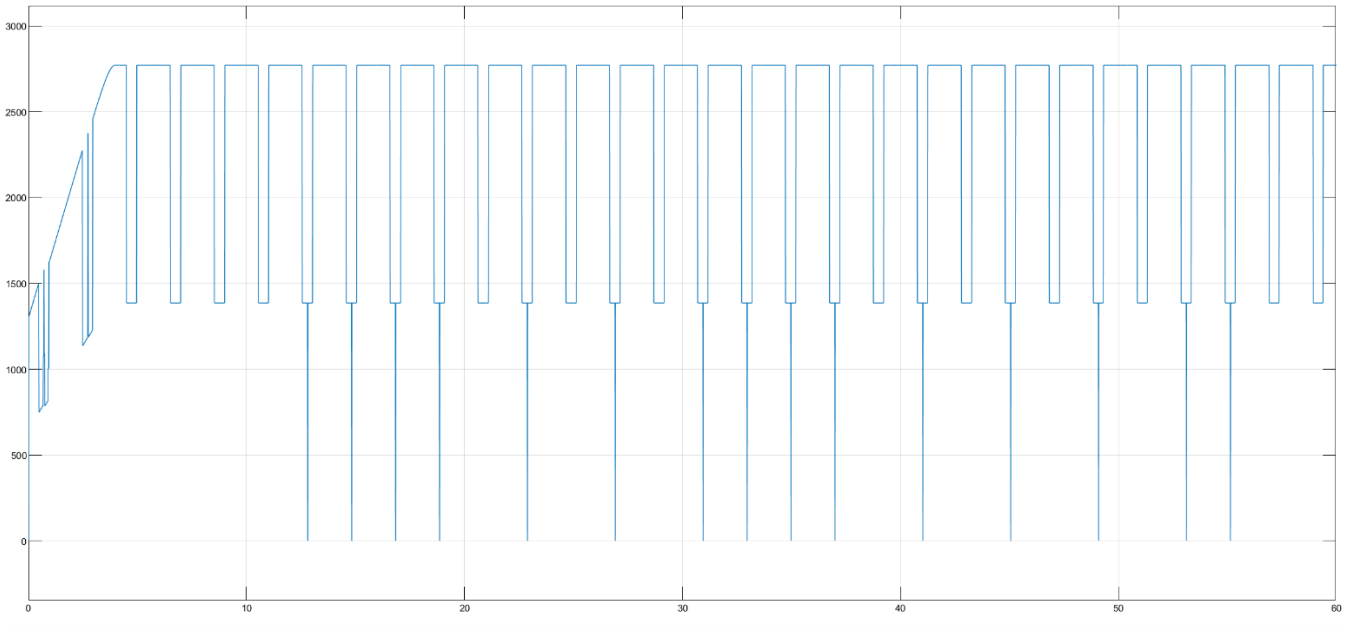

Figure 8.12. *PV array DC power evolution over one minute, controlled by MPPT.*

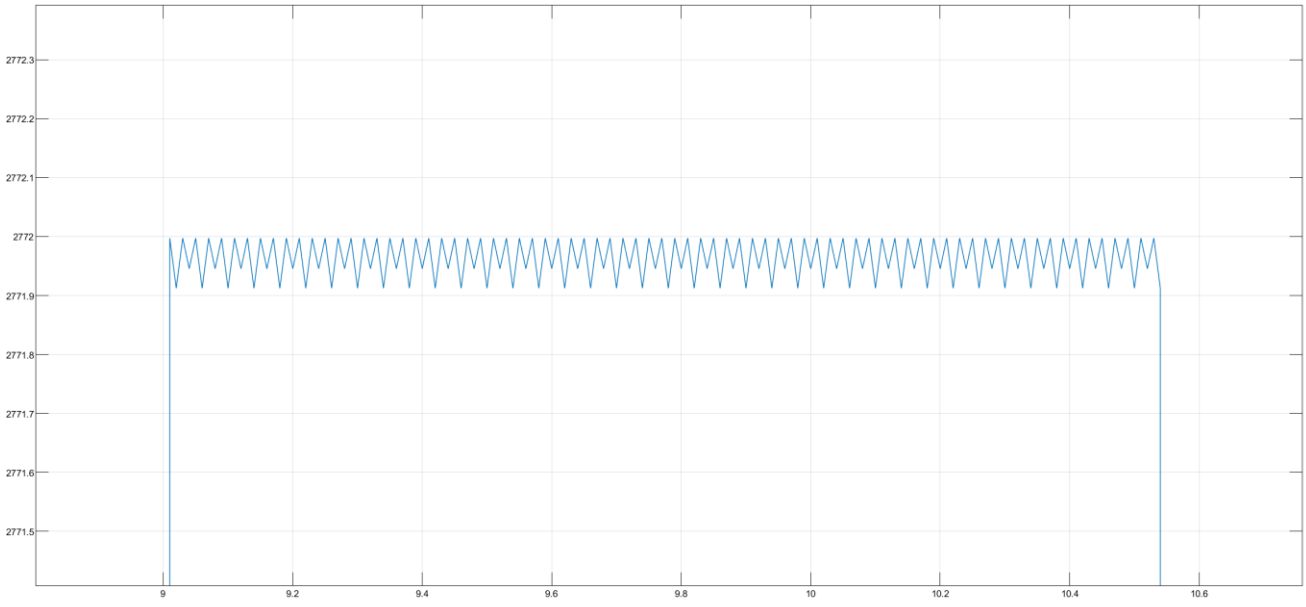

Figure 8.13. *MPPT operation on PV array DC power.*

As it can be seen, the P&O MPPT algorithm operates until it reaches the MPP values by changing voltage seen by PV array. Then, it continuously fluctuates around those values, depending on duty cycle step value, until irradiance condition changes again. When the simple PV array is completely shined in standard test conditions, its voltage oscillates around 80.25 V, current around 34.53 A and DC power around 2771.95 W (comparable to datasheet values). The evolution trends are similar to the ones obtained by SIMULINK model diagrams of PV array in Chapter 7 (see Figures 7.13, 7.14, 7.15). However, the difference is that, for very small periods, the simple PV array total current and

power outputs decrease to zero in the electrical circuit, since it happens that different string modules can be shadowed in the same or near instants and there is electrical inertia during their variations; this is not the circumstance of Chapter 7 models, where power and current are never zero (it is not an electrical circuit). Instead, during voltage evolution, the shading condition is so short and fast that array voltage reduction is really small (before all panels are shined again and the MPPT does its work). Furthermore, the MPPT is fast enough to reply in case of irradiance changes due to blades rotation, allowing the exploitation of modules nearby aerogenerators even in conditions of shadow flickering phenomenon appearance. The amplitude of PV array voltage variation around MPP value, due to P&O algorithm operation, depends on the size of fixed duty cycle step. For instance, a shorter duty cycle step is able to decrease voltage fluctuations, but the MPPT is slower; on the other hand, a wider step makes it faster but with bigger voltage oscillations, increasing power losses. Instead, the MPPT update frequency is connected to the actual speed of P&O algorithm on tracking peak power after panel working conditions change. In general, the best matching for a MPPT is a fast update rate and a small duty cycle step, a good compromise between voltage oscillations (power losses) and quick response. In the previous electrical circuit, the duty cycle step was 0.1% while the update frequency was 100 Hz. By increasing the first to 1% and decreasing the latter to 40 Hz (the update frequency used by “Microchip Technology Inc” in some tests [40]), which means a simulation and measurements each 2.5 hundredths of second, the PV array voltage becomes more swinging and the MPPT slower in its reply.

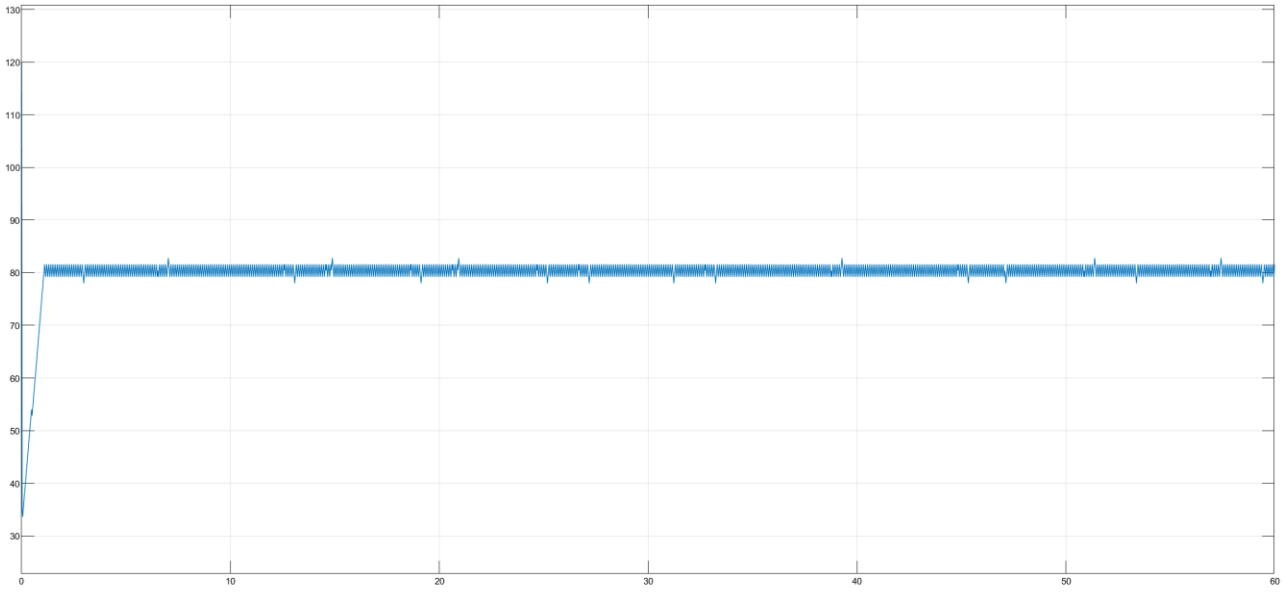

Figure 8.14. *New PV array voltage evolution.*

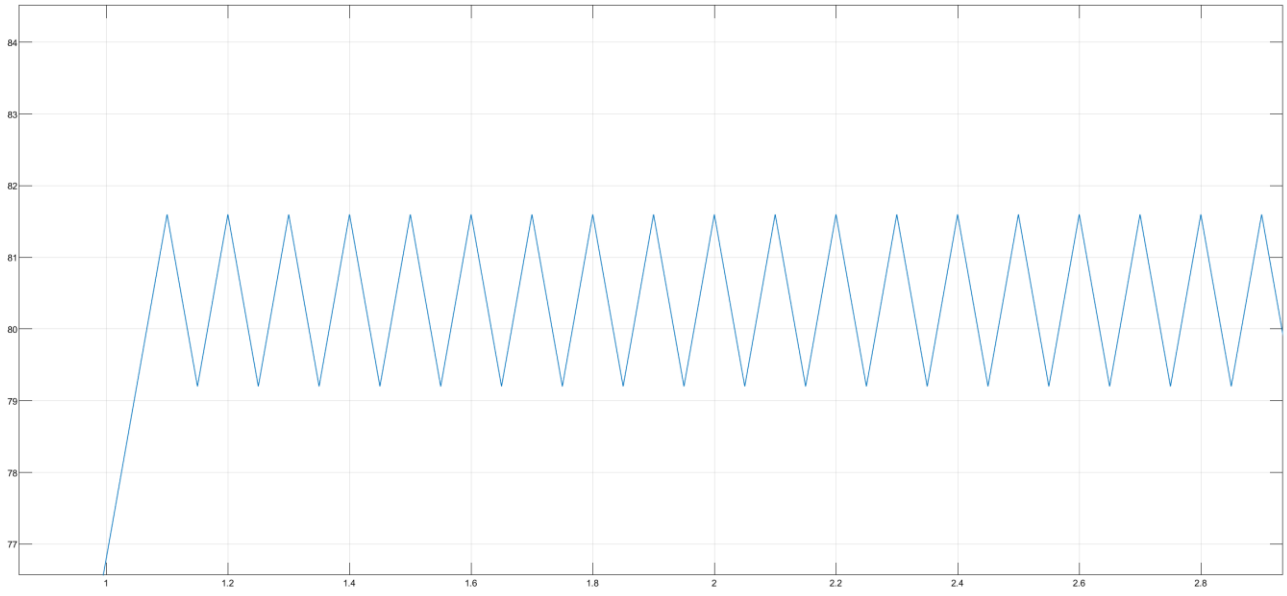

Figure 8.15. *New PV array voltage fluctuations amplitude.*

From the pictures above, it can be noticed that the wider duty cycle step, from 0.1% to 1%, makes the MPPT faster in its response than the first case, even if its update frequency is decreased from 100 Hz to 40 Hz. The PV array voltage overall oscillation is raised from 0.23 V (with 0.1% step) to 2.3 V (with 1% step).

CONCLUSIONS

European Countries and private companies are starting to invest more on renewable energy for decarbonising current energy sector. The lack of free land with right features to decrease as much as possible all impacts and a strict bureaucratic system are pushing enterprises and policymakers towards new solutions. The hybrid power plants are surely one of these options, consisting of a wind farm operating together with one or more photovoltaic plants. This thesis proved the feasibility of such kind of technology in the real world, not just in theory. In fact, even if the shadow casted by turbines and especially blades shadow oscillation over time can be quite a problem in terms of electrical grid quality and stability, the overall annual energy production by a PV plant installed below aerogenerators is poorly affected by shadow flickering phenomenon. However, grid stability issues can be solved with the adoption of devices named synchronous compensators or STATCOM; for instance TERNA, the Italian transmission system operator, is spending a lot of money right now on this technology to make electrical grid more resilient, allowing the conversion from a monodirectional central generation system to a bidirectional distributed generation one, where renewables are the dominant sources and consumers are instead prosumers (both producers and consumers). The energy generation losses due to wind turbine shadings are less than 2 % (the theoretical maximum is 1.84 % according to PVSYST, see the extreme model in Chapter 5) and they are lower than other types of losses (the panel mutual shading is 4.89 % from PVSYST). Therefore, the only problem related to PV plants integration into wind parks is the intermittency during a day of the solar irradiance reaching sensible surfaces because of blades rotation around hub axis. In Chapter 6 it was demonstrated that the blade shading condition lasts only some tenths of second (around two or three tenths of second) on a single module placed in the neighbourhood of an aerogenerator, while the period between two consecutive blade shadowings is approximately two seconds. Anyway, if a fast response MPPT algorithm and a control system are integrated into the solar inverters connected to PV array, the trouble associated to array maximum power operation, when its working conditions change, will be fixed. Besides, this shadow flickering phenomenon persists two and a half hours during the worst day of the year in terms of length of shadow casted by turbines (on the 21st of December, Winter solstice), as demonstrated in Chapter 6 for a single module at a given distance. This means that a larger number of panels nearby a wind turbine is involved during seasons when the solar day duration, the light presence without clouds and the solar energy availability is less (Winter and Autumn), while in

Summer, when the solar days are much wider and the energy available is abundant, Sun has its highest values of solar elevation and so shadow length by turbines is way shorter: less modules are influenced by the shading issues described before, and thus there is absence of power production losses and intermittent generation for almost all panels in the best period of the year, referring to the solar primary energy presence. In conclusion, panels can be installed close to an aerogenerator, but considering the time required for returning the investment that is linked to PV plant annual energy productivity, the closer the modules are to the wind turbine tower the higher is the number of shadow minutes per year and per day (see Chapter 4 pictures), thus lowering the energy generation. Then, a suggestion is to perform the shadow flickering analysis as it was done in this thesis, choosing the right distance of panels from aerogenerator tower axis: for the examined case, the suggested distance is 100 m, as written in Chapter 4. If the designer wish is to avoid any possible power output oscillation due to rotating blade shadows, the other suggestion is to install modules at longer distances than the shadow length casted by whole turbines during Winter solstice. In this thesis case, from Chapter 6 pictures obtained by the shadow evolution MATLAB models, the distance between tower axis and the PV plant panels must follow the shadow spatial trend on ground and it must be at least greater than 420 m. Whatever would be the engineering decision, hybrid power plants are the future of renewables cooperation. A single technology is not able to satisfy a global energy demand that is rising year after year, but a basket made by different solutions that can be integrated and implemented in the same location, saving land for other purposes too, can have the potential to achieve a more sustainable society worldwide. After all bad news and frustration feeling that followed the last Conference of Parties not taken decisions by policymakers and stakeholders, this is without doubts a new hope for both planet Earth and humankind next generations, that are angrily and rightfully waiting for answers.

APPENDIX A

- **TRINASOLAR VERTEX PV MODULE CATALOGUE**

Vertex

BIFACIAL DUAL GLASS MONOCRYSTALLINE MODULE

PRODUCT: TSM-DEG21C.20

POWER RANGE: 645-665W

665W	0~+5W	21.4%
MAXIMUM POWER OUTPUT	POSITIVE POWER TOLERANCE	MAXIMUM EFFICIENCY

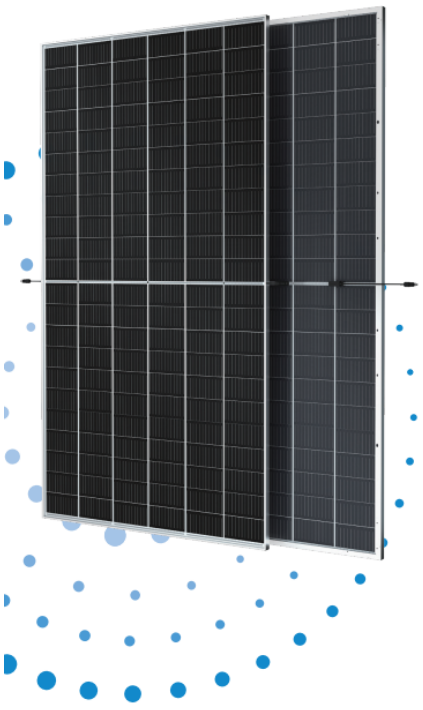

High customer value

- Lower LCOE (Levelized Cost Of Energy), reduced BOS (Balance of System) cost, shorter payback time
- Lowest guaranteed first year and annual degradation;
- Designed for compatibility with existing mainstream system components

High power up to 665W

- Up to 21.4% module efficiency with high density interconnect technology
- Multi-busbar technology for better light trapping effect, lower series resistance and improved current collection

High reliability

- Minimized micro-cracks with innovative non-destructive cutting technology
- Ensured PID resistance through cell process and module material control
- Resistant to harsh environments such as salt, ammonia, sand, high temperature and high humidity areas
- Mechanical performance up to 5400 Pa positive load and 2400 Pa negative load

High energy yield

- Excellent IAM (Incident Angle Modifier) and low irradiation performance, validated by 3rd party certifications
- The unique design provides optimized energy production under inter-row shading conditions
- Lower temperature coefficient (-0.34%) and operating temperature
- Up to 25% additional power gain from back side depending on albedo

Trina Solar's Vertex Bifacial Dual Glass Performance Warranty

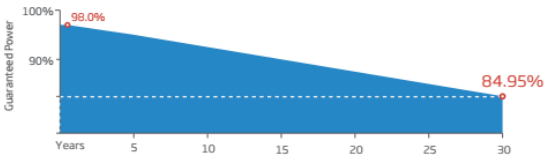

Comprehensive Products and System Certificates

IEC61215/IEC61730/IEC61701/IEC62716/UL61730
ISO 9001: Quality Management System
ISO 14001: Environmental Management System
ISO14064: Greenhouse Gases Emissions Verification
ISO45001: Occupational Health and Safety Management System

Trinasolar

Vertex BIFACIAL DUAL GLASS MONOCRYSTALLINE MODULE

DIMENSIONS OF PV MODULE(mm)

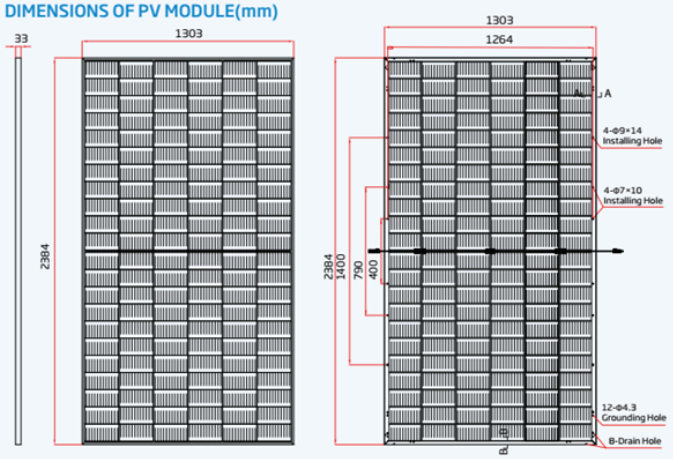

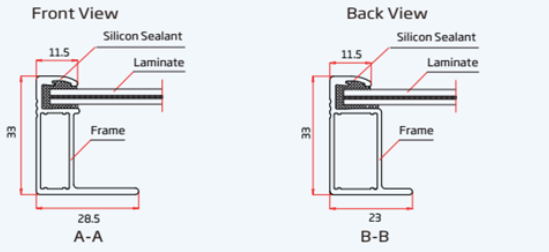

I-V CURVES OF PV MODULE(650 W)

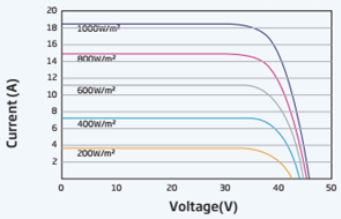

P-V CURVES OF PV MODULE(650W)

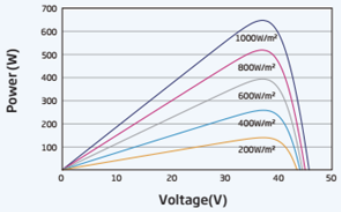

I-V CURVES OF PV MODULE(650 W)

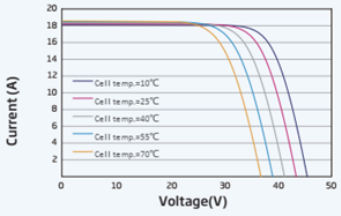

ELECTRICAL DATA (STC)

Peak Power Watts-PMAX (Wp)*	645	650	655	660	665
Power Tolerance-PMAX (W)			0 ~ +5		
Maximum Power Voltage-VMPP (V)	37.5	37.7	37.9	38.1	38.3
Maximum Power Current-IMPP (A)	17.23	17.27	17.31	17.35	17.39
Open Circuit Voltage-Voc (V)	45.3	45.5	45.7	45.9	46.1
Short Circuit Current-Isc (A)	18.31	18.35	18.40	18.45	18.50
Module Efficiency η m (%)	20.8	20.9	21.1	21.2	21.4

STC: Irradiance 1000W/m2, Cell Temperature 25℃, Air Mass AM1.5. *Measuring tolerance: ±3%.

Electrical characteristics with different power bin (reference to 10% Irradiance ratio)

Total Equivalent power -PMAX (Wp)	690	696	701	706	712
Maximum Power Voltage-VMPP (V)	37.5	37.7	37.9	38.1	38.3
Maximum Power Current-IMPP (A)	18.44	18.48	18.52	18.56	18.60
Open Circuit Voltage-Voc (V)	45.3	45.5	45.7	45.9	46.1
Short Circuit Current-Isc (A)	19.59	19.63	19.69	19.74	19.79
Irradiance ratio (rear/front)			10%		

Power Bifaciality:70±5%.

ELECTRICAL DATA (NOCT)

Maximum Power-PMAX (Wp)	488	492	495	499	504
Maximum Power Voltage-VMPP (V)	34.9	35.1	35.2	35.4	35.6
Maximum Power Current-IMPP (A)	13.98	14.01	14.05	14.10	14.16
Open Circuit Voltage-Voc (V)	42.7	42.9	43.0	43.2	43.4
Short Circuit Current-Isc (A)	14.75	14.79	14.83	14.87	14.91

NOCT: Irradiance at 800W/m², Ambient Temperature 20℃, Wind Speed 1m/s.

MECHANICAL DATA

Solar Cells	Monocrystalline
No. of cells	132 cells
Module Dimensions	2384×1303×33 mm (93.86×51.30×1.30 inches)
Weight	38.3 kg (84.4 lb)
Front Glass	2.0 mm (0.08 inches), High Transmission, AR Coated Heat Strengthened Glass
Encapsulant material	POE/EVA
Back Glass	2.0 mm (0.08 inches), Heat Strengthened Glass (White Grid Glass)
Frame	33mm(1.30 inches) Anodized Aluminium Alloy
J-Box	IP 68 rated
Cables	Photovoltaic Technology Cable 4.0mm² (0.006 inches²), Portrait: 350/280 mm(13.78/11.02 inches) Length can be customized
Connector	MC4 EVO2 / TS4*

*Please refer to regional datasheet for specified connector.

TEMPERATURE RATINGS

NOCT (Nominal Operating Cell Temperature)	43℃ (±2℃)
Temperature Coefficient of PMAX	- 0.34%/℃
Temperature Coefficient of Voc	- 0.25%/℃
Temperature Coefficient of Isc	0.04%/℃

MAXIMUMRATINGS

Operational Temperature	-40~+85℃
Maximum System Voltage	1500V DC (IEC)
	1500V DC (UL)
Max Series Fuse Rating	35A

WARRANTY

12 year Product Workmanship Warranty

30 year Power Warranty

2% first year degradation

0.45% Annual Power Attenuation

(Please refer to product warranty for details)

PACKAGING CONFIGUREATION

Modules per box: 33 pieces

Modules per 40' container : 594 pieces

Trinasolar

CAUTION: READ SAFETY AND INSTALLATION INSTRUCTIONS BEFORE USING THE PRODUCT.

Version number: TSM_EN_2022_A

www.trinasolar.com

- **SUNGROW SG350HX INVERTER CATALOGUE**

SG350HX

Multi-MPPT String Inverter for 1500 Vdc System

HIGH YIELD

- Up to 16 MPPTs with max. efficiency 99%
- 20A per string, compatible with 500Wp+ module
- Data exchange with tracker system, improving yield

LOW COST

- Q at night function, save investment
- Power line communication (PLC)
- Smart IV Curve diagnosis,active O&M

GRID SUPPORT

- SCR≥1.16 stable operation in extremely weak grid
- Reactive power response time <30ms
- Compliant with global grid code

PROVEN SAFETY

- 2 strings per MPPT, no fear of string reverse connection
- Integrated DC switch, automatically cut off the fault
- 24h real-time AC and DC insulation monitoring

CIRCUIT DIAGRAM

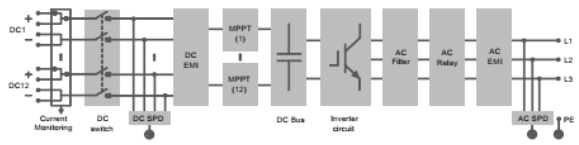

EFFICIENCY CURVE

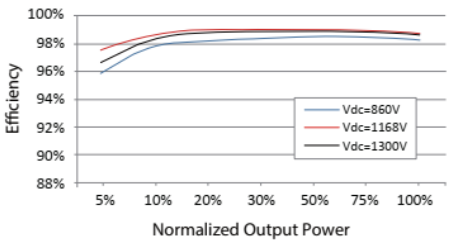

SUNGROW
Clean power for all

Type designation	SG350HX
Input (DC)	
Max. PV input voltage	1500 V
Min. PV input voltage / Startup input voltage	500 V / 550 V
Nominal PV input voltage	1080 V
MPP voltage range	500 V – 1500 V
No. of independent MPP inputs	12 (optional: 14/16)
Max. number of input connector per MPPT	2
Max. PV input current	12 * 40 A (Optional: 14 * 30 A / 16 * 30 A)
Max. DC short-circuit current per MPPT	60 A
Output (AC)	
AC output power	352 kVA @ 30℃ / 320 kVA @40 ℃ / 295 kVA @50℃
Max. AC output current	254 A
Nominal AC voltage	3 / PE, 800 V
AC voltage range	640 – 920V
Nominal grid frequency / Grid frequency range	50 Hz / 45 – 55 Hz, 60 Hz / 55 – 65 Hz
THD	< 3 % (at nominal power)
DC current injection	< 0.5 % In
Power factor at nominal power / Adjustable power factor	> 0.99 / 0.8 leading – 0.8 lagging
Feed-in phases / Connection phases	3 / 3
Efficiency	
Max. efficiency / European efficiency / CEC efficiency	99.02 % / 98.8 % / 98.5%
Protection	
DC reverse connection protection	Yes
AC short circuit protection	Yes
Leakage current protection	Yes
Grid monitoring	Yes
Ground fault monitoring	Yes
DC switch / AC switch	Yes / No
PV string current monitoring	Yes
Q at night function	Yes
Anti-PID and PID recovery function	Optional
Surge protection	DC Type II / AC Type II
General Data	
Dimensions (W*H*D)	1136 * 870 * 361 mm (44.7'' * 34.3'' * 14.2'')
Weight	≤116 kg(≤255.7 lbs)
Isolation method	Transformerless
Degree of protection	IP66 (NEMA 4X)
Power consumption at night	< 6 W
Operating ambient temperature range	-30 to 60℃(-22 to 140 ℉)
Allowable relative humidity range	0 – 100 %
Cooling method	Smart forced air cooling
Max. operating altitude	4000 m (> 3000 m derating) / 13123 ft (> 9843 ft derating)
Display	LED, Bluetooth+APP
Communication	RS485 / PLC
DC connection type	MC4-Evo2 (Max. 6 mm², optional 10mm² / Max. 10AWG, optional 8AWG)
AC connection type	Support OT/DT terminal (Max. 400 mm² / 789 Kcmil)
Compliance	IEC 62109, IEC 61727, IEC 62116, IEC 60068, IEC 61683, VDE-AR-N 4110:2018, VDE-AR-N 4120:2018, EN 50549-1/2, UNE 206007-1:2013, P.O.12.3, UTE C15-712-1:2013, UL1741, UL1741SA, IEEE1547, IEEE1547.1, CSA C22.2 107.1-01-2001, California Rule 21, UL1699B
Grid Support	Q at night function, LVRT, HVRT,active & reactive power control and power ramp rate control, Q-U control, P-f control

APPENDIX B

SHADOW - Map

Calculation: WORST CASE WTG04 E WTG05

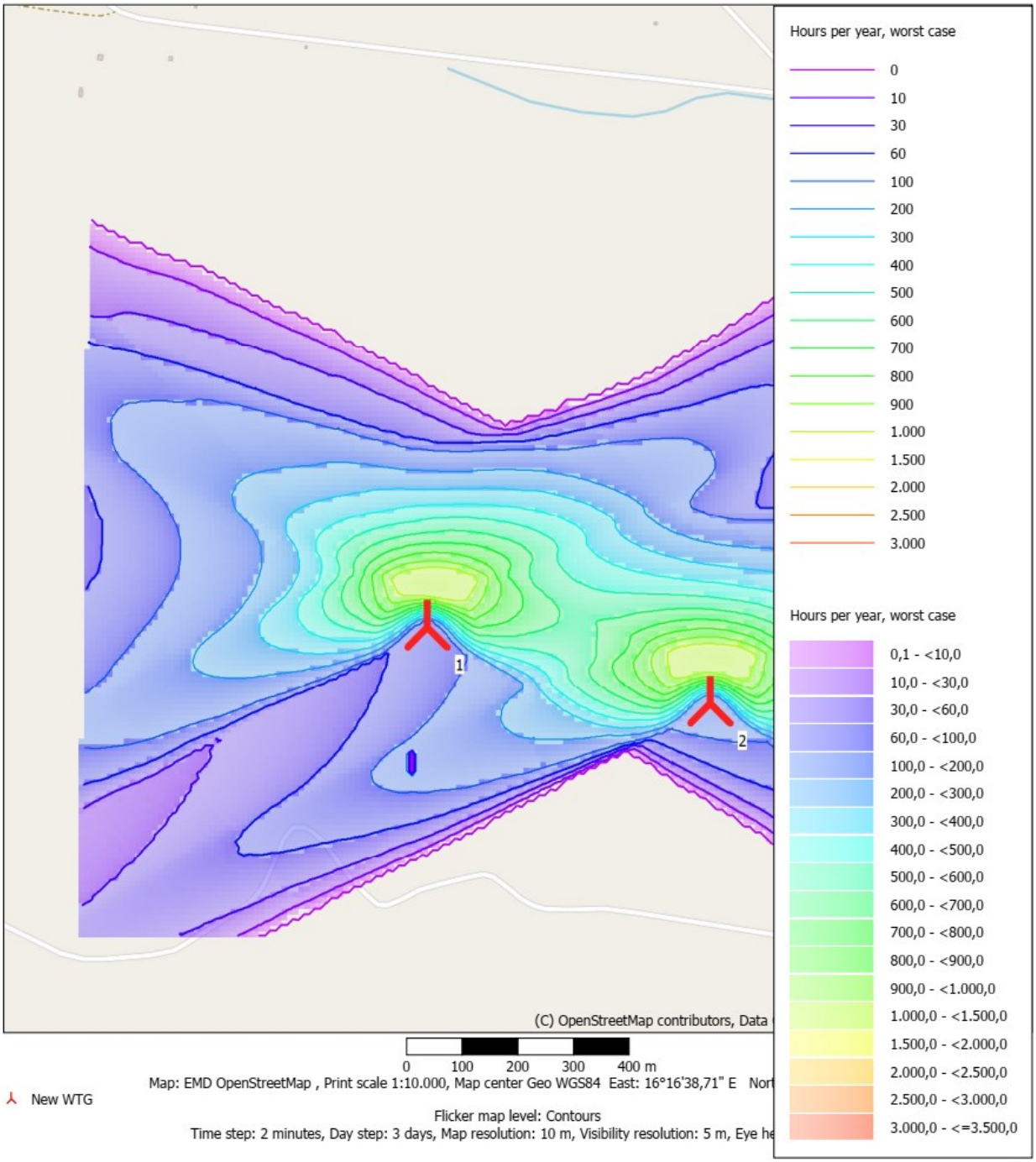

SHADOW - Map

Calculation: WORST CASE WTG04 E WTG05

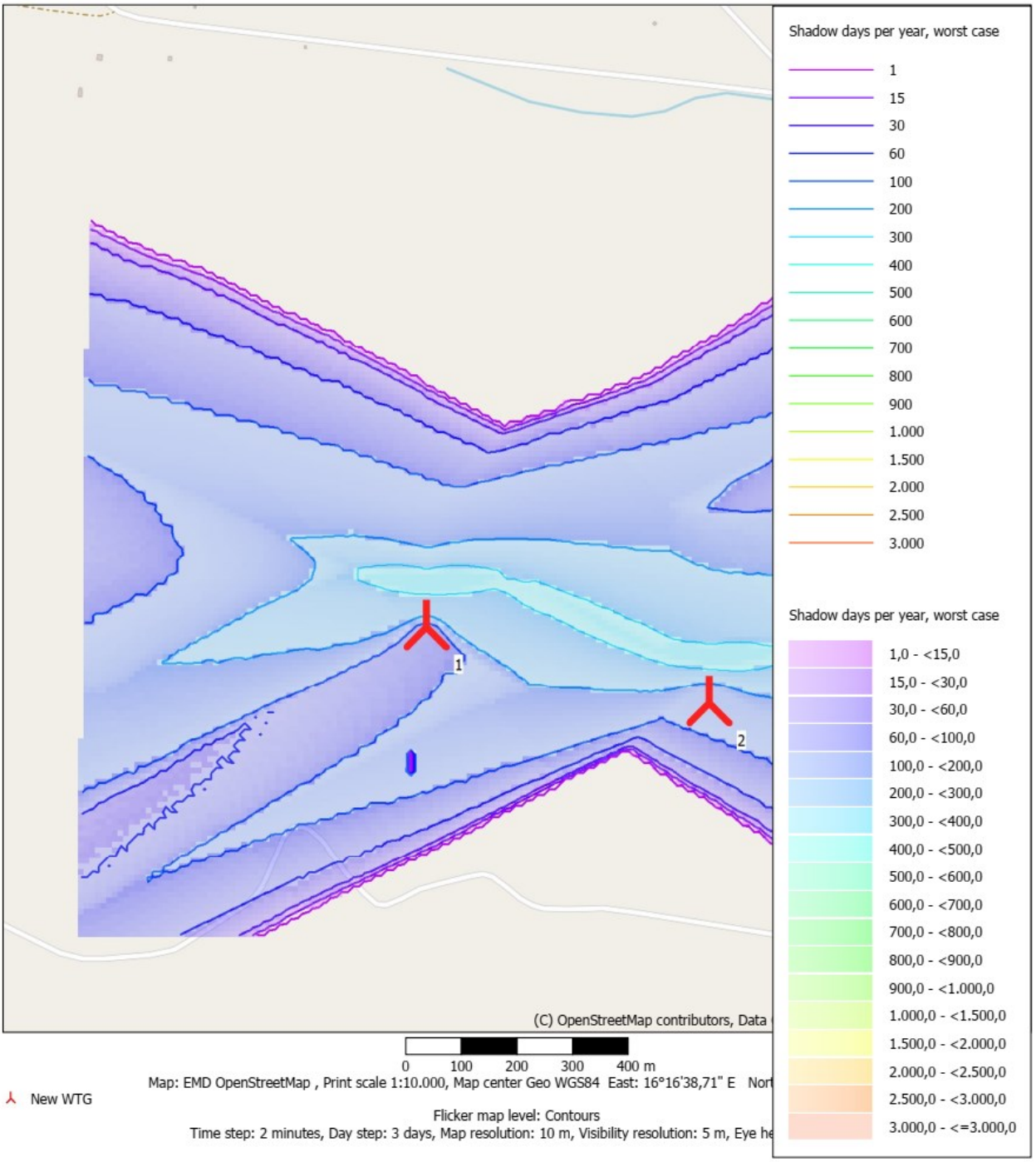

SHADOW - Map

Calculation: WORST CASE WTG04 E WTG05

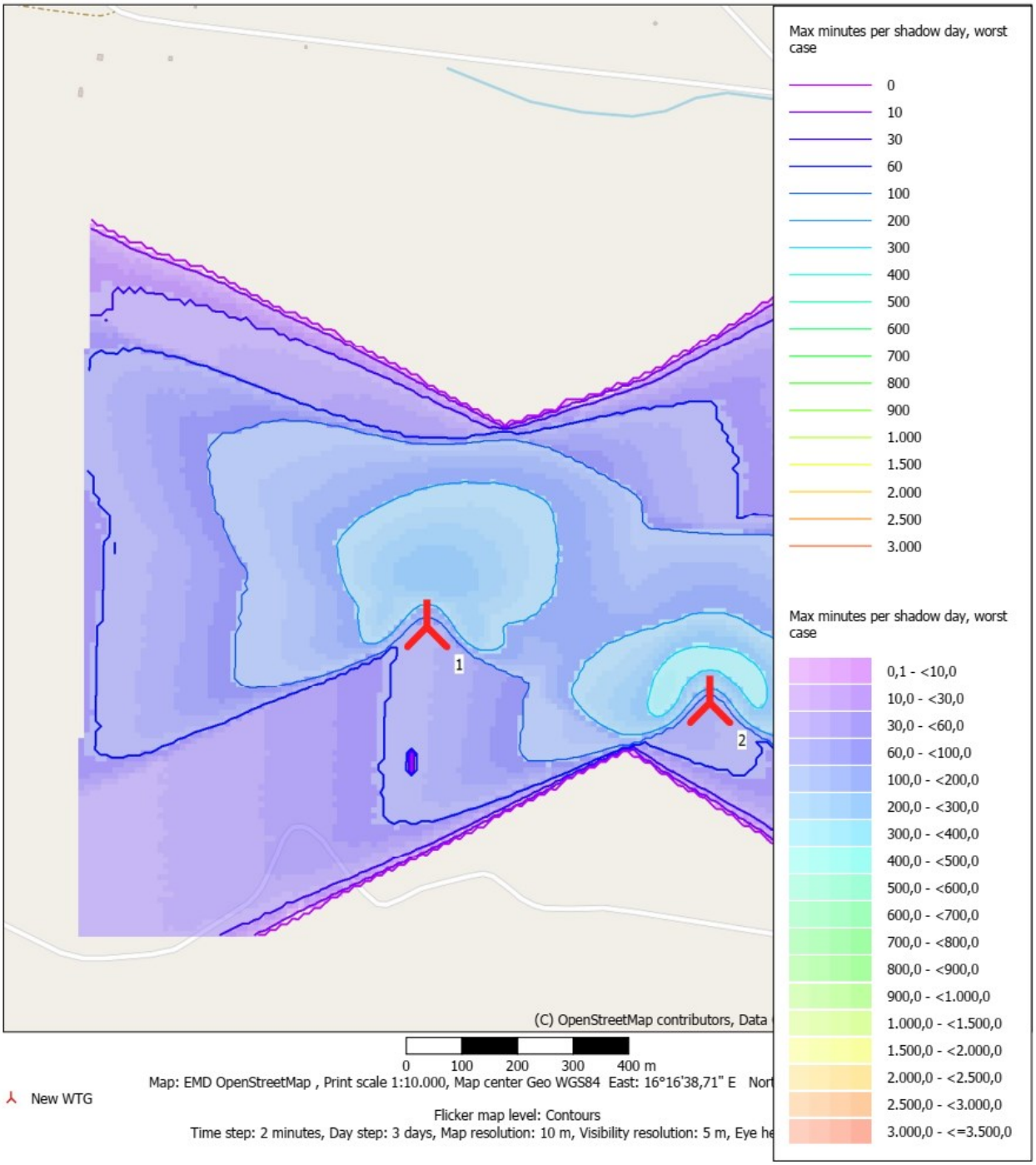

APPENDIX C

- **PVSYST REPORT FOR THREE-BLADED TURBINES CASE**

PVsyst V7.2.8
VC4, Simulation date:
05/11/22 00:03
with v7.2.8

Project: IMPIANTO PV GRAVINA IN PUGLIA

Variant: Prestazioni AEP impianto VC3 con OMBRA AEROGENERATORI STATICI

Project summary

Geographical Site	Situation		Project settings	
GRAVINA IN PUGLIA	Latitude	40.84 °N	Albedo	0.20
Italia	Longitude	16.28 °E		
	Altitude	375 m		
	Time zone	UTC+1		

Meteo data
GRAVINA IN PUGLIA
PVGIS-SARAH averages 01/01/05 to 31/12/16 - Sintetico

System summary

Grid-Connected System — **Tracking system with backtracking**

PV Field Orientation	Near Shadings	User's needs
Tracking plane, horizontal N-S axis	Linear shadings	Unlimited load (grid)
Axis azimuth 0 °		

System information

PV Array		Inverters	
Nb. of modules	76531 units	Nb. of units	125 units
Pnom total	51.28 MWp	Pnom total	40.00 MWac
		Pnom ratio	1.282

Results summary

Produced Energy	92648 MWh/year	Specific production	1807 kWh/kWp/year	Perf. Ratio PR	84.80 %

General parameters

Grid-Connected System

Tracking system with backtracking

PV Field Orientation

Orientation
Tracking plane, horizontal N-S axis
Axis azimuth 0 °

Backtracking strategy
Nb. of trackers 2639 units

Sizes
Tracker Spacing 6.00 m
Collector width 2.38 m
Ground Cov. Ratio (GCR) 39.7 %
Phi min / max. -/+ 60.0 °

Backtracking limit angle
Phi limits +/- 66.4 °

Models used
Transposition Perez
Diffuse Perez, Meteonorm
Circumsolar separate

Horizon
Free Horizon

Near Shadings
Linear shadings

User's needs
Unlimited load (grid)

PV Array Characteristics

PV module

Manufacturer	Trina Solar
Model	TSM-670DEG21C.20
(Original PVsyst database)	
Unit Nom. Power	670 Wp
Number of PV modules	76531 units
Nominal (STC)	51.28 MWp
Modules	2639 Strings x 29 In series
At operating cond. (50°C)	
Pmpp	47.05 MWp
U mpp	1006 V
I mpp	46784 A

Inverter

Manufacturer	Sungrow
Model	SG350HX-20A-Preliminary
(Original PVsyst database)	
Unit Nom. Power	320 kWac
Number of inverters	125 units
Total power	40000 kWac
Operating voltage	500-1500 V
Max. power (=>30°C)	352 kWac
Pnom ratio (DC:AC)	1.28

Total PV power

Nominal (STC)	51276 kWp
Total	76531 modules
Module area	237732 m²
Cell area	222751 m²

Total inverter power

Total power	40000 kWac
Nb. of inverters	125 units
Pnom ratio	1.28

Array losses

Array Soiling Losses
Loss Fraction 1.0 %

Thermal Loss factor
Module temperature according to irradiance
Uc (const) 29.0 W/m²K
Uv (wind) 0.0 W/m²K/m/s

DC wiring losses
Global array res. 0.35 mΩ
Loss Fraction 1.5 % at STC

LID - Light Induced Degradation
Loss Fraction 2.0 %

Module Quality Loss
Loss Fraction -0.8 %

Module mismatch losses
Loss Fraction 2.0 % at MPP

Strings Mismatch loss
Loss Fraction 0.1 %

IAM loss factor
Incidence effect (IAM): User defined profile

0°	40°	50°	60°	70°	75°	80°	85°	90°
1.000	1.000	0.998	0.992	0.983	0.961	0.933	0.853	0.000

AC wiring losses

Inv. output line up to injection point

Inverter voltage	800 Vac tri
Loss Fraction	1.04 % at STC
Inverter: SG350HX-20A-Preliminary	
Wire section (125 Inv.)	Copper 125 x 3 x 185 mm²
Average wires length	161 m

Near shadings parameter

Perspective of the PV-field and surrounding shading scene

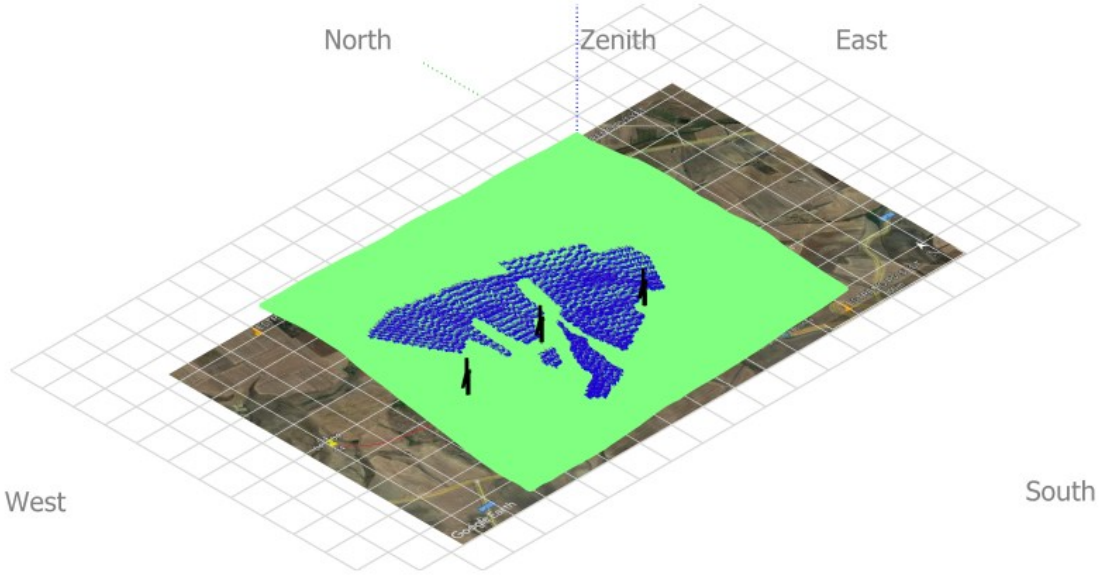

Iso-shadings diagram

IMPIANTO PV GRAVINA IN PUGLIA - Legal Time

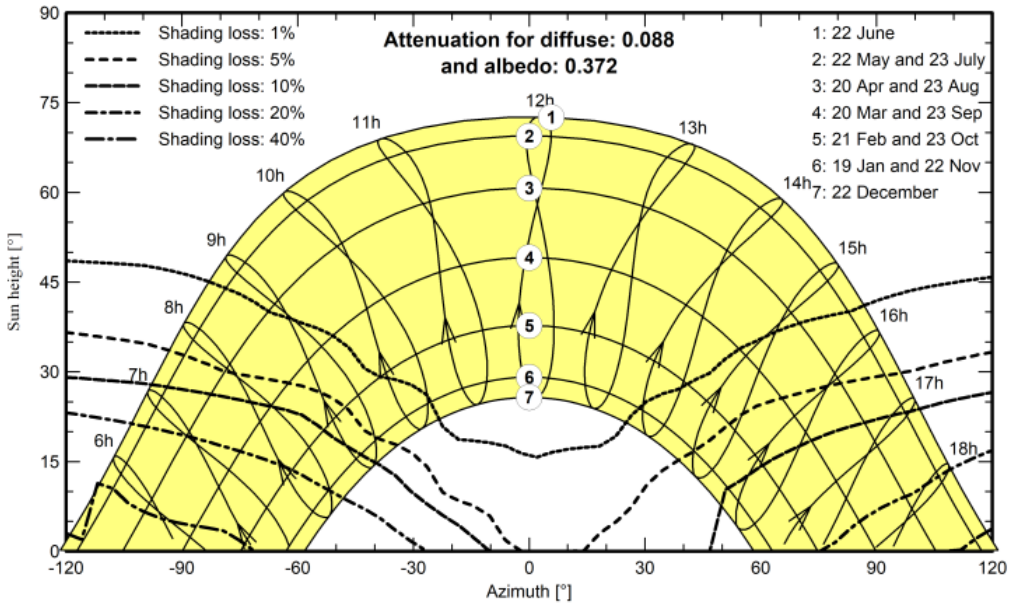

Main results

System Production

Produced Energy	92648 MWh/year	Specific production	1807 kWh/kWp/year
		Performance Ratio PR	84.80 %

Normalized productions (per installed kWp)

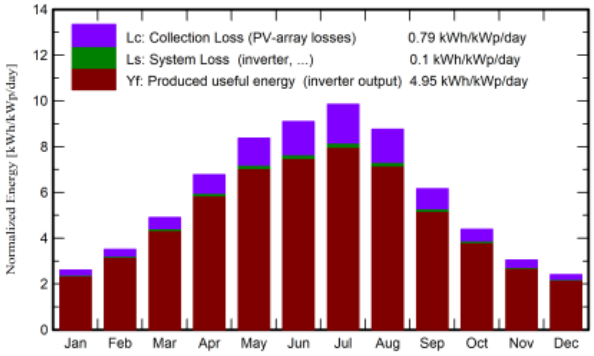

Performance Ratio PR

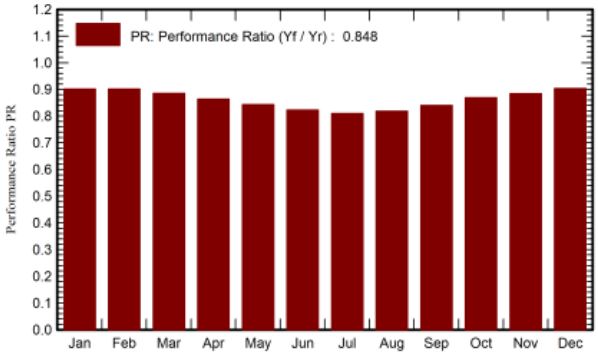

Balances and main results

	GlobHor kWh/m²	DiffHor kWh/m²	T_Amb °C	GlobInc kWh/m²	GlobEff kWh/m²	EArray MWh	E_Grid MWh	PR ratio
January	61.0	27.90	6.52	80.9	75.5	3809	3741	0.902
February	74.9	35.10	6.66	98.4	92.0	4628	4548	0.901
March	117.6	51.40	9.35	152.0	142.7	7036	6903	0.886
April	154.8	64.40	13.00	203.3	190.8	9191	9005	0.864
May	199.2	75.70	17.46	259.3	243.7	11456	11218	0.844
June	208.7	74.50	22.32	273.1	256.0	11772	11521	0.823
July	227.3	66.70	25.84	305.5	286.6	12977	12696	0.810
August	201.8	62.10	25.59	271.4	255.8	11643	11389	0.818
September	140.3	54.10	20.86	185.0	173.5	8135	7973	0.840
October	101.9	42.50	15.93	136.1	127.5	6178	6064	0.869
November	67.1	29.50	11.45	91.3	84.9	4210	4138	0.884
December	55.4	25.00	7.31	74.5	69.3	3509	3452	0.904
Year	1610.0	608.90	15.24	2130.8	1998.6	94545	92648	0.848

Legends

GlobHor	Global horizontal irradiation
DiffHor	Horizontal diffuse irradiation
T_Amb	Ambient Temperature
GlobInc	Global incident in coll. plane
GlobEff	Effective Global, corr. for IAM and shadings
EArray	Effective energy at the output of the array
E_Grid	Energy injected into grid
PR	Performance Ratio

Loss diagram

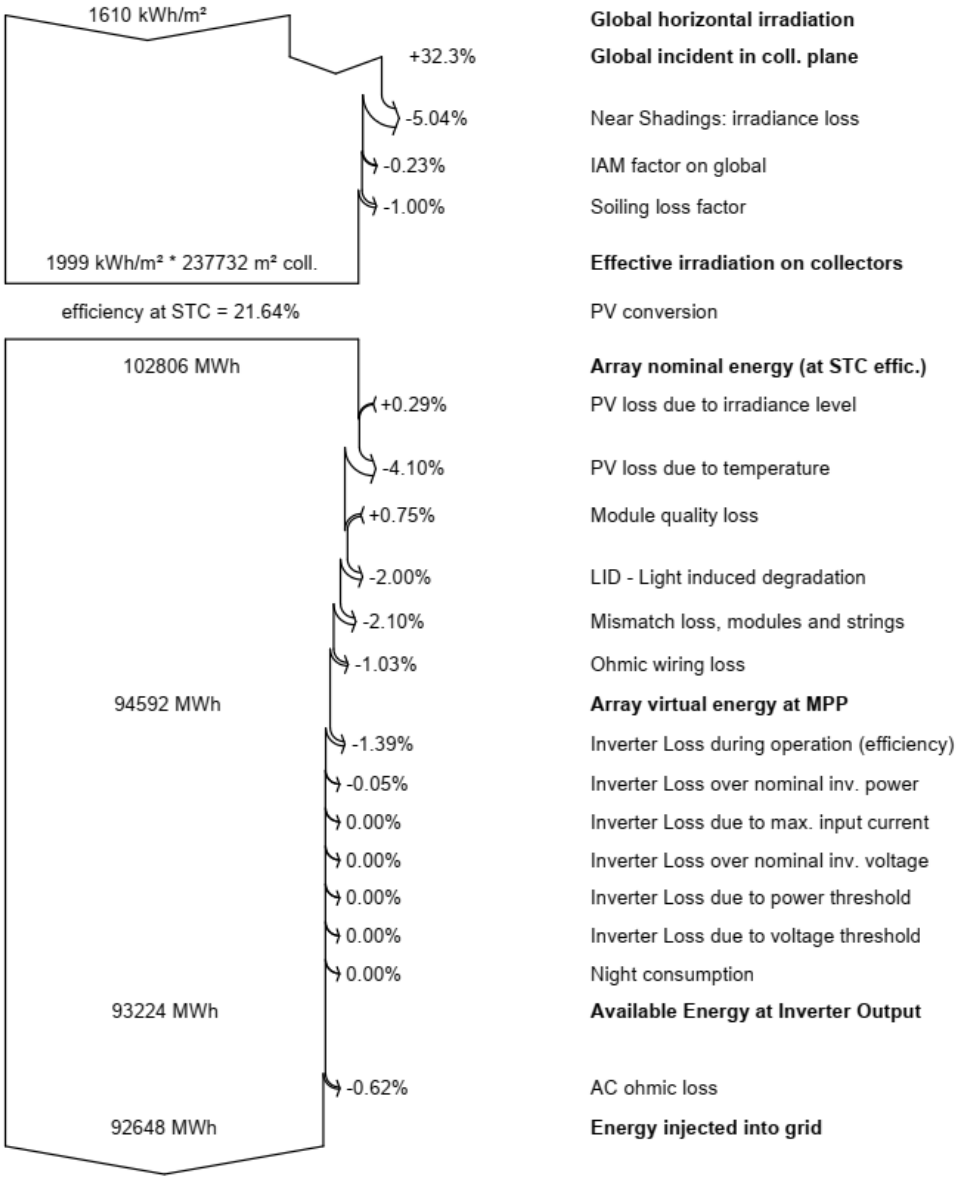

Special graphs

Diagramma giornaliero entrata/uscita

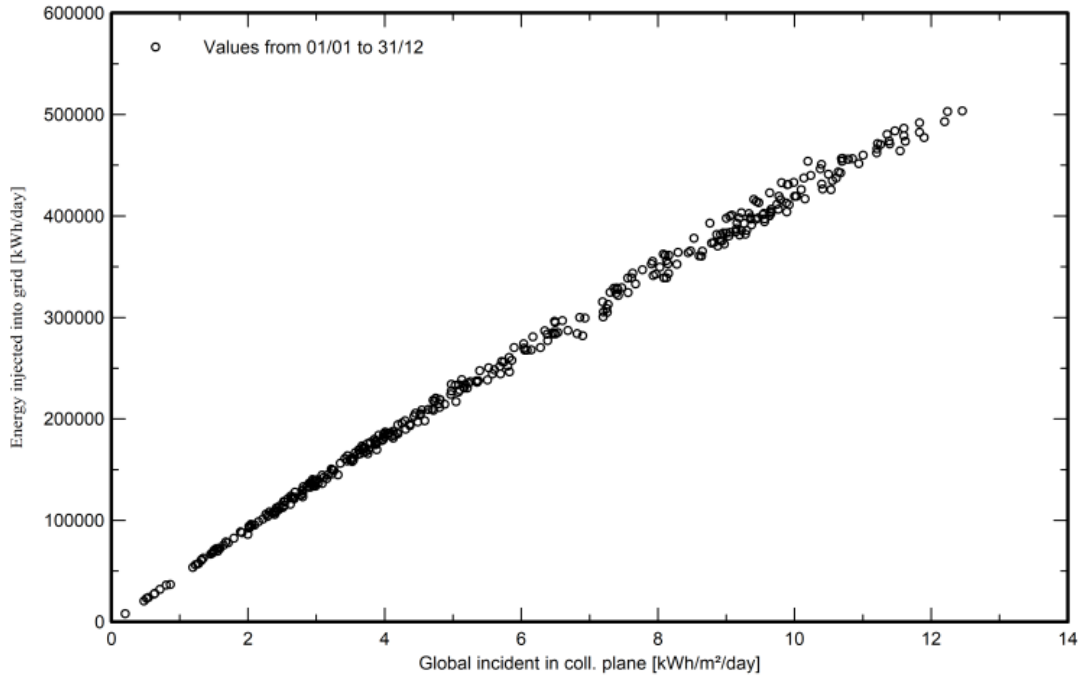

Distribuzione potenza in uscita sistema

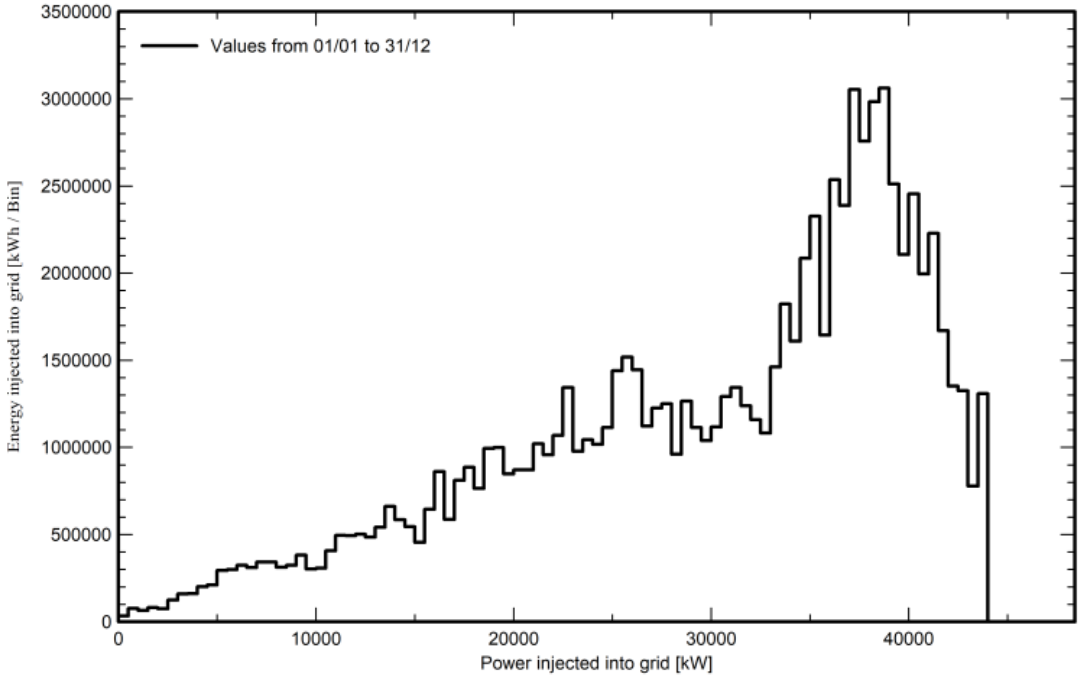

- **PVSYST REPORT FOR EXTREME CASE WITH DISCS**

Project: IMPIANTO PV GRAVINA IN PUGLIA

Variant: Variante con disco

PVsyst V7.2.8
VC7, Simulation date:
13/12/22 10:12
with v7.2.8

Project summary

Geographical Site
GRAVINA IN PUGLIA
Italy

Situation

Latitude	40.84 °N
Longitude	16.28 °E
Altitude	375 m
Time zone	UTC+1

Project settings

Albedo	0.20

Meteo data
GRAVINA IN PUGLIA
PVGIS-SARAH averages 01/01/05 to 31/12/16 - Sintetico

System summary

Grid-Connected System

Tracking system with backtracking

PV Field Orientation
Tracking plane, horizontal N-S axis
Axis azimuth 0 °

Near Shadings
Linear shadings

User's needs
Unlimited load (grid)

System information

PV Array

Nb. of modules	76531 units
Pnom total	51.28 MWp

Inverters

Nb. of units	125 units
Pnom total	40.00 MWac
Pnom ratio	1.282

Results summary

Produced Energy	91110 MWh/year	Specific production	1777 kWh/kWp/year	Perf. Ratio PR	83.39 %

General parameters

Grid-Connected System

Tracking system with backtracking

PV Field Orientation

Orientation	
Tracking plane, horizontal N-S axis	
Axis azimuth	0 °

Backtracking strategy	
Nb. of trackers	2639 units
Sizes	
Tracker Spacing	6.00 m
Collector width	2.38 m
Ground Cov. Ratio (GCR)	39.7 %
Phi min / max.	-/+ 60.0 °
Backtracking limit angle	
Phi limits	+/- 66.4 °

Models used	
Transposition	Perez
Diffuse	Perez, Meteonorm
Circumsolar	separate

Horizon
Free Horizon

Near Shadings
Linear shadings

User's needs
Unlimited load (grid)

PV Array Characteristics

PV module

Manufacturer	Trina Solar
Model	TSM-670DEG21C.20
(Original PVsyst database)	
Unit Nom. Power	670 Wp
Number of PV modules	76531 units
Nominal (STC)	51.28 MWp
Modules	2639 Strings x 29 In series
At operating cond. (50°C)	
Pmpp	47.05 MWp
U mpp	1006 V
I mpp	46784 A

Inverter

Manufacturer	Sungrow
Model	SG350HX-20A-Preliminary
(Original PVsyst database)	
Unit Nom. Power	320 kWac
Number of inverters	125 units
Total power	40000 kWac
Operating voltage	500-1500 V
Max. power (=>30°C)	352 kWac
Pnom ratio (DC:AC)	1.28

Total PV power

Nominal (STC)	51276 kWp
Total	76531 modules
Module area	237732 m²
Cell area	222751 m²

Total inverter power

Total power	40000 kWac
Nb. of inverters	125 units
Pnom ratio	1.28

Array losses

Array Soiling Losses
Loss Fraction 1.0 %

Thermal Loss factor
Module temperature according to irradiance
Uc (const) 29.0 W/m²K
Uv (wind) 0.0 W/m²K/m/s

DC wiring losses
Global array res. 0.35 mΩ
Loss Fraction 1.5 % at STC

LID - Light Induced Degradation
Loss Fraction 2.0 %

Module Quality Loss
Loss Fraction -0.8 %

Module mismatch losses
Loss Fraction 2.0 % at MPP

Strings Mismatch loss
Loss Fraction 0.1 %

IAM loss factor
Incidence effect (IAM): User defined profile

0°	40°	50°	60°	70°	75°	80°	85°	90°
1.000	1.000	0.998	0.992	0.983	0.961	0.933	0.853	0.000

AC wiring losses

Inv. output line up to injection point

Inverter voltage	800 Vac tri
Loss Fraction	1.04 % at STC
Inverter: SG350HX-20A-Preliminary	
Wire section (125 Inv.)	Copper 125 x 3 x 185 mm²
Average wires length	162 m

Near shadings parameter

Perspective of the PV-field and surrounding shading scene

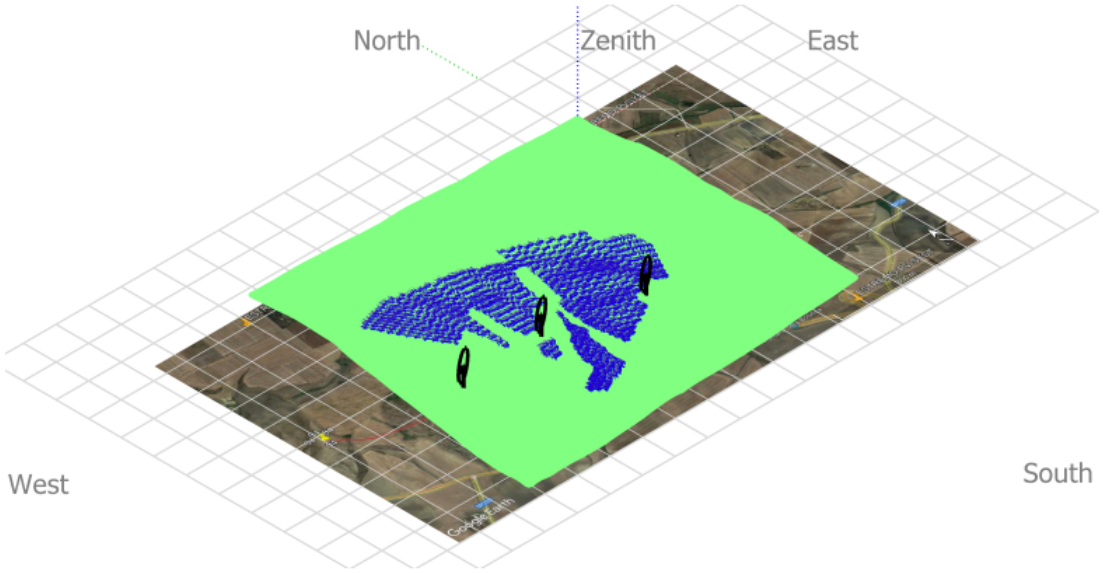

Iso-shadings diagram

IMPIANTO PV GRAVINA IN PUGLIA - Legal Time

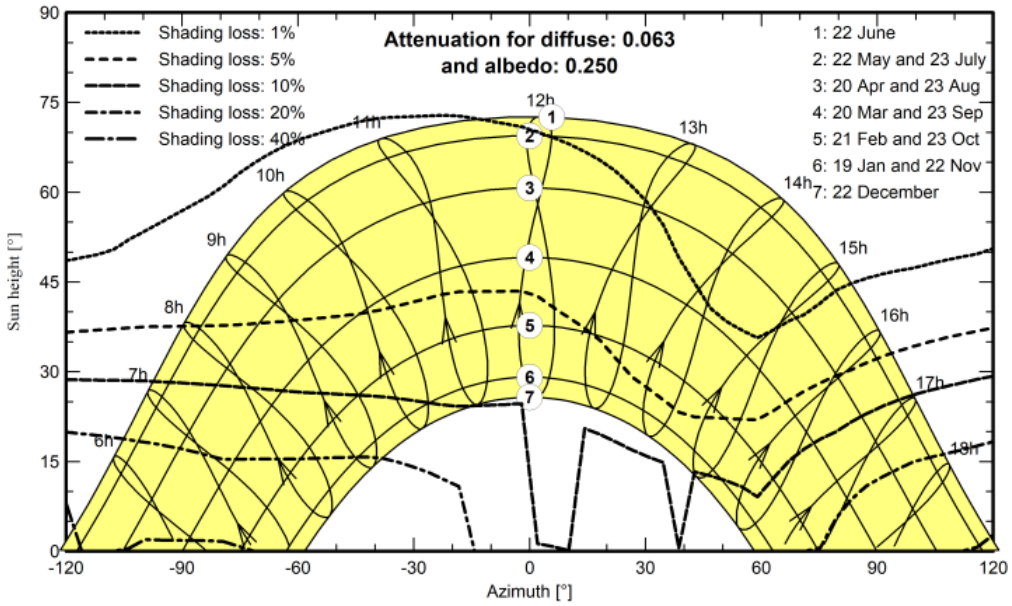

Main results

System Production

Produced Energy	91110 MWh/year	Specific production	1777 kWh/kWp/year
		Performance Ratio PR	83.39 %

Normalized productions (per installed kWp)

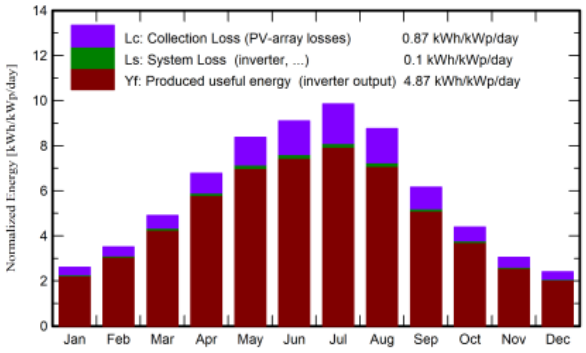

Performance Ratio PR

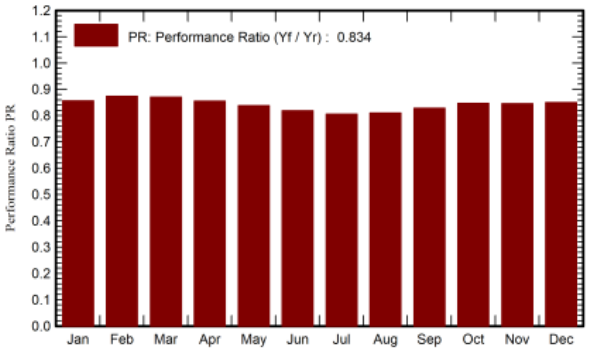

Balances and main results

	GlobHor kWh/m²	DiffHor kWh/m²	T_Amb °C	GlobInc kWh/m²	GlobEff kWh/m²	EArray MWh	E_Grid MWh	PR ratio
January	61.0	27.90	6.52	80.9	71.6	3615	3552	0.856
February	74.9	35.10	6.66	98.4	89.1	4487	4410	0.874
March	117.6	51.40	9.35	152.0	140.0	6911	6781	0.870
April	154.8	64.40	13.00	203.3	188.5	9093	8910	0.855
May	199.2	75.70	17.46	259.3	241.7	11375	11139	0.838
June	208.7	74.50	22.32	273.1	254.4	11714	11465	0.819
July	227.3	66.70	25.84	305.5	284.3	12897	12619	0.805
August	201.8	62.10	25.59	271.4	252.8	11521	11271	0.810
September	140.3	54.10	20.86	185.0	170.6	8015	7856	0.828
October	101.9	42.50	15.93	136.1	124.0	6016	5906	0.846
November	67.1	29.50	11.45	91.3	81.0	4024	3956	0.845
December	55.4	25.00	7.31	74.5	65.1	3299	3246	0.850
Year	1610.0	608.90	15.24	2130.8	1963.2	92966	91110	0.834

Legends

GlobHor	Global horizontal irradiation	EArray	Effective energy at the output of the array
DiffHor	Horizontal diffuse irradiation	E_Grid	Energy injected into grid
T_Amb	Ambient Temperature	PR	Performance Ratio
GlobInc	Global incident in coll. plane		
GlobEff	Effective Global, corr. for IAM and shadings		

Loss diagram

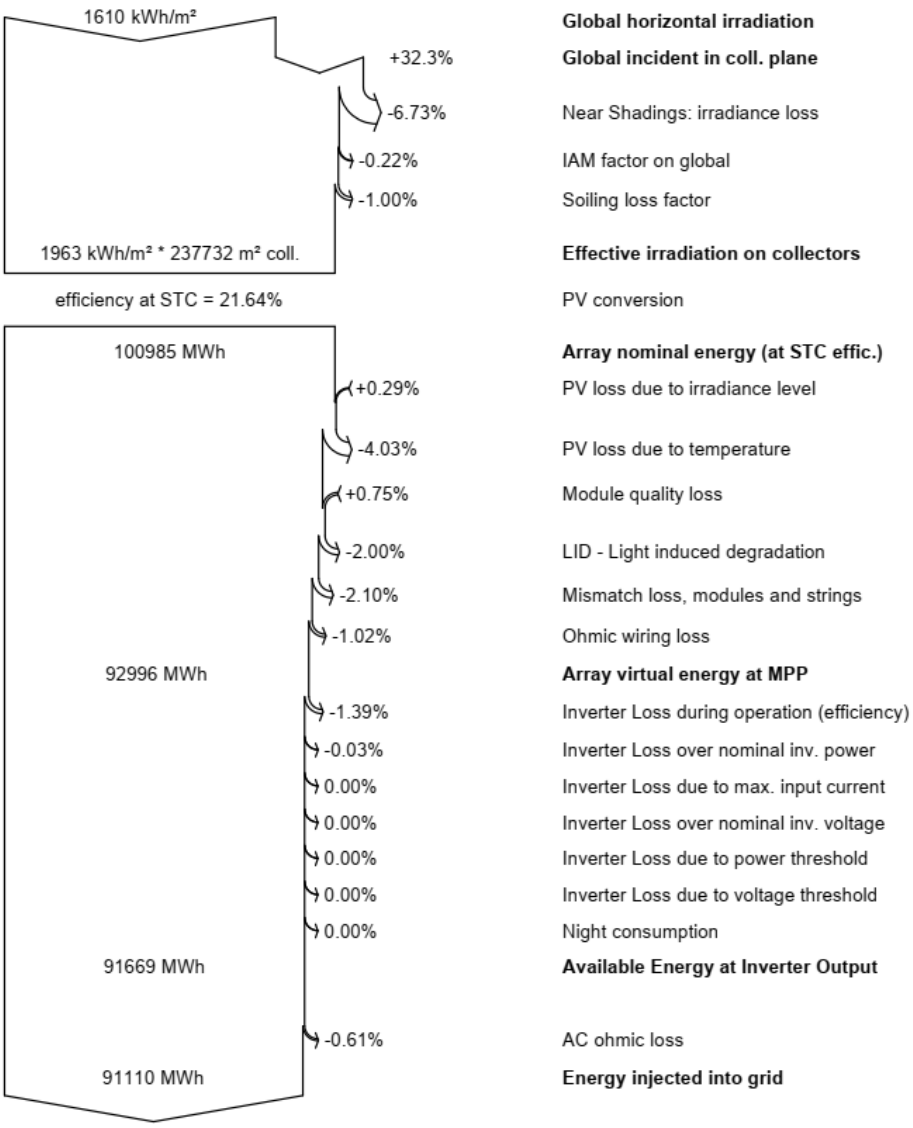

Special graphs

Diagramma giornaliero entrata/uscita

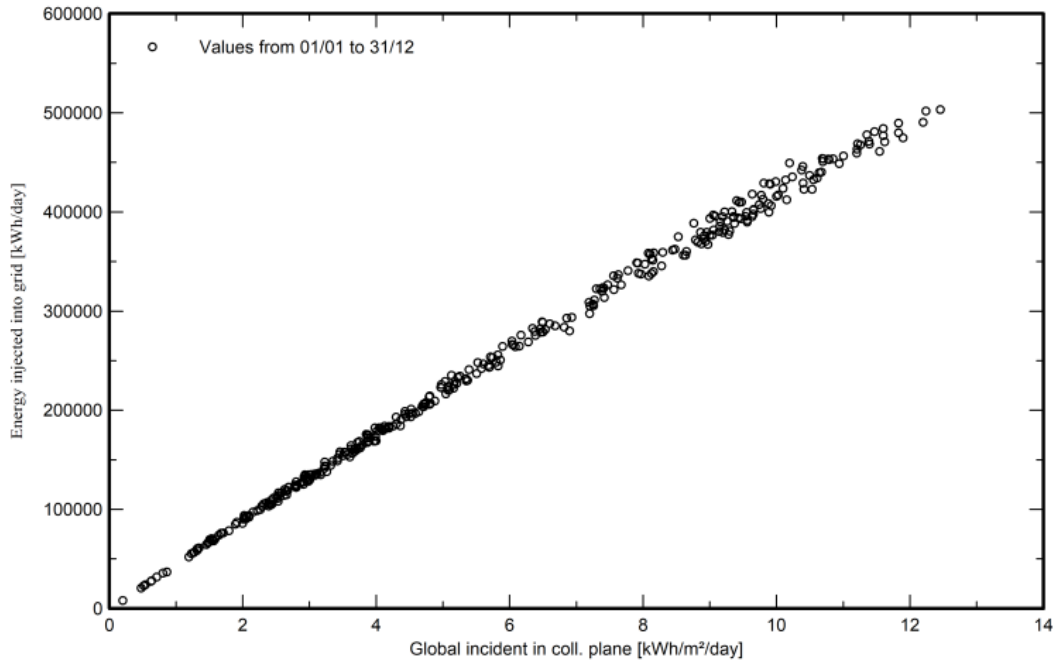

Distribuzione potenza in uscita sistema

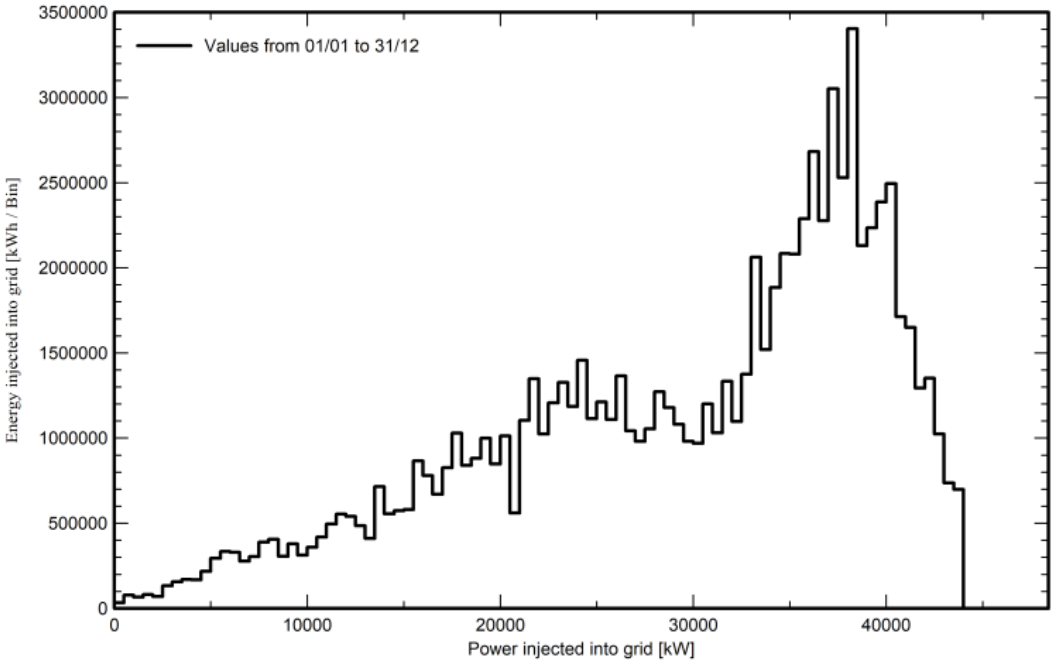

- **PVSYST REPORT FOR PV PLANT WITHOUT TURBINES LOSSES**

Project: IMPIANTO PV GRAVINA IN PUGLIA

Variant: Impianto PV VC2 con perdite dettagliate

PVsyst V7.2.8
VC3, Simulation date:
04/11/22 23:06
with v7.2.8

Loss diagram

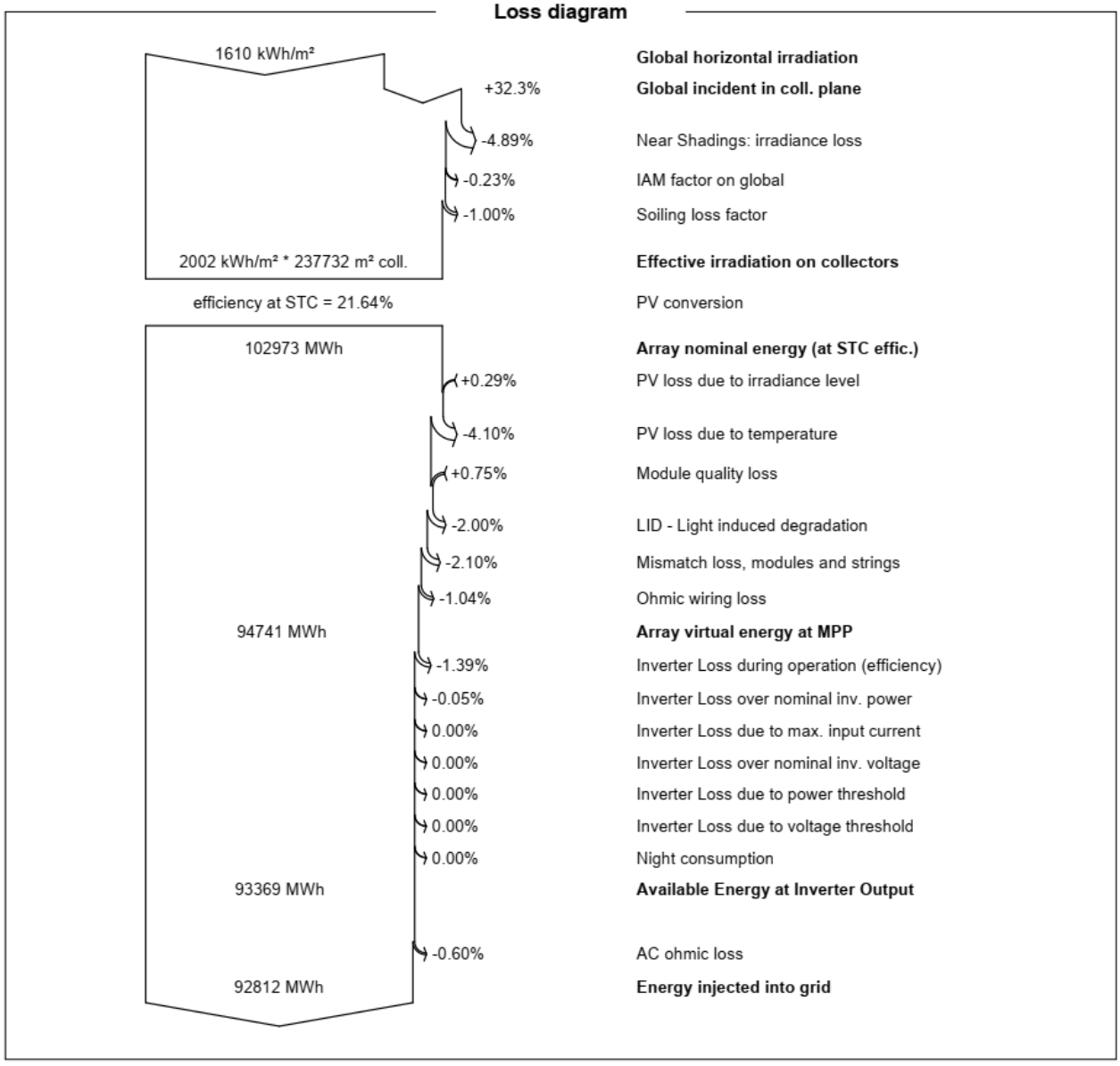

APPENDIX D

- **AREA AROUND WTG04 AEP**

Solar PV - Main

Calculation: PROVA CALCOLO AEP CON OMBRE INTORNO TURBINA WTG04

Setup

Accept gap filled data:	yes
Gapfilled:	0,0%
Calculation type:	AEP
Data start:	01/01/2021
Data end:	01/01/2022
Tracking included:	Yes
Bifacial included:	Yes

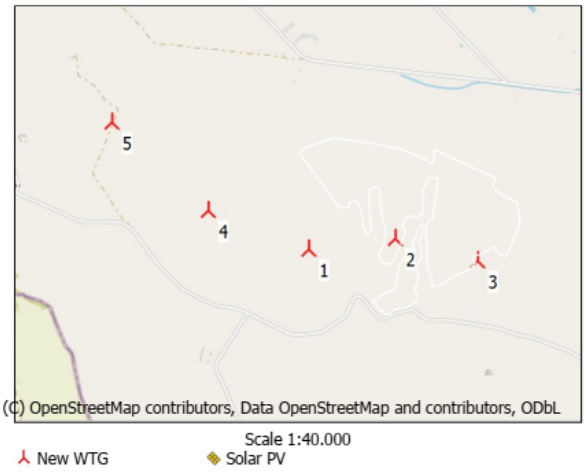

Shading calculation includes:

	Included	Settings	Number/data
Obstacles	no		0
Panels	no	only in area	
WTG Towers	yes		5
WTG Rotor	yes	Reduce to 50%	5
Topography	no		

Meteo data:

Raw input data:

	Name	Min	Max	Average	Recovery	Energy
Solar irradiation	ERA5 (Gaussian Grid)_N40,889915_E016,20 (23).2,00m -	0,0 W/m²	969,3 W/m²	187,4 W/m²	100,0%	1642 kWh/m²/y
Temperature	ERA5 (Gaussian Grid)_N40,889915_E016,20 (23).2,00m -	-5,8 deg C	38,5 deg C	15,0 deg C	100,0%	
Humidity		-	-	-	0.0%	

Energy value: Gap filled, not scaled

Scaling

Scaling used: no

Main Results - Annual Energy Production

Design area (ha)	22,72
Panel area (1000 m²)	76,78
Rated power (DC) [kW]	16.561,1
Rated power (AC) [kW]	14.400,0
Average AC/DC ratio	0,87
Panels	24.718
Inverters	45
Avg. inv. size (kW AC)	320,0
ha/MW	1,58
Performance ratio (1 year)	79,3%
Net production (1 year) MWh/y	**32.437,1**
Net production (20 year) MWh/y	**26.561,1**

	GROSS *1)	**Losses *2)**						**Net**	**Cap. f.**	
		Shading loss	Before inverter	Inverter clipping	Inv. DC/AC conversion	After inverter	All loss			Performance ratio *3)
	MWh/y	[%]	[%]	[%]	[%]	[%]	[%]	MWh/y	[%]	[%]
Year 1	36287,8	1,26	5,92	0,53	1,18	1,72	10,61	32437,1	25,7	79,3
20 year average	36287,8	1,26	23,15	0,00	0,98	1,41	26,80	**26561,1**	21,1	64,9

Solar PV - Main

Calculation: PROVA CALCOLO AEP CON OMBRE INTORNO TURBINA WTG04

*1) Gross includes reduction due to incidence angle modifier.
*2) Loss percentages all relates to gross production.
*3) Performance ratio is here calculated NET (except after inverter loss) relative to irradiance on the inclined plane multiplied with panel efficiency at Standard Test Conditions.

Production per area

Area	Panels	Power	Inverters	Power	Design area	Design area	Gross	Net Year 1	Net Year 20	Cap. f. Year 1	Cap. f. Year 20	Performance
	No	kW DC	No	kW AC	ha	ha/MW	MWh/y	MWh/y	MWh/y	%	%	Ratio % (20y)
Area_1 - 16,6 ha	18081	12114,3	33	10560,0	16,59	1,57	26665,8	23753,5	19442,5	25,7	21,0	64,6
Area_2 - 6,1 ha	6637	4446,8	12	3840,0	6,14	1,60	9622,0	8683,6	7118,6	25,8	21,2	65,8
Total	**24718**	**16561,1**	**45**	**14400,0**	**22,72**	**1,58**	**36287,8**	**32437,1**	**26561,1**	**25,7**	**21,1**	**64,9**

Shading losses per area (% of gross)

Area	Gross	Panel and diffuse red.	Obstacles	WTG Towers	WTG rotors	Topo	Combined
	MWh/y	%	%	%	%	%	%
Area_1 - 16,6 ha	26665,8	NA	NA	0,41	1,35	NA	1,65
Area_2 - 6,1 ha	9622,0	NA	NA	0,07	0,17	NA	0,20
Total	**36287,8**	**NA**	**NA**	**0,32**	**1,03**	**NA**	**1,26**

Other losses per area (1. year) (% of gross)

Area	Gross	Before inverter	Inverter clipping	DC/AC conversion	After inverter	Combined
	MWh/y	%	%	%	%	%
Area_1 - 16,6 ha	26665,8	5,90	0,49	1,17	1,72	9,27
Area_2 - 6,1 ha	9622,0	5,98	0,64	1,19	1,74	9,55
Total	**36287,8**	**5,92**	**0,53**	**1,18**	**1,72**	**9,35**

Other losses per area (20. year) (% of gross)

Area	Gross	Before inverter	Inverter clipping	DC/AC conversion	After inverter	Combined
	MWh/y	%	%	%	%	%
Area_1 - 16,6 ha	26665,8	23,06	0,00	0,98	1,41	25,44
Area_2 - 6,1 ha	9622,0	23,40	0,00	0,99	1,43	25,82
Total	**36287,8**	**23,15**	**0,00**	**0,98**	**1,41**	**25,54**

Total losses per area (% of gross)

Area	Gross	Shading losses	Other losses (1y)	Other losses (20y)	**All losses (1y)**	**All losses (20y)**
	MWh/y	%	%	%	%	%
Area_1 - 16,6 ha	26665,8	1,65	9,27	25,44	10,92	27,09
Area_2 - 6,1 ha	9622,0	0,20	9,55	25,82	9,75	26,02
Total	**36287,8**	**1,26**	**9,35**	**25,54**	**10,61**	**26,80**

Panel details per area: (W refer to W DC)

Area	Type/name	Orientation	Size	Power Max / Panel	TC	NOCT	Bypass diodes:	Bypass orientation	Bifacial	BF	Degradation
			m x m	W	%/°C	°C					%/y
Area_1 - 16,6 ha	A	Portrait	1,30 x 2,38	670,0	-0,340	43,0	3	Short side	Yes	0,75	2,0
Area_2 - 6,1 ha	B	Portrait	1,30 x 2,38	670,0	-0,340	43,0	3	Short side	Yes	0,75	2,0

A: Userdefined_Vertex_665W_1,303x2,384Monocrystalline_3xBypass.PVPanel
B: Userdefined_Vertex_665W_1,303x2,384Monocrystalline_3xBypass.PVPanel

Details per area

Area	Row count	Row distance	Tilt	Azimuth	Ground offset	Irradiation on panel: Direct	Diffuse	Reflected	Albedo	Total
		m	°	°	m	kWh/m²/y	kWh/m²/y	kWh/m²/y		kWh/m²/y
Area_1 - 16,6 ha	98	6,0	#	90	3,0	1406,2	815,0	311,7	0,2	2532,8
Area_2 - 6,1 ha	60	6,0	#	90	3,0	1367,1	801,5	311,5	0,2	2480,1

Solar PV - Time Varying production

Calculation: PROVA CALCOLO AEP CON OMBRE INTORNO TURBINA WTG04

Production MWh/y

Values are averages for the calculation period 01/01/2021 - 01/01/2022 with all calculated losses deducted. Also average degradation losses of 2,0% per year for 20 years are deducted

Hour	Jan	Feb	Mar	Apr	May	Jun	Jul	Aug	Sep	Oct	Nov	Dec	All
0	0,0	0,0	0,0	0,0	0,0	0,0	0,0	0,0	0,0	0,0	0,0	0,0	**-0,1**
1	0,0	0,0	0,0	0,0	0,0	0,0	0,0	0,0	0,0	0,0	0,0	0,0	**-0,1**
2	0,0	0,0	0,0	0,0	0,0	0,0	0,0	0,0	0,0	0,0	0,0	0,0	**-0,1**
3	0,0	0,0	0,0	0,0	0,0	0,0	0,0	0,0	0,0	0,0	0,0	0,0	**-0,1**
4	0,0	0,0	0,0	0,0	0,0	0,0	0,0	0,0	0,0	0,0	0,0	0,0	**-0,1**
5	0,0	0,0	0,0	1,4	23,4	37,8	23,5	3,0	0,0	0,0	0,0	0,0	**89,1**
6	0,0	0,0	9,8	61,4	148,1	174,1	152,9	93,6	37,5	3,9	0,0	0,0	**681,4**
7	0,3	23,6	116,8	227,7	342,7	336,6	339,6	294,8	196,5	84,0	16,3	0,9	**1.980,0**
8	57,9	151,7	285,4	287,5	327,0	316,1	322,6	321,0	300,4	204,7	89,6	68,1	**2.732,0**
9	150,2	220,4	274,7	280,4	332,3	331,5	329,2	316,9	280,7	196,9	127,2	153,9	**2.994,5**
10	141,4	201,9	261,7	287,4	333,7	327,7	333,7	320,9	270,6	198,4	131,5	132,8	**2.941,9**
11	140,2	191,0	256,3	276,5	319,2	321,9	328,4	313,0	257,5	185,1	122,4	123,9	**2.835,3**
12	133,5	187,2	248,6	267,9	318,2	311,1	323,0	304,9	255,4	180,6	118,7	120,6	**2.769,8**
13	129,3	192,2	249,0	253,6	312,5	308,9	319,4	299,4	244,6	164,5	107,1	118,5	**2.698,9**
14	117,8	190,3	242,9	233,6	295,5	295,5	306,5	280,6	213,4	142,9	92,3	104,2	**2.515,5**
15	78,5	168,4	217,6	210,6	280,5	266,7	276,5	248,9	175,2	99,7	45,8	46,6	**2.115,1**
16	10,7	79,4	147,0	167,8	242,0	215,0	230,0	210,9	116,6	24,9	0,2	0,0	**1.444,5**
17	0,0	0,2	27,5	64,6	130,8	151,0	156,2	109,7	19,9	0,0	0,0	0,0	**659,9**
18	0,0	0,0	0,0	0,2	18,0	40,7	37,5	8,0	0,0	0,0	0,0	0,0	**104,2**
19	0,0	0,0	0,0	0,0	0,0	0,0	0,0	0,0	0,0	0,0	0,0	0,0	**-0,1**
20	0,0	0,0	0,0	0,0	0,0	0,0	0,0	0,0	0,0	0,0	0,0	0,0	**-0,1**
21	0,0	0,0	0,0	0,0	0,0	0,0	0,0	0,0	0,0	0,0	0,0	0,0	**-0,1**
22	0,0	0,0	0,0	0,0	0,0	0,0	0,0	0,0	0,0	0,0	0,0	0,0	**-0,1**
23	0,0	0,0	0,0	0,0	0,0	0,0	0,0	0,0	0,0	0,0	0,0	0,0	**-0,1**
All	**959,8**	**1.606,2**	**2.337,3**	**2.620,5**	**3.423,8**	**3.434,6**	**3.478,9**	**3.125,5**	**2.368,4**	**1.485,5**	**851,1**	**869,5**	**26.561,1**

Hourly power (kW AC)

Hour	Jan	Feb	Mar	Apr	May	Jun	Jul	Aug	Sep	Oct	Nov	Dec	All (avg)
0	0	0	0	0	0	0	0	0	0	0	0	0	**0**
1	0	0	0	0	0	0	0	0	0	0	0	0	**0**
2	0	0	0	0	0	0	0	0	0	0	0	0	**0**
3	0	0	0	0	0	0	0	0	0	0	0	0	**0**
4	0	0	0	0	0	0	0	0	0	0	0	0	**0**
5	0	0	0	47	754	1.261	760	96	0	0	0	0	**244**
6	0	0	317	2.046	4.778	5.803	4.933	3.020	1.249	127	0	0	**1.865**
7	10	834	3.769	7.591	11.056	11.221	10.956	9.511	6.550	2.709	543	30	**5.421**
8	1.868	5.371	9.206	9.582	10.549	10.536	10.407	10.356	10.014	6.603	2.987	2.195	**7.480**
9	4.845	7.803	8.863	9.347	10.719	11.050	10.621	10.224	9.358	6.350	4.241	4.965	**8.198**
10	4.563	7.148	8.443	9.580	10.764	10.925	10.766	10.351	9.022	6.401	4.382	4.285	**8.055**
11	4.522	6.762	8.267	9.216	10.297	10.731	10.593	10.096	8.583	5.970	4.079	3.997	**7.763**
12	4.306	6.628	8.018	8.931	10.264	10.370	10.418	9.835	8.515	5.827	3.958	3.891	**7.583**
13	4.170	6.803	8.034	8.453	10.079	10.297	10.302	9.658	8.153	5.306	3.572	3.823	**7.389**
14	3.801	6.735	7.835	7.787	9.533	9.850	9.887	9.052	7.115	4.609	3.076	3.363	**6.887**
15	2.534	5.960	7.020	7.022	9.049	8.890	8.919	8.028	5.840	3.217	1.527	1.504	**5.791**
16	346	2.810	4.742	5.592	7.805	7.167	7.419	6.802	3.888	803	8	0	**3.955**
17	0	7	886	2.154	4.221	5.032	5.038	3.539	664	0	0	0	**1.807**
18	0	0	0	5	580	1.356	1.208	257	0	0	0	0	**285**
19	0	0	0	0	0	0	0	0	0	0	0	0	**0**
20	0	0	0	0	0	0	0	0	0	0	0	0	**0**
21	0	0	0	0	0	0	0	0	0	0	0	0	**0**
22	0	0	0	0	0	0	0	0	0	0	0	0	**0**
23	0	0	0	0	0	0	0	0	0	0	0	0	**0**
All (avg)	**1.290**	**2.369**	**3.142**	**3.640**	**4.602**	**4.770**	**4.676**	**4.201**	**3.289**	**1.997**	**1.182**	**1.169**	**3.030**

Solar PV - Time Varying production

Calculation: PROVA CALCOLO AEP CON OMBRE INTORNO TURBINA WTG04

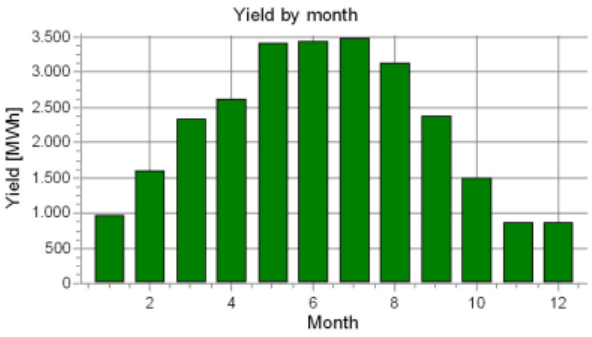

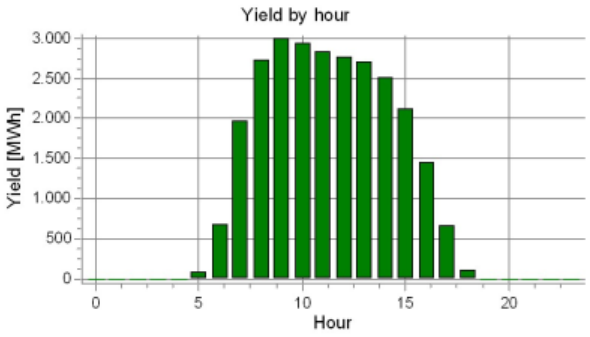

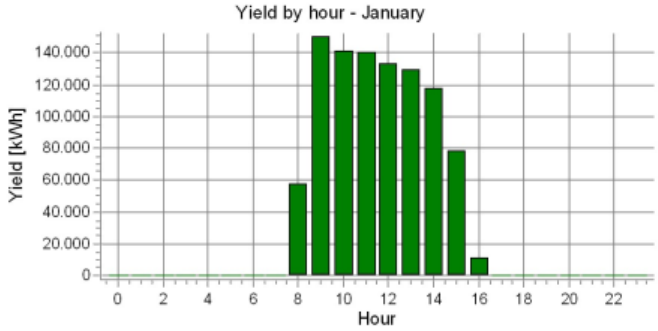

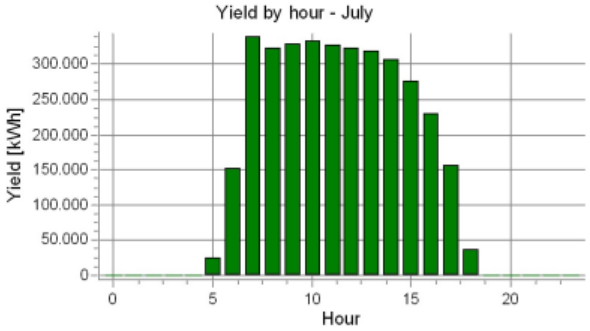

Please note that the duration table and graph is without degradation loss

Hours	Hours [%]	Hours accumulated	Power kW
630,0	7,2	630,0	13.421 - 14.128
265,0	3,0	895,0	12.715 - 13.421
200,0	2,3	1095,0	12.009 - 12.715
183,0	2,1	1278,0	11.302 - 12.009
180,0	2,1	1458,0	10.596 - 11.302
160,0	1,8	1618,0	9.889,4 - 10.596
180,0	2,1	1798,0	9.183,0 - 9.889,4
153,0	1,7	1951,0	8.476,6 - 9.183,0
161,0	1,8	2112,0	7.770,2 - 8.476,6
182,0	2,1	2294,0	7.063,8 - 7.770,2
201,0	2,3	2495,0	6.357,5 - 7.063,8
175,0	2,0	2670,0	5.651,1 - 6.357,5
165,0	1,9	2835,0	4.944,7 - 5.651,1
170,0	1,9	3005,0	4.238,3 - 4.944,7
139,0	1,6	3144,0	3.531,9 - 4.238,3
159,0	1,8	3303,0	2.825,5 - 3.531,9
179,0	2,0	3482,0	2.119,2 - 2.825,5
209,0	2,4	3691,0	1.412,8 - 2.119,2
226,0	2,6	3917,0	706,4 - 1.412,8
289,0	3,3	4206,0	0,0 - 706,4
4554,0	52,0	8760,0	0,0

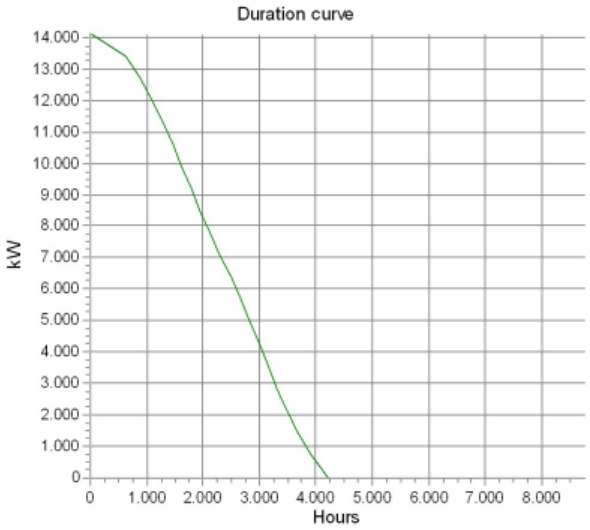

Solar PV - Panels

Calculation: PROVA CALCOLO AEP CON OMBRE INTORNO TURBINA WTG04

Panels per area

Area	No. panels	Panel name
Area_1 - 16,6 ha	18081	Userdefined_Vertex_665W_1,303x2,384Monocrystalline_3xBypass.PVPanel
Area_2 - 6,1 ha	6637	Userdefined_Vertex_665W_1,303x2,384Monocrystalline_3xBypass.PVPanel

Userdefined_Vertex_665W_1,303x2,384Monocrystalline_3xBypass.PVPanel

Panel name Userdefined_Vertex_665W_1,303x2,384Monocrystalline_3xBypass.PVPanel
Panel type: Monocrystalline

	Long side [m]	Short side [m]	Orientation	Area [m²]
Panel size (outer):	2,384	1,303	Portrait	3,106

	W DC	W/m²	Panel efficiency [%] *)
Pmax:	670,000	215,687	21,569

*) At standard test conditions, irradiance 1000W/m², module temp 25 deg C, air mass 1.5 spectrum

Temperature Coefficient [%/deg C]	-0,340
Auto calculated	no
TC by auto calculation [%/deg C]	-0,460
NOCT (Nominal Operating Cell Temperature, deg C)	43,000

Bypass diodes:

Bypass diodes used:	Short side
- Number	3
Threshold for shading reduction	0,0%

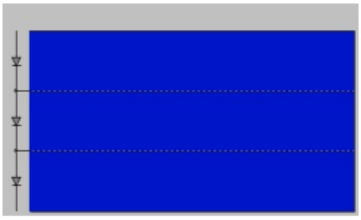

Bifacial

Bifacial Yes

Solar PV - Inverter(s)

Calculation: PROVA CALCOLO AEP CON OMBRE INTORNO TURBINA WTG04

Inverter specifications:

	Area	AC/DC spec.	DC-power [kW]	Inv.Size [kW]	No. Of inverters	AC power [kW]	AC/DC realized
A	Area_1 - 16,6 ha	0,9	12114,3	320,0	33	10560,0	0,87
A	Area_2 - 6,1 ha	0,9	4446,8	320,0	12	3840,0	0,86

Inverter efficiency: A

	Default used	Default value	Used value
Maximum AC power [kW]		-	320,0
Efficiency at maximum AC outp...	no	98,5	98,8
Power consumption during oper...	no	2560 (0,800%)	260 (0,081%)
Power consumption no operatio...	no	80 (0,025%)	6 (0,002%)

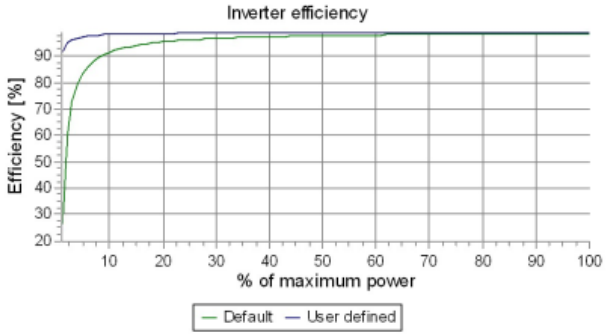

- **AREA AROUND WTG05 AEP**

Solar PV - Main

Calculation: PROVA AEP CON OMBRE ATTORNO WTG05

Setup

Accept gap filled data:	yes
Gapfilled:	0,0%
Calculation type:	AEP
Data start:	01/01/2021
Data end:	01/01/2022
Tracking included:	Yes
Bifacial included:	Yes

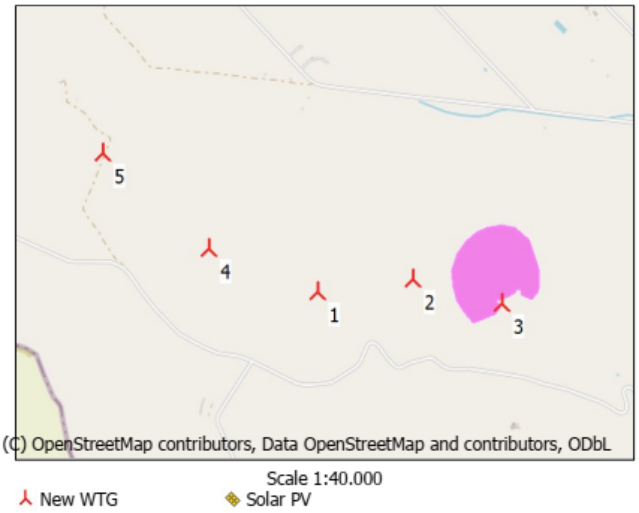

Shading calculation includes:

	Included	Settings	Number/data
Obstacles	no		0
Panels	no	only in area	
WTG Towers	yes		5
WTG Rotor	yes	Reduce to 50%	5
Topography	no		

Meteo data:

Raw input data:

	Name	Min	Max	Average	Recovery	Energy
Solar irradiation	ERA5 (Gaussian Grid)_N40,889915_E016,20 (23).2,00m -	0,0 W/m²	969,3 W/m²	187,4 W/m²	100,0%	1642 kWh/m²/y
Temperature	ERA5 (Gaussian Grid)_N40,889915_E016,20 (23).2,00m -	-5,8 deg C	38,5 deg C	15,0 deg C	100,0%	
Humidity		-	-	-	0.0%	

Energy value: Gap filled, not scaled

Scaling

Scaling used: no

Main Results - Annual Energy Production

Design area (ha)	18,49
Panel area (1000 m²)	63,19
Rated power (DC) [kW]	13.629,1
Rated power (AC) [kW]	11.840,0
Average AC/DC ratio	0,87
Panels	20.342
Inverters	37
Avg. inv. size (kW AC)	320,0
ha/MW	1,56
Performance ratio (1 year)	78,7%
Net production (1 year) MWh/y	**26.700,4**
Net production (20 year) MWh/y	**21.855,1**

	GROSS *1)	**Losses *2)**						**Net**	**Cap. f.**	
		Shading loss	Before inverter	Inverter clipping	Inv. DC/AC conversion	After inverter	All loss			Performance ratio *3)
	MWh/y	[%]	[%]	[%]	[%]	[%]	[%]	MWh/y	[%]	[%]
Year 1	30027,3	1,82	5,89	0,49	1,17	1,71	11,08	26700,4	25,7	78,7
20 year average	30027,3	1,82	23,02	0,00	0,98	1,40	27,22	**21855,1**	21,1	64,5

Solar PV - Main

Calculation: PROVA AEP CON OMBRE ATTORNO WTG05

*1) Gross includes reduction due to incidence angle modifier.
*2) Loss percentages all relates to gross production.
*3) Performance ratio is here calculated NET (except after inverter loss) relative to irradiance on the inclined plane multiplied with panel efficiency at Standard Test Conditions.

Production per area

Area	Panels	Power	Inverters	Power	Design area	Design area	Gross	Net Year 1	Net Year 20	Cap. f. Year 1	Cap. f. Year 20	Performance
	No	kW DC	No	kW AC	ha	ha/MW	MWh/y	MWh/y	MWh/y	%	%	Ratio % (20y)
Area_1 - 18,5 ha	20342	13629,1	37	11840,0	18,49	1,56	30027,3	26700,4	21855,1	25,7	21,1	64,5
Total	**20342**	**13629,1**	**37**	**11840,0**	**18,49**	**1,56**	**30027,3**	**26700,4**	**21855,1**	**25,7**	**21,1**	**64,5**

Shading losses per area (% of gross)

Area	Gross	Panel and diffuse red.	Obstacles	WTG Towers	WTG rotors	Topo	Combined
	MWh/y	%	%	%	%	%	%
Area_1 - 18,5 ha	30027,3	NA	NA	0,30	1,68	NA	1,82
Total	**30027,3**	**NA**	**NA**	**0,30**	**1,68**	**NA**	**1,82**

Other losses per area (1. year) (% of gross)

Area	Gross	Before inverter	Inverter clipping	DC/AC conversion	After inverter	Combined
	MWh/y	%	%	%	%	%
Area_1 - 18,5 ha	30027,3	5,89	0,49	1,17	1,71	9,26
Total	**30027,3**	**5,89**	**0,49**	**1,17**	**1,71**	**9,26**

Other losses per area (20. year) (% of gross)

Area	Gross	Before inverter	Inverter clipping	DC/AC conversion	After inverter	Combined
	MWh/y	%	%	%	%	%
Area_1 - 18,5 ha	30027,3	23,02	0,00	0,98	1,40	25,40
Total	**30027,3**	**23,02**	**0,00**	**0,98**	**1,40**	**25,40**

Total losses per area (% of gross)

Area	Gross	Shading losses	Other losses (1y)	Other losses (20y)	All losses (1y)	All losses (20y)
	MWh/y	%	%	%	%	%
Area_1 - 18,5 ha	30027,3	1,82	9,26	25,40	11,08	27,22
Total	**30027,3**	**1,82**	**9,26**	**25,40**	**11,08**	**27,22**

Panel details per area: (W refer to W DC)

Area	Type/name	Orientation	Size	Power Max / Panel	TC	NOCT	Bypass diodes:	Bypass orientation	Bifacial	BF	Degradation
			m x m	W	%/°C	°C					%/y
Area_1 - 18,5 ha	A	Portrait	1,30 x 2,38	670,0	-0,340	43,0	3	Short side	Yes	0,75	2,0

A: Userdefined_Vertex_665W_1,303x2,384Monocrystalline_3xBypass.PVPanel

Details per area

Area	Row count	Row distance	Tilt	Azimuth	Ground offset	Irradiation on panel: Direct	Diffuse	Reflected	Albedo	Total
		m	°	°	m	kWh/m²/y	kWh/m²/y	kWh/m²/y		kWh/m²/y
Area_1 - 18,5 ha	84	6,0	#	90	3,0	1408,4	815,8	311,7	0,2	2535,8

 # Tracking settings

Area	Backtracking	Min angle	Max angle	Manual tilt angles: Date:
Area_1 - 18,5 ha	Yes	-60,0	60,0	Continuous tracking

Production MWh/y

Values are averages for the calculation period 01/01/2021 - 01/01/2022 with all calculated losses deducted. Also average degradation losses of 2,0% per year for 20 years are deducted

Hour	Jan	Feb	Mar	Apr	May	Jun	Jul	Aug	Sep	Oct	Nov	Dec	All
0	0,0	0,0	0,0	0,0	0,0	0,0	0,0	0,0	0,0	0,0	0,0	0,0	**-0,1**
1	0,0	0,0	0,0	0,0	0,0	0,0	0,0	0,0	0,0	0,0	0,0	0,0	**-0,1**
2	0,0	0,0	0,0	0,0	0,0	0,0	0,0	0,0	0,0	0,0	0,0	0,0	**-0,1**
3	0,0	0,0	0,0	0,0	0,0	0,0	0,0	0,0	0,0	0,0	0,0	0,0	**-0,1**
4	0,0	0,0	0,0	0,0	0,0	0,0	0,0	0,0	0,0	0,0	0,0	0,0	**-0,1**
5	0,0	0,0	0,0	1,2	21,1	35,2	21,9	2,6	0,0	0,0	0,0	0,0	**81,9**
6	0,0	0,0	9,0	56,2	131,3	155,3	137,3	84,7	35,6	3,7	0,0	0,0	**613,2**
7	0,4	23,5	109,4	201,4	282,4	276,0	280,7	259,1	178,6	78,2	15,9	0,9	**1.706,5**
8	56,5	138,2	240,6	233,6	267,1	259,0	264,1	261,4	242,8	167,8	80,6	67,3	**2.279,0**
9	121,2	175,8	220,7	227,3	271,2	271,4	269,1	257,6	226,2	157,5	101,5	123,4	**2.423,0**
10	112,5	161,7	212,0	234,4	273,4	269,1	273,7	262,0	220,3	161,3	106,4	106,1	**2.392,8**
11	114,2	155,9	209,8	226,9	262,9	265,5	270,6	257,0	211,1	151,3	99,9	100,9	**2.326,1**
12	108,9	152,8	203,1	219,8	262,8	257,4	267,0	250,9	208,6	147,3	97,0	98,3	**2.273,9**
13	105,3	156,0	202,4	208,3	258,6	256,0	264,5	246,8	199,2	133,4	87,3	96,6	**2.214,2**
14	95,4	152,4	196,1	191,7	244,1	244,2	253,4	231,3	173,3	114,9	74,9	85,5	**2.057,4**
15	64,7	136,4	176,2	173,1	231,6	220,1	228,3	205,0	142,7	79,7	36,6	38,7	**1.733,0**
16	7,8	60,0	115,0	137,3	199,4	177,2	189,6	173,6	92,2	18,3	0,1	0,0	**1.170,5**
17	0,0	0,1	19,1	48,7	100,7	119,1	123,2	84,4	14,1	0,0	0,0	0,0	**509,4**
18	0,0	0,0	0,0	0,0	12,0	30,2	27,4	5,4	0,0	0,0	0,0	0,0	**75,0**
19	0,0	0,0	0,0	0,0	0,0	0,0	0,0	0,0	0,0	0,0	0,0	0,0	**-0,1**
20	0,0	0,0	0,0	0,0	0,0	0,0	0,0	0,0	0,0	0,0	0,0	0,0	**-0,1**
21	0,0	0,0	0,0	0,0	0,0	0,0	0,0	0,0	0,0	0,0	0,0	0,0	**-0,1**
22	0,0	0,0	0,0	0,0	0,0	0,0	0,0	0,0	0,0	0,0	0,0	0,0	**-0,1**
23	0,0	0,0	0,0	0,0	0,0	0,0	0,0	0,0	0,0	0,0	0,0	0,0	**-0,1**
All	**786,8**	**1.312,8**	**1.913,4**	**2.159,9**	**2.818,6**	**2.835,7**	**2.870,6**	**2.581,7**	**1.944,5**	**1.213,3**	**700,2**	**717,6**	**21.855,1**

Hourly power (kW AC)

Hour	Jan	Feb	Mar	Apr	May	Jun	Jul	Aug	Sep	Oct	Nov	Dec	All (avg)
0	-0,2	-0,2	-0,2	-0,2	-0,2	-0,2	-0,2	-0,2	-0,2	-0,2	-0,2	-0,2	**-0,2**
1	-0,2	-0,2	-0,2	-0,2	-0,2	-0,2	-0,2	-0,2	-0,2	-0,2	-0,2	-0,2	**-0,2**
2	-0,2	-0,2	-0,2	-0,2	-0,2	-0,2	-0,2	-0,2	-0,2	-0,2	-0,2	-0,2	**-0,2**
3	-0,2	-0,2	-0,2	-0,2	-0,2	-0,2	-0,2	-0,2	-0,2	-0,2	-0,2	-0,2	**-0,2**
4	-0,2	-0,2	-0,2	-0,2	-0,2	-0,2	-0,2	-0,2	-0,2	-0,2	-0,2	-0,2	**-0,2**
5	-0,2	-0,2	-0,2	40,6	680,0	1.172,3	707,6	82,8	-0,2	-0,2	-0,2	-0,2	**224,3**
6	-0,2	-0,2	290,4	1.873,8	4.236,0	5.177,5	4.429,6	2.733,6	1.186,8	119,7	-0,2	-0,2	**1.678,9**
7	11,7	832,5	3.530,3	6.713,1	9.110,8	9.200,9	9.054,1	8.358,8	5.951,9	2.522,4	528,5	29,9	**4.672,2**
8	1.823,4	4.893,2	7.761,3	7.785,6	8.616,0	8.632,1	8.518,0	8.432,6	8.092,9	5.413,7	2.688,1	2.171,2	**6.239,6**
9	3.908,8	6.224,6	7.118,2	7.577,0	8.749,9	9.048,0	8.681,8	8.308,2	7.540,5	5.080,8	3.384,3	3.981,2	**6.633,9**
10	3.630,6	5.722,2	6.839,1	7.813,9	8.819,8	8.971,5	8.828,4	8.450,2	7.342,6	5.202,4	3.545,5	3.422,0	**6.551,2**
11	3.685,2	5.518,5	6.768,1	7.564,7	8.479,1	8.851,3	8.728,1	8.291,5	7.035,2	4.881,3	3.331,0	3.254,9	**6.368,5**
12	3.512,6	5.410,2	6.552,3	7.327,2	8.476,7	8.580,2	8.613,0	8.092,3	6.953,6	4.750,6	3.232,4	3.171,3	**6.225,5**
13	3.397,5	5.521,6	6.528,2	6.942,2	8.341,2	8.531,9	8.531,0	7.960,9	6.639,5	4.303,8	2.910,9	3.115,7	**6.062,3**
14	3.077,4	5.395,8	6.325,3	6.391,6	7.875,6	8.141,3	8.173,5	7.461,7	5.777,7	3.705,9	2.498,3	2.756,6	**5.632,7**
15	2.085,8	4.828,8	5.684,5	5.769,0	7.470,2	7.337,5	7.363,0	6.614,0	4.757,0	2.569,6	1.219,8	1.248,1	**4.744,7**
16	251,7	2.124,1	3.710,4	4.575,7	6.432,4	5.906,9	6.116,6	5.598,5	3.073,0	591,0	4,7	-0,2	**3.204,7**
17	-0,2	2,6	617,1	1.624,4	3.249,9	3.969,1	3.973,7	2.721,6	469,0	-0,2	-0,2	-0,2	**1.394,5**
18	-0,2	-0,2	-0,2	0,4	388,2	1.005,1	883,5	175,0	-0,2	-0,2	-0,2	-0,2	**205,3**
19	-0,2	-0,2	-0,2	-0,2	-0,2	-0,2	-0,2	-0,2	-0,2	-0,2	-0,2	-0,2	**-0,2**
20	-0,2	-0,2	-0,2	-0,2	-0,2	-0,2	-0,2	-0,2	-0,2	-0,2	-0,2	-0,2	**-0,2**
21	-0,2	-0,2	-0,2	-0,2	-0,2	-0,2	-0,2	-0,2	-0,2	-0,2	-0,2	-0,2	**-0,2**
22	-0,2	-0,2	-0,2	-0,2	-0,2	-0,2	-0,2	-0,2	-0,2	-0,2	-0,2	-0,2	**-0,2**
23	-0,2	-0,2	-0,2	-0,2	-0,2	-0,2	-0,2	-0,2	-0,2	-0,2	-0,2	-0,2	**-0,2**
All (avg)	**1.057,6**	**1.936,3**	**2.571,8**	**2.999,9**	**3.788,5**	**3.938,5**	**3.858,3**	**3.470,0**	**2.700,7**	**1.630,8**	**972,5**	**964,5**	**2.493,2**

Solar PV - Time Varying production

Calculation: PROVA AEP CON OMBRE ATTORNO WTG05

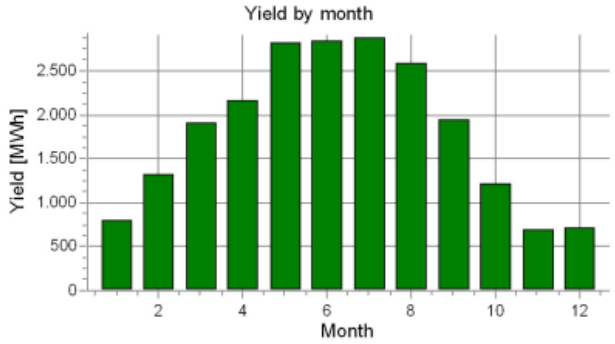

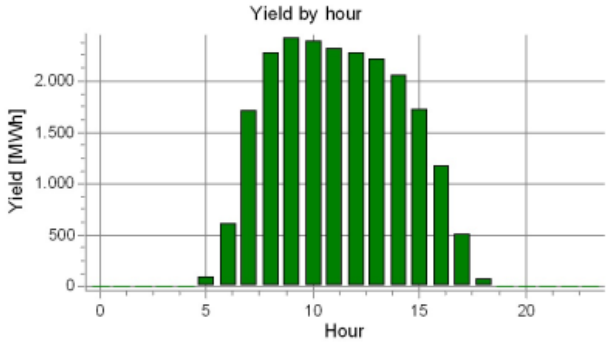

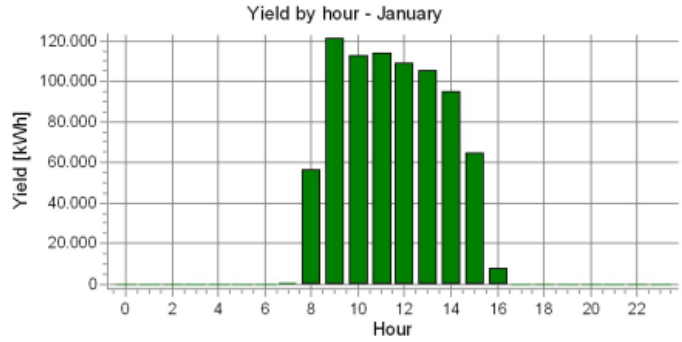

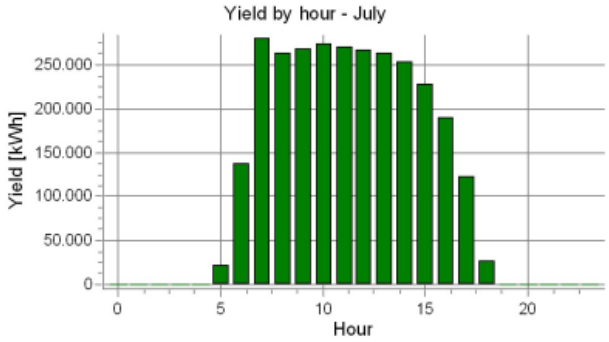

Please note that the duration table and graph is without degradation loss

Hours	Hours [%]	Hours accumulated	Power kW
638,0	7,3	638,0	11.035 - 11.616
251,0	2,9	889,0	10.454 - 11.035
202,0	2,3	1091,0	9.873,7 - 10.454
177,0	2,0	1268,0	9.292,9 - 9.873,7
182,0	2,1	1450,0	8.712,1 - 9.292,9
173,0	2,0	1623,0	8.131,3 - 8.712,1
166,0	1,9	1789,0	7.550,5 - 8.131,3
162,0	1,8	1951,0	6.969,7 - 7.550,5
180,0	2,1	2131,0	6.388,9 - 6.969,7
153,0	1,7	2284,0	5.808,1 - 6.388,9
206,0	2,4	2490,0	5.227,2 - 5.808,1
168,0	1,9	2658,0	4.646,4 - 5.227,2
183,0	2,1	2841,0	4.065,6 - 4.646,4
163,0	1,9	3004,0	3.484,8 - 4.065,6
157,0	1,8	3161,0	2.904,0 - 3.484,8
160,0	1,8	3321,0	2.323,2 - 2.904,0
154,0	1,8	3475,0	1.742,4 - 2.323,2
219,0	2,5	3694,0	1.161,6 - 1.742,4
217,0	2,5	3911,0	580,8 - 1.161,6
288,0	3,3	4199,0	0,0 - 580,8
4561,0	52,1	8760,0	0,0

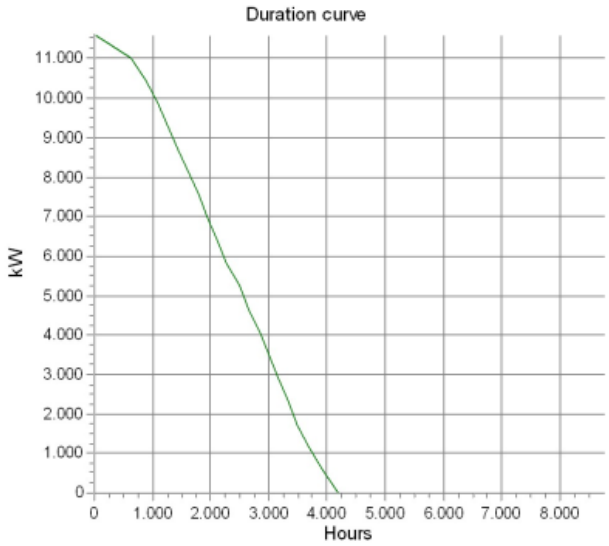

- **REMAINING AREA AEP**

Solar PV - Main

Calculation: PROVA CALCOLO AEP ZONA SENZA OMBRE

Setup

Accept gap filled data:	yes
Gapfilled:	0,0%
Calculation type:	AEP
Data start:	01/01/2021
Data end:	01/01/2022
Tracking included:	Yes
Bifacial included:	Yes

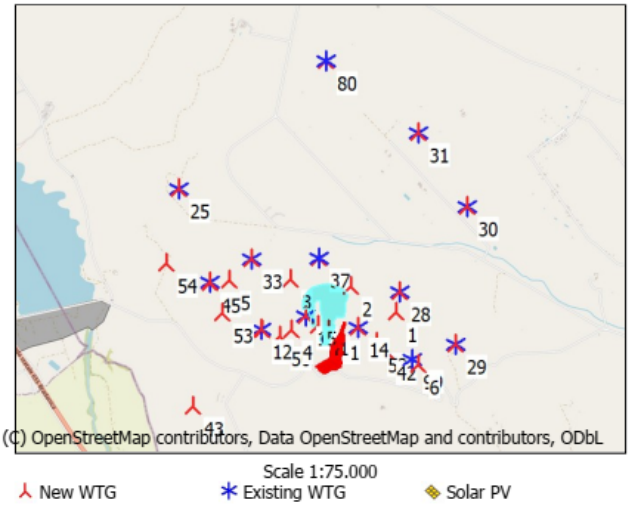

Shading calculation includes:

	Included	Settings	Number/data
Obstacles	no		
Panels	no	only in area	
WTG Towers	no		
WTG Rotor	no		
Topography	no		

Meteo data:

Raw input data:

	Name	Min	Max	Average	Recovery	Energy
Solar irradiation	ERA5 (Gaussian Grid)_N40,889915_E016,20 (23).2,00m -	0,0 W/m²	969,3 W/m²	187,4 W/m²	100,0%	1642 kWh/m²/y
Temperature	ERA5 (Gaussian Grid)_N40,889915_E016,20 (23).2,00m -	-5,8 deg C	38,5 deg C	15,0 deg C	100,0%	
Humidity		-	-	-	0.0%	

Energy value: Gap filled, not scaled

Scaling

Scaling used: no

Main Results - Annual Energy Production

Design area (ha)	25,45
Panel area (1000 m²)	85,89
Rated power (DC) [kW]	18.524,8
Rated power (AC) [kW]	16.000,0
Average AC/DC ratio	0,86
Panels	27.649
Inverters	50
Avg. inv. size (kW AC)	320,0
ha/MW	1,59
Performance ratio (1 year)	80,3%
Net production (1 year) MWh/y	**37.289,5**
Net production (20 year) MWh/y	**30.611,2**

	GROSS *1)	**Losses *2)** Shading loss	Before inverter	Inverter clipping	Inv. DC/AC conversion	After inverter	All loss	**Net**	**Cap. f.** Performance ratio *3)
	MWh/y	[%]	[%]	[%]	[%]	[%]	[%]	MWh/y	[%]	[%]
Year 1	41228,7	0,00	5,88	0,75	1,19	1,74	9,55	37289,5	26,6	80,3
20 year average	41228,7	0,00	23,33	0,00	0,99	1,43	25,75	**30611,2**	21,8	65,9

Solar PV - Main

Calculation: PROVA CALCOLO AEP ZONA SENZA OMBRE

*1) Gross includes reduction due to incidence angle modifier.
*2) Loss percentages all relates to gross production.
*3) Performance ratio is here calculated NET (except after inverter loss) relative to irradiance on the inclined plane multiplied with panel efficiency at Standard Test Conditions.

Production per area

Area	Panels	Power	Inverters	Power	Design area	Design area	Gross	Net Year 1	Net Year 20	Cap. f. Year 1	Cap. f. Year 20	Performance
	No	kW DC	No	kW AC	ha	ha/MW	MWh/y	MWh/y	MWh/y	%	%	Ratio % (20y)
Area_1 - 25,4 ha	27649	18524,8	50	16000,0	25,45	1,59	41228,7	37289,5	30611,2	26,6	21,8	65,9
Total	**27649**	**18524,8**	**50**	**16000,0**	**25,45**	**1,59**	**41228,7**	**37289,5**	**30611,2**	**26,6**	**21,8**	**65,9**

Shading losses per area (% of gross)

Area	Gross	Panel and diffuse red.	Obstacles	WTG Towers	WTG rotors	Topo	Combined
	MWh/y	%	%	%	%	%	%
Area_1 - 25,4 ha	41228,7	NA	NA	NA	NA	NA	NA
Total	**41228,7**	**NA**	**NA**	**NA**	**NA**	**NA**	**NA**

Other losses per area (1. year) (% of gross)

Area	Gross	Before inverter	Inverter clipping	DC/AC conversion	After inverter	Combined
	MWh/y	%	%	%	%	%
Area_1 - 25,4 ha	41228,7	5,88	0,75	1,19	1,74	9,55
Total	**41228,7**	**5,88**	**0,75**	**1,19**	**1,74**	**9,55**

Other losses per area (20. year) (% of gross)

Area	Gross	Before inverter	Inverter clipping	DC/AC conversion	After inverter	Combined
	MWh/y	%	%	%	%	%
Area_1 - 25,4 ha	41228,7	23,33	0,00	0,99	1,43	25,75
Total	**41228,7**	**23,33**	**0,00**	**0,99**	**1,43**	**25,75**

Total losses per area (% of gross)

Area	Gross	Shading losses	Other losses (1y)	Other losses (20y)	**All losses (1y)**	**All losses (20y)**
	MWh/y	%	%	%	%	%
Area_1 - 25,4 ha	41228,7	0,00	9,55	25,75	9,55	25,75
Total	**41228,7**	**0,00**	**9,55**	**25,75**	**9,55**	**25,75**

Panel details per area: (W refer to W DC)

Area	Type/name	Orientation	Size	Power Max / Panel	TC	NOCT	Bypass diodes:	Bypass orientation	Bifacial	BF	Degradation
			m x m	W	%/°C	°C					%/y
Area_1 - 25,4 ha	A	Portrait	1,30 x 2,38	670,0	-0,340	43,0	3	Short side	Yes	0,75	2,0

A: Userdefined_Vertex_665W_1,303x2,384Monocrystalline_3xBypass.PVPanel

Details per area

Area	Row count	Row distance	Tilt	Azimuth	Ground offset	Irradiation on panel: Direct	Diffuse	Reflected	Albedo	Total
		m	°	°	m	kWh/m²/y	kWh/m²/y	kWh/m²/y		kWh/m²/y
Area_1 - 25,4 ha	265	6,0	#	90	3,0	1419,1	824,0	311,8	0,2	2554,9

 # Tracking settings

Area	Backtracking	Min angle	Max angle	Manual tilt angles: Date:
Area_1 - 25,4 ha	Yes	-60,0	60,0	Continuous tracking

Solar PV - Time Varying production

Calculation: PROVA CALCOLO AEP ZONA SENZA OMBRE

Production MWh/y

Values are averages for the calculation period 01/01/2021 - 01/01/2022 with all calculated losses deducted. Also average degradation losses of 2,0% per year for 20 years are deducted

Hour	Jan	Feb	Mar	Apr	May	Jun	Jul	Aug	Sep	Oct	Nov	Dec	All
0	0,0	0,0	0,0	0,0	0,0	0,0	0,0	0,0	0,0	0,0	0,0	0,0	**-0,1**
1	0,0	0,0	0,0	0,0	0,0	0,0	0,0	0,0	0,0	0,0	0,0	0,0	**-0,1**
2	0,0	0,0	0,0	0,0	0,0	0,0	0,0	0,0	0,0	0,0	0,0	0,0	**-0,1**
3	0,0	0,0	0,0	0,0	0,0	0,0	0,0	0,0	0,0	0,0	0,0	0,0	**-0,1**
4	0,0	0,0	0,0	0,0	0,0	0,0	0,0	0,0	0,0	0,0	0,0	0,0	**-0,1**
5	0,0	0,0	0,0	1,6	23,5	38,6	23,0	3,8	0,0	0,0	0,0	0,0	**90,4**
6	0,0	0,0	10,3	67,2	158,4	184,1	162,5	101,5	42,4	4,2	0,0	0,0	**730,5**
7	0,4	28,5	136,5	260,9	385,8	377,2	383,5	347,1	228,5	102,5	21,5	1,3	**2.273,8**
8	116,6	192,6	335,4	323,3	366,9	354,4	361,7	360,6	338,9	236,2	122,1	137,5	**3.246,2**
9	173,1	251,5	311,1	315,8	373,6	372,5	369,9	356,7	317,1	223,5	145,3	177,5	**3.387,5**
10	162,4	231,4	298,2	325,8	376,9	369,5	376,4	363,2	308,5	228,0	151,5	153,5	**3.345,3**
11	163,5	222,3	294,8	315,2	362,0	364,3	371,8	356,3	295,2	213,4	141,4	144,7	**3.244,8**
12	155,6	217,8	285,2	304,6	360,5	351,9	365,7	346,4	291,7	207,7	137,3	140,9	**3.165,3**
13	151,1	222,6	283,4	286,3	352,4	348,1	360,2	338,3	276,7	187,9	124,1	139,1	**3.070,2**
14	136,2	217,7	273,8	262,8	332,3	332,0	344,5	315,7	239,7	161,0	105,3	121,1	**2.842,0**
15	94,8	190,5	244,5	236,7	314,9	299,2	310,3	279,6	197,0	115,4	62,2	69,2	**2.414,3**
16	27,3	129,5	179,3	188,4	271,4	241,1	257,9	236,5	144,5	46,1	1,2	0,0	**1.723,3**
17	0,0	2,3	68,4	104,3	169,4	179,3	185,9	148,8	43,5	0,0	0,0	0,0	**901,9**
18	0,0	0,0	0,0	2,3	33,1	53,3	62,1	26,1	0,0	0,0	0,0	0,0	**176,7**
19	0,0	0,0	0,0	0,0	0,0	0,0	0,0	0,0	0,0	0,0	0,0	0,0	**-0,1**
20	0,0	0,0	0,0	0,0	0,0	0,0	0,0	0,0	0,0	0,0	0,0	0,0	**-0,1**
21	0,0	0,0	0,0	0,0	0,0	0,0	0,0	0,0	0,0	0,0	0,0	0,0	**-0,1**
22	0,0	0,0	0,0	0,0	0,0	0,0	0,0	0,0	0,0	0,0	0,0	0,0	**-0,1**
23	0,0	0,0	0,0	0,0	0,0	0,0	0,0	0,0	0,0	0,0	0,0	0,0	**-0,1**
All	**1.180,7**	**1.906,6**	**2.720,9**	**2.995,2**	**3.881,0**	**3.865,4**	**3.935,4**	**3.580,4**	**2.723,6**	**1.725,6**	**1.011,8**	**1.084,6**	**30.611,2**

Hourly power (kW AC)

Hour	Jan	Feb	Mar	Apr	May	Jun	Jul	Aug	Sep	Oct	Nov	Dec	All (avg)
0	0	0	0	0	0	0	0	0	0	0	0	0	**0**
1	0	0	0	0	0	0	0	0	0	0	0	0	**0**
2	0	0	0	0	0	0	0	0	0	0	0	0	**0**
3	0	0	0	0	0	0	0	0	0	0	0	0	**0**
4	0	0	0	0	0	0	0	0	0	0	0	0	**0**
5	0	0	0	53	760	1.287	741	121	0	0	0	0	**248**
6	0	0	333	2.239	5.110	6.136	5.242	3.273	1.412	136	0	0	**2.000**
7	12	1.010	4.404	8.697	12.446	12.575	12.370	11.198	7.617	3.305	717	41	**6.225**
8	3.760	6.816	10.818	10.777	11.837	11.813	11.669	11.631	11.295	7.621	4.070	4.436	**8.888**
9	5.583	8.904	10.035	10.528	12.053	12.415	11.933	11.505	10.570	7.208	4.842	5.726	**9.275**
10	5.237	8.190	9.618	10.861	12.159	12.318	12.143	11.715	10.282	7.355	5.051	4.951	**9.159**
11	5.274	7.868	9.509	10.506	11.678	12.142	11.995	11.492	9.842	6.883	4.714	4.669	**8.884**
12	5.019	7.709	9.201	10.155	11.628	11.730	11.797	11.175	9.722	6.700	4.578	4.546	**8.666**
13	4.873	7.880	9.143	9.544	11.367	11.605	11.619	10.913	9.224	6.060	4.135	4.487	**8.406**
14	4.393	7.706	8.833	8.760	10.718	11.066	11.114	10.184	7.992	5.192	3.510	3.905	**7.781**
15	3.059	6.744	7.887	7.891	10.157	9.973	10.010	9.021	6.567	3.722	2.073	2.231	**6.610**
16	880	4.584	5.785	6.280	8.754	8.038	8.319	7.629	4.818	1.488	40	0	**4.718**
17	0	81	2.208	3.476	5.463	5.977	5.998	4.800	1.451	0	0	0	**2.469**
18	0	0	0	77	1.066	1.776	2.002	841	0	0	0	0	**484**
19	0	0	0	0	0	0	0	0	0	0	0	0	**0**
20	0	0	0	0	0	0	0	0	0	0	0	0	**0**
21	0	0	0	0	0	0	0	0	0	0	0	0	**0**
22	0	0	0	0	0	0	0	0	0	0	0	0	**0**
23	0	0	0	0	0	0	0	0	0	0	0	0	**0**
All (avg)	**1.587**	**2.812**	**3.657**	**4.160**	**5.216**	**5.369**	**5.290**	**4.812**	**3.783**	**2.319**	**1.405**	**1.458**	**3.492**

Solar PV - Time Varying production

Calculation: PROVA CALCOLO AEP ZONA SENZA OMBRE

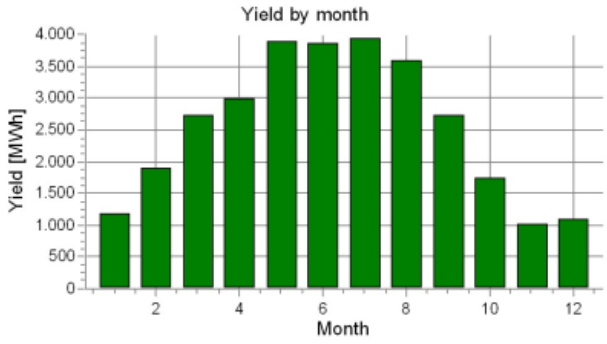

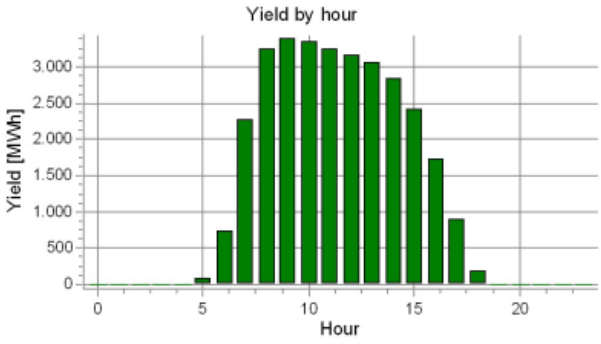

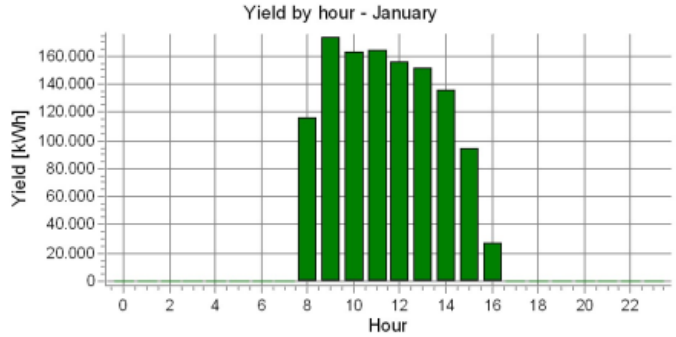

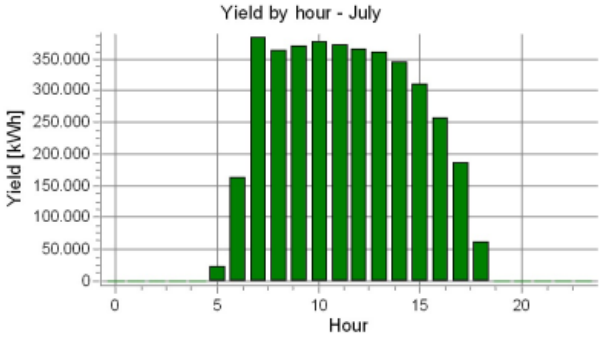

Please note that the duration table and graph is without degradation loss

Hours	Hours [%]	Hours accumulated	Power kW
727,0	8,3	727,0	14.913 - 15.697
236,0	2,7	963,0	14.128 - 14.913
184,0	2,1	1147,0	13.343 - 14.128
194,0	2,2	1341,0	12.558 - 13.343
193,0	2,2	1534,0	11.773 - 12.558
151,0	1,7	1685,0	10.988 - 11.773
175,0	2,0	1860,0	10.203 - 10.988
171,0	2,0	2031,0	9.418,5 - 10.203
166,0	1,9	2197,0	8.633,6 - 9.418,5
205,0	2,3	2402,0	7.848,7 - 8.633,6
188,0	2,1	2590,0	7.063,8 - 7.848,7
172,0	2,0	2762,0	6.279,0 - 7.063,8
163,0	1,9	2925,0	5.494,1 - 6.279,0
167,0	1,9	3092,0	4.709,2 - 5.494,1
146,0	1,7	3238,0	3.924,4 - 4.709,2
168,0	1,9	3406,0	3.139,5 - 3.924,4
175,0	2,0	3581,0	2.354,6 - 3.139,5
164,0	1,9	3745,0	1.569,7 - 2.354,6
224,0	2,6	3969,0	784,9 - 1.569,7
242,0	2,8	4211,0	0,0 - 784,9
4549,0	51,9	8760,0	0,0

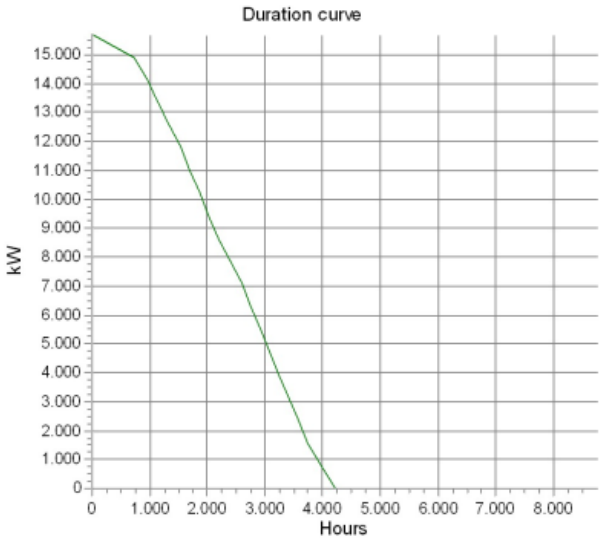

- **WindPRO SIMULATION OF TOTAL PV PLANT AREA WITHOUT SHADINGS**

Solar PV - Main

Calculation: AEP INTERO IMPIANTO SENZA OMBRE

Setup

Accept gap filled data:	yes
Gapfilled:	0,0%
Calculation type:	AEP
Data start:	01/01/2021
Data end:	01/01/2022
Tracking included:	Yes
Bifacial included:	Yes

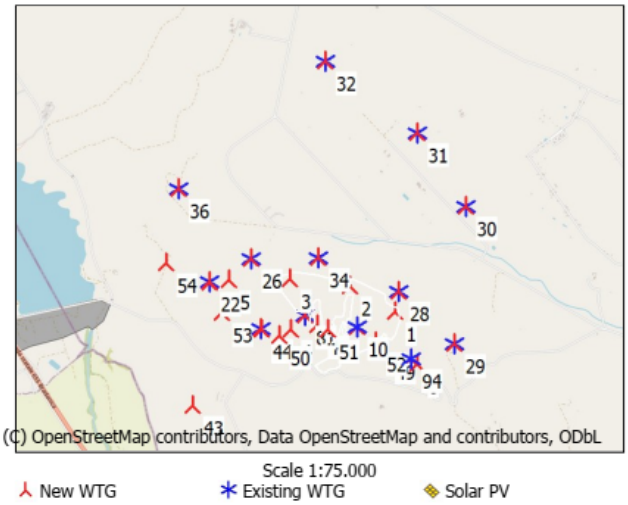

Shading calculation includes:

	Included	Settings	Number/data
Obstacles	no		
Panels	no	only in area	
WTG Towers	no		
WTG Rotor	no		
Topography	no		

Meteo data:

Raw input data:

	Name	Min	Max	Average	Recovery	Energy
Solar irradiation	ERA5 (Gaussian Grid)_N40,889915_E016,20 (23).2,00m -	0,0 W/m²	969,3 W/m²	187,4 W/m²	100,0%	1642 kWh/m²/y
Temperature	ERA5 (Gaussian Grid)_N40,889915_E016,20 (23).2,00m -	-5,8 deg C	38,5 deg C	15,0 deg C	100,0%	
Humidity		-	-	-	0.0%	

Energy value: Gap filled, not scaled

Scaling

Scaling used: no

Main Results - Annual Energy Production

Design area (ha)	66,6
Panel area (1000 m²)	227,3
Rated power (DC) [kW]	49.017,2
Rated power (AC) [kW]	41.920,0
Average AC/DC ratio	0,86
Panels	73.160
Inverters	131
Avg. inv. size (kW AC)	320,0
ha/MW	1,59
Performance ratio (1 year)	80,1%
Net production (1 year) MWh/y	**96.788,7**
Net production (20 year) MWh/y	**79.531,9**

	GROSS *1)	**Losses *2)**						**Net**	**Cap. f.**	
		Shading loss	Before inverter	Inverter clipping	Inv. DC/AC conversion	After inverter	All loss			Performance ratio *3)
	MWh/y	[%]	[%]	[%]	[%]	[%]	[%]	MWh/y	[%]	[%]
Year 1	107211,8	0,00	5,94	0,85	1,19	1,74	9,72	96788,7	26,4	80,1
20 year average	107211,8	0,00	23,39	0,01	0,99	1,43	25,82	**79531,9**	21,7	65,8

Solar PV - Main

Calculation: AEP INTERO IMPIANTO SENZA OMBRE

*1) Gross includes reduction due to incidence angle modifier.
*2) Loss percentages all relates to gross production.
*3) Performance ratio is here calculated NET (except after inverter loss) relative to irradiance on the inclined plane multiplied with panel efficiency at Standard Test Conditions.

Production per area

Area	Panels	Power	Inverters	Power	Design area	Design area	Gross	Net Year 1	Net Year 20	Cap. f. Year 1	Cap. f. Year 20	Performance
	No	kW DC	No	kW AC	ha	ha/MW	MWh/y	MWh/y	MWh/y	%	%	Ratio % (20y)
PV_1 - 60,5 ha	66520	44568,4	119	38080,0	60,51	1,59	97666,9	88147,8	72457,3	26,4	21,7	65,8
PV_2 - 6,1 ha	6640	4448,8	12	3840,0	6,13	1,60	9545,0	8640,8	7074,6	25,7	21,0	66,0
Total	**73160**	**49017,2**	**131**	**41920,0**	**66,64**	**1,59**	**107211,8**	**96788,7**	**79531,9**	**26,4**	**21,7**	**65,8**

Shading losses per area (% of gross)

Area	Gross	Panel and diffuse red.	Obstacles	WTG Towers	WTG rotors	Topo	Combined
	MWh/y	%	%	%	%	%	%
PV_1 - 60,5 ha	97666,9	NA	NA	NA	NA	NA	NA
PV_2 - 6,1 ha	9545,0	NA	NA	NA	NA	NA	NA
Total	**107211,8**	**NA**	**NA**	**NA**	**NA**	**NA**	**NA**

Other losses per area (1. year) (% of gross)

Area	Gross	Before inverter	Inverter clipping	DC/AC conversion	After inverter	Combined
	MWh/y	%	%	%	%	%
PV_1 - 60,5 ha	97666,9	5,93	0,88	1,19	1,74	9,75
PV_2 - 6,1 ha	9545,0	6,00	0,53	1,19	1,74	9,47
Total	**107211,8**	**5,94**	**0,85**	**1,19**	**1,74**	**9,72**

Other losses per area (20. year) (% of gross)

Area	Gross	Before inverter	Inverter clipping	DC/AC conversion	After inverter	Combined
	MWh/y	%	%	%	%	%
PV_1 - 60,5 ha	97666,9	23,38	0,01	0,99	1,43	25,81
PV_2 - 6,1 ha	9545,0	23,45	0,00	1,00	1,43	25,88
Total	**107211,8**	**23,39**	**0,01**	**0,99**	**1,43**	**25,82**

Total losses per area (% of gross)

Area	Gross	Shading losses	Other losses (1y)	Other losses (20y)	**All losses (1y)**	**All losses (20y)**
	MWh/y	%	%	%	%	%
PV_1 - 60,5 ha	97666,9	0,00	9,75	25,81	9,75	25,81
PV_2 - 6,1 ha	9545,0	0,00	9,47	25,88	9,47	25,88
Total	**107211,8**	**0,00**	**9,72**	**25,82**	**9,72**	**25,82**

Panel details per area: (W refer to W DC)

Area	Type/name	Orientation	Size	Power Max / Panel	TC	NOCT	Bypass diodes:	Bypass orientation	Bifacial	BF	Degradation
			m x m	W	%/°C	°C					%/y
PV_1 - 60,5 ha	A	Portrait	1,30 x 2,38	670,0	-0,340	43,0	3	Short side	Yes	0,75	2,0
PV_2 - 6,1 ha	B	Portrait	1,30 x 2,38	670,0	-0,340	43,0	3	Short side	Yes	0,75	2,0

A: Userdefined_Vertex_665W_1,303x2,384Monocrystalline_3xBypass.PVPanel
B: Userdefined_Vertex_665W_1,303x2,384Monocrystalline_3xBypass.PVPanel

Details per area

Area	Row count	Row distance	Tilt	Azimuth	Ground offset	Irradiation on panel Direct	Diffuse	Reflected	Albedo	Total
		m	°	°	m	kWh/m²/y	kWh/m²/y	kWh/m²/y		kWh/m²/y
PV_1 - 60,5 ha	258	6,0	#	90	3,0	1394,3	813,5	311,9	0,2	2519,7
PV_2 - 6,1 ha	60	6,0	#	90	3,0	1347,4	797,5	311,7	0,2	2456,6

Solar PV - Time Varying production

Calculation: AEP INTERO IMPIANTO SENZA OMBRE

Production MWh/y

Values are averages for the calculation period 01/01/2021 - 01/01/2022 with all calculated losses deducted, except for degradation losses (for Year 1)

Hour	Jan	Feb	Mar	Apr	May	Jun	Jul	Aug	Sep	Oct	Nov	Dec	All
0	0,0	0,0	0,0	0,0	0,0	0,0	0,0	0,0	0,0	0,0	0,0	0,0	**-0,3**
1	0,0	0,0	0,0	0,0	0,0	0,0	0,0	0,0	0,0	0,0	0,0	0,0	**-0,3**
2	0,0	0,0	0,0	0,0	0,0	0,0	0,0	0,0	0,0	0,0	0,0	0,0	**-0,3**
3	0,0	0,0	0,0	0,0	0,0	0,0	0,0	0,0	0,0	0,0	0,0	0,0	**-0,3**
4	0,0	0,0	0,0	0,0	0,0	0,0	0,0	0,0	0,0	0,0	0,0	0,0	**-0,3**
5	0,0	0,0	0,0	11,6	118,1	169,8	79,1	42,7	0,0	0,0	0,0	0,0	**421,0**
6	0,0	0,0	28,7	246,8	713,5	744,4	479,0	279,5	205,8	16,7	0,0	0,0	**2.714,4**
7	2,3	85,9	371,4	692,5	1.156,7	1.150,1	1.129,0	848,5	891,4	325,4	79,2	8,5	**6.740,9**
8	211,2	544,1	975,0	971,1	1.146,6	1.144,0	1.171,0	1.151,7	1.047,5	761,5	388,3	317,3	**9.829,3**
9	554,1	821,4	1.009,3	992,6	1.167,3	1.175,4	1.180,8	1.154,1	1.018,9	727,3	467,9	561,8	**10.830,7**
10	529,1	751,6	967,1	1.028,0	1.176,5	1.163,3	1.196,4	1.175,6	991,1	740,7	493,7	498,9	**10.712,0**
11	533,9	722,2	957,5	1.006,7	1.141,0	1.156,3	1.192,0	1.154,1	947,5	693,1	461,0	469,1	**10.434,3**
12	506,7	707,2	923,7	975,5	1.147,0	1.119,9	1.173,2	1.116,5	941,5	675,2	448,4	455,6	**10.190,4**
13	492,9	722,5	917,4	913,9	1.129,3	1.112,2	1.156,7	1.090,0	893,9	611,3	405,6	451,4	**9.897,0**
14	445,2	706,6	886,3	839,9	1.071,2	1.066,7	1.111,4	1.018,6	775,6	524,8	345,6	395,9	**9.187,7**
15	311,4	619,3	792,8	764,8	1.017,9	966,7	1.003,3	904,5	640,5	367,5	175,9	192,3	**7.757,0**
16	45,8	302,0	574,7	602,9	880,3	782,6	835,4	766,0	392,5	92,1	1,1	0,0	**5.275,6**
17	0,0	1,7	115,0	248,3	414,1	517,4	605,3	448,5	56,7	0,0	0,0	0,0	**2.406,9**
18	0,0	0,0	0,0	1,4	44,5	136,0	172,0	40,5	0,0	0,0	0,0	0,0	**394,2**
19	0,0	0,0	0,0	0,0	0,0	0,0	0,0	0,0	0,0	0,0	0,0	0,0	**-0,3**
20	0,0	0,0	0,0	0,0	0,0	0,0	0,0	0,0	0,0	0,0	0,0	0,0	**-0,3**
21	0,0	0,0	0,0	0,0	0,0	0,0	0,0	0,0	0,0	0,0	0,0	0,0	**-0,3**
22	0,0	0,0	0,0	0,0	0,0	0,0	0,0	0,0	0,0	0,0	0,0	0,0	**-0,3**
23	0,0	0,0	0,0	0,0	0,0	0,0	0,0	0,0	0,0	0,0	0,0	0,0	**-0,3**
All	**3.632,2**	**5.984,3**	**8.518,5**	**9.295,7**	**12.323,7**	**12.404,6**	**12.484,2**	**11.190,7**	**8.802,6**	**5.535,2**	**3.266,4**	**3.350,5**	**96.788,7**

Hourly power (kW AC)

Hour	Jan	Feb	Mar	Apr	May	Jun	Jul	Aug	Sep	Oct	Nov	Dec	All (avg)
0	-1	-1	-1	-1	-1	-1	-1	-1	-1	-1	-1	-1	**-1**
1	-1	-1	-1	-1	-1	-1	-1	-1	-1	-1	-1	-1	**-1**
2	-1	-1	-1	-1	-1	-1	-1	-1	-1	-1	-1	-1	**-1**
3	-1	-1	-1	-1	-1	-1	-1	-1	-1	-1	-1	-1	**-1**
4	-1	-1	-1	-1	-1	-1	-1	-1	-1	-1	-1	-1	**-1**
5	-1	-1	-1	385	3.809	5.659	2.551	1.377	-1	-1	-1	-1	**1.153**
6	-1	-1	926	8.228	23.018	24.814	15.450	9.017	6.860	539	-1	-1	**7.432**
7	73	3.040	11.980	23.082	37.313	38.338	36.420	27.372	29.715	10.496	2.641	273	**18.455**
8	6.812	19.262	31.450	32.369	36.987	38.134	37.775	37.151	34.915	24.566	12.944	10.237	**26.911**
9	17.873	29.075	32.559	33.087	37.653	39.181	38.090	37.229	33.962	23.460	15.595	18.122	**29.653**
10	17.068	26.605	31.197	34.267	37.951	38.776	38.592	37.923	33.035	23.893	16.458	16.094	**29.328**
11	17.221	25.566	30.886	33.556	36.807	38.544	38.450	37.228	31.585	22.356	15.368	15.132	**28.568**
12	16.344	25.033	29.796	32.516	37.001	37.329	37.847	36.018	31.384	21.782	14.946	14.697	**27.900**
13	15.900	25.576	29.593	30.463	36.428	37.073	37.312	35.161	29.797	19.718	13.519	14.562	**27.097**
14	14.361	25.014	28.592	27.995	34.554	35.557	35.850	32.857	25.853	16.928	11.519	12.772	**25.155**
15	10.045	21.923	25.573	25.494	32.837	32.224	32.363	29.179	21.350	11.855	5.864	6.204	**21.238**
16	1.479	10.690	18.540	20.098	28.398	26.086	26.949	24.711	13.084	2.971	38	-1	**14.444**
17	-1	59	3.709	8.278	13.358	17.246	19.527	14.469	1.889	-1	-1	-1	**6.590**
18	-1	-1	-1	47	1.436	4.532	5.548	1.307	-1	-1	-1	-1	**1.079**
19	-1	-1	-1	-1	-1	-1	-1	-1	-1	-1	-1	-1	**-1**
20	-1	-1	-1	-1	-1	-1	-1	-1	-1	-1	-1	-1	**-1**
21	-1	-1	-1	-1	-1	-1	-1	-1	-1	-1	-1	-1	**-1**
22	-1	-1	-1	-1	-1	-1	-1	-1	-1	-1	-1	-1	**-1**
23	-1	-1	-1	-1	-1	-1	-1	-1	-1	-1	-1	-1	**-1**
All (avg)	**4.882**	**8.826**	**11.450**	**12.911**	**16.564**	**17.229**	**16.780**	**15.041**	**12.226**	**7.440**	**4.537**	**4.503**	**11.041**

Solar PV - Time Varying production

Calculation: AEP INTERO IMPIANTO SENZA OMBRE

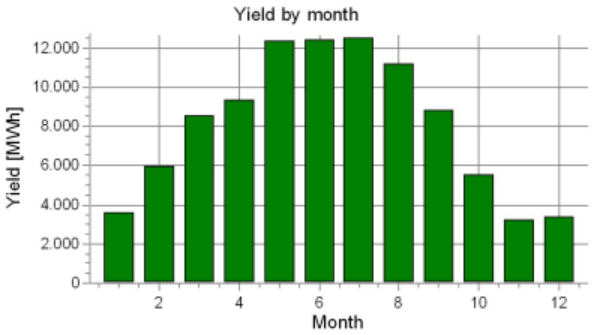

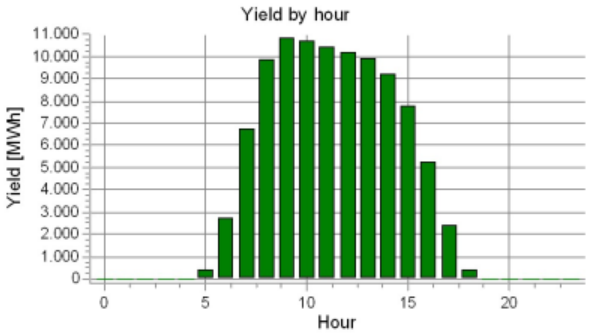

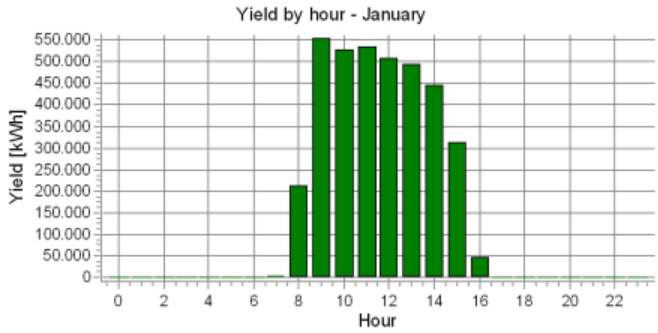

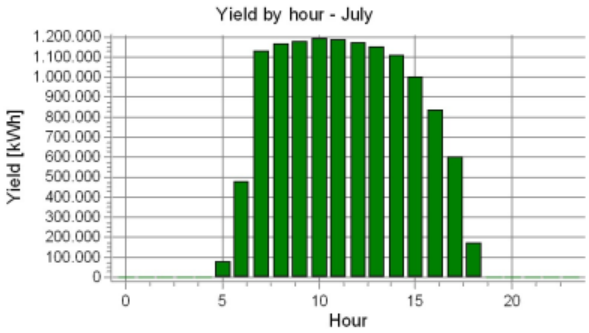

Please note that the duration table and graph is without degradation loss

Hours	Hours [%]	Hours accumulated	Power kW
755,0	8,6	755,0	39.071 - 41.127
218,0	2,5	973,0	37.015 - 39.071
185,0	2,1	1158,0	34.958 - 37.015
186,0	2,1	1344,0	32.902 - 34.958
199,0	2,3	1543,0	30.845 - 32.902
157,0	1,8	1700,0	28.789 - 30.845
187,0	2,1	1887,0	26.733 - 28.789
161,0	1,8	2048,0	24.676 - 26.733
140,0	1,6	2188,0	22.620 - 24.676
167,0	1,9	2355,0	20.564 - 22.620
165,0	1,9	2520,0	18.507 - 20.564
181,0	2,1	2701,0	16.451 - 18.507
169,0	1,9	2870,0	14.395 - 16.451
151,0	1,7	3021,0	12.338 - 14.395
161,0	1,8	3182,0	10.282 - 12.338
155,0	1,8	3337,0	8.225,5 - 10.282
180,0	2,1	3517,0	6.169,1 - 8.225,5
157,0	1,8	3674,0	4.112,7 - 6.169,1
256,0	2,9	3930,0	2.056,4 - 4.112,7
270,0	3,1	4200,0	0,0 - 2.056,4
4560,0	52,1	8760,0	0,0

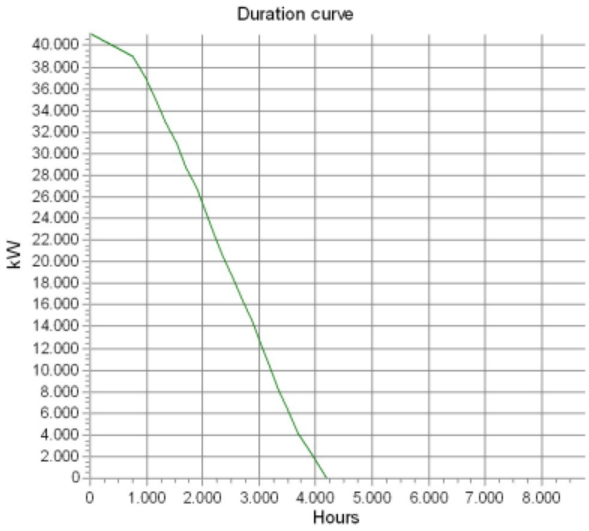

APPENDIX E

1) WTG SHADOW EVOLUTION MODEL IN A SINGLE DAY AT GRAVINA IN PUGLIA

(input day = 355, whatever TAPVA_distance and TANSTA_distance)

```
% GLOBAL GRAVINA IN PUGLIA WTG SHADOW MODEL DURING A SINGLE DAY
% WTG rotor fixed normal direction = North-North-West

clear all
close all
clc
% model to compute shadow coordinates on an area and on a PV module surface
% considering its evolution during each minute of a single day
% (X,Y) reference system plane with origin in WTG tower axis
% East: X positive ; West: X negative
% North: Y positive ; South: Y negative
% all angles inside sin() and cos() functions are in radians, [rad]

Hmod=2.384;     % PV module height [m]
Wmod=1.303;     % PV module width [m]
PV_mod_area=Hmod*Wmod;    % PV module area [m^2]
lat=40.837;     % latitude of WTG 04 tower position in Gravina in Puglia site [°]
long=16.272;    % longitude of WTG 04 tower position in Gravina in Puglia site [°]
rot=1.038;  % [rad/s], angular speed of a single blade/wind rotor

% PV module position on (X,Y) plane
TAPVA_distance=input('Insert PV module center of gravity position along N-S [m] = ');  %
[m], tower-PV module axis/center of gravity distance (I choose position of PV module)
TANSTA_distance=input('Insert PV module center of gravity position along W-E [m] = ');
% [m], tower axis - NorthSouth tracker axis distance (I choose position of PV module)

day=input('Insert n° day of the year = ');  % number of day in the year [-]
    B=(360/365*(day-1))*0.017453292; % [rad]   1° = 0.017453292 rad  ,  1 rad =
57.29577951°
    decl=(23.45*sin((360/365*(day+284))*0.017453292))*0.017453292;  % [rad]
    ET=229.2*(0.000075+(0.001868*cos(B))-(0.032077*sin(B))-(0.014615*cos(2*B))-
(0.04089*sin(2*B)));   % Equation of Time [min], correction factor for true solar time
TST calculation

%% SHADOW MODEL OF WTG TOWER IN A SINGLE DAY
for z=1:121  % altitude of a point from ground along tower height [m]
HEIGHT(z)=z;
diam(z)=4.3-(0.004962779*z);   % WTG tower diameter at different elevation [m], supposing
linear reduction of tower diameter

    for j= 480:960  % analysis of shadow position will be done every minute from 8:00
a.m. to 16:00 p.m.
        LT(z,j)=j;    % legal time of a day [min]

        if day>=1 & day<=85     % change of solar hour at 27 March 2022
           summertime_difference=0; % [min], legal time one hour change
        elseif day>=86 & day<=302   % change of solar hour at 30 October 2022
            summertime_difference=-60; % [min]
        else
             summertime_difference=0; % [min]
        end

        diff_GMT=-60;  % [min], difference with Greenwich Mean Time of our Time Zone
        TST(z,j)=(LT(z,j)+diff_GMT+((long/15)*60)+ET+summertime_difference)/60;  % True
Solar Time [h]
        HRA(z,j)=(15*(TST(z,j)-12))*0.017453292;   % hour angle [rad]

alfa(z,j)=asin((cos(decl)*cos(lat*0.017453292)*cos(HRA(z,j)))+(sin(decl)*sin(lat*0.017453
292)));  % solar height angle [rad]
```

```
        gammas(z,j)=asin((cos(decl)*sin(HRA(z,j)))/cos(alfa(z,j)));   % solar azimuth
angle [rad]

        Lshad_axis(z,j)=z/tan(alfa(z,j));   % shadow length of WTG tower axis [m]
        xshad_axis(z,j)=Lshad_axis(z,j)*sin(gammas(z,j));  % x coordinate of axis shadow
[m]
        yshad_axis(z,j)=Lshad_axis(z,j)*cos(gammas(z,j));  % y coordinate of axis shadow
[m]

        xshad_w(z,j)=xshad_axis(z,j)-((diam(z)*cos(gammas(z,j)))/2);   % x coordinate of
western tower point shadow [m]
        yshad_w(z,j)=yshad_axis(z,j)+((diam(z)*sin(gammas(z,j)))/2);   % y coordinate of
western tower point shadow [m]

        xshad_e(z,j)=xshad_axis(z,j)+((diam(z)*cos(gammas(z,j)))/2);   % x coordinate of
eastern tower point shadow [m]
        yshad_e(z,j)=yshad_axis(z,j)-((diam(z)*sin(gammas(z,j)))/2);   % y coordinate of
eastern tower point shadow [m]

        % WTG SHADOW MARGIN COORDINATES ON PV MODULE SURFACE (ORIGIN AT BOTTOM-LEFT
CORNER OF PV MODULE)
        % PV module distance from WTG on (X,Y) plane
        dpvy=TAPVA_distance-(Hmod/2);  % distance along y axis between tower axis and PV
module center of gravity [m]
        dpvx=TANSTA_distance-(Wmod/2);  % distance along x axis between tower axis and
North-South horizontal tracker axis [m]

            % (X,Y) coordinates of tower axis shadow on PV module surface
            if  (xshad_axis(z,j)-dpvx)>0 & (xshad_axis(z,j)-dpvx)<=1.303
                 xshad_axis_mod(z,j)=xshad_axis(z,j)-dpvx;  % x coordinate on PV module
surface of shadow axis [m]
            elseif  (xshad_axis(z,j)-dpvx)>1.303
                 xshad_axis_mod(z,j)=1.303;
            else
                 xshad_axis_mod(z,j)=0;
            end

            if (yshad_axis(z,j)-dpvy)>0 & (yshad_axis(z,j)-dpvy)<=2.384
                yshad_axis_mod(z,j)=yshad_axis(z,j)-dpvy;  % y coordinate on PV module
surface of shadow axis [m]
            elseif  (yshad_axis(z,j)-dpvy)>2.384
                yshad_axis_mod(z,j)=2.384;
            else
                yshad_axis_mod(z,j)=0;
            end

            % (X,Y) coordinates of tower western point shadow on PV module surface
            if (xshad_w(z,j)-dpvx)>0 & (xshad_w(z,j)-dpvx)<=1.303
                xshad_w_mod(z,j)=xshad_w(z,j)-dpvx;  % x coordinate on PV module surface
of tower western point shadow [m]
            elseif  (xshad_w(z,j)-dpvx)>1.303
                xshad_w_mod(z,j)=1.303;
            else
                xshad_w_mod(z,j)=0;
            end

            if (yshad_w(z,j)-dpvy)>0 & (yshad_w(z,j)-dpvy)<=2.384
                yshad_w_mod(z,j)=yshad_w(z,j)-dpvy;  % y coordinate on PV module surface
of tower western point shadow [m]
            elseif  (yshad_w(z,j)-dpvy)>2.384
                yshad_w_mod(z,j)=2.384;
            else
                yshad_w_mod(z,j)=0;
            end

            % (X,Y) coordinates of tower eastern point shadow on PV module surface
            if (xshad_e(z,j)-dpvx)>0 & (xshad_e(z,j)-dpvx)<=1.303
                xshad_e_mod(z,j)=xshad_e(z,j)-dpvx;  % x coordinate on PV module surface
of tower eastern point shadow [m]
```

```
            elseif (xshad_e(z,j)-dpvx)>1.303
                xshad_e_mod(z,j)=1.303;
            else
                xshad_e_mod(z,j)=0;
            end

            if (yshad_e(z,j)-dpvy)>0 & (yshad_e(z,j)-dpvy)<=2.384
                yshad_e_mod(z,j)=yshad_e(z,j)-dpvy;  % y coordinate on PV module surface
of tower eastern point shadow [m]
            elseif  (yshad_e(z,j)-dpvy)>2.384
                yshad_e_mod(z,j)=2.384;
            else
                yshad_e_mod(z,j)=0;
            end

            %%%%% SHADOW BY WTG TOWER LOSS APPROXIMATION
            Ashad_mod(z,j)=((yshad_e_mod(z,j)+yshad_w_mod(z,j))*(xshad_e_mod(z,j)-
xshad_w_mod(z,j)))/2;   % PV module tower shaded area approximation [m^2]
            Shading_loss(z,j)=(Ashad_mod(z,j)/PV_mod_area)*100;   % percentage of
irradiance lost by WTG tower shading

    end
end



%% SHADOW MODEL OF THREE BLADES IN A SINGLE DAY
% Hypothesis: rotor plane (X,Z) with normal direction always fixed towards North-North-
West direction (30°=0.523599)
% Highest wind direction frequency at Gravina in Puglia site
angle=30*0.017453292;
for R=1:79    % [m] radial position of a point along blades
    Rad(R)=R;
if R>=0 & R<23.7
   z(R)=3-cos(R/7.543944303);   % [m] blade width at radial position
  elseif R>=23.7 & R<71.1
         z(R)=5.349999993-(0.056962025*R);
  else
      z(R)=6.842105264-((R^2)/912.1461538);
end

for j= 480:960  % analysis of shadow position will be done every minute from 8:00 a.m. to
16:00 p.m.
        LT(R,j)=j;    % legal time of a day [min]

        if day>=1 & day<=85     % change of solar hour at 27 March 2022
           summertime_difference=0; % [min], legal time one hour change
        elseif day>=86 & day<=302   % change of solar hour at 30 October 2022
            summertime_difference=-60; % [min]
        else
             summertime_difference=0; % [min]
        end

        diff_GMT=-60;  % [min], difference with Greenwich Mean Time of our Time Zone
        TST(R,j)=(LT(R,j)+diff_GMT+((long/15)*60)+ET+summertime_difference)/60;  % True
Solar Time [h]
        HRA(R,j)=(15*(TST(R,j)-12))*0.017453292;   % hour angle [rad]

alfa(R,j)=asin((cos(decl)*cos(lat*0.017453292)*cos(HRA(R,j)))+(sin(decl)*sin(lat*0.017453
292)));  % solar height angle [rad]
        gammas(R,j)=asin((cos(decl)*sin(HRA(R,j)))/cos(alfa(R,j)));   % solar azimuth
angle [rad]


        %%%%% LEADING EDGE (polar coordinates of leading edge points on (X,Z) rotor
plane)
        teta_le1(R,j)=(-rot)*LT(R,j)*60;  % [rad], polar coordinates angle related to
blade towards 0° direction
```

```
                                        % minus sign because rotation direction of GE
CYPRESS WTG rotor is clockwise
        teta_le2(R,j)=((-rot)*LT(R,j)*60)+((2/3)*pi);  % [rad], polar coordinates angle
related to blade towards +120° direction
        teta_le3(R,j)=((-rot)*LT(R,j)*60)-((2/3)*pi);  % [rad], polar coordinates angle
related to blade towards -120° direction

        rho_le1(R,j)=R;    % [m], polar coordinates module related to blade towards 0°
direction
        rho_le2(R,j)=R;    % [m], polar coordinates module related to blade towards +120°
direction
        rho_le3(R,j)=R;    % [m], polar coordinates module related to blade towards -120°
direction

        rho_x_le1(R,j)=rho_le1(R,j)*cos(teta_le1(R,j));  % [m], x axis component (WEST-
EAST) of polar coordinates module
        rho_x_le2(R,j)=rho_le2(R,j)*cos(teta_le2(R,j));
        rho_x_le3(R,j)=rho_le3(R,j)*cos(teta_le3(R,j));

        rho_z_le1(R,j)=(rho_le1(R,j)*sin(teta_le1(R,j)))+120.9;  % [m], z axis component
(ALTITUDE) of polar coordinates module
        rho_z_le2(R,j)=(rho_le2(R,j)*sin(teta_le2(R,j)))+120.9;
        rho_z_le3(R,j)=(rho_le3(R,j)*sin(teta_le3(R,j)))+120.9;



        %%%%% TRAILING EDGE (polar coordinates of trailing edge points on (X,Z) rotor
plane)
        teta_te1(R,j)=teta_le1(R,j)+atan(z(R)/R);   % [rad], polar coordinates angle
related to blade towards 0° direction
        teta_te2(R,j)=teta_le2(R,j)+atan(z(R)/R);   % [rad], polar coordinates angle
related to blade towards +120° direction
        teta_te3(R,j)=teta_le3(R,j)+atan(z(R)/R);   % [rad], polar coordinates angle
related to blade towards -120° direction

        rho_te1(R,j)=sqrt((R^2)+(z(R)^2));   % [m], polar coordinates module related to
blade towards 0° direction
        rho_te2(R,j)=sqrt((R^2)+(z(R)^2));   % [m], polar coordinates module related to
blade towards +120° direction
        rho_te3(R,j)=sqrt((R^2)+(z(R)^2));   % [m], polar coordinates module related to
blade towards -120° direction

        rho_x_te1(R,j)=rho_te1(R,j)*cos(teta_te1(R,j));  % [m], x axis component (WEST-
EAST) of polar coordinates module on rotor (X,Z) plane
        rho_x_te2(R,j)=rho_te2(R,j)*cos(teta_te2(R,j));
        rho_x_te3(R,j)=rho_te3(R,j)*cos(teta_te3(R,j));

        rho_z_te1(R,j)=(rho_te1(R,j)*sin(teta_te1(R,j)))+120.9;  % [m], z axis component
(ALTITUDE) of polar coordinates module on rotor (X,Z) plane
        rho_z_te2(R,j)=(rho_te2(R,j)*sin(teta_te2(R,j)))+120.9;
        rho_z_te3(R,j)=(rho_te3(R,j)*sin(teta_te3(R,j)))+120.9;


        %%%%% LEADING EDGE POINT SHADOW COMPONENTS ON (X,Y) PLANE, WTG TOWER AXIS ORIGIN
        % BLADE 1 (0°)
        Lshad_le1(R,j)=rho_z_le1(R,j)/tan(alfa(R,j));   % shadow length
        xshad_le1(R,j)=(Lshad_le1(R,j)*sin(gammas(R,j)))+(rho_x_le1(R,j)*cos(angle));  %
x shadow length coordinate on (X,Y) plane
        yshad_le1(R,j)=(Lshad_le1(R,j)*cos(gammas(R,j)))+(rho_x_le1(R,j)*sin(angle));  %
y shadow length coordinate on (X,Y) plane

        % BLADE 2 (+120°)
        Lshad_le2(R,j)=rho_z_le2(R,j)/tan(alfa(R,j));
        xshad_le2(R,j)=(Lshad_le2(R,j)*sin(gammas(R,j)))+(rho_x_le2(R,j)*cos(angle));
        yshad_le2(R,j)=(Lshad_le2(R,j)*cos(gammas(R,j)))+(rho_x_le2(R,j)*sin(angle));

        % BLADE 3 (-120°)
        Lshad_le3(R,j)=rho_z_le3(R,j)/tan(alfa(R,j));
        xshad_le3(R,j)=(Lshad_le3(R,j)*sin(gammas(R,j)))+(rho_x_le3(R,j)*cos(angle));
```

```
        yshad_le3(R,j)=(Lshad_le3(R,j)*cos(gammas(R,j)))+(rho_x_le3(R,j)*sin(angle));


        %%%%% TRAILING EDGE POINT SHADOW COMPONENTS ON (X,Y) PLANE, WTG TOWER AXIS ORIGIN
        % BLADE 1 (0°)
        Lshad_te1(R,j)=rho_z_te1(R,j)/tan(alfa(R,j));   % shadow length
        xshad_te1(R,j)=(Lshad_te1(R,j)*sin(gammas(R,j)))+(rho_x_te1(R,j)*cos(angle));   %
x shadow length coordinate on (X,Y) plane
        yshad_te1(R,j)=(Lshad_te1(R,j)*cos(gammas(R,j)))+(rho_x_te1(R,j)*sin(angle));   %
y shadow length coordinate on (X,Y) plane

        % BLADE 2 (+120°)
        Lshad_te2(R,j)=rho_z_te2(R,j)/tan(alfa(R,j));
        xshad_te2(R,j)=(Lshad_te2(R,j)*sin(gammas(R,j)))+(rho_x_te2(R,j)*cos(angle));
        yshad_te2(R,j)=(Lshad_te2(R,j)*cos(gammas(R,j)))+(rho_x_te2(R,j)*sin(angle));

        % BLADE 3 (-120°)
        Lshad_te3(R,j)=rho_z_te3(R,j)/tan(alfa(R,j));
        xshad_te3(R,j)=(Lshad_te3(R,j)*sin(gammas(R,j)))+(rho_x_te3(R,j)*cos(angle));
        yshad_te3(R,j)=(Lshad_te3(R,j)*cos(gammas(R,j)))+(rho_x_te3(R,j)*sin(angle));



        % BLADE LEADING AND TRAILING EDGES COORDINATES ON PV MODULE SURFACE (ORIGIN AT
BOTTOM-LEFT CORNER OF PV MODULE)
        % (X,Y) coordinates of BLADE 1 (0°) shadow on PV module surface
             if  (xshad_le1(R,j)-dpvx)>0 & (xshad_le1(R,j)-dpvx)<=1.303
                  xshad_le1_mod(R,j)=xshad_le1(R,j)-dpvx;  % x coordinate on PV module
surface of leading edge shadow [m]
             elseif  (xshad_le1(R,j)-dpvx)>1.303
                  xshad_le1_mod(R,j)=1.303;
             else
                  xshad_le1_mod(R,j)=0;
             end

             if (yshad_le1(R,j)-dpvy)>0 & (yshad_le1(R,j)-dpvy)<=2.384
                 yshad_le1_mod(R,j)=yshad_le1(R,j)-dpvy;  % y coordinate on PV module
surface of leading edge shadow [m]
             elseif  (yshad_le1(R,j)-dpvy)>2.384
                 yshad_le1_mod(R,j)=2.384;
             else
                 yshad_le1_mod(R,j)=0;
             end

             if  (xshad_te1(R,j)-dpvx)>0 & (xshad_te1(R,j)-dpvx)<=1.303
                  xshad_te1_mod(R,j)=xshad_te1(R,j)-dpvx;  % x coordinate on PV module
surface of trailing edge shadow [m]
             elseif  (xshad_te1(R,j)-dpvx)>1.303
                  xshad_te1_mod(R,j)=1.303;
             else
                  xshad_te1_mod(R,j)=0;
             end

             if (yshad_te1(R,j)-dpvy)>0 & (yshad_te1(R,j)-dpvy)<=2.384
                 yshad_te1_mod(R,j)=yshad_te1(R,j)-dpvy;  % y coordinate on PV module
surface of trailing edge shadow [m]
             elseif  (yshad_te1(R,j)-dpvy)>2.384
                 yshad_te1_mod(R,j)=2.384;
             else
                 yshad_te1_mod(R,j)=0;
             end

             % (X,Y) coordinates of BLADE 2 (+120°) shadow on PV module surface (ORIGIN
AT BOTTOM-LEFT CORNER OF PV MODULE)
             if  (xshad_le2(R,j)-dpvx)>0 & (xshad_le2(R,j)-dpvx)<=1.303
                  xshad_le2_mod(R,j)=xshad_le2(R,j)-dpvx;  % x coordinate on PV module
surface of leading edge shadow [m]
             elseif  (xshad_le2(R,j)-dpvx)>1.303
                  xshad_le2_mod(R,j)=1.303;
```

```
            else
                 xshad_le2_mod(R,j)=0;
            end

            if (yshad_le2(R,j)-dpvy)>0 & (yshad_le2(R,j)-dpvy)<=2.384
                yshad_le2_mod(R,j)=yshad_le2(R,j)-dpvy;  % y coordinate on PV module
surface of leading edge shadow [m]
            elseif  (yshad_le2(R,j)-dpvy)>2.384
                yshad_le2_mod(R,j)=2.384;
            else
                yshad_le2_mod(R,j)=0;
            end

            if  (xshad_te2(R,j)-dpvx)>0 & (xshad_te2(R,j)-dpvx)<=1.303
                 xshad_te2_mod(R,j)=xshad_te2(R,j)-dpvx;  % x coordinate on PV module
surface of trailing edge shadow [m]
            elseif  (xshad_te2(R,j)-dpvx)>1.303
                 xshad_te2_mod(R,j)=1.303;
            else
                 xshad_te2_mod(R,j)=0;
            end

            if (yshad_te2(R,j)-dpvy)>0 & (yshad_te2(R,j)-dpvy)<=2.384
                yshad_te2_mod(R,j)=yshad_te2(R,j)-dpvy;  % y coordinate on PV module
surface of trailing edge shadow [m]
            elseif  (yshad_te2(R,j)-dpvy)>2.384
                yshad_te2_mod(R,j)=2.384;
            else
                yshad_te2_mod(R,j)=0;
            end

            % (X,Y) coordinates of BLADE 3 (-120°) shadow on PV module surface (ORIGIN
AT BOTTOM-LEFT CORNER OF PV MODULE)
             if  (xshad_le3(R,j)-dpvx)>0 & (xshad_le3(R,j)-dpvx)<=1.303
                 xshad_le3_mod(R,j)=xshad_le3(R,j)-dpvx;  % x coordinate on PV module
surface of leading edge shadow [m]
            elseif  (xshad_le3(R,j)-dpvx)>1.303
                 xshad_le3_mod(R,j)=1.303;
            else
                 xshad_le3_mod(R,j)=0;
            end

            if (yshad_le3(R,j)-dpvy)>0 & (yshad_le3(R,j)-dpvy)<=2.384
                yshad_le3_mod(R,j)=yshad_le3(R,j)-dpvy;  % y coordinate on PV module
surface of leading edge shadow [m]
            elseif  (yshad_le3(R,j)-dpvy)>2.384
                yshad_le3_mod(R,j)=2.384;
            else
                yshad_le3_mod(R,j)=0;
            end

            if  (xshad_te3(R,j)-dpvx)>0 & (xshad_te3(R,j)-dpvx)<=1.303
                 xshad_te3_mod(R,j)=xshad_te3(R,j)-dpvx;  % x coordinate on PV module
surface of trailing edge shadow [m]
            elseif  (xshad_te3(R,j)-dpvx)>1.303
                 xshad_te3_mod(R,j)=1.303;
            else
                 xshad_te3_mod(R,j)=0;
            end

            if (yshad_te3(R,j)-dpvy)>0 & (yshad_te3(R,j)-dpvy)<=2.384
                yshad_te3_mod(R,j)=yshad_te3(R,j)-dpvy;  % y coordinate on PV module
surface of trailing edge shadow [m]
            elseif  (yshad_te3(R,j)-dpvy)>2.384
                yshad_te3_mod(R,j)=2.384;
            else
                yshad_te3_mod(R,j)=0;
            end
```

```
            %%%%%% SHADOW BY BLADES LOSS APPROXIMATION

Ashad_blade1_mod(R,j)=((yshad_le1_mod(R,j)+yshad_te1_mod(R,j))*abs((xshad_le1_mod(R,j)-
xshad_te1_mod(R,j))))/2;   % PV module shaded area by BLADE 1 (0°) approximation [m^2]
            Shading_blade1_loss(R,j)=(Ashad_blade1_mod(R,j)/PV_mod_area)*100;   % [%]
percentage of irradiance lost by BLADE 1 (0°) shading approximation


Ashad_blade2_mod(R,j)=((yshad_le2_mod(R,j)+yshad_te2_mod(R,j))*abs((xshad_le2_mod(R,j)-
xshad_te2_mod(R,j))))/2;   % PV module shaded area by BLADE 2 (+120°) approximation [m^2]
            Shading_blade2_loss(R,j)=(Ashad_blade2_mod(R,j)/PV_mod_area)*100;   % [%]
percentage of irradiance lost by BLADE 2 (+120°) shading approximation


Ashad_blade3_mod(R,j)=((yshad_le3_mod(R,j)+yshad_te3_mod(R,j))*abs((xshad_le3_mod(R,j)-
xshad_te3_mod(R,j))))/2;   % PV module shaded area by BLADE 3 (-120°) approximation [m^2]
            Shading_blade3_loss(R,j)=(Ashad_blade3_mod(R,j)/PV_mod_area)*100;   % [%]
percentage of irradiance lost by BLADE 3 (-120°) shading approximation

    end
end


  %%%%% RESULTING FIGURES
  figure(1)
  plot(xshad_axis,yshad_axis,'.')
  title('TOWER AXIS SHADOW POSITION IN A SINGLE DAY')
  xlabel('WEST - EAST  [m]')
  ylabel('NORTH - SOUTH  [m]')
  grid on

  figure(2)
  plot(xshad_w,yshad_w,'.')
  title('TOWER WERSTERN POINT SHADOW POSITION IN A SINGLE DAY')
  xlabel('WEST - EAST  [m]')
  ylabel('NORTH - SOUTH  [m]')
  grid on

  figure(3)
  plot(xshad_e,yshad_e,'.')
  title('TOWER EASTERN POINT SHADOW POSITION IN A SINGLE DAY')
  xlabel('WEST - EAST  [m]')
  ylabel('NORTH - SOUTH  [m]')
  grid on

 figure(4)
  plot(xshad_axis,yshad_axis,'.',xshad_w,yshad_w,'.',xshad_e,yshad_e,'.')
  title('OVERALL TOWER SHADOW POSITION IN A SINGLE DAY')
  xlabel('WEST - EAST  [m]')
  ylabel('NORTH - SOUTH  [m]')
  grid on

  figure(5)
  plot(xshad_axis_mod,yshad_axis_mod,'*')
  title('TOWER AXIS SHADOW POSITION ON PV MODULE SURFACE IN A SINGLE DAY')
  xlabel('PV MODULE WIDTH [m]')
  ylabel('PV MODULE HEIGHT [m]')
  axis([0 1.303 0 2.384])
  grid on

  figure(6)
  plot(xshad_w_mod,yshad_w_mod,'*')
  title('TOWER WESTERN POINT SHADOW POSITION ON PV MODULE SURFACE IN A SINGLE DAY')
  xlabel('PV MODULE WIDTH [m]')
  ylabel('PV MODULE HEIGHT [m]')
  axis([0 1.303 0 2.384])
  grid on
```

```
  figure(7)
  plot(xshad_e_mod,yshad_e_mod,'*')
  title('TOWER EASTERN POINT SHADOW POSITION ON PV MODULE SURFACE IN A SINGLE DAY')
  xlabel('PV MODULE WIDTH [m]')
  ylabel('PV MODULE HEIGHT [m]')
  axis([0 1.303 0 2.384])
  grid on

  figure(8)
  plot(xshad_le1,yshad_le1,'.',xshad_te1,yshad_te1,'*')
  title('FIRST BLADE [0°] SHADOW POSITION IN A SINGLE DAY')
  xlabel('WEST - EAST  [m]')
  ylabel('NORTH - SOUTH  [m]')
  grid on

  figure(9)
  plot(xshad_le2,yshad_le2,'.',xshad_te2,yshad_te2,'*')
  title('SECOND BLADE [+120°] SHADOW POSITION IN A SINGLE DAY')
  xlabel('WEST - EAST  [m]')
  ylabel('NORTH - SOUTH  [m]')
  grid on

  figure(10)
  plot(xshad_le3,yshad_le3,'.',xshad_te3,yshad_te3,'*')
  title('THIRD BLADE [-120°] SHADOW POSITION IN A SINGLE DAY')
  xlabel('WEST - EAST  [m]')
  ylabel('NORTH - SOUTH  [m]')
  grid on

  figure(11)

plot(xshad_le1,yshad_le1,'*',xshad_te1,yshad_te1,'*',xshad_le2,yshad_le2,'*',xshad_te2,ys
had_te2,'*',xshad_le3,yshad_le3,'*',xshad_te3,yshad_te3,'*')
  title('OVERALL THREE BLADES SHADOW POSITION IN A SINGLE DAY')
  xlabel('WEST - EAST  [m]')
  ylabel('NORTH - SOUTH  [m]')
  grid on

  figure(12)
  plot(xshad_le1_mod,yshad_le1_mod,'.',xshad_te1_mod,yshad_te1_mod,'*')
  title('BLADE 1 [0°] LE AND TE SHADOW POSITION ON PV MODULE SURFACE IN A SINGLE DAY')
  xlabel('PV MODULE WIDTH [m]')
  ylabel('PV MODULE HEIGHT [m]')
  axis([0 1.303 0 2.384])
  grid on

  figure(13)
  plot(xshad_le2_mod,yshad_le2_mod,'.',xshad_te2_mod,yshad_te2_mod,'*')
  title('BLADE 2 [+120°] LE AND TE SHADOW POSITION ON PV MODULE SURFACE IN A SINGLE DAY')
  xlabel('PV MODULE WIDTH [m]')
  ylabel('PV MODULE HEIGHT [m]')
  axis([0 1.303 0 2.384])
  grid on

  figure(14)
  plot(xshad_le3_mod,yshad_le3_mod,'.',xshad_te3_mod,yshad_te3_mod,'*')
  title('BLADE 3 [-120°] LE AND TE SHADOW POSITION ON PV MODULE SURFACE IN A SINGLE DAY')
  xlabel('PV MODULE WIDTH [m]')
  ylabel('PV MODULE HEIGHT [m]')
  axis([0 1.303 0 2.384])
  grid on

  figure(15)

plot(xshad_axis,yshad_axis,'.',xshad_w,yshad_w,'.',xshad_e,yshad_e,'.',xshad_le1,yshad_le
1,'*',xshad_te1,yshad_te1,'*',xshad_le2,yshad_le2,'*',xshad_te2,yshad_te2,'*',xshad_le3,y
shad_le3,'*',xshad_te3,yshad_te3,'*')
  title('OVERALL WTG TOWER AND THREE BLADES SHADOW POSITION IN A SINGLE DAY')
  xlabel('WEST - EAST  [m]')
```

```
  ylabel('NORTH - SOUTH  [m]')
  grid on

%% WTG BLADES PROFILE MODEL
figure(16)
plot(Rad,z,'k-')
title('WTG BLADE PROFILE')
xlabel('Radial position [m]')
ylabel('Chord length [m]')
axis([0 79 0 20])
grid on
```

2) WTG SHADOW TIME SERIES IN SECONDS MODEL ON A SINGLE PV PANEL (input day = 355, TAPVA_distance = 240 m and TANSTA_distance = 0 m)

```
clear
close all
clc
% model to see when a PV module is shaded, a time series in seconds
% considering WTG shadow evolution during a single day
% (X,Y) reference system plane with origin in WTG tower axis
% East: X positive ; West: X negative
% North: Y positive ; South: Y negative
% all angles inside sin() and cos() functions are in radians, [rad]

Hmod=2.384;     % PV module height [m]
Wmod=1.303;     % PV module width [m]
PV_mod_area=Hmod*Wmod;    % PV module area [m^2]
lat=40.837;     % latitude of WTG 04 tower position at Gravina in Puglia site [°]
long=16.272;    % longitude of WTG 04 tower position at Gravina in Puglia site [°]
rot=1.038;  % [rad/s], angular speed of a single blade/wind rotor

% PV module position on (X,Y) plane
TAPVA_distance=input('Insert PV module center of gravity position along N-S [m] = ');  %
[m], tower-PV module axis/center of gravity distance
TANSTA_distance=input('Insert PV module center of gravity position along W-E [m] = ');
% [m], tower axis - NorthSouth tracker axis distance

% PV module distance from WTG on (X,Y) plane
dpvy=TAPVA_distance-(Hmod/2);  % distance along y axis between tower axis and PV module
center of gravity [m]
dpvx=TANSTA_distance-(Wmod/2);  % distance along x axis between tower axis and North-
South horizontal tracker axis [m]

x_modposition_e=TANSTA_distance+(Wmod/2);    % eastern x coordinate of PV module on (X,Y)
plane
x_modposition_w=TANSTA_distance-(Wmod/2);    % western x coordinate of PV module on (X,Y)
plane
y_modposition_n=TAPVA_distance+(Hmod/2);     % northern y coordinate of PV module on (X,Y)
plane
y_modposition_s=TAPVA_distance-(Hmod/2);     % southern y coordinate of PV module on (X,Y)
plane

day=input('Insert n° day of the year = ');  % number of day in the year [-]
    B=(360/365*(day-1))*0.017453292; % [rad]   1° = 0.017453292 rad  ,  1 rad =
57.29577951°
    decl=(23.45*sin((360/365*(day+284))*0.017453292))*0.017453292;  % [rad]
    ET=229.2*(0.000075+(0.001868*cos(B))-(0.032077*sin(B))-(0.014615*cos(2*B))-
(0.04089*sin(2*B)));   % Equation of Time [min], correction factor for true solar time
TST calculation

%% SHADOW MODEL OF WTG TOWER IN A SINGLE DAY
for z=1:121  % altitude of a point from ground along tower height [m]
HEIGHT(z)=z;
diam(z)=4.3-(0.004962779*z);   % WTG tower diameter at different elevation [m], supposing
linear reduction of tower diameter
```

```
    for j= 28800:57600  % [s] analysis of shadow position will be done every second from
8:00 a.m. to 16:00 p.m.

        LT(z,j)=j/60;    % legal time of a day [min]

        if day>=1 & day<=85     % change of solar hour at 27 March 2022
           summertime_difference=0; % [min], legal time one hour change
        elseif day>=86 & day<=302   % change of solar hour at 30 October 2022
            summertime_difference=-60; % [min]
        else
             summertime_difference=0; % [min]
        end

        diff_GMT=-60;  % [min], difference with Greenwich Mean Time of our Time Zone
        TST(z,j)=(LT(z,j)+diff_GMT+((long/15)*60)+ET+summertime_difference)*60;  % True
Solar Time [s]
        HRA(z,j)=(0.004166666*(TST(z,j)-43200))*0.017453292;   % hour angle [rad]

alfa(z,j)=asin((cos(decl)*cos(lat*0.017453292)*cos(HRA(z,j)))+(sin(decl)*sin(lat*0.017453
292)));  % solar height angle [rad]
        gammas(z,j)=asin((cos(decl)*sin(HRA(z,j)))/cos(alfa(z,j)));   % solar azimuth
angle [rad]

        Lshad_axis(z,j)=z/tan(alfa(z,j));   % shadow length of WTG tower axis [m]
        xshad_axis(z,j)=Lshad_axis(z,j)*sin(gammas(z,j));  % x coordinate of axis shadow
[m]
        yshad_axis(z,j)=Lshad_axis(z,j)*cos(gammas(z,j));  % y coordinate of axis shadow
[m]

        xshad_w(z,j)=xshad_axis(z,j)-((diam(z)*cos(gammas(z,j)))/2);   % x coordinate of
western tower point shadow [m]
        yshad_w(z,j)=yshad_axis(z,j)+((diam(z)*sin(gammas(z,j)))/2);   % y coordinate of
western tower point shadow [m]

        xshad_e(z,j)=xshad_axis(z,j)+((diam(z)*cos(gammas(z,j)))/2);   % x coordinate of
eastern tower point shadow [m]
        yshad_e(z,j)=yshad_axis(z,j)-((diam(z)*sin(gammas(z,j)))/2);   % y coordinate of
eastern tower point shadow [m]

        xshad_wa1(z,j)=xshad_axis(z,j)-((diam(z)*cos(gammas(z,j)))/8);   % x coordinate
fraction of western tower point shadow [m]
        yshad_wa1(z,j)=yshad_axis(z,j)+((diam(z)*sin(gammas(z,j)))/8);   % y coordinate
fraction of western tower point shadow [m]

        xshad_wa2(z,j)=xshad_axis(z,j)-((diam(z)*cos(gammas(z,j)))/4);
        yshad_wa2(z,j)=yshad_axis(z,j)+((diam(z)*sin(gammas(z,j)))/4);

        xshad_wa3(z,j)=xshad_axis(z,j)-((diam(z)*cos(gammas(z,j)))*3/8);
        yshad_wa3(z,j)=yshad_axis(z,j)+((diam(z)*sin(gammas(z,j)))*3/8);

        xshad_ea1(z,j)=xshad_axis(z,j)+((diam(z)*cos(gammas(z,j)))/8);   % x coordinate
fraction of eastern tower point shadow [m]
        yshad_ea1(z,j)=yshad_axis(z,j)-((diam(z)*sin(gammas(z,j)))/8);   % y coordinate
fraction of eastern tower point shadow [m]

        xshad_ea2(z,j)=xshad_axis(z,j)+((diam(z)*cos(gammas(z,j)))/4);
        yshad_ea2(z,j)=yshad_axis(z,j)-((diam(z)*sin(gammas(z,j)))/4);

        xshad_ea3(z,j)=xshad_axis(z,j)+((diam(z)*cos(gammas(z,j)))*3/8);
        yshad_ea3(z,j)=yshad_axis(z,j)-((diam(z)*sin(gammas(z,j)))*3/8);


            if (x_modposition_w<=xshad_axis(z,j) & xshad_axis(z,j)<=x_modposition_e) |
(x_modposition_w<=xshad_w(z,j) & xshad_w(z,j)<=x_modposition_e) |
(x_modposition_w<=xshad_e(z,j) & xshad_e(z,j)<=x_modposition_e) |
(x_modposition_w<=xshad_ea1(z,j) & xshad_ea1(z,j)<=x_modposition_e) |
(x_modposition_w<=xshad_wa1(z,j) & xshad_wa1(z,j)<=x_modposition_e) |
(x_modposition_w<=xshad_ea2(z,j) & xshad_ea2(z,j)<=x_modposition_e) |
```

```
(x_modposition_w<=xshad_wa2(z,j) & xshad_wa2(z,j)<=x_modposition_e) |
(x_modposition_w<=xshad_ea3(z,j) & xshad_ea3(z,j)<=x_modposition_e) |
(x_modposition_w<=xshad_wa3(z,j) & xshad_wa3(z,j)<=x_modposition_e)
                Timeseries_modshad_x_tower(z,j)=1;   % 1 = there is tower shadow on PV
module
            else
                Timeseries_modshad_x_tower(z,j)=0;   % 0 = there is not tower shadow on
PV module
            end

            if (y_modposition_s<=yshad_axis(z,j) & yshad_axis(z,j)<=y_modposition_n) |
(y_modposition_s<=yshad_w(z,j) & yshad_w(z,j)<=y_modposition_n) |
(y_modposition_s<=yshad_e(z,j) & yshad_e(z,j)<=y_modposition_n)
                Timeseries_modshad_y_tower(z,j)=1;   % 1 = there is tower shadow on PV
module
            else
                Timeseries_modshad_y_tower(z,j)=0;   % 0 = there is not tower shadow on
PV module
            end

                Timeseries_modshad_tower(z,j)=Timeseries_modshad_x_tower(z,j).*
Timeseries_modshad_y_tower(z,j); % overall tower shadow presence on PV module matrix

    end
end

Timeseries_t=linspace(1,1,121)*Timeseries_modshad_tower;   % tower shadow on PV module
time series vector

for j= 28800:57600
    if Timeseries_t(1,j)>=1
        Timeseries_t(1,j)=1;  % there is tower shadow
    elseif Timeseries_t(1,j)<1
        Timeseries_t(1,j)=0;  % there is not tower shadow
    end
end

figure(1)
plot(Timeseries_t,'k')
title('TOWER SHADOW ON PV MODULE')
xlabel('Time [seconds]')
ylabel('0 = not shaded PV, 1 = shaded PV')
axis([0 57600 -0.05 1.05])


%% SHADOW MODEL OF THREE BLADES IN A SINGLE DAY
% Hypothesis: rotor plane (X,Z) with normal direction always fixed towards North-North-
West direction (30°=0.523599)
% Highest wind direction frequency at Gravina in Puglia site
angle=30*0.017453292;
for R=1:79    % [m] radial position of a point along blades
    Rad(R)=R;
if R>=0 & R<23.7
   z(R)=3-cos(R/7.543944303);   % [m] blade width at radial position
  elseif R>=23.7 & R<71.1
         z(R)=5.349999993-(0.056962025*R);
  else
      z(R)=6.842105264-((R^2)/912.1461538);
end

for j= 28800:57600  % analysis of shadow position will be done every second from 8:00
a.m. to 16:00 p.m.
LT(R,j)=j/60;    % legal time of a day [min]

        if day>=1 & day<=85     % change of solar hour at 27 March 2022
           summertime_difference=0; % [min], legal time one hour change
        elseif day>=86 & day<=302   % change of solar hour at 30 October 2022
            summertime_difference=-60; % [min]
        else
```

```
            summertime_difference=0; % [min]
        end

        diff_GMT=-60;  % [min], difference with Greenwich Mean Time of our Time Zone
        TST(R,j)=(LT(R,j)+diff_GMT+((long/15)*60)+ET+summertime_difference)*60;  % True
Solar Time [s]
        HRA(R,j)=(0.004166666*(TST(R,j)-43200))*0.017453292;   % hour angle [rad]

alfa(R,j)=asin((cos(decl)*cos(lat*0.017453292)*cos(HRA(R,j)))+(sin(decl)*sin(lat*0.017453
292)));  % solar height angle [rad]
        gammas(R,j)=asin((cos(decl)*sin(HRA(R,j)))/cos(alfa(R,j)));   % solar azimuth
angle [rad]


        %%%%% LEADING EDGE (polar coordinates of leading edge points on (X,Z) rotor
plane)
        teta_le1(R,j)=(-rot)*LT(R,j)*60;  % [rad], polar coordinates angle related to
blade towards 0° direction
                                          % minus sign because rotation direction of GE
CYPRESS WTG rotor is clockwise
        teta_le2(R,j)=((-rot)*LT(R,j)*60)+((2/3)*pi);  % [rad], polar coordinates angle
related to blade towards +120° direction
        teta_le3(R,j)=((-rot)*LT(R,j)*60)-((2/3)*pi);  % [rad], polar coordinates angle
related to blade towards -120° direction

        rho_le1(R,j)=R;    % [m], polar coordinates module related to blade towards 0°
direction
        rho_le2(R,j)=R;    % [m], polar coordinates module related to blade towards +120°
direction
        rho_le3(R,j)=R;    % [m], polar coordinates module related to blade towards -120°
direction

        rho_x_le1(R,j)=rho_le1(R,j)*cos(teta_le1(R,j));  % [m], x axis component (WEST-
EAST) of polar coordinates module
        rho_x_le2(R,j)=rho_le2(R,j)*cos(teta_le2(R,j));
        rho_x_le3(R,j)=rho_le3(R,j)*cos(teta_le3(R,j));

        rho_z_le1(R,j)=(rho_le1(R,j)*sin(teta_le1(R,j)))+120.9;  % [m], z axis component
(ALTITUDE) of polar coordinates module
        rho_z_le2(R,j)=(rho_le2(R,j)*sin(teta_le2(R,j)))+120.9;
        rho_z_le3(R,j)=(rho_le3(R,j)*sin(teta_le3(R,j)))+120.9;



        %%%%% TRAILING EDGE (polar coordinates of trailing edge points on (X,Z) rotor
plane)
        teta_te1(R,j)=teta_le1(R,j)+atan(z(R)/R);   % [rad], polar coordinates angle
related to blade towards 0° direction
        teta_te2(R,j)=teta_le2(R,j)+atan(z(R)/R);   % [rad], polar coordinates angle
related to blade towards +120° direction
        teta_te3(R,j)=teta_le3(R,j)+atan(z(R)/R);   % [rad], polar coordinates angle
related to blade towards -120° direction

        rho_te1(R,j)=sqrt((R^2)+(z(R)^2));   % [m], polar coordinates module related to
blade towards 0° direction
        rho_te2(R,j)=sqrt((R^2)+(z(R)^2));   % [m], polar coordinates module related to
blade towards +120° direction
        rho_te3(R,j)=sqrt((R^2)+(z(R)^2));   % [m], polar coordinates module related to
blade towards -120° direction

        rho_x_te1(R,j)=rho_te1(R,j)*cos(teta_te1(R,j));  % [m], x axis component (WEST-
EAST) of polar coordinates module on rotor (X,Z) plane
        rho_x_te2(R,j)=rho_te2(R,j)*cos(teta_te2(R,j));
        rho_x_te3(R,j)=rho_te3(R,j)*cos(teta_te3(R,j));

        rho_z_te1(R,j)=(rho_te1(R,j)*sin(teta_te1(R,j)))+120.9;  % [m], z axis component
(ALTITUDE) of polar coordinates module on rotor (X,Z) plane
        rho_z_te2(R,j)=(rho_te2(R,j)*sin(teta_te2(R,j)))+120.9;
        rho_z_te3(R,j)=(rho_te3(R,j)*sin(teta_te3(R,j)))+120.9;
```

```
        %%%%% LEADING EDGE POINT SHADOW COMPONENTS ON (X,Y) PLANE, WTG TOWER AXIS ORIGIN
        % BLADE 1 (0°)
        Lshad_le1(R,j)=rho_z_le1(R,j)/tan(alfa(R,j));    % shadow length
        xshad_le1(R,j)=(Lshad_le1(R,j)*sin(gammas(R,j)))+(rho_x_le1(R,j)*cos(angle));  %
x shadow length coordinate on (X,Y) plane
        yshad_le1(R,j)=(Lshad_le1(R,j)*cos(gammas(R,j)))+(rho_x_le1(R,j)*sin(angle));  %
y shadow length coordinate on (X,Y) plane

        % BLADE 2 (+120°)
        Lshad_le2(R,j)=rho_z_le2(R,j)/tan(alfa(R,j));
        xshad_le2(R,j)=(Lshad_le2(R,j)*sin(gammas(R,j)))+(rho_x_le2(R,j)*cos(angle));
        yshad_le2(R,j)=(Lshad_le2(R,j)*cos(gammas(R,j)))+(rho_x_le2(R,j)*sin(angle));

        % BLADE 3 (-120°)
        Lshad_le3(R,j)=rho_z_le3(R,j)/tan(alfa(R,j));
        xshad_le3(R,j)=(Lshad_le3(R,j)*sin(gammas(R,j)))+(rho_x_le3(R,j)*cos(angle));
        yshad_le3(R,j)=(Lshad_le3(R,j)*cos(gammas(R,j)))+(rho_x_le3(R,j)*sin(angle));


        %%%%% TRAILING EDGE POINT SHADOW COMPONENTS ON (X,Y) PLANE, WTG TOWER AXIS ORIGIN
        % BLADE 1 (0°)
        Lshad_te1(R,j)=rho_z_te1(R,j)/tan(alfa(R,j));    % shadow length
        xshad_te1(R,j)=(Lshad_te1(R,j)*sin(gammas(R,j)))+(rho_x_te1(R,j)*cos(angle));    %
x shadow length coordinate on (X,Y) plane
        yshad_te1(R,j)=(Lshad_te1(R,j)*cos(gammas(R,j)))+(rho_x_te1(R,j)*sin(angle));    %
y shadow length coordinate on (X,Y) plane

        % BLADE 2 (+120°)
        Lshad_te2(R,j)=rho_z_te2(R,j)/tan(alfa(R,j));
        xshad_te2(R,j)=(Lshad_te2(R,j)*sin(gammas(R,j)))+(rho_x_te2(R,j)*cos(angle));
        yshad_te2(R,j)=(Lshad_te2(R,j)*cos(gammas(R,j)))+(rho_x_te2(R,j)*sin(angle));

        % BLADE 3 (-120°)
        Lshad_te3(R,j)=rho_z_te3(R,j)/tan(alfa(R,j));
        xshad_te3(R,j)=(Lshad_te3(R,j)*sin(gammas(R,j)))+(rho_x_te3(R,j)*cos(angle));
        yshad_te3(R,j)=(Lshad_te3(R,j)*cos(gammas(R,j)))+(rho_x_te3(R,j)*sin(angle));



%% BLADE POINTS SHADOW TIME SERIES ON SINGLE PANEL
% BLADE 1
        if rho_z_le1(R,j)>=120.9
             if (xshad_te1(R,j)<=x_modposition_w & x_modposition_w<=xshad_le1(R,j)) |
(xshad_te1(R,j)<=x_modposition_e & x_modposition_e<=xshad_le1(R,j))
                 Timeseries_modshad_x1(R,j)=1;    % 1 = there is leading edge points shadow
on PV module
             else
                  Timeseries_modshad_x1(R,j)=0;    % 0 = there is not leading edge points
shadow on PV module
             end
        else
             if (xshad_le1(R,j)<=x_modposition_w & x_modposition_w<=xshad_te1(R,j)) |
(xshad_le1(R,j)<=x_modposition_e & x_modposition_e<=xshad_te1(R,j))
                 Timeseries_modshad_x1(R,j)=1;    % 1 = there is leading edge points shadow
on PV module
             else
                  Timeseries_modshad_x1(R,j)=0;    % 0 = there is not leading edge points
shadow on PV module
             end
        end

        if  rho_x_le1(R,j)<=0
             if (yshad_te1(R,j)<=y_modposition_s & y_modposition_s<=yshad_le1(R,j)) |
(yshad_te1(R,j)<=y_modposition_n & y_modposition_n<=yshad_le1(R,j))
                 Timeseries_modshad_y1(R,j)=1;    % 1 = there is leading edge points shadow
on PV module
             else
```

```
                Timeseries_modshad_y1(R,j)=0;    % 0 = there is not leading edge points
shadow on PV module
             end
         else
             if (yshad_le1(R,j)<=y_modposition_s & y_modposition_s<=yshad_te1(R,j)) |
(yshad_le1(R,j)<=y_modposition_n & y_modposition_n<=yshad_te1(R,j))
                Timeseries_modshad_y1(R,j)=1;    % 1 = there is leading edge points shadow
on PV module
             else
                Timeseries_modshad_y1(R,j)=0;    % 0 = there is not leading edge points
shadow on PV module
             end
         end


Timeseries_modshad_1(R,j)=Timeseries_modshad_x1(R,j)*Timeseries_modshad_y1(R,j);  %
overall leading edge points shadow presence on PV module matrix

% BLADE 2
         if rho_z_le2(R,j)>=120.9
             if (xshad_te2(R,j)<=x_modposition_w & x_modposition_w<=xshad_le2(R,j)) |
(xshad_te2(R,j)<=x_modposition_e & x_modposition_e<=xshad_le2(R,j))
                Timeseries_modshad_x2(R,j)=1;    % 1 = there is leading edge points shadow
on PV module
             else
                 Timeseries_modshad_x2(R,j)=0;    % 0 = there is not leading edge points
shadow on PV module
             end
         else
             if (xshad_le2(R,j)<=x_modposition_w & x_modposition_w<=xshad_te2(R,j)) |
(xshad_le2(R,j)<=x_modposition_e & x_modposition_e<=xshad_te2(R,j))
                Timeseries_modshad_x2(R,j)=1;    % 1 = there is leading edge points shadow
on PV module
             else
                 Timeseries_modshad_x2(R,j)=0;    % 0 = there is not leading edge points
shadow on PV module
             end
         end

         if  rho_x_le2(R,j)<=0
             if (yshad_te2(R,j)<=y_modposition_s & y_modposition_s<=yshad_le2(R,j)) |
(yshad_te2(R,j)<=y_modposition_n & y_modposition_n<=yshad_le2(R,j))
                Timeseries_modshad_y2(R,j)=1;    % 1 = there is leading edge points shadow
on PV module
             else
                Timeseries_modshad_y2(R,j)=0;    % 0 = there is not leading edge points
shadow on PV module
             end
         else
             if (yshad_le2(R,j)<=y_modposition_s & y_modposition_s<=yshad_te2(R,j)) |
(yshad_le2(R,j)<=y_modposition_n & y_modposition_n<=yshad_te2(R,j))
                Timeseries_modshad_y2(R,j)=1;    % 1 = there is leading edge points shadow
on PV module
             else
                Timeseries_modshad_y2(R,j)=0;    % 0 = there is not leading edge points
shadow on PV module
             end
         end


Timeseries_modshad_2(R,j)=Timeseries_modshad_x2(R,j)*Timeseries_modshad_y2(R,j);  %
overall leading edge points shadow presence on PV module matrix


% BLADE 3
         if rho_z_le3(R,j)>=120.9
             if (xshad_te3(R,j)<=x_modposition_w & x_modposition_w<=xshad_le3(R,j)) |
(xshad_te3(R,j)<=x_modposition_e & x_modposition_e<=xshad_le3(R,j))
```

```
                Timeseries_modshad_x3(R,j)=1;    % 1 = there is leading edge points shadow
on PV module
            else
                Timeseries_modshad_x3(R,j)=0;    % 0 = there is not leading edge points
shadow on PV module
            end
        else
            if (xshad_le3(R,j)<=x_modposition_w & x_modposition_w<=xshad_te3(R,j)) |
(xshad_le3(R,j)<=x_modposition_e & x_modposition_e<=xshad_te3(R,j))
                Timeseries_modshad_x3(R,j)=1;    % 1 = there is leading edge points shadow
on PV module
            else
                Timeseries_modshad_x3(R,j)=0;    % 0 = there is not leading edge points
shadow on PV module
            end
        end

        if  rho_x_le3(R,j)<=0
            if (yshad_te3(R,j)<=y_modposition_s & y_modposition_s<=yshad_le3(R,j)) |
(yshad_te3(R,j)<=y_modposition_n & y_modposition_n<=yshad_le3(R,j))
                Timeseries_modshad_y3(R,j)=1;    % 1 = there is leading edge points shadow
on PV module
            else
                Timeseries_modshad_y3(R,j)=0;    % 0 = there is not leading edge points
shadow on PV module
            end
        else
            if (yshad_le3(R,j)<=y_modposition_s & y_modposition_s<=yshad_te3(R,j)) |
(yshad_le3(R,j)<=y_modposition_n & y_modposition_n<=yshad_te3(R,j))
                Timeseries_modshad_y3(R,j)=1;    % 1 = there is leading edge points shadow
on PV module
            else
                Timeseries_modshad_y3(R,j)=0;    % 0 = there is not leading edge points
shadow on PV module
            end
        end


Timeseries_modshad_3(R,j)=Timeseries_modshad_x3(R,j)*Timeseries_modshad_y3(R,j);  %
overall leading edge points shadow presence on PV module matrix

end
end


% BLADE 1 POINTS SHADOW TIME SERIES ON SINGLE PV PANEL FIGURE
Timeseries_1=linspace(1,1,79)*Timeseries_modshad_1;  % leading edge points shadow on PV
module time series vector

for j= 28800:57600
    if Timeseries_1(1,j)>=1
       Timeseries_1(1,j)=1;  % there is trailing edge points shadow
    elseif Timeseries_1(1,j)<1
       Timeseries_1(1,j)=0;  % there is not trailing edge points shadow
    end
end

figure(2)
plot(Timeseries_1,'r')
title('BLADE 1 (0°) SHADOW TIME SERIES ON PV MODULE')
xlabel('Time [seconds]')
ylabel('0 = not shaded PV, 1 = shaded PV')
axis([0 57600 -0.05 1.05])


% BLADE 2 POINTS SHADOW TIME SERIES ON SINGLE PV PANEL FIGURE
Timeseries_2=linspace(1,1,79)*Timeseries_modshad_2;  % leading edge points shadow on PV
module time series vector
```

```
for j= 28800:57600
    if Timeseries_2(1,j)>=1
       Timeseries_2(1,j)=1;  % there is trailing edge points shadow
    elseif Timeseries_2(1,j)<1
       Timeseries_2(1,j)=0;  % there is not trailing edge points shadow
    end
end

figure(3)
plot(Timeseries_2,'b')
title('BLADE 2 (+120°) SHADOW TIME SERIES ON PV MODULE')
xlabel('Time [seconds]')
ylabel('0 = not shaded PV, 1 = shaded PV')
axis([0 57600 -0.05 1.05])


% BLADE 3 POINTS SHADOW TIME SERIES ON SINGLE PV PANEL FIGURE
Timeseries_3=linspace(1,1,79)*Timeseries_modshad_3;  % leading edge points shadow on PV
module time series vector

for j= 28800:57600
    if Timeseries_3(1,j)>=1
       Timeseries_3(1,j)=1;  % there is trailing edge points shadow
    elseif Timeseries_3(1,j)<1
       Timeseries_3(1,j)=0;  % there is not trailing edge points shadow
    end
end

figure(4)
plot(Timeseries_3,'k')
title('BLADE 3 (-120°) SHADOW TIME SERIES ON PV MODULE')
xlabel('Time [seconds]')
ylabel('0 = not shaded PV, 1 = shaded PV')
axis([0 57600 -0.05 1.05])


% SUM OF BLADE 1,2,3 SHADOWs TIME SERIES ON SINGLE PV MODULE
Timeseries_modshad_blades=[Timeseries_modshad_1(:,:); Timeseries_modshad_2(:,:);
Timeseries_modshad_3(:,:)];  % overall blades shadow presence on PV module matrix
Timeseries_blades=linspace(1,1,237)*Timeseries_modshad_blades;  % overall blades shadow
on PV module time series vector

for j= 28800:57600
    if Timeseries_blades(1,j)>=1
        Timeseries_blades(1,j)=1;  % there is blades shadow
    elseif Timeseries_blades(1,j)<1
        Timeseries_blades(1,j)=0;  % there is not blades shadow
    end
end


figure(5)
hold on
plot(Timeseries_1,'r')
plot(Timeseries_2,'b')
plot(Timeseries_3,'k')
hold off
title('WTG BLADES SHADOW TIME SERIES ON PV MODULE')
xlabel('Time [seconds]')
ylabel('0 = not shaded PV, 1 = shaded PV')
axis([0 57600 -0.05 1.05])
legend('Blade 1 (0°)','Blade 2 (+120°)','Blade 3 (-120°)')

figure(6)
plot(Timeseries_blades)
title('OVERALL WTG BLADES SHADOW TIME SERIES ON PV MODULE')
xlabel('Time [seconds]')
ylabel('0 = not shaded PV, 1 = shaded PV')
axis([0 57600 -0.05 1.05])
```

```
figure(7)
subplot(5,1,1)
plot(Timeseries_1,'r')
title('BLADE 1 (0°) SHADOW')
xlabel('Time [seconds]')
ylabel('0 = not shaded PV, 1 = shaded PV')
axis([0 57600 -0.05 1.05])
subplot(5,1,2)
plot(Timeseries_2,'b')
title('BLADE 2 (+120°) SHADOW')
xlabel('Time [seconds]')
axis([0 57600 -0.05 1.05])
subplot(5,1,3)
plot(Timeseries_3,'k')
title('BLADE 3 (-120°) SHADOW')
xlabel('Time [seconds]')
axis([0 57600 -0.05 1.05])
subplot(5,1,4)
hold on
plot(Timeseries_1,'r')
plot(Timeseries_2,'b')
plot(Timeseries_3,'k')
hold off
title('WTG BLADES SHADOW')
xlabel('Time [seconds]')
axis([0 57600 -0.05 1.05])
legend('Blade 1 (0°)','Blade 2 (+120°)','Blade 3 (-120°)')
subplot(5,1,5)
plot(Timeseries_blades)
title('OVERALL WTG BLADES SHADOW')
xlabel('Time [seconds]')
axis([0 57600 -0.05 1.05])


Timeseries=[Timeseries_modshad_tower(:,:); Timeseries_modshad_blades(:,:)];  % overall
tower and blades shadow presence on PV module matrix
Timeseries_tb=linspace(1,1,358)*Timeseries;  % overall tower and blades shadow on PV
module time series vector

for j= 28800:57600
    if Timeseries_tb(1,j)>=1
        Timeseries_tb(1,j)=1;  % there is tower and/or blades shadow
    elseif Timeseries_tb(1,j)<1
        Timeseries_tb(1,j)=0;  % there is not both tower and blades shadow
    end
end

figure(8)
hold on
plot(Timeseries_blades,'r')
plot(Timeseries_t,'k')
hold off
title('WTG SHADOW TIME SERIES ON PV MODULE')
xlabel('Time [seconds]')
ylabel('0 = not shaded PV, 1 = shaded PV')
axis([0 57600 -0.05 1.05])

figure(9)
plot(Timeseries_tb)
title('OVERALL WTG SHADOW TIME SERIES ON PV MODULE')
xlabel('Time [seconds]')
ylabel('0 = not shaded PV, 1 = shaded PV')
axis([0 57600 -0.05 1.05])

figure(10)
subplot(4,1,1)
plot(Timeseries_t,'k')
title('TOWER SHADOW ON PV MODULE')
```

```
xlabel('Time [seconds]')
ylabel('0 = not shaded PV, 1 = shaded PV')
axis([0 57600 -0.05 1.05])
subplot(4,1,2)
plot(Timeseries_blades,'r')
title('THREE BLADES SHADOW ON PV MODULE')
xlabel('Time [seconds]')
axis([0 57600 -0.05 1.05])
subplot(4,1,3)
hold on
plot(Timeseries_blades,'r')
plot(Timeseries_t,'k')
hold off
title('OVERALL WTG SHADOW ON PV MODULE')
xlabel('Time [seconds]')
axis([0 57600 -0.05 1.05])
subplot(4,1,4)
plot(Timeseries_tb)
title('OVERALL WTG SHADOW ON PV MODULE')
xlabel('Time [seconds]')
axis([0 57600 -0.05 1.05])
```

3) WTG SHADOW SMALLER TIME SERIES MODEL ON A SINGLE PV PANEL (input day = 355, TAPVA_distance = 240 m and TANSTA_distance = 0 m)

```
% Smaller time series shadow evolution for a single PV module

clear
close all
clc
% model to see when a PV module is shaded, a time series in tenth of seconds
% considering WTG shadow evolution in a small time period
% (X,Y) reference system plane with origin in WTG tower axis
% East: X positive ; West: X negative
% North: Y positive ; South: Y negative
% all angles inside sin() and cos() functions are in radians, [rad]

Hmod=2.384;     % PV module height [m]
Wmod=1.303;     % PV module width [m]
PV_mod_area=Hmod*Wmod;    % PV module area [m^2]
lat=40.837;     % latitude of WTG 04 tower position in Gravina in Puglia site [°]
long=16.272;    % longitude of WTG 04 tower position in Gravina in Puglia site [°]
rot=1.038;  % [rad/s], angular speed of a single blade/wind rotor

% PV module position on (X,Y) plane
TAPVA_distance=input('Insert PV module center of gravity position along N-S [m] = ');  %
[m], tower-PV module axis/center of gravity distance
TANSTA_distance=input('Insert PV module center of gravity position along W-E [m] = ');
% [m], tower axis - NorthSouth tracker axis distance

% PV module distance from WTG axis on (X,Y) plane
dpvy=TAPVA_distance-(Hmod/2);  % distance along y axis between tower axis and PV module
center of gravity [m]
dpvx=TANSTA_distance-(Wmod/2);  % distance along x axis between tower axis and North-
South horizontal tracker axis [m]

x_modposition_e=dpvx+Wmod;    % eastern x coordinate of PV module on (X,Y) plane
x_modposition_w=dpvx;    % western x coordinate of PV module on (X,Y) plane
y_modposition_n=dpvy+Hmod;     % northern y coordinate of PV module on (X,Y) plane
y_modposition_s=dpvy;     % southern y coordinate of PV module on (X,Y) plane

day=input('Insert n° day of the year = ');  % number of day in the year [-]
    B=(360/365*(day-1))*0.017453292; % [rad]   1° = 0.017453292 rad  ,  1 rad =
57.29577951°
    decl=(23.45*sin((360/365*(day+284))*0.017453292))*0.017453292;  % [rad]
```

```
    ET=229.2*(0.000075+(0.001868*cos(B))-(0.032077*sin(B))-(0.014615*cos(2*B))-
(0.04089*sin(2*B)));   % Equation of Time [min], correction factor for true solar time
TST calculation

%% SHADOW MODEL OF WTG TOWER IN A SINGLE DAY
for z=1:121  % altitude of a point from ground along tower height [m]
HEIGHT(z)=z;
diam(z)=4.3-(0.004962779*z);   % WTG tower diameter at different elevation [m], supposing
linear reduction of tower diameter

    for j= 1:18000  % [ds] analysis of shadow position will be done every tenth of a
second from 11:35 a.m. to 12:05 p.m. (30 minutes)

        LT(z,j)=(11.583*60)+(j/600);    % legal time of a day [min]

        if day>=1 & day<=85     % change of solar hour at 27 March 2022
           summertime_difference=0; % [min], legal time one hour change
        elseif day>=86 & day<=302   % change of solar hour at 30 October 2022
            summertime_difference=-60; % [min]
        else
             summertime_difference=0; % [min]
        end

        diff_GMT=-60;  % [min], difference with Greenwich Mean Time of our Time Zone
        TST(z,j)=(LT(z,j)+diff_GMT+((long/15)*60)+ET+summertime_difference)*60;  % True
Solar Time [s]
        HRA(z,j)=(0.004166666*(TST(z,j)-43200))*0.017453292;   % hour angle [rad]

alfa(z,j)=asin((cos(decl)*cos(lat*0.017453292)*cos(HRA(z,j)))+(sin(decl)*sin(lat*0.017453
292)));  % solar height angle [rad]
        gammas(z,j)=asin((cos(decl)*sin(HRA(z,j)))/cos(alfa(z,j)));   % solar azimuth
angle [rad]

        Lshad_axis(z,j)=z/tan(alfa(z,j));   % shadow length of WTG tower axis [m]
        xshad_axis(z,j)=Lshad_axis(z,j)*sin(gammas(z,j));  % x coordinate of axis shadow
[m]
        yshad_axis(z,j)=Lshad_axis(z,j)*cos(gammas(z,j));  % y coordinate of axis shadow
[m]

        xshad_w(z,j)=xshad_axis(z,j)-((diam(z)/2)*cos(gammas(z,j)));   % x coordinate of
western tower point shadow [m]
        yshad_w(z,j)=yshad_axis(z,j)+((diam(z)/2)*sin(gammas(z,j)));   % y coordinate of
western tower point shadow [m]

        xshad_e(z,j)=xshad_axis(z,j)+((diam(z)/2)*cos(gammas(z,j)));   % x coordinate of
eastern tower point shadow [m]
        yshad_e(z,j)=yshad_axis(z,j)-((diam(z)/2)*sin(gammas(z,j)));   % y coordinate of
eastern tower point shadow [m]

        xshad_wa1(z,j)=xshad_axis(z,j)-((diam(z)*cos(gammas(z,j)))/8);   % x coordinate
fraction of western tower point shadow [m]
        yshad_wa1(z,j)=yshad_axis(z,j)+((diam(z)*sin(gammas(z,j)))/8);   % y coordinate
fraction of western tower point shadow [m]

        xshad_wa2(z,j)=xshad_axis(z,j)-((diam(z)*cos(gammas(z,j)))/4);
        yshad_wa2(z,j)=yshad_axis(z,j)+((diam(z)*sin(gammas(z,j)))/4);

        xshad_wa3(z,j)=xshad_axis(z,j)-((diam(z)*cos(gammas(z,j)))*3/8);
        yshad_wa3(z,j)=yshad_axis(z,j)+((diam(z)*sin(gammas(z,j)))*3/8);

        xshad_ea1(z,j)=xshad_axis(z,j)+((diam(z)*cos(gammas(z,j)))/8);   % x coordinate
fraction of eastern tower point shadow [m]
        yshad_ea1(z,j)=yshad_axis(z,j)-((diam(z)*sin(gammas(z,j)))/8);   % y coordinate
fraction of eastern tower point shadow [m]

        xshad_ea2(z,j)=xshad_axis(z,j)+((diam(z)*cos(gammas(z,j)))/4);
        yshad_ea2(z,j)=yshad_axis(z,j)-((diam(z)*sin(gammas(z,j)))/4);

        xshad_ea3(z,j)=xshad_axis(z,j)+((diam(z)*cos(gammas(z,j)))*3/8);
```

```
        yshad_ea3(z,j)=yshad_axis(z,j)-((diam(z)*sin(gammas(z,j)))*3/8);

        if (x_modposition_w<=xshad_axis(z,j) & xshad_axis(z,j)<=x_modposition_e) |
(x_modposition_w<=xshad_w(z,j) & xshad_w(z,j)<=x_modposition_e) |
(x_modposition_w<=xshad_e(z,j) & xshad_e(z,j)<=x_modposition_e) |
(x_modposition_w<=xshad_ea1(z,j) & xshad_ea1(z,j)<=x_modposition_e) |
(x_modposition_w<=xshad_wa1(z,j) & xshad_wa1(z,j)<=x_modposition_e) |
(x_modposition_w<=xshad_ea2(z,j) & xshad_ea2(z,j)<=x_modposition_e) |
(x_modposition_w<=xshad_wa2(z,j) & xshad_wa2(z,j)<=x_modposition_e) |
(x_modposition_w<=xshad_ea3(z,j) & xshad_ea3(z,j)<=x_modposition_e) |
(x_modposition_w<=xshad_wa3(z,j) & xshad_wa3(z,j)<=x_modposition_e)
                Timeseries_modshad_x_tower(z,j)=1;   % 1 = there is tower shadow on PV
module
            else
                Timeseries_modshad_x_tower(z,j)=0;   % 0 = there is not tower shadow on
PV module
            end

            if (y_modposition_s<=yshad_axis(z,j) & yshad_axis(z,j)<=y_modposition_n) |
(y_modposition_s<=yshad_w(z,j) & yshad_w(z,j)<=y_modposition_n) |
(y_modposition_s<=yshad_e(z,j) & yshad_e(z,j)<=y_modposition_n)
                Timeseries_modshad_y_tower(z,j)=1;   % 1 = there is tower shadow on PV
module
            else
                Timeseries_modshad_y_tower(z,j)=0;   % 0 = there is not tower shadow on
PV module
            end

               Timeseries_modshad_tower(z,j)=Timeseries_modshad_x_tower(z,j).*
Timeseries_modshad_y_tower(z,j);  % overall tower shadow presence on PV module matrix

    end
end

Timeseries_t=linspace(1,1,121)*Timeseries_modshad_tower;   % tower shadow on PV module
time series vector

for j= 1:18000
    if Timeseries_t(1,j)>=1
        Timeseries_t(1,j)=1;   % there is tower shadow
    elseif Timeseries_t(1,j)<1
        Timeseries_t(1,j)=0;   % there is not tower shadow
    end
end

figure(1)
plot(Timeseries_t,'k')
title('TOWER SHADOW TIME SERIES ON PV MODULE')
xlabel('Time [tenths of second]')
ylabel('0 = not shaded PV, 1 = shaded PV')
axis([0 18000 -0.05 1.05])


%% SHADOW MODEL OF THREE BLADES IN A SINGLE DAY
% Hypothesis: rotor plane (X,Z) with normal direction always fixed towards North-North-
West direction (30°=0.523599)
% Highest wind direction frequency at Gravina in Puglia site
angle=30*0.017453292;
for R=1:79    % [m] radial position of a point along blades
    Rad(R)=R;
if R>=0 & R<23.7
   z(R)=3-cos(R/7.543944303);   % [m] blade width at radial position
  elseif R>=23.7 & R<71.1
         z(R)=5.349999993-(0.056962025*R);
  else
      z(R)=6.842105264-((R^2)/912.1461538);
end
```

```
for j= 1:18000  % analysis of shadow position will be done every tenth of second in a
minute from 11:35 am to 12:05 pm (30 minutes)
    LT(R,j)=(11.583*60)+(j/600);    % legal time of a day [min]

        if day>=1 & day<=85     % change of solar hour at 27 March 2022
           summertime_difference=0; % [min], legal time one hour change
        elseif day>=86 & day<=302   % change of solar hour at 30 October 2022
            summertime_difference=-60; % [min]
        else
             summertime_difference=0; % [min]
        end

        diff_GMT=-60;  % [min], difference with Greenwich Mean Time of our Time Zone
        TST(R,j)=(LT(R,j)+diff_GMT+((long/15)*60)+ET+summertime_difference)*60;  % True
Solar Time [s]
        HRA(R,j)=(0.004166666*(TST(R,j)-43200))*0.017453292;   % hour angle [rad]

alfa(R,j)=asin((cos(decl)*cos(lat*0.017453292)*cos(HRA(R,j)))+(sin(decl)*sin(lat*0.017453
292)));  % solar height angle [rad]
        gammas(R,j)=asin((cos(decl)*sin(HRA(R,j)))/cos(alfa(R,j)));   % solar azimuth
angle [rad]


        %%%%% LEADING EDGE (polar coordinates of leading edge points on (X,Z) rotor
plane)
        teta_le1(R,j)=(-rot)*LT(R,j)*60;  % [rad], polar coordinates angle related to
blade towards 0° direction
                                          % minus sign because rotation direction of GE
CYPRESS WTG rotor is clockwise
        teta_le2(R,j)=((-rot)*LT(R,j)*60)+((2/3)*pi);  % [rad], polar coordinates angle
related to blade towards +120° direction
        teta_le3(R,j)=((-rot)*LT(R,j)*60)-((2/3)*pi);  % [rad], polar coordinates angle
related to blade towards -120° direction

        rho_le1(R,j)=R;    % [m], polar coordinates module related to blade towards 0°
direction
        rho_le2(R,j)=R;    % [m], polar coordinates module related to blade towards +120°
direction
        rho_le3(R,j)=R;    % [m], polar coordinates module related to blade towards -120°
direction

        rho_x_le1(R,j)=rho_le1(R,j)*cos(teta_le1(R,j));  % [m], x axis component (WEST-
EAST) of polar coordinates module
        rho_x_le2(R,j)=rho_le2(R,j)*cos(teta_le2(R,j));
        rho_x_le3(R,j)=rho_le3(R,j)*cos(teta_le3(R,j));

        rho_z_le1(R,j)=(rho_le1(R,j)*sin(teta_le1(R,j)))+120.9;  % [m], z axis component
(ALTITUDE) of polar coordinates module
        rho_z_le2(R,j)=(rho_le2(R,j)*sin(teta_le2(R,j)))+120.9;
        rho_z_le3(R,j)=(rho_le3(R,j)*sin(teta_le3(R,j)))+120.9;



        %%%%% TRAILING EDGE (polar coordinates of trailing edge points on (X,Z) rotor
plane)
        teta_te1(R,j)=teta_le1(R,j)+atan(z(R)/R);   % [rad], polar coordinates angle
related to blade towards 0° direction
        teta_te2(R,j)=teta_le2(R,j)+atan(z(R)/R);   % [rad], polar coordinates angle
related to blade towards +120° direction
        teta_te3(R,j)=teta_le3(R,j)+atan(z(R)/R);   % [rad], polar coordinates angle
related to blade towards -120° direction

        rho_te1(R,j)=sqrt((R^2)+(z(R)^2));   % [m], polar coordinates module related to
blade towards 0° direction
        rho_te2(R,j)=sqrt((R^2)+(z(R)^2));   % [m], polar coordinates module related to
blade towards +120° direction
        rho_te3(R,j)=sqrt((R^2)+(z(R)^2));   % [m], polar coordinates module related to
blade towards -120° direction
```

```
        rho_x_te1(R,j)=rho_te1(R,j)*cos(teta_te1(R,j));  % [m], x axis component (WEST-
EAST) of polar coordinates module on rotor (X,Z) plane
        rho_x_te2(R,j)=rho_te2(R,j)*cos(teta_te2(R,j));
        rho_x_te3(R,j)=rho_te3(R,j)*cos(teta_te3(R,j));

        rho_z_te1(R,j)=(rho_te1(R,j)*sin(teta_te1(R,j)))+120.9;  % [m], z axis component
(ALTITUDE) of polar coordinates module on rotor (X,Z) plane
        rho_z_te2(R,j)=(rho_te2(R,j)*sin(teta_te2(R,j)))+120.9;
        rho_z_te3(R,j)=(rho_te3(R,j)*sin(teta_te3(R,j)))+120.9;


        %%%%% LEADING EDGE POINT SHADOW COMPONENTS ON (X,Y) PLANE, WTG TOWER AXIS ORIGIN
        % BLADE 1 (0°)
        Lshad_le1(R,j)=rho_z_le1(R,j)/tan(alfa(R,j));   % shadow length
        xshad_le1(R,j)=(Lshad_le1(R,j)*sin(gammas(R,j)))+(rho_x_le1(R,j)*cos(angle));  %
x shadow length coordinate on (X,Y) plane
        yshad_le1(R,j)=(Lshad_le1(R,j)*cos(gammas(R,j)))+(rho_x_le1(R,j)*sin(angle));  %
y shadow length coordinate on (X,Y) plane

        % BLADE 2 (+120°)
        Lshad_le2(R,j)=rho_z_le2(R,j)/tan(alfa(R,j));
        xshad_le2(R,j)=(Lshad_le2(R,j)*sin(gammas(R,j)))+(rho_x_le2(R,j)*cos(angle));
        yshad_le2(R,j)=(Lshad_le2(R,j)*cos(gammas(R,j)))+(rho_x_le2(R,j)*sin(angle));

        % BLADE 3 (-120°)
        Lshad_le3(R,j)=rho_z_le3(R,j)/tan(alfa(R,j));
        xshad_le3(R,j)=(Lshad_le3(R,j)*sin(gammas(R,j)))+(rho_x_le3(R,j)*cos(angle));
        yshad_le3(R,j)=(Lshad_le3(R,j)*cos(gammas(R,j)))+(rho_x_le3(R,j)*sin(angle));


        %%%%% TRAILING EDGE POINT SHADOW COMPONENTS ON (X,Y) PLANE, WTG TOWER AXIS ORIGIN
        % BLADE 1 (0°)
        Lshad_te1(R,j)=rho_z_te1(R,j)/tan(alfa(R,j));   % shadow length
        xshad_te1(R,j)=(Lshad_te1(R,j)*sin(gammas(R,j)))+(rho_x_te1(R,j)*cos(angle));   %
x shadow length coordinate on (X,Y) plane
        yshad_te1(R,j)=(Lshad_te1(R,j)*cos(gammas(R,j)))+(rho_x_te1(R,j)*sin(angle));   %
y shadow length coordinate on (X,Y) plane

        % BLADE 2 (+120°)
        Lshad_te2(R,j)=rho_z_te2(R,j)/tan(alfa(R,j));
        xshad_te2(R,j)=(Lshad_te2(R,j)*sin(gammas(R,j)))+(rho_x_te2(R,j)*cos(angle));
        yshad_te2(R,j)=(Lshad_te2(R,j)*cos(gammas(R,j)))+(rho_x_te2(R,j)*sin(angle));

        % BLADE 3 (-120°)
        Lshad_te3(R,j)=rho_z_te3(R,j)/tan(alfa(R,j));
        xshad_te3(R,j)=(Lshad_te3(R,j)*sin(gammas(R,j)))+(rho_x_te3(R,j)*cos(angle));
        yshad_te3(R,j)=(Lshad_te3(R,j)*cos(gammas(R,j)))+(rho_x_te3(R,j)*sin(angle));

%% BLADE POINTS SHADOW TIME SERIES ON SINGLE PANEL
% BLADE 1
if rho_z_le1(R,j)>=120.9

            if (xshad_te1(R,j)<=x_modposition_w & x_modposition_w<=xshad_le1(R,j)) |
(xshad_te1(R,j)<=x_modposition_e & x_modposition_e<=xshad_le1(R,j))
                Timeseries_modshad_x1(R,j)=1;   % 1 = there is leading edge points shadow
on PV module
            else
                Timeseries_modshad_x1(R,j)=0;   % 0 = there is not leading edge points
shadow on PV module
            end
else
            if (xshad_le1(R,j)<=x_modposition_w & x_modposition_w<=xshad_te1(R,j)) |
(xshad_le1(R,j)<=x_modposition_e & x_modposition_e<=xshad_te1(R,j))
                Timeseries_modshad_x1(R,j)=1;   % 1 = there is leading edge points shadow
on PV module
            else
                Timeseries_modshad_x1(R,j)=0;   % 0 = there is not leading edge points
shadow on PV module
            end
```

```
end

if  rho_x_le1(R,j)<=0

             if (yshad_te1(R,j)<=y_modposition_s & y_modposition_s<=yshad_le1(R,j)) |
(yshad_te1(R,j)<=y_modposition_n & y_modposition_n<=yshad_le1(R,j))
                Timeseries_modshad_y1(R,j)=1;    % 1 = there is leading edge points shadow
on PV module
             else
                Timeseries_modshad_y1(R,j)=0;    % 0 = there is not leading edge points
shadow on PV module
             end
else
             if (yshad_le1(R,j)<=y_modposition_s & y_modposition_s<=yshad_te1(R,j)) |
(yshad_le1(R,j)<=y_modposition_n & y_modposition_n<=yshad_te1(R,j))
                Timeseries_modshad_y1(R,j)=1;    % 1 = there is leading edge points shadow
on PV module
             else
                Timeseries_modshad_y1(R,j)=0;    % 0 = there is not leading edge points
shadow on PV module
             end
end


Timeseries_modshad_1(R,j)=Timeseries_modshad_x1(R,j)*Timeseries_modshad_y1(R,j);  %
overall leading edge points shadow presence on PV module matrix

% BLADE 2
if rho_z_le2(R,j)>=120.9

             if (xshad_te2(R,j)<=x_modposition_w & x_modposition_w<=xshad_le2(R,j)) |
(xshad_te2(R,j)<=x_modposition_e & x_modposition_e<=xshad_le2(R,j))
                Timeseries_modshad_x2(R,j)=1;    % 1 = there is leading edge points shadow
on PV module
             else
                 Timeseries_modshad_x2(R,j)=0;    % 0 = there is not leading edge points
shadow on PV module
             end
else
             if (xshad_le2(R,j)<=x_modposition_w & x_modposition_w<=xshad_te2(R,j)) |
(xshad_le2(R,j)<=x_modposition_e & x_modposition_e<=xshad_te2(R,j))
                Timeseries_modshad_x2(R,j)=1;    % 1 = there is leading edge points shadow
on PV module
             else
                 Timeseries_modshad_x2(R,j)=0;    % 0 = there is not leading edge points
shadow on PV module
             end
end

if  rho_x_le2(R,j)<=0

             if (yshad_te2(R,j)<=y_modposition_s & y_modposition_s<=yshad_le2(R,j)) |
(yshad_te2(R,j)<=y_modposition_n & y_modposition_n<=yshad_le2(R,j))
                Timeseries_modshad_y2(R,j)=1;    % 1 = there is leading edge points shadow
on PV module
             else
                Timeseries_modshad_y2(R,j)=0;    % 0 = there is not leading edge points
shadow on PV module
             end
else
             if (yshad_le2(R,j)<=y_modposition_s & y_modposition_s<=yshad_te2(R,j)) |
(yshad_le2(R,j)<=y_modposition_n & y_modposition_n<=yshad_te2(R,j))
                Timeseries_modshad_y2(R,j)=1;    % 1 = there is leading edge points shadow
on PV module
             else
                Timeseries_modshad_y2(R,j)=0;    % 0 = there is not leading edge points
shadow on PV module
             end
end
```

```
Timeseries_modshad_2(R,j)=Timeseries_modshad_x2(R,j)*Timeseries_modshad_y2(R,j);  %
overall leading edge points shadow presence on PV module matrix


% BLADE 3
if rho_z_le3(R,j)>=120.9

             if (xshad_te3(R,j)<=x_modposition_w & x_modposition_w<=xshad_le3(R,j)) |
(xshad_te3(R,j)<=x_modposition_e & x_modposition_e<=xshad_le3(R,j))
                Timeseries_modshad_x3(R,j)=1;    % 1 = there is leading edge points shadow
on PV module
             else
                 Timeseries_modshad_x3(R,j)=0;    % 0 = there is not leading edge points
shadow on PV module
             end
else
             if (xshad_le3(R,j)<=x_modposition_w & x_modposition_w<=xshad_te3(R,j)) |
(xshad_le3(R,j)<=x_modposition_e & x_modposition_e<=xshad_te3(R,j))
                Timeseries_modshad_x3(R,j)=1;    % 1 = there is leading edge points shadow
on PV module
             else
                 Timeseries_modshad_x3(R,j)=0;    % 0 = there is not leading edge points
shadow on PV module
             end
end

if  rho_x_le3(R,j)<=0

             if (yshad_te3(R,j)<=y_modposition_s & y_modposition_s<=yshad_le3(R,j)) |
(yshad_te3(R,j)<=y_modposition_n & y_modposition_n<=yshad_le3(R,j))
                Timeseries_modshad_y3(R,j)=1;    % 1 = there is leading edge points shadow
on PV module
             else
                Timeseries_modshad_y3(R,j)=0;    % 0 = there is not leading edge points
shadow on PV module
             end
else
             if (yshad_le3(R,j)<=y_modposition_s & y_modposition_s<=yshad_te3(R,j)) |
(yshad_le3(R,j)<=y_modposition_n & y_modposition_n<=yshad_te3(R,j))
                Timeseries_modshad_y3(R,j)=1;    % 1 = there is leading edge points shadow
on PV module
             else
                Timeseries_modshad_y3(R,j)=0;    % 0 = there is not leading edge points
shadow on PV module
             end
end


Timeseries_modshad_3(R,j)=Timeseries_modshad_x3(R,j)*Timeseries_modshad_y3(R,j);  %
overall leading edge points shadow presence on PV module matrix

end
end


% BLADE 1 POINTS SHADOW TIME SERIES ON SINGLE PV PANEL FIGURE
Timeseries_1=linspace(1,1,79)*Timeseries_modshad_1;  % leading edge points shadow on PV
module time series vector

for j= 1:18000
    if Timeseries_1(1,j)>=1
       Timeseries_1(1,j)=1;  % there is trailing edge points shadow
    elseif Timeseries_1(1,j)<1
       Timeseries_1(1,j)=0;  % there is not trailing edge points shadow
    end
end
```

```
figure(2)
plot(Timeseries_1,'r')
title('BLADE 1 (0°) SHADOW TIME SERIES ON PV MODULE')
xlabel('Time [tenths of second]')
ylabel('0 = not shaded PV, 1 = shaded PV')
axis([0 18000 -0.05 1.05])


% BLADE 2 POINTS SHADOW TIME SERIES ON SINGLE PV PANEL FIGURE
Timeseries_2=linspace(1,1,79)*Timeseries_modshad_2;  % leading edge points shadow on PV
module time series vector

for j= 1:18000
    if Timeseries_2(1,j)>=1
       Timeseries_2(1,j)=1;  % there is trailing edge points shadow
    elseif Timeseries_2(1,j)<1
       Timeseries_2(1,j)=0;  % there is not trailing edge points shadow
    end
end

figure(3)
plot(Timeseries_2,'b')
title('BLADE 2 (+120°) SHADOW TIME SERIES ON PV MODULE')
xlabel('Time [tenths of second]')
ylabel('0 = not shaded PV, 1 = shaded PV')
axis([0 18000 -0.05 1.05])


% BLADE 3 POINTS SHADOW TIME SERIES ON SINGLE PV PANEL FIGURE
Timeseries_3=linspace(1,1,79)*Timeseries_modshad_3;  % leading edge points shadow on PV
module time series vector

for j= 1:18000
    if Timeseries_3(1,j)>=1
       Timeseries_3(1,j)=1;  % there is trailing edge points shadow
    elseif Timeseries_3(1,j)<1
       Timeseries_3(1,j)=0;  % there is not trailing edge points shadow
    end
end

figure(4)
plot(Timeseries_3,'k')
title('BLADE 3 (-120°) SHADOW TIME SERIES ON PV MODULE')
xlabel('Time [tenths of second]')
ylabel('0 = not shaded PV, 1 = shaded PV')
axis([0 18000 -0.05 1.05])


% SUM OF BLADE 1,2,3 SHADOWs TIME SERIES ON SINGLE PV MODULE
Timeseries_modshad_blades=[Timeseries_modshad_1(:,:); Timeseries_modshad_2(:,:);
Timeseries_modshad_3(:,:)];  % overall blades shadow presence on PV module matrix
Timeseries_blades=linspace(1,1,237)*Timeseries_modshad_blades;  % overall blades shadow
on PV module time series vector

for j= 1:18000
    if Timeseries_blades(1,j)>=1
        Timeseries_blades(1,j)=1;  % there is blades shadow
    elseif Timeseries_blades(1,j)<1
        Timeseries_blades(1,j)=0;  % there is not blades shadow
    end
end


figure(5)
hold on
plot(Timeseries_1,'r')
plot(Timeseries_2,'b')
plot(Timeseries_3,'k')
hold off
```

```
title('WTG BLADES SHADOW TIME SERIES ON PV MODULE')
xlabel('Time [tenths of second]')
ylabel('0 = not shaded PV, 1 = shaded PV')
axis([0 18000 -0.05 1.05])
legend('Blade 1 (0°)','Blade 2 (+120°)','Blade 3 (-120°)')

figure(6)
plot(Timeseries_blades)
title('OVERALL WTG BLADES SHADOW TIME SERIES ON PV MODULE')
xlabel('Time [tenths of second]')
ylabel('0 = not shaded PV, 1 = shaded PV')
axis([0 18000 -0.05 1.05])

figure(7)
subplot(5,1,1)
plot(Timeseries_1,'r')
title('BLADE 1 (0°) SHADOW')
xlabel('Time [tenths of second]')
ylabel('0 = not shaded PV, 1 = shaded PV')
axis([0 18000 -0.05 1.05])
subplot(5,1,2)
plot(Timeseries_2,'b')
title('BLADE 2 (+120°) SHADOW')
xlabel('Time [tenths of second]')
axis([0 18000 -0.05 1.05])
subplot(5,1,3)
plot(Timeseries_3,'k')
title('BLADE 3 (-120°) SHADOW')
xlabel('Time [tenths of second]')
axis([0 18000 -0.05 1.05])
subplot(5,1,4)
hold on
plot(Timeseries_1,'r')
plot(Timeseries_2,'b')
plot(Timeseries_3,'k')
hold off
title('WTG BLADES SHADOW')
xlabel('Time [tenths of second]')
axis([0 18000 -0.05 1.05])
legend('Blade 1 (0°)','Blade 2 (+120°)','Blade 3 (-120°)')
subplot(5,1,5)
plot(Timeseries_blades)
title('OVERALL WTG BLADES SHADOW')
xlabel('Time [tenths of second]')
axis([0 18000 -0.05 1.05])


Timeseries=[Timeseries_modshad_tower(:,:); Timeseries_modshad_blades(:,:)];  % overall
tower and blades shadow presence on PV module matrix
Timeseries_tb=linspace(1,1,358)*Timeseries;  % overall tower and blades shadow on PV
module time series vector

for j= 1:18000
    if Timeseries_tb(1,j)>=1
        Timeseries_tb(1,j)=1;  % there is tower and/or blades shadow
    elseif Timeseries_tb(1,j)<1
        Timeseries_tb(1,j)=0;  % there is not both tower and blades shadow
    end
end

figure(8)
hold on
plot(Timeseries_blades,'r')
plot(Timeseries_t,'k')
hold off
title('WTG SHADOW TIME SERIES ON PV MODULE')
xlabel('Time [tenths of second]')
ylabel('0 = not shaded PV, 1 = shaded PV')
axis([0 18000 -0.05 1.05])
```

```
figure(9)
plot(Timeseries_tb)
title('OVERALL WTG SHADOW TIME SERIES ON PV MODULE')
xlabel('Time [tenths of second]')
ylabel('0 = not shaded PV, 1 = shaded PV')
axis([0 18000 -0.05 1.05])

figure(10)
subplot(4,1,1)
plot(Timeseries_t,'k')
title('TOWER SHADOW ON PV MODULE')
xlabel('Time [tenths of second]')
ylabel('0 = not shaded PV, 1 = shaded PV')
axis([0 18000 -0.05 1.05])
subplot(4,1,2)
plot(Timeseries_blades,'r')
title('THREE BLADES SHADOW ON PV MODULE')
xlabel('Time [tenths of second]')
axis([0 18000 -0.05 1.05])
subplot(4,1,3)
hold on
plot(Timeseries_blades,'r')
plot(Timeseries_t,'k')
hold off
title('OVERALL WTG SHADOW ON PV MODULE')
xlabel('Time [tenths of second]')
axis([0 18000 -0.05 1.05])
subplot(4,1,4)
plot(Timeseries_tb)
title('OVERALL WTG SHADOW ON PV MODULE')
xlabel('Time [tenths of second]')
axis([0 18000 -0.05 1.05])
```

4) BLADES SHADOW ONE MINUTE TIME SERIES ON A SINGLE PV PANEL

(input TAPVA_distance = 300 m, TANSTA_distance = 0 m, hour = 11 and minutes = 45, day = 355)

```
% Smaller time series with only blades shadow evolution for a single PV module

clear
close all
clc
% model to see when a PV module is shaded separately by blades,
% in a time series in hundredths of second
% time period of one minute (6000 hundredths of second)
% (X,Y) reference system plane with origin in WTG tower axis
% East: X positive ; West: X negative
% North: Y positive ; South: Y negative
% all angles inside sin() and cos() functions are in radians, [rad]

Hmod=2.384;     % PV module height [m]
Wmod=1.303;     % PV module width [m]
PV_mod_area=Hmod*Wmod;    % PV module area [m^2]
lat=40.837;     % latitude of WTG 04 tower position in Gravina in Puglia site [°]
long=16.272;    % longitude of WTG 04 tower position in Gravina in Puglia site [°]
rot=1.038;  % [rad/s], angular speed of a single blade/wind rotor

% PV module position on (X,Y) plane
TAPVA_distance=input('Insert PV module center of gravity position along N-S [m] = ');  %
[m], tower-PV module axis/center of gravity distance
TANSTA_distance=input('Insert PV module center of gravity position along W-E [m] = ');
% [m], tower axis - NorthSouth tracker axis distance

 % PV module distance from WTG axis on (X,Y) plane
```

```
 dpvy=TAPVA_distance-(Hmod/2);  % distance along y axis between tower axis and PV module
center of gravity [m]
 dpvx=TANSTA_distance-(Wmod/2);  % distance along x axis between tower axis and North-
South horizontal tracker axis [m]

 x_modposition_e=dpvx+Wmod;   % eastern x coordinate of PV module on (X,Y) plane
 x_modposition_w=dpvx;   % western x coordinate of PV module on (X,Y) plane
 y_modposition_n=dpvy+Hmod;    % northern y coordinate of PV module on (X,Y) plane
 y_modposition_s=dpvy;    % southern y coordinate of PV module on (X,Y) plane

hour=input('Insert hour [h] = ');   % hour of the day
minutes=input('Insert minutes [min] = ');  % minutes of that hour of the day

day=input('Insert n° day of the year = ');  % number of day in the year [-]
    B=(360/365*(day-1))*0.017453292; % [rad]   1° = 0.017453292 rad  ,  1 rad =
57.29577951°
    decl=(23.45*sin((360/365*(day+284))*0.017453292))*0.017453292;  % [rad]
    ET=229.2*(0.000075+(0.001868*cos(B))-(0.032077*sin(B))-(0.014615*cos(2*B))-
(0.04089*sin(2*B)));   % Equation of Time [min], correction factor for true solar time
TST calculation

%% SHADOW MODEL OF THREE BLADES IN A SINGLE DAY
% Hypothesis: rotor plane (X,Z) with normal direction always fixed towards North-North-
West direction (30°=0.523599)
% Highest wind direction frequency at Gravina in Puglia site
angle=30*0.017453292;
for R=1:79    % [m] radial position of a point along blades
    Rad(R)=R;
if R>=0 & R<23.7
   z(R)=3-cos(R/7.543944303);   % [m] blade width at radial position
  elseif R>=23.7 & R<71.1
         z(R)=5.349999993-(0.056962025*R);
  else
      z(R)=6.842105264-((R^2)/912.1461538);
end

for j= 1:6000  % analysis of shadow position will be done every hundredths of second in
one minute (from 11:45 am to 11:46 am)
LT(R,j)=((hour*60)+minutes)+(j/6000);    % legal time of a day [min]

        if day>=1 & day<=85     % change of solar hour at 27 March 2022
           summertime_difference=0; % [min], legal time one hour change
        elseif day>=86 & day<=302   % change of solar hour at 30 October 2022
            summertime_difference=-60; % [min]
        else
             summertime_difference=0; % [min]
        end

        diff_GMT=-60;  % [min], difference with Greenwich Mean Time of our Time Zone
        TST(R,j)=(LT(R,j)+diff_GMT+((long/15)*60)+ET+summertime_difference)*60;  % True
Solar Time [s]
        HRA(R,j)=(0.004166666*(TST(R,j)-43200))*0.017453292;   % hour angle [rad]

alfa(R,j)=asin((cos(decl)*cos(lat*0.017453292)*cos(HRA(R,j)))+(sin(decl)*sin(lat*0.017453
292)));  % solar height angle [rad]
        gammas(R,j)=asin((cos(decl)*sin(HRA(R,j)))/cos(alfa(R,j)));   % solar azimuth
angle [rad]


        %%%%% LEADING EDGE (polar coordinates of leading edge points on (X,Z) rotor
plane)
        teta_le1(R,j)=(-rot)*LT(R,j)*60;  % [rad], polar coordinates angle related to
blade towards 0° direction
                                    % minus sign because rotation direction of GE
CYPRESS WTG rotor is clockwise
        teta_le2(R,j)=((-rot)*LT(R,j)*60)+((2/3)*pi);  % [rad], polar coordinates angle
related to blade towards +120° direction
        teta_le3(R,j)=((-rot)*LT(R,j)*60)-((2/3)*pi);  % [rad], polar coordinates angle
related to blade towards -120° direction
```

```
        rho_le1(R,j)=R;    % [m], polar coordinates module related to blade towards 0°
direction
        rho_le2(R,j)=R;    % [m], polar coordinates module related to blade towards +120°
direction
        rho_le3(R,j)=R;    % [m], polar coordinates module related to blade towards -120°
direction

        rho_x_le1(R,j)=rho_le1(R,j)*cos(teta_le1(R,j));  % [m], x axis component (WEST-
EAST) of polar coordinates module
        rho_x_le2(R,j)=rho_le2(R,j)*cos(teta_le2(R,j));
        rho_x_le3(R,j)=rho_le3(R,j)*cos(teta_le3(R,j));

        rho_z_le1(R,j)=(rho_le1(R,j)*sin(teta_le1(R,j)))+120.9;  % [m], z axis component
(ALTITUDE) of polar coordinates module
        rho_z_le2(R,j)=(rho_le2(R,j)*sin(teta_le2(R,j)))+120.9;
        rho_z_le3(R,j)=(rho_le3(R,j)*sin(teta_le3(R,j)))+120.9;



        %%%%% TRAILING EDGE (polar coordinates of trailing edge points on (X,Z) rotor
plane)
        teta_te1(R,j)=teta_le1(R,j)+atan(z(R)/R);   % [rad], polar coordinates angle
related to blade towards 0° direction
        teta_te2(R,j)=teta_le2(R,j)+atan(z(R)/R);   % [rad], polar coordinates angle
related to blade towards +120° direction
        teta_te3(R,j)=teta_le3(R,j)+atan(z(R)/R);   % [rad], polar coordinates angle
related to blade towards -120° direction

        rho_te1(R,j)=sqrt((R^2)+(z(R)^2));   % [m], polar coordinates module related to
blade towards 0° direction
        rho_te2(R,j)=sqrt((R^2)+(z(R)^2));   % [m], polar coordinates module related to
blade towards +120° direction
        rho_te3(R,j)=sqrt((R^2)+(z(R)^2));   % [m], polar coordinates module related to
blade towards -120° direction

        rho_x_te1(R,j)=rho_te1(R,j)*cos(teta_te1(R,j));  % [m], x axis component (WEST-
EAST) of polar coordinates module on rotor (X,Z) plane
        rho_x_te2(R,j)=rho_te2(R,j)*cos(teta_te2(R,j));
        rho_x_te3(R,j)=rho_te3(R,j)*cos(teta_te3(R,j));

        rho_z_te1(R,j)=(rho_te1(R,j)*sin(teta_te1(R,j)))+120.9;  % [m], z axis component
(ALTITUDE) of polar coordinates module on rotor (X,Z) plane
        rho_z_te2(R,j)=(rho_te2(R,j)*sin(teta_te2(R,j)))+120.9;
        rho_z_te3(R,j)=(rho_te3(R,j)*sin(teta_te3(R,j)))+120.9;


        %%%%% LEADING EDGE POINT SHADOW COMPONENTS ON (X,Y) PLANE, WTG TOWER AXIS ORIGIN
        % BLADE 1 (0°)
        Lshad_le1(R,j)=rho_z_le1(R,j)/tan(alfa(R,j));   % shadow length
        xshad_le1(R,j)=(Lshad_le1(R,j)*sin(gammas(R,j)))+(rho_x_le1(R,j)*cos(angle));  %
x shadow length coordinate on (X,Y) plane
        yshad_le1(R,j)=(Lshad_le1(R,j)*cos(gammas(R,j)))+(rho_x_le1(R,j)*sin(angle));  %
y shadow length coordinate on (X,Y) plane

        % BLADE 2 (+120°)
        Lshad_le2(R,j)=rho_z_le2(R,j)/tan(alfa(R,j));
        xshad_le2(R,j)=(Lshad_le2(R,j)*sin(gammas(R,j)))+(rho_x_le2(R,j)*cos(angle));
        yshad_le2(R,j)=(Lshad_le2(R,j)*cos(gammas(R,j)))+(rho_x_le2(R,j)*sin(angle));

        % BLADE 3 (-120°)
        Lshad_le3(R,j)=rho_z_le3(R,j)/tan(alfa(R,j));
        xshad_le3(R,j)=(Lshad_le3(R,j)*sin(gammas(R,j)))+(rho_x_le3(R,j)*cos(angle));
        yshad_le3(R,j)=(Lshad_le3(R,j)*cos(gammas(R,j)))+(rho_x_le3(R,j)*sin(angle));


        %%%%% TRAILING EDGE POINT SHADOW COMPONENTS ON (X,Y) PLANE, WTG TOWER AXIS ORIGIN
        % BLADE 1 (0°)
        Lshad_te1(R,j)=rho_z_te1(R,j)/tan(alfa(R,j));   % shadow length
```

```
        xshad_te1(R,j)=(Lshad_te1(R,j)*sin(gammas(R,j)))+(rho_x_te1(R,j)*cos(angle));    %
x shadow length coordinate on (X,Y) plane
        yshad_te1(R,j)=(Lshad_te1(R,j)*cos(gammas(R,j)))+(rho_x_te1(R,j)*sin(angle));    %
y shadow length coordinate on (X,Y) plane

        % BLADE 2 (+120°)
        Lshad_te2(R,j)=rho_z_te2(R,j)/tan(alfa(R,j));
        xshad_te2(R,j)=(Lshad_te2(R,j)*sin(gammas(R,j)))+(rho_x_te2(R,j)*cos(angle));
        yshad_te2(R,j)=(Lshad_te2(R,j)*cos(gammas(R,j)))+(rho_x_te2(R,j)*sin(angle));

        % BLADE 3 (-120°)
        Lshad_te3(R,j)=rho_z_te3(R,j)/tan(alfa(R,j));
        xshad_te3(R,j)=(Lshad_te3(R,j)*sin(gammas(R,j)))+(rho_x_te3(R,j)*cos(angle));
        yshad_te3(R,j)=(Lshad_te3(R,j)*cos(gammas(R,j)))+(rho_x_te3(R,j)*sin(angle));

%% BLADE POINTS SHADOW TIME SERIES ON SINGLE PANEL
% BLADE 1
if rho_z_le1(R,j)>=120.9

            if (xshad_te1(R,j)<=x_modposition_w & x_modposition_w<=xshad_le1(R,j)) |
(xshad_te1(R,j)<=x_modposition_e & x_modposition_e<=xshad_le1(R,j))
                Timeseries_modshad_x1(R,j)=1;    % 1 = there is leading edge points shadow
on PV module
            else
                Timeseries_modshad_x1(R,j)=0;    % 0 = there is not leading edge points
shadow on PV module
            end
else
            if (xshad_le1(R,j)<=x_modposition_w & x_modposition_w<=xshad_te1(R,j)) |
(xshad_le1(R,j)<=x_modposition_e & x_modposition_e<=xshad_te1(R,j))
                Timeseries_modshad_x1(R,j)=1;    % 1 = there is leading edge points shadow
on PV module
            else
                Timeseries_modshad_x1(R,j)=0;    % 0 = there is not leading edge points
shadow on PV module
            end
end

if  rho_x_le1(R,j)<0

            if (yshad_te1(R,j)<=y_modposition_s & y_modposition_s<=yshad_le1(R,j)) |
(yshad_te1(R,j)<=y_modposition_n & y_modposition_n<=yshad_le1(R,j))
                Timeseries_modshad_y1(R,j)=1;    % 1 = there is leading edge points shadow
on PV module
            else
                Timeseries_modshad_y1(R,j)=0;    % 0 = there is not leading edge points
shadow on PV module
            end
else
            if (yshad_le1(R,j)<=y_modposition_s & y_modposition_s<=yshad_te1(R,j)) |
(yshad_le1(R,j)<=y_modposition_n & y_modposition_n<=yshad_te1(R,j))
                Timeseries_modshad_y1(R,j)=1;    % 1 = there is leading edge points shadow
on PV module
            else
                Timeseries_modshad_y1(R,j)=0;    % 0 = there is not leading edge points
shadow on PV module
            end
end


Timeseries_modshad_1(R,j)=Timeseries_modshad_x1(R,j)*Timeseries_modshad_y1(R,j);  %
overall leading edge points shadow presence on PV module matrix

% BLADE 2
if rho_z_le2(R,j)>=120.9

            if (xshad_te2(R,j)<=x_modposition_w & x_modposition_w<=xshad_le2(R,j)) |
(xshad_te2(R,j)<=x_modposition_e & x_modposition_e<=xshad_le2(R,j))
```

```
                Timeseries_modshad_x2(R,j)=1;    % 1 = there is leading edge points shadow
on PV module
            else
                Timeseries_modshad_x2(R,j)=0;    % 0 = there is not leading edge points
shadow on PV module
            end
else
            if (xshad_le2(R,j)<=x_modposition_w & x_modposition_w<=xshad_te2(R,j)) |
(xshad_le2(R,j)<=x_modposition_e & x_modposition_e<=xshad_te2(R,j))
                Timeseries_modshad_x2(R,j)=1;    % 1 = there is leading edge points shadow
on PV module
            else
                Timeseries_modshad_x2(R,j)=0;    % 0 = there is not leading edge points
shadow on PV module
            end
end

if  rho_x_le2(R,j)<=0

            if (yshad_te2(R,j)<=y_modposition_s & y_modposition_s<=yshad_le2(R,j)) |
(yshad_te2(R,j)<=y_modposition_n & y_modposition_n<=yshad_le2(R,j))
                Timeseries_modshad_y2(R,j)=1;    % 1 = there is leading edge points shadow
on PV module
            else
                Timeseries_modshad_y2(R,j)=0;    % 0 = there is not leading edge points
shadow on PV module
            end
else
            if (yshad_le2(R,j)<=y_modposition_s & y_modposition_s<=yshad_te2(R,j)) |
(yshad_le2(R,j)<=y_modposition_n & y_modposition_n<=yshad_te2(R,j))
                Timeseries_modshad_y2(R,j)=1;    % 1 = there is leading edge points shadow
on PV module
            else
                Timeseries_modshad_y2(R,j)=0;    % 0 = there is not leading edge points
shadow on PV module
            end
end


Timeseries_modshad_2(R,j)=Timeseries_modshad_x2(R,j)*Timeseries_modshad_y2(R,j);  %
overall leading edge points shadow presence on PV module matrix


% BLADE 3
if rho_z_le3(R,j)>=120.9

            if (xshad_te3(R,j)<=x_modposition_w & x_modposition_w<=xshad_le3(R,j)) |
(xshad_te3(R,j)<=x_modposition_e & x_modposition_e<=xshad_le3(R,j))
                Timeseries_modshad_x3(R,j)=1;    % 1 = there is leading edge points shadow
on PV module
            else
                Timeseries_modshad_x3(R,j)=0;    % 0 = there is not leading edge points
shadow on PV module
            end
else
            if (xshad_le3(R,j)<=x_modposition_w & x_modposition_w<=xshad_te3(R,j)) |
(xshad_le3(R,j)<=x_modposition_e & x_modposition_e<=xshad_te3(R,j))
                Timeseries_modshad_x3(R,j)=1;    % 1 = there is leading edge points shadow
on PV module
            else
                Timeseries_modshad_x3(R,j)=0;    % 0 = there is not leading edge points
shadow on PV module
            end
end

if  rho_x_le3(R,j)<=0

            if (yshad_te3(R,j)<=y_modposition_s & y_modposition_s<=yshad_le3(R,j)) |
(yshad_te3(R,j)<=y_modposition_n & y_modposition_n<=yshad_le3(R,j))
```

```
                Timeseries_modshad_y3(R,j)=1;    % 1 = there is leading edge points shadow
on PV module
            else
                Timeseries_modshad_y3(R,j)=0;    % 0 = there is not leading edge points
shadow on PV module
            end
else
            if (yshad_le3(R,j)<=y_modposition_s & y_modposition_s<=yshad_te3(R,j)) |
(yshad_le3(R,j)<=y_modposition_n & y_modposition_n<=yshad_te3(R,j))
                Timeseries_modshad_y3(R,j)=1;    % 1 = there is leading edge points shadow
on PV module
            else
                Timeseries_modshad_y3(R,j)=0;    % 0 = there is not leading edge points
shadow on PV module
            end
end


Timeseries_modshad_3(R,j)=Timeseries_modshad_x3(R,j)*Timeseries_modshad_y3(R,j);  %
overall leading edge points shadow presence on PV module matrix

end
end


% BLADE 1 POINTS SHADOW TIME SERIES ON SINGLE PV PANEL FIGURE
Timeseries_1=linspace(1,1,79)*Timeseries_modshad_1;  % leading edge points shadow on PV
module time series vector

for j= 1:6000
    if Timeseries_1(1,j)>=1
       Timeseries_1(1,j)=1;  % there is trailing edge points shadow
    elseif Timeseries_1(1,j)<1
       Timeseries_1(1,j)=0;  % there is not trailing edge points shadow
    end
end

figure(1)
plot(Timeseries_1,'r')
title('BLADE 1 (0°) SHADOW TIME SERIES ON PV MODULE')
xlabel('Time [hundredths of second]')
ylabel('0 = not shaded PV, 1 = shaded PV')
axis([0 6000 -0.05 1.05])


% BLADE 2 POINTS SHADOW TIME SERIES ON SINGLE PV PANEL FIGURE
Timeseries_2=linspace(1,1,79)*Timeseries_modshad_2;  % leading edge points shadow on PV
module time series vector

for j= 1:6000
    if Timeseries_2(1,j)>=1
       Timeseries_2(1,j)=1;  % there is trailing edge points shadow
    elseif Timeseries_2(1,j)<1
       Timeseries_2(1,j)=0;  % there is not trailing edge points shadow
    end
end

figure(2)
plot(Timeseries_2,'b')
title('BLADE 2 (+120°) SHADOW TIME SERIES ON PV MODULE')
xlabel('Time [hundredths of second]')
ylabel('0 = not shaded PV, 1 = shaded PV')
axis([0 6000 -0.05 1.05])


% BLADE 3 POINTS SHADOW TIME SERIES ON SINGLE PV PANEL FIGURE
Timeseries_3=linspace(1,1,79)*Timeseries_modshad_3;  % leading edge points shadow on PV
module time series vector
```

```
for j= 1:6000
    if Timeseries_3(1,j)>=1
       Timeseries_3(1,j)=1;  % there is trailing edge points shadow
    elseif Timeseries_3(1,j)<1
       Timeseries_3(1,j)=0;  % there is not trailing edge points shadow
    end
end

figure(3)
plot(Timeseries_3,'k')
title('BLADE 3 (-120°) SHADOW TIME SERIES ON PV MODULE')
xlabel('Time [hundredths of second]')
ylabel('0 = not shaded PV, 1 = shaded PV')
axis([0 6000 -0.05 1.05])


% SUM OF BLADE 1,2,3 SHADOWs TIME SERIES ON SINGLE PV MODULE
Timeseries=[Timeseries_modshad_1(:,:); Timeseries_modshad_2(:,:);
Timeseries_modshad_3(:,:)];  % overall blades shadow presence on PV module matrix
Timeseries_blades=linspace(1,1,237)*Timeseries;  % overall blades shadow on PV module
time series vector

for j= 1:6000
    if Timeseries_blades(1,j)>=1
        Timeseries_blades(1,j)=1;  % there is blades shadow
    elseif Timeseries_blades(1,j)<1
        Timeseries_blades(1,j)=0;  % there is not blades shadow
    end
end


figure(4)
hold on
plot(Timeseries_1,'r')
plot(Timeseries_2,'b')
plot(Timeseries_3,'k')
hold off
title('WTG BLADES SHADOW TIME SERIES ON PV MODULE')
xlabel('Time [hundredths of second]')
ylabel('0 = not shaded PV, 1 = shaded PV')
axis([0 6000 -0.05 1.05])
legend('Blade 1 (0°)','Blade 2 (+120°)','Blade 3 (-120°)')

figure(5)
plot(Timeseries_blades)
title('OVERALL WTG BLADES SHADOW TIME SERIES ON PV MODULE')
xlabel('Time [hundredths of second]')
ylabel('0 = not shaded PV, 1 = shaded PV')
axis([0 6000 -0.05 1.05])

figure(6)
subplot(5,1,1)
plot(Timeseries_1,'r')
title('BLADE 1 (0°) POINTS SHADOW')
xlabel('Time [hundredths of second]')
ylabel('0 = not shaded PV, 1 = shaded PV')
axis([0 6000 -0.05 1.05])
subplot(5,1,2)
plot(Timeseries_2,'b')
title('BLADE 2 (+120°) POINTS SHADOW')
xlabel('Time [hundredths of second]')
axis([0 6000 -0.05 1.05])
subplot(5,1,3)
plot(Timeseries_3,'k')
title('BLADE 3 (-120°) POINTS SHADOW')
xlabel('Time [hundredths of second]')
axis([0 6000 -0.05 1.05])
subplot(5,1,4)
hold on
```

```
plot(Timeseries_1,'r')
plot(Timeseries_2,'b')
plot(Timeseries_3,'k')
hold off
title('WTG BLADES SHADOW')
xlabel('Time [hundredths of second]')
axis([0 6000 -0.05 1.05])
legend('Blade 1 (0°)','Blade 2 (+120°)','Blade 3 (-120°)')
subplot(5,1,5)
plot(Timeseries_blades)
title('OVERALL WTG BLADES SHADOW')
xlabel('Time [hundredths of second]')
axis([0 6000 -0.05 1.05])
```

5) BLADES SHADOW ONE MINUTE TIME SERIES ON A SIMPLE PV ARRAY

(input TAPVA_distance = 300 m, TANSTA_distance = 0 m, hour = 11 and minutes = 45, day = 355)

```
% Small time series with only shadow evolution on a small PV array (nPV X nstring)

clear
close all
clc
% model to see when a PV module is shaded by blades, a time series in hundredths of
second
% considering its evolution during a small time period
% (X,Y) reference system plane with origin in WTG tower axis
% East: X positive ; West: X negative
% North: Y positive ; South: Y negative
% all angles inside sin() and cos() functions are in radians, [rad]

Hmod=2.384;     % PV module height [m]
Wmod=1.303;     % PV module width [m]
PV_mod_area=Hmod*Wmod;    % PV module area [m^2]
lat=40.837;     % latitude of WTG 04 tower position at Gravina in Puglia site [°]
long=16.272;    % longitude of WTG 04 tower position at Gravina in Puglia site [°]
rot=1.038;  % [rad/s], angular speed of a single blade/wind rotor

% PV module position on (X,Y) plane
TAPVA_distance1=input('Insert first PV module center of gravity position along N-S [m] =
');  % [m], tower-PV module axis/center of gravity distance
TANSTA_distance1=input('Insert first PV module center of gravity position along W-E [m] =
');    % [m], tower axis - NorthSouth tracker axis distance

hour=input('Insert hour [h] = ');    % hour of the day
minutes=input('Insert minutes [min] = ');     % minutes of that hour of the day

day=input('Insert n° day of the year = ');  % number of day in the year [-]
    B=(360/365*(day-1))*0.017453292; % [rad]   1° = 0.017453292 rad  ,  1 rad =
57.29577951°
    decl=(23.45*sin((360/365*(day+284))*0.017453292))*0.017453292;  % [rad]
    ET=229.2*(0.000075+(0.001868*cos(B))-(0.032077*sin(B))-(0.014615*cos(2*B))-
(0.04089*sin(2*B)));    % Equation of Time [min], correction factor for true solar time
TST calculation

for nstring=1:2    % number of strings connected in parallel
for nPV=1:2        % number of panel connected in series in the string

    if nstring==1
        number=nPV;
    elseif nstring==2
        number=2+nPV;
    end

% PV module distance from WTG axis on (X,Y) plane
```

```
dpvy=TAPVA_distance1-(Hmod/2)+(nPV*Hmod)-Hmod+(nPV*0.2)-0.2;  % distance between two
modules in the same string along y axis is 20 cm [m]
dpvx=TANSTA_distance1-(Wmod/2)+(nstring*6)-6;  % distance between two contiguous strings
along x axis is 6 m [m]

x_modposition_e=dpvx+Wmod;   % eastern x coordinate of PV module on (X,Y) plane
x_modposition_w=dpvx;   % western x coordinate of PV module on (X,Y) plane
y_modposition_n=dpvy+Hmod;    % northern y coordinate of PV module on (X,Y) plane
y_modposition_s=dpvy;    % southern y coordinate of PV module on (X,Y) plane

% SHADOW MODEL OF THREE BLADES IN A SINGLE DAY
% Hypothesis: rotor plane (X,Z) with normal direction always fixed towards North-North-
West direction (30°=0.523599)
% Highest wind direction frequency at Gravina in Puglia site
angle=30*0.017453292;
for R=1:79    % [m] radial position of a point along blades
    Rad(R)=R;
if R>=0 & R<23.7
   z(R)=3-cos(R/7.543944303);   % [m] blade width at radial position
  elseif R>=23.7 & R<71.1
         z(R)=5.349999993-(0.056962025*R);
  else
      z(R)=6.842105264-((R^2)/912.1461538);
end

for j= 1:6000  % analysis of shadow position will be done every hundredths of second in
one minute (from 11:45 a.m. to 11:46 a.m.)
LT(R,j)=((hour*60)+minutes)+(j/6000);    % legal time of a day [min]

        if day>=1 & day<=85     % change of solar hour at 27 March 2022
           summertime_difference=0; % [min], legal time one hour change
        elseif day>=86 & day<=302   % change of solar hour at 30 October 2022
            summertime_difference=-60; % [min]
        else
             summertime_difference=0; % [min]
        end

        diff_GMT=-60;  % [min], difference with Greenwich Mean Time of our Time Zone
        TST(R,j)=(LT(R,j)+diff_GMT+((long/15)*60)+ET+summertime_difference)*60;  % True
Solar Time [s]
        HRA(R,j)=(0.004166666*(TST(R,j)-43200))*0.017453292;   % hour angle [rad]

alfa(R,j)=asin((cos(decl)*cos(lat*0.017453292)*cos(HRA(R,j)))+(sin(decl)*sin(lat*0.017453
292)));  % solar height angle [rad]
        gammas(R,j)=asin((cos(decl)*sin(HRA(R,j)))/cos(alfa(R,j)));   % solar azimuth
angle [rad]


        %%%%% LEADING EDGE (polar coordinates of leading edge points on (X,Z) rotor
plane)
        teta_le1(R,j)=(-rot)*LT(R,j)*60;  % [rad], polar coordinates angle related to
blade towards 0° direction
                                          % minus sign because rotation direction of GE
CYPRESS WTG rotor is clockwise
        teta_le2(R,j)=((-rot)*LT(R,j)*60)+((2/3)*pi);  % [rad], polar coordinates angle
related to blade towards +120° direction
        teta_le3(R,j)=((-rot)*LT(R,j)*60)-((2/3)*pi);  % [rad], polar coordinates angle
related to blade towards -120° direction

        rho_le1(R,j)=R;    % [m], polar coordinates module related to blade towards 0°
direction
        rho_le2(R,j)=R;    % [m], polar coordinates module related to blade towards +120°
direction
        rho_le3(R,j)=R;    % [m], polar coordinates module related to blade towards -120°
direction

        rho_x_le1(R,j)=rho_le1(R,j)*cos(teta_le1(R,j));  % [m], x axis component (WEST-
EAST) of polar coordinates module
        rho_x_le2(R,j)=rho_le2(R,j)*cos(teta_le2(R,j));
```

```
        rho_x_le3(R,j)=rho_le3(R,j)*cos(teta_le3(R,j));

        rho_z_le1(R,j)=(rho_le1(R,j)*sin(teta_le1(R,j)))+120.9;  % [m], z axis component
(ALTITUDE) of polar coordinates module
        rho_z_le2(R,j)=(rho_le2(R,j)*sin(teta_le2(R,j)))+120.9;
        rho_z_le3(R,j)=(rho_le3(R,j)*sin(teta_le3(R,j)))+120.9;



        %%%%% TRAILING EDGE (polar coordinates of trailing edge points on (X,Z) rotor
plane)
        teta_te1(R,j)=teta_le1(R,j)+atan(z(R)/R);   % [rad], polar coordinates angle
related to blade towards 0° direction
        teta_te2(R,j)=teta_le2(R,j)+atan(z(R)/R);   % [rad], polar coordinates angle
related to blade towards +120° direction
        teta_te3(R,j)=teta_le3(R,j)+atan(z(R)/R);   % [rad], polar coordinates angle
related to blade towards -120° direction

        rho_te1(R,j)=sqrt((R^2)+(z(R)^2));   % [m], polar coordinates module related to
blade towards 0° direction
        rho_te2(R,j)=sqrt((R^2)+(z(R)^2));   % [m], polar coordinates module related to
blade towards +120° direction
        rho_te3(R,j)=sqrt((R^2)+(z(R)^2));   % [m], polar coordinates module related to
blade towards -120° direction

        rho_x_te1(R,j)=rho_te1(R,j)*cos(teta_te1(R,j));  % [m], x axis component (WEST-
EAST) of polar coordinates module on rotor (X,Z) plane
        rho_x_te2(R,j)=rho_te2(R,j)*cos(teta_te2(R,j));
        rho_x_te3(R,j)=rho_te3(R,j)*cos(teta_te3(R,j));

        rho_z_te1(R,j)=(rho_te1(R,j)*sin(teta_te1(R,j)))+120.9;  % [m], z axis component
(ALTITUDE) of polar coordinates module on rotor (X,Z) plane
        rho_z_te2(R,j)=(rho_te2(R,j)*sin(teta_te2(R,j)))+120.9;
        rho_z_te3(R,j)=(rho_te3(R,j)*sin(teta_te3(R,j)))+120.9;


        %%%%% LEADING EDGE POINT SHADOW COMPONENTS ON (X,Y) PLANE, WTG TOWER AXIS ORIGIN
        % BLADE 1 (0°)
        Lshad_le1(R,j)=rho_z_le1(R,j)/tan(alfa(R,j));   % shadow length
        xshad_le1(R,j)=(Lshad_le1(R,j)*sin(gammas(R,j)))+(rho_x_le1(R,j)*cos(angle));  %
x shadow length coordinate on (X,Y) plane
        yshad_le1(R,j)=(Lshad_le1(R,j)*cos(gammas(R,j)))+(rho_x_le1(R,j)*sin(angle));  %
y shadow length coordinate on (X,Y) plane

        % BLADE 2 (+120°)
        Lshad_le2(R,j)=rho_z_le2(R,j)/tan(alfa(R,j));
        xshad_le2(R,j)=(Lshad_le2(R,j)*sin(gammas(R,j)))+(rho_x_le2(R,j)*cos(angle));
        yshad_le2(R,j)=(Lshad_le2(R,j)*cos(gammas(R,j)))+(rho_x_le2(R,j)*sin(angle));

        % BLADE 3 (-120°)
        Lshad_le3(R,j)=rho_z_le3(R,j)/tan(alfa(R,j));
        xshad_le3(R,j)=(Lshad_le3(R,j)*sin(gammas(R,j)))+(rho_x_le3(R,j)*cos(angle));
        yshad_le3(R,j)=(Lshad_le3(R,j)*cos(gammas(R,j)))+(rho_x_le3(R,j)*sin(angle));


        %%%%% TRAILING EDGE POINT SHADOW COMPONENTS ON (X,Y) PLANE, WTG TOWER AXIS ORIGIN
        % BLADE 1 (0°)
        Lshad_te1(R,j)=rho_z_te1(R,j)/tan(alfa(R,j));   % shadow length
        xshad_te1(R,j)=(Lshad_te1(R,j)*sin(gammas(R,j)))+(rho_x_te1(R,j)*cos(angle));   %
x shadow length coordinate on (X,Y) plane
        yshad_te1(R,j)=(Lshad_te1(R,j)*cos(gammas(R,j)))+(rho_x_te1(R,j)*sin(angle));   %
y shadow length coordinate on (X,Y) plane

        % BLADE 2 (+120°)
        Lshad_te2(R,j)=rho_z_te2(R,j)/tan(alfa(R,j));
        xshad_te2(R,j)=(Lshad_te2(R,j)*sin(gammas(R,j)))+(rho_x_te2(R,j)*cos(angle));
        yshad_te2(R,j)=(Lshad_te2(R,j)*cos(gammas(R,j)))+(rho_x_te2(R,j)*sin(angle));

        % BLADE 3 (-120°)
```

```
        Lshad_te3(R,j)=rho_z_te3(R,j)/tan(alfa(R,j));
        xshad_te3(R,j)=(Lshad_te3(R,j)*sin(gammas(R,j)))+(rho_x_te3(R,j)*cos(angle));
        yshad_te3(R,j)=(Lshad_te3(R,j)*cos(gammas(R,j)))+(rho_x_te3(R,j)*sin(angle));


%% BLADE POINTS SHADOW TIME SERIES ON SINGLE PANEL
% BLADE 1
if rho_z_le1(R,j)>=120.9

             if (xshad_te1(R,j)<=x_modposition_w & x_modposition_w<=xshad_le1(R,j)) |
(xshad_te1(R,j)<=x_modposition_e & x_modposition_e<=xshad_le1(R,j))
                Timeseries_modshad_x1(R,j)=1;    % 1 = there is leading edge points shadow
on PV module
             else
                 Timeseries_modshad_x1(R,j)=0;    % 0 = there is not leading edge points
shadow on PV module
             end
else
             if (xshad_le1(R,j)<=x_modposition_w & x_modposition_w<=xshad_te1(R,j)) |
(xshad_le1(R,j)<=x_modposition_e & x_modposition_e<=xshad_te1(R,j))
                Timeseries_modshad_x1(R,j)=1;    % 1 = there is leading edge points shadow
on PV module
             else
                 Timeseries_modshad_x1(R,j)=0;    % 0 = there is not leading edge points
shadow on PV module
             end
end

if  rho_x_le1(R,j)<=0

             if (yshad_te1(R,j)<=y_modposition_s & y_modposition_s<=yshad_le1(R,j)) |
(yshad_te1(R,j)<=y_modposition_n & y_modposition_n<=yshad_le1(R,j))
                Timeseries_modshad_y1(R,j)=1;    % 1 = there is leading edge points shadow
on PV module
             else
                Timeseries_modshad_y1(R,j)=0;    % 0 = there is not leading edge points
shadow on PV module
             end
else
             if (yshad_le1(R,j)<=y_modposition_s & y_modposition_s<=yshad_te1(R,j)) |
(yshad_le1(R,j)<=y_modposition_n & y_modposition_n<=yshad_te1(R,j))
                Timeseries_modshad_y1(R,j)=1;    % 1 = there is leading edge points shadow
on PV module
             else
                Timeseries_modshad_y1(R,j)=0;    % 0 = there is not leading edge points
shadow on PV module
             end
end


Timeseries_modshad_1(R,j)=Timeseries_modshad_x1(R,j)*Timeseries_modshad_y1(R,j);  %
overall leading edge points shadow presence on PV module matrix

% BLADE 2
if rho_z_le2(R,j)>=120.9

             if (xshad_te2(R,j)<=x_modposition_w & x_modposition_w<=xshad_le2(R,j)) |
(xshad_te2(R,j)<=x_modposition_e & x_modposition_e<=xshad_le2(R,j))
                Timeseries_modshad_x2(R,j)=1;    % 1 = there is leading edge points shadow
on PV module
             else
                 Timeseries_modshad_x2(R,j)=0;    % 0 = there is not leading edge points
shadow on PV module
             end
else
             if (xshad_le2(R,j)<=x_modposition_w & x_modposition_w<=xshad_te2(R,j)) |
(xshad_le2(R,j)<=x_modposition_e & x_modposition_e<=xshad_te2(R,j))
                Timeseries_modshad_x2(R,j)=1;    % 1 = there is leading edge points shadow
on PV module
```

```
            else
                Timeseries_modshad_x2(R,j)=0;    % 0 = there is not leading edge points
shadow on PV module
            end
end

if  rho_x_le2(R,j)<=0

            if (yshad_te2(R,j)<=y_modposition_s & y_modposition_s<=yshad_le2(R,j)) |
(yshad_te2(R,j)<=y_modposition_n & y_modposition_n<=yshad_le2(R,j))
               Timeseries_modshad_y2(R,j)=1;    % 1 = there is leading edge points shadow
on PV module
            else
               Timeseries_modshad_y2(R,j)=0;    % 0 = there is not leading edge points
shadow on PV module
            end
else
            if (yshad_le2(R,j)<=y_modposition_s & y_modposition_s<=yshad_te2(R,j)) |
(yshad_le2(R,j)<=y_modposition_n & y_modposition_n<=yshad_te2(R,j))
               Timeseries_modshad_y2(R,j)=1;    % 1 = there is leading edge points shadow
on PV module
            else
               Timeseries_modshad_y2(R,j)=0;    % 0 = there is not leading edge points
shadow on PV module
            end
end


Timeseries_modshad_2(R,j)=Timeseries_modshad_x2(R,j)*Timeseries_modshad_y2(R,j);  %
overall leading edge points shadow presence on PV module matrix


% BLADE 3
if rho_z_le3(R,j)>=120.9

            if (xshad_te3(R,j)<=x_modposition_w & x_modposition_w<=xshad_le3(R,j)) |
(xshad_te3(R,j)<=x_modposition_e & x_modposition_e<=xshad_le3(R,j))
               Timeseries_modshad_x3(R,j)=1;    % 1 = there is leading edge points shadow
on PV module
            else
                Timeseries_modshad_x3(R,j)=0;    % 0 = there is not leading edge points
shadow on PV module
            end
else
            if (xshad_le3(R,j)<=x_modposition_w & x_modposition_w<=xshad_te3(R,j)) |
(xshad_le3(R,j)<=x_modposition_e & x_modposition_e<=xshad_te3(R,j))
               Timeseries_modshad_x3(R,j)=1;    % 1 = there is leading edge points shadow
on PV module
            else
                Timeseries_modshad_x3(R,j)=0;    % 0 = there is not leading edge points
shadow on PV module
            end
end

if  rho_x_le3(R,j)<=0

            if (yshad_te3(R,j)<=y_modposition_s & y_modposition_s<=yshad_le3(R,j)) |
(yshad_te3(R,j)<=y_modposition_n & y_modposition_n<=yshad_le3(R,j))
               Timeseries_modshad_y3(R,j)=1;    % 1 = there is leading edge points shadow
on PV module
            else
               Timeseries_modshad_y3(R,j)=0;    % 0 = there is not leading edge points
shadow on PV module
            end
else
            if (yshad_le3(R,j)<=y_modposition_s & y_modposition_s<=yshad_te3(R,j)) |
(yshad_le3(R,j)<=y_modposition_n & y_modposition_n<=yshad_te3(R,j))
               Timeseries_modshad_y3(R,j)=1;    % 1 = there is leading edge points shadow
on PV module
```

```
            else
               Timeseries_modshad_y3(R,j)=0;    % 0 = there is not leading edge points
shadow on PV module
            end
end


Timeseries_modshad_3(R,j)=Timeseries_modshad_x3(R,j)*Timeseries_modshad_y3(R,j);  %
overall leading edge points shadow presence on PV module matrix

end
end


% BLADE 1 POINTS SHADOW TIME SERIES ON SINGLE PV PANEL FIGURE
Timeseries_1=linspace(1,1,79)*Timeseries_modshad_1;  % leading edge points shadow on PV
module time series vector
Timeseries_blade1(number,:)=Timeseries_1;

for j= 1:6000
    if Timeseries_blade1(number,j)>=1
       Timeseries_blade1(number,j)=1;  % there is trailing edge points shadow
    elseif Timeseries_blade1(number,j)<1
       Timeseries_blade1(number,j)=0;  % there is not trailing edge points shadow
    end
end

% BLADE 2 POINTS SHADOW TIME SERIES ON SINGLE PV PANEL FIGURE
Timeseries_2=linspace(1,1,79)*Timeseries_modshad_2;  % leading edge points shadow on PV
module time series vector
Timeseries_blade2(number,:)=Timeseries_2;

for j= 1:6000
    if Timeseries_blade2(number,j)>=1
       Timeseries_blade2(number,j)=1;  % there is trailing edge points shadow
    elseif Timeseries_blade2(number,j)<1
       Timeseries_blade2(number,j)=0;  % there is not trailing edge points shadow
    end
end

% BLADE 3 POINTS SHADOW TIME SERIES ON SINGLE PV PANEL FIGURE
Timeseries_3=linspace(1,1,79)*Timeseries_modshad_3;  % leading edge points shadow on PV
module time series vector
Timeseries_blade3(number,:)=Timeseries_3;

for j= 1:6000
    if Timeseries_blade3(number,j)>=1
       Timeseries_blade3(number,j)=1;  % there is trailing edge points shadow
    elseif Timeseries_blade3(number,j)<1
       Timeseries_blade3(number,j)=0;  % there is not trailing edge points shadow
    end
end

% SUM OF BLADE 1,2,3 SHADOWS TIME SERIES ON SINGLE PV MODULE
Timeseries=[Timeseries_modshad_1(:,:); Timeseries_modshad_2(:,:);
Timeseries_modshad_3(:,:)];  % overall blades shadow presence on PV module matrix
Timeseries_blades(number,:)=linspace(1,1,237)*Timeseries;  % overall blades shadow on PV
module time series vector

for j= 1:6000
    if Timeseries_blades(number,j)>=1
        Timeseries_blades(number,j)=1;  % there is blades shadow
    elseif Timeseries_blades(number,j)<1
        Timeseries_blades(number,j)=0;  % there is not blades shadow
    end
end

end
end
```

```
figure(1)
hold on
plot(Timeseries_blade1(1,:),'r')
plot(Timeseries_blade1(2,:),'b')
plot(Timeseries_blade1(3,:),'k')
plot(Timeseries_blade1(4,:),'g')
hold off
title('BLADE 1 (0°) SHADOW TIME SERIES ON PV ARRAY')
xlabel('Time [hundredths of second]')
ylabel('0 = not shaded PV, 1 = shaded PV')
legend('Module1-string1','Module2-string1','Module1-string2','Module2-string2')
axis([0 6000 -0.05 1.05])

figure(2)
hold on
plot(Timeseries_blade2(1,:),'r')
plot(Timeseries_blade2(2,:),'b')
plot(Timeseries_blade2(3,:),'k')
plot(Timeseries_blade2(4,:),'g')
hold off
title('BLADE 2 (+120°) SHADOW TIME SERIES ON PV ARRAY')
xlabel('Time [hundredths of second]')
ylabel('0 = not shaded PV, 1 = shaded PV')
legend('Module1-string1','Module2-string1','Module1-string2','Module2-string2')
axis([0 6000 -0.05 1.05])

figure(3)
hold on
plot(Timeseries_blade3(1,:),'r')
plot(Timeseries_blade3(2,:),'b')
plot(Timeseries_blade3(3,:),'k')
plot(Timeseries_blade3(4,:),'g')
hold off
title('BLADE 3 (-120°) SHADOW TIME SERIES ON PV ARRAY')
xlabel('Time [hundredths of second]')
ylabel('0 = not shaded PV, 1 = shaded PV')
legend('Module1-string1','Module2-string1','Module1-string2','Module2-string2')
axis([0 6000 -0.05 1.05])

figure(4)
subplot(4,1,1)
hold on
plot(Timeseries_blade1(1,:),'r')
plot(Timeseries_blade1(2,:),'b')
plot(Timeseries_blade1(3,:),'k')
plot(Timeseries_blade1(4,:),'g')
hold off
title('BLADE 1 (0°) SHADOW TIME SERIES ON PV ARRAY')
xlabel('Time [hundredths of second]')
ylabel('0 = not shaded PV, 1 = shaded PV')
legend('Module1-string1','Module2-string1','Module1-string2','Module2-string2')
axis([0 6000 -0.05 1.05])
subplot(4,1,2)
hold on
plot(Timeseries_blade2(1,:),'r')
plot(Timeseries_blade2(2,:),'b')
plot(Timeseries_blade2(3,:),'k')
plot(Timeseries_blade2(4,:),'g')
hold off
title('BLADE 2 (+120°) SHADOW TIME SERIES ON PV ARRAY')
xlabel('Time [hundredths of second]')
legend('Module1-string1','Module2-string1','Module1-string2','Module2-string2')
axis([0 6000 -0.05 1.05])
subplot(4,1,3)
hold on
plot(Timeseries_blade3(1,:),'r')
plot(Timeseries_blade3(2,:),'b')
plot(Timeseries_blade3(3,:),'k')
```

```
plot(Timeseries_blade3(4,:),'g')
hold off
title('BLADE 3 (-120°) SHADOW TIME SERIES ON PV ARRAY')
xlabel('Time [hundredths of second]')
legend('Module1-string1','Module2-string1','Module1-string2','Module2-string2')
axis([0 6000 -0.05 1.05])
subplot(4,1,4)
hold on
plot(Timeseries_blade1(1,:),'r')
plot(Timeseries_blade1(2,:),'r')
plot(Timeseries_blade1(3,:),'r')
plot(Timeseries_blade1(4,:),'r')
plot(Timeseries_blade2(1,:),'b')
plot(Timeseries_blade2(2,:),'b')
plot(Timeseries_blade2(3,:),'b')
plot(Timeseries_blade2(4,:),'b')
plot(Timeseries_blade3(1,:),'k')
plot(Timeseries_blade3(2,:),'k')
plot(Timeseries_blade3(3,:),'k')
plot(Timeseries_blade3(4,:),'k')
hold off
title('BLADES SHADOW TIME SERIES ON PV ARRAY')
xlabel('Time [hundredths of second]')
legend('Blade1 (0°)','','','','Blade2 (+120°)','','','','Blade3 (-120°)')
axis([0 6000 -0.05 1.05])

figure(5)
plot(Timeseries_blades(1,:),'r')
title('BLADES SHADOW TIME SERIES MODULE1-STRING1')
xlabel('Time [hundredths of second]')
ylabel('0 = not shaded PV, 1 = shaded PV')
legend('Module1-string1')
axis([0 6000 -0.05 1.05])

figure(6)
plot(Timeseries_blades(2,:),'b')
title('BLADES SHADOW TIME SERIES MODULE2-STRING1')
xlabel('Time [hundredths of second]')
ylabel('0 = not shaded PV, 1 = shaded PV')
legend('Module2-string1')
axis([0 6000 -0.05 1.05])

figure(7)
plot(Timeseries_blades(3,:),'k')
title('BLADES SHADOW TIME SERIES MODULE1-STRING2')
xlabel('Time [hundredths of second]')
ylabel('0 = not shaded PV, 1 = shaded PV')
legend('Module1-string2')
axis([0 6000 -0.05 1.05])

figure(8)
plot(Timeseries_blades(4,:),'g')
title('BLADES SHADOW TIME SERIES MODULE2-STRING2')
xlabel('Time [hundredths of second]')
ylabel('0 = not shaded PV, 1 = shaded PV')
legend('Module2-string2')
axis([0 6000 -0.05 1.05])

figure(9)
hold on
plot(Timeseries_blades(1,:),'r')
plot(Timeseries_blades(2,:),'b')
plot(Timeseries_blades(3,:),'k')
plot(Timeseries_blades(4,:),'g')
hold off
title('BLADES SHADOW TIME SERIES ON EACH ARRAY PV MODULE')
xlabel('Time [hundredths of second]')
ylabel('0 = not shaded PV, 1 = shaded PV')
legend('Module1-string1','Module2-string1','Module1-string2','Module2-string2')
```

```
axis([0 6000 -0.05 1.05])

figure(10)
subplot(5,1,1)
plot(Timeseries_blades(1,:),'r')
title('BLADES SHADOW TIME SERIES MODULE1-STRING1')
xlabel('Time [hundredths of second]')
ylabel('0 = not shaded PV, 1 = shaded PV')
legend('Module1-string1')
axis([0 6000 -0.05 1.05])
subplot(5,1,2)
plot(Timeseries_blades(2,:),'b')
title('BLADES SHADOW TIME SERIES MODULE2-STRING1')
xlabel('Time [hundredths of second]')
legend('Module2-string1')
axis([0 6000 -0.05 1.05])
subplot(5,1,3)
plot(Timeseries_blades(3,:),'k')
title('BLADES SHADOW TIME SERIES MODULE1-STRING2')
xlabel('Time [hundredths of second]')
legend('Module1-string2')
axis([0 6000 -0.05 1.05])
subplot(5,1,4)
plot(Timeseries_blades(4,:),'g')
title('BLADES SHADOW TIME SERIES MODULE2-STRING2')
xlabel('Time [hundredths of second]')
legend('Module2-string2')
axis([0 6000 -0.05 1.05])
subplot(5,1,5)
hold on
plot(Timeseries_blades(1,:),'r')
plot(Timeseries_blades(2,:),'b')
plot(Timeseries_blades(3,:),'k')
plot(Timeseries_blades(4,:),'g')
hold off
title('BLADES SHADOW TIME SERIES ON EACH ARRAY PV MODULE')
xlabel('Time [hundredths of second]')
legend('Module1-string1','Module2-string1','Module1-string2','Module2-string2')
axis([0 6000 -0.05 1.05])
```

APPENDIX F

- **WTG BLADE SHADOWS CODE IN SIMULINK MATLAB FUNCTION BLOCKS**

```
function Mod1_str1 =fun1(u)

% model to see when a PV module is shaded by blades, a time series in hundredths of
second
% considering its evolution during a small time period
% (X,Y) reference system plane with origin in WTG tower axis
% East: X positive ; West: X negative
% North: Y positive ; South: Y negative
% all angles inside sin() and cos() functions are in radians, [rad]

Hmod=2.384;     % PV module height [m]
Wmod=1.303;     % PV module width [m]
lat=40.837;     % latitude of WTG 04 tower position at Gravina in Puglia site [°]
long=16.272;    % longitude of WTG 04 tower position at Gravina in Puglia site [°]
rot=1.038;  % [rad/s], angular speed of a single blade/wind rotor

B=(360/365*(u(5)-1))*0.017453292; % [rad]   1° = 0.017453292 rad  ,  1 rad = 57.29577951°
decl=(23.45*sin((360/365*(u(5)+284))*0.017453292))*0.017453292;  % [rad]
ET=229.2*(0.000075+(0.001868*cos(B))-(0.032077*sin(B))-(0.014615*cos(2*B))-
(0.04089*sin(2*B)));   % Equation of Time [min], correction factor for true solar time
TST calculation


% PV module distance from WTG axis on (X,Y) plane
dpvy=u(1)-(Hmod/2);  % distance between two modules in the same string along y axis is 20
cm [m]
dpvx=u(2)-(Wmod/2);  % distance between two contiguous strings along x axis is 6 m [m]

x_modposition_e=dpvx+Wmod;   % eastern x coordinate of PV module on (X,Y) plane
x_modposition_w=dpvx;   % western x coordinate of PV module on (X,Y) plane
y_modposition_n=dpvy+Hmod;    % northern y coordinate of PV module on (X,Y) plane
y_modposition_s=dpvy;    % southern y coordinate of PV module on (X,Y) plane


j= u(6);  % analysis of shadow position will be done every hundredths of second in one
minute (from 11:45 a.m. to 11:46 a.m.)
LT=((u(3)*60)+u(4))+(j/6000);    % legal time of a day [min]

        if u(5)>=1 & u(5)<=85     % change of solar hour at 27 March 2022
           summertime_difference=0; % [min], legal time one hour change
        elseif u(5)>=86 & u(5)<=302   % change of solar hour at 30 October 2022
            summertime_difference=-60; % [min]
        else
             summertime_difference=0; % [min]
        end

        diff_GMT=-60;  % [min], difference with Greenwich Mean Time of our Time Zone
        TST=(LT+diff_GMT+((long/15)*60)+ET+summertime_difference)*60;  % True Solar Time
[s]
        HRA=(0.004166666*(TST-43200))*0.017453292;   % hour angle [rad]

alfa=asin((cos(decl)*cos(lat*0.017453292)*cos(HRA))+(sin(decl)*sin(lat*0.017453292)));  %
solar height angle [rad]
        gammas=asin((cos(decl)*sin(HRA))/cos(alfa));   % solar azimuth angle [rad]

Timeseries_modsh_1=linspace(0,0,79)';
Timeseries_modsh_2=linspace(0,0,79)';
Timeseries_modsh_3=linspace(0,0,79)';

a=1;
```

```
% SHADOW MODEL OF THREE BLADES IN A SINGLE DAY
% Hypothesis: rotor plane (X,Z) with normal direction always fixed towards North-North-
West direction (30°=0.523599)
% Highest wind direction frequency at Gravina in Puglia site
angle=30*0.017453292;
for R=1:79    % [m] radial position of a point along blades

if R>=0 & R<23.7
   z=3-cos(R/7.543944303);   % [m] blade width at radial position
  elseif R>=23.7 & R<71.1
         z=5.349999993-(0.056962025*R);
  else
      z=6.842105264-((R^2)/912.1461538);
end

        %%%%% LEADING EDGE (polar coordinates of leading edge points on (X,Z) rotor
plane)
        teta_le1=(-rot)*LT*60;  % [rad], polar coordinates angle related to blade towards
0° direction
                                        % minus sign because rotation direction of GE
CYPRESS WTG rotor is clockwise
        teta_le2=((-rot)*LT*60)+((2/3)*pi);  % [rad], polar coordinates angle related to
blade towards +120° direction
        teta_le3=((-rot)*LT*60)-((2/3)*pi);  % [rad], polar coordinates angle related to
blade towards -120° direction

        rho_le1=R;    % [m], polar coordinates module related to blade towards 0°
direction
        rho_le2=R;    % [m], polar coordinates module related to blade towards +120°
direction
        rho_le3=R;    % [m], polar coordinates module related to blade towards -120°
direction

        rho_x_le1=rho_le1*cos(teta_le1);  % [m], x axis component (WEST-EAST) of polar
coordinates module
        rho_x_le2=rho_le2*cos(teta_le2);
        rho_x_le3=rho_le3*cos(teta_le3);

        rho_z_le1=(rho_le1*sin(teta_le1))+120.9;  % [m], z axis component (ALTITUDE) of
polar coordinates module
        rho_z_le2=(rho_le2*sin(teta_le2))+120.9;
        rho_z_le3=(rho_le3*sin(teta_le3))+120.9;


        %%%%% TRAILING EDGE (polar coordinates of trailing edge points on (X,Z) rotor
plane)
        teta_te1=teta_le1+atan(z/R);   % [rad], polar coordinates angle related to blade
towards 0° direction
        teta_te2=teta_le2+atan(z/R);   % [rad], polar coordinates angle related to blade
towards +120° direction
        teta_te3=teta_le3+atan(z/R);   % [rad], polar coordinates angle related to blade
towards -120° direction

        rho_te1=sqrt((R^2)+(z^2));   % [m], polar coordinates module related to blade
towards 0° direction
        rho_te2=sqrt((R^2)+(z^2));   % [m], polar coordinates module related to blade
towards +120° direction
        rho_te3=sqrt((R^2)+(z^2));   % [m], polar coordinates module related to blade
towards -120° direction

        rho_x_te1=rho_te1*cos(teta_te1);  % [m], x axis component (WEST-EAST) of polar
coordinates module on rotor (X,Z) plane
        rho_x_te2=rho_te2*cos(teta_te2);
        rho_x_te3=rho_te3*cos(teta_te3);

        rho_z_te1=(rho_te1*sin(teta_te1))+120.9;  % [m], z axis component (ALTITUDE) of
polar coordinates module on rotor (X,Z) plane
        rho_z_te2=(rho_te2*sin(teta_te2))+120.9;
        rho_z_te3=(rho_te3*sin(teta_te3))+120.9;
```

```
        %%%%% LEADING EDGE POINT SHADOW COMPONENTS ON (X,Y) PLANE, WTG TOWER AXIS ORIGIN
        % BLADE 1 (0°)
        Lshad_le1=rho_z_le1/tan(alfa);    % shadow length
        xshad_le1=(Lshad_le1*sin(gammas))+(rho_x_le1*cos(angle));  % x shadow length
coordinate on (X,Y) plane
        yshad_le1=(Lshad_le1*cos(gammas))+(rho_x_le1*sin(angle));  % y shadow length
coordinate on (X,Y) plane

        % BLADE 2 (+120°)
        Lshad_le2=rho_z_le2/tan(alfa);
        xshad_le2=(Lshad_le2*sin(gammas))+(rho_x_le2*cos(angle));
        yshad_le2=(Lshad_le2*cos(gammas))+(rho_x_le2*sin(angle));

        % BLADE 3 (-120°)
        Lshad_le3=rho_z_le3/tan(alfa);
        xshad_le3=(Lshad_le3*sin(gammas))+(rho_x_le3*cos(angle));
        yshad_le3=(Lshad_le3*cos(gammas))+(rho_x_le3*sin(angle));


        %%%%% TRAILING EDGE POINT SHADOW COMPONENTS ON (X,Y) PLANE, WTG TOWER AXIS ORIGIN
        % BLADE 1 (0°)
        Lshad_te1=rho_z_te1/tan(alfa);    % shadow length
        xshad_te1=(Lshad_te1*sin(gammas))+(rho_x_te1*cos(angle));    % x shadow length
coordinate on (X,Y) plane
        yshad_te1=(Lshad_te1*cos(gammas))+(rho_x_te1*sin(angle));    % y shadow length
coordinate on (X,Y) plane

        % BLADE 2 (+120°)
        Lshad_te2=rho_z_te2/tan(alfa);
        xshad_te2=(Lshad_te2*sin(gammas))+(rho_x_te2*cos(angle));
        yshad_te2=(Lshad_te2*cos(gammas))+(rho_x_te2*sin(angle));

        % BLADE 3 (-120°)
        Lshad_te3=rho_z_te3/tan(alfa);
        xshad_te3=(Lshad_te3*sin(gammas))+(rho_x_te3*cos(angle));
        yshad_te3=(Lshad_te3*cos(gammas))+(rho_x_te3*sin(angle));


%% BLADE POINTS SHADOW TIME SERIES ON SINGLE PANEL
% BLADE 1
if rho_z_le1>=120.9

            if (xshad_te1<=x_modposition_w & x_modposition_w<=xshad_le1) |
(xshad_te1<=x_modposition_e & x_modposition_e<=xshad_le1)
                Timeseries_modshad_x1=1;    % 1 = there is leading edge points shadow on
PV module
            else
                Timeseries_modshad_x1=0;    % 0 = there is not leading edge points shadow
on PV module
            end
else
            if (xshad_le1<=x_modposition_w & x_modposition_w<=xshad_te1) |
(xshad_le1<=x_modposition_e & x_modposition_e<=xshad_te1)
                Timeseries_modshad_x1=1;    % 1 = there is leading edge points shadow on
PV module
            else
                Timeseries_modshad_x1=0;    % 0 = there is not leading edge points shadow
on PV module
            end
end


if  rho_x_le1<=0

            if (yshad_te1<=y_modposition_s & y_modposition_s<=yshad_le1) |
(yshad_te1<=y_modposition_n & y_modposition_n<=yshad_le1)
```

```
                Timeseries_modshad_y1=1;    % 1 = there is leading edge points shadow on
PV module
            else
                Timeseries_modshad_y1=0;    % 0 = there is not leading edge points shadow
on PV module
            end
else
            if (yshad_le1<=y_modposition_s & y_modposition_s<=yshad_te1) |
(yshad_le1<=y_modposition_n & y_modposition_n<=yshad_te1)
                Timeseries_modshad_y1=1;    % 1 = there is leading edge points shadow on
PV module
            else
                Timeseries_modshad_y1=0;    % 0 = there is not leading edge points shadow
on PV module
            end
end

            Timeseries_modshad_1=Timeseries_modshad_x1*Timeseries_modshad_y1;  % overall
leading edge points shadow presence on PV module matrix
            Timeseries_modsh_1(a,1)=Timeseries_modshad_1;


% BLADE 2
if rho_z_le2>=120.9

            if (xshad_te2<=x_modposition_w & x_modposition_w<=xshad_le2) |
(xshad_te2<=x_modposition_e & x_modposition_e<=xshad_le2)
                Timeseries_modshad_x2=1;    % 1 = there is leading edge points shadow on
PV module
            else
                 Timeseries_modshad_x2=0;    % 0 = there is not leading edge points shadow
on PV module
            end
else
            if (xshad_le2<=x_modposition_w & x_modposition_w<=xshad_te2) |
(xshad_le2<=x_modposition_e & x_modposition_e<=xshad_te2)
                Timeseries_modshad_x2=1;    % 1 = there is leading edge points shadow on
PV module
            else
                 Timeseries_modshad_x2=0;    % 0 = there is not leading edge points shadow
on PV module
            end
end


if  rho_x_le2<=0

            if (yshad_te2<=y_modposition_s & y_modposition_s<=yshad_le2) |
(yshad_te2<=y_modposition_n & y_modposition_n<=yshad_le2)
                Timeseries_modshad_y2=1;    % 1 = there is leading edge points shadow on
PV module
            else
                Timeseries_modshad_y2=0;    % 0 = there is not leading edge points shadow
on PV module
            end
else
            if (yshad_le2<=y_modposition_s & y_modposition_s<=yshad_te2) |
(yshad_le2<=y_modposition_n & y_modposition_n<=yshad_te2)
                Timeseries_modshad_y2=1;    % 1 = there is leading edge points shadow on
PV module
            else
                Timeseries_modshad_y2=0;    % 0 = there is not leading edge points shadow
on PV module
            end
end


            Timeseries_modshad_2=Timeseries_modshad_x2*Timeseries_modshad_y2;  % overall
leading edge points shadow presence on PV module matrix
```

```
            Timeseries_modsh_2(a,1)=Timeseries_modshad_2;


% BLADE 3
if rho_z_le3>=120.9

            if (xshad_te3<=x_modposition_w & x_modposition_w<=xshad_le3) |
(xshad_te3<=x_modposition_e & x_modposition_e<=xshad_le3)
                Timeseries_modshad_x3=1;    % 1 = there is leading edge points shadow on
PV module
            else
                Timeseries_modshad_x3=0;    % 0 = there is not leading edge points shadow
on PV module
            end
else
            if (xshad_le3<=x_modposition_w & x_modposition_w<=xshad_te3) |
(xshad_le3<=x_modposition_e & x_modposition_e<=xshad_te3)
                Timeseries_modshad_x3=1;    % 1 = there is leading edge points shadow on
PV module
            else
                Timeseries_modshad_x3=0;    % 0 = there is not leading edge points shadow
on PV module
            end
end



if  rho_x_le3<=0

            if (yshad_te3<=y_modposition_s & y_modposition_s<=yshad_le3) |
(yshad_te3<=y_modposition_n & y_modposition_n<=yshad_le3)
                Timeseries_modshad_y3=1;    % 1 = there is leading edge points shadow on
PV module
            else
                Timeseries_modshad_y3=0;    % 0 = there is not leading edge points shadow
on PV module
            end
else
            if (yshad_le3<=y_modposition_s & y_modposition_s<=yshad_te3) |
(yshad_le3<=y_modposition_n & y_modposition_n<=yshad_te3)
                Timeseries_modshad_y3=1;    % 1 = there is leading edge points shadow on
PV module
            else
                Timeseries_modshad_y3=0;    % 0 = there is not leading edge points shadow
on PV module
            end
end


            Timeseries_modshad_3=Timeseries_modshad_x3*Timeseries_modshad_y3;  % overall
leading edge points shadow presence on PV module matrix
            Timeseries_modsh_3(a,1)=Timeseries_modshad_3;

            a=a+1;
end

% SUM OF BLADE 1,2,3 SHADOWS TIME SERIES ON SINGLE PV MODULE
Timeseries=[Timeseries_modsh_1(:,1); Timeseries_modsh_2(:,1); Timeseries_modsh_3(:,1)];
% overall blades shadow presence on PV module matrix
Timeseries_blades=linspace(1,1,237)*Timeseries;  % overall blades shadow on PV module
time series vector

    if Timeseries_blades>=1
        Timeseries_blades=1;  % there is blades shadow
    elseif Timeseries_blades<1
        Timeseries_blades=0;  % there is not blades shadow
    end

% Four modules shading time series 0,1 vectors
```

```
Mod1_str1=Timeseries_blades;

end
```

- **BLOCKING DIODES PV ARRAY CURRENT MATLAB FUNCTION BLOCK**

```
function Iarray = fcn(shadow,I)
% function for modelling blocking diode behaviour for PV array output current

if (shadow(1)==1 & shadow(2)==0 & shadow(3)==0 & shadow(4)==0) | (shadow(1)==0 &
shadow(2)==1 & shadow(3)==0 & shadow(4)==0) | (shadow(1)==0 & shadow(2)==0 & shadow(3)==1
& shadow(4)==0) | (shadow(1)==0 & shadow(2)==0 & shadow(3)==0 & shadow(4)==1)
    Iarray=I/2;
else
    Iarray=I;
end

end
```

- **BLOCKING DIODES PV ARRAY POWER MATLAB FUNCTION BLOCK**

```
function realP = fcn(P,shad)
% function for modelling blocking diode behaviour for PV array output power

Pnew=1;
if shad==0 | shad==4 | shad==2 | shad==3
    Pnew = P;
elseif shad==1   % blocking diode effect
    Pnew=P*(2/3);
end

realP=Pnew;

end
```

APPENDIX G

- **PERTURB AND OBSERVE MPPT ALGORITHM USED INSIDE MODEL**

```
% function to integrate MPPT perturb and observe algorithm and logical flow
% depending on measured voltage and current, duty cycle is calculated
% function taken from the one created by: CARLOS OSORIO, MATHWORKS

function Duty = PandO(Varray,Iarray)

persistent Dprev Pprev Vprev  % these variables are permanently saved in this function

% Initialization of internal voltage, power and duty cycle values
if isempty(Dprev)  % logical case of first iteration, initial values
    Dprev=0.7;
    Vprev=76.6;   % voltage at MPP in STC of two modules in series (2 x 38.3 V)
    Pprev=2660;  % all modules are producing (4 x 665 W)
end

% Duty cycle parameter variation in MPPT
deltaDuty=0.001;  % 0.1% duty cycle variation

% Array power calculation, from instantaneous voltage and current measurements
Parray=Varray*Iarray;

% MPPT perturb and observe algorithm logical flow
if (Parray-Pprev)~=0
    if (Parray-Pprev)>0
        if (Varray-Vprev)>0
            Duty=Dprev-deltaDuty;
        else
            Duty=Dprev+deltaDuty;
        end
    else
        if (Varray-Vprev)>0
            Duty=Dprev+deltaDuty;
        else
```

```
            Duty=Dprev-deltaDuty;
        end
    end
else
    Duty=Dprev;
end

% Memorised internal values update
Dprev=Duty;
Vprev=Varray;
Pprev=Parray;

end
```

- **PERTURB AND OBSERVE LOGICAL STATEFLOW CHART**

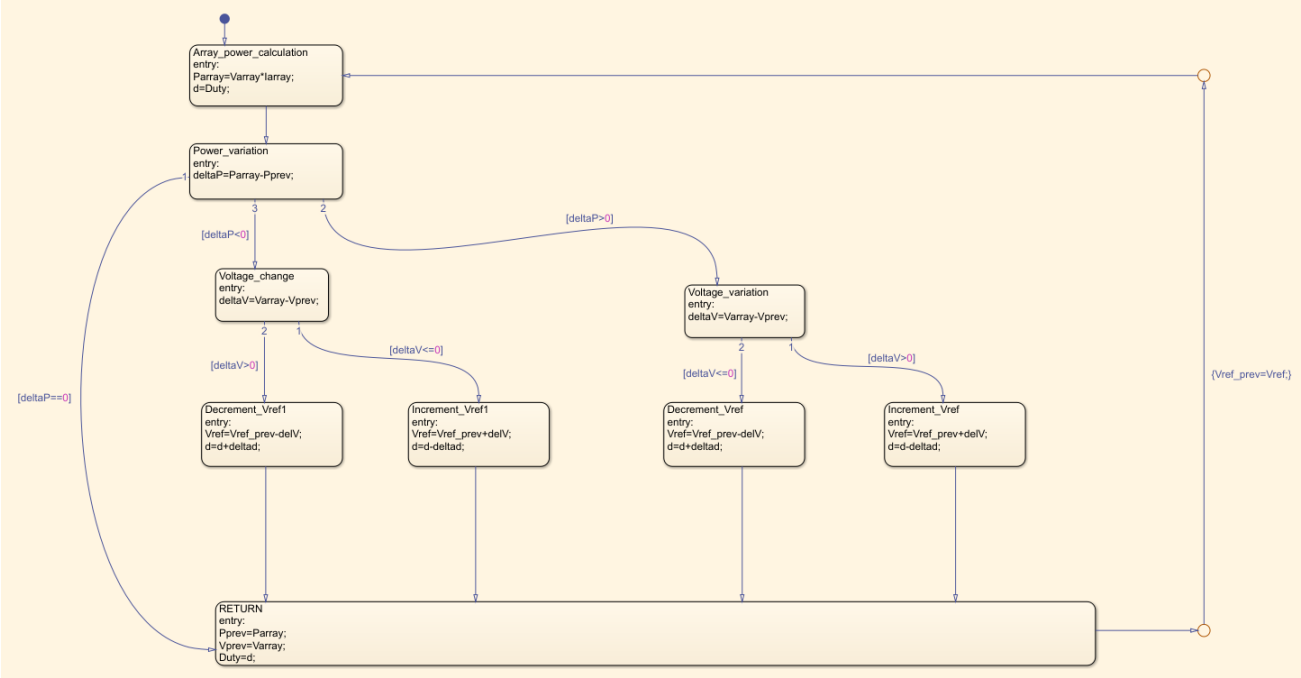

NOMENCLATURE

E = energy (MeV)

Δm = mass variation (a.m.u.)

c = speed of light in vacuum, wave propagation velocity in the medium (m/s)

a = absorptivity (-)

r = reflectivity (-)

t = transmittivity (-)

Ibb = emitted irradiance of a black body (W/m^2)

Eph = photon energy (eV)

h = Planck constant (eVs)

Gsc = solar constant (W/m^2)

$G_{0,d}$ = outside the atmosphere solar irradiance (W/m^2)

d = number of a day in the year (-)

ΔTz = time difference of position time zone compared to Greenwich mean time (h)

ΔTs = summer time difference (h)

i = incidence angle (°)

Ior = direct irradiance on a horizontal unitary plane (W/m^2)

Id = irradiance of the direct radiation on a tilted unitary surface (W/m^2)

Dor = irradiance of diffused radiation on horizontal unitary surface (W/m^2)

Dd = irradiance of diffused radiation on tilted surface (W/m^2)

Gor = overall irradiance incident on horizontal plane (W/m^2)

Rr = reflected irradiance on tilted surface (W/m^2)

G = total irradiance reaching an inclined plane (W/m^2)

AM = air mass (-)

Eg = energy bandgap (eV)

E_k = average thermal kinetic energy (J)

T = absolute temperature (K)

k = Boltzmann constant, $8.62 \cdot 10^{-5}\text{eV/K}$, $1.38 \cdot 10^{-23}\text{eV/K}$

n_0 = electron thermal concentration (cm^{-3})

p_0 = hole thermal concentration (cm^{-3})

n' = light electron concentration (cm^{-3})

p' = light hole electron concentration (cm^{-3})

n = overall electron concentration (cm^{-3})

p = overall hole concentration (cm^{-3})

$I(x, \lambda)$ = intensity of a monochromatic radiation ($\frac{\text{W}}{\text{m}^2 \cdot \mu\text{m}}$)

I_0 = initial intensity of a monochromatic radiation ($\frac{\text{W}}{\text{m}^2 \cdot \mu\text{m}}$)

n_1, n_2 = refractive index real components of entering and exiting mediums (-)

θ_1, θ_2 = incident angles of radiation with normal to interface (°)

J_n = total diffusion current density (A/cm^2) = ($\frac{\text{C}}{\text{s} \cdot \text{cm}^2}$)

$J_{n,diff}$ = electron diffusion current density (A/cm^2) = ($\frac{\text{C}}{\text{s} \cdot \text{cm}^2}$)

$J_{p,diff}$ = hole diffusion current density (A/cm^2) = ($\frac{\text{C}}{\text{s} \cdot \text{cm}^2}$)

q = $1.602 \cdot 10^{-19}$ C fundamental electric charge (C)

$\frac{dn}{dx}$ = electron concentration gradient ($\frac{\text{cm}^{-3}}{\text{cm}}$)

$\frac{dp}{dx}$ = hole concentration gradient ($\frac{\text{cm}^{-3}}{\text{cm}}$)

Dn = electron diffusion coefficient ($\frac{\text{cm}^2}{\text{s}}$)

Dp = hole diffusion coefficient ($\frac{cm^2}{s}$)

L_n = electron diffusion length (cm)

L_p = hole diffusion length (cm)

CP = collection probability (-)

I_L = light generated current (A)

J_L = light generated current density ($\frac{A}{cm^2}$)

A = front and/or back surface of PV cell (cm^2)

x = position along the thickness of the device (cm)

f = incident photon flux ($cm^{-1} \cdot s^{-1}$)

I_D = forward diode current (A)

I_0 = reverse saturation current (A)

V = applied voltage (V)

Tc = cell temperature (°C)

Isc = short-circuit current (A)

Voc = open-circuit voltage (V)

Imp = maximum power point current (A)

Vmp = maximum power point voltage (V)

T_{env} = environmental temperature (°C)

NOCT = nominal operating cell temperature (°C)

G_{NOTC} = total irradiance in NOTC conditions ($\frac{W}{m^2}$)

Pmp = cell peak power (W)

n = not ideality factor (-)

FF = cell/module/generator fill factor (-)

A = cell/module/generator area (m^2)

Rs = series resistance (Ω)

Rp = shunt resistance (Ω)

P_0 = PV generator rated DC power (W)

$P_{mod,STC}$ = single module STC peak power (W)

N = number of same I-V characteristic modules in a PV array (-)

Hmod = PV module height (m)

Wmod = PV module width (m)

Rtip = blade radius (m)

GREEK LETTERS:

σ = Stefan-Boltzmann constant ($\frac{W}{m^2 \cdot K^4}$)

λ = wavelength (nm)

λ_1, λ_2 = minimum and maximum wavelength of solar spectrum (nm)

δ = declination angle (°)

φ = latitude (°)

α = solar height angle (°)

$\alpha(\lambda)$ = medium absorption coefficient for that specific wavelength (cm^{-1})

α = current temperature variation coefficient (%/°C)

ω = hour angle (°)

ψ = longitude (°)

γs = solar azimuth (°)

γ = power temperature variation coefficient (%/°C)

β = inclination angle (°)

β = voltage temperature variation coefficient (%/°C)

ρa = albedo of soil material (-)

ϑ = zenith angle (°)

τ = recombination lifetime (ms)

λ_1, λ_2 = minimum and maximum wavelength of solar spectrum (nm)

η = cell/module/generator solar energy conversion efficiency (-)

ACRONYMS:

WTG = Wind Turbine Generator

OECD = Organisation for Economic Co-operation and Development

GHG = GreenHouse Gases

RED II = Renewable Energy Directive II

PNIEC = Piano Nazionale Integrato Energia e Clima

ETS = Emission Trading System

PNRR = Piano Nazionale Ripresa e Resilienza

RES = Renewable Energy Sources

MPPT = Maximum Power Point Tracker

NREL = National Renewable Energy Laboratory

LCOE = Levelized Cost Of Electricity

CAPEX = CAPital EXpenditure

TST = True Solar Time

LT = Legal Time

GMT = Greenwich Mean Time

ET = Equation of Time

ENEA = Ente per le nuove tecnologie, l'energia e l'ambiente

UV = UltraViolet

STC = Standard Test Conditions

ehp = electron-hole pair

ARC = Anti Reflection Coating

BSF = Back Surface Field

TIR = Total Internal Reflection

TCO = Transparent Conducting Oxide

EVA = Ethylene Vinyl Acetate

PVF = PolyVinyl Fluoride

MPP = Maximum Power Point

rpm = revolutions per minute

AEP = Annual Energy Production

DTM = Digital Terrain Model

PR = Performance Ratio

IAM = Incidence Angle Modifier

LID = Light Induced Degradation

RAM = Random Access Memory

LE = Leading Edge

TE = Trailing Edge

P&O = Perturb and Observe

REFERENCES

[1] https://www.mite.gov.it/pagina/cop-21-laccordo-di-parigi

[2] Direttiva (UE) 2018/2001 del Parlamento Europeo e del Consiglio dell'11 dicembre 2018 sulla promozione dell'uso dell'energia da fonti rinnovabili, Gazzetta Ufficiale dell'Unione Europea, https://eur-lex.europa.eu/legal-content/IT/TXT/PDF/?uri=CELEX:32018L2001

[3] https://www.rinnovabili.it/energia/politiche-energetiche/direttiva-energia-rinnovabili-2030-consiglio-ue/

[4] Piano Nazionale Integrato Energia e Clima, page 11

[5] Legislative Decree 8 November 2021 number 199, Gazzetta Ufficiale della Repubblica Italiana, https://www.gazzettaufficiale.it/eli/id/2021/11/30/21G00214/sg

[6] Piano Nazionale Ripresa e Resilienza, page 120

[7] US Department of Energy, Energy Efficiency and Renewable Energy (EERE), https://www1.eere.energy.gov/solar/pdfs/solar_timeline.pdf

[8] *"Photovoltaics: coming of age"*, Martin A. Green, Univerity of New South Wales, Kensington, Australia

[9] *"Solar cells: from basics to advanced systems"*. Chenming Hu, Richard M. White. University of California, Berkeley. McGraw-Hill Book Company, chapter 9, pages 182-183

[10] https://www.bellsystemmemorial.com/belllabs_photovoltaics.html

[11] http://www.natcoresolar.com/corporate/science-advisory-board/david-carlson

[12] *"Best research-cell efficiency chart"*. NREL, https://www.nrel.gov/pv/cell-efficiency.html

[13] "*Trasmissione del calore"*. Bonacina, Cavallini, Mattarolo. CLEUP

[14] "*Solar Engineering of Thermal Processes, Photovoltaics and Wind"*. Duffie, Beckman. WILEY

[15] "*Elementi di Fisica: meccanica e termodinamica"*. Mazzoldi, Nigro, Voci. EdiSES

[16] *"Solar cells, from basics to advanced systems"*. Chenming Hu, Richard White, University of California, Berkeley. McGraw-Hill Book Company

[17] "*Termodinamica applicata"*. Cavallini, Mattarolo. CLEUP

[18] https://www.pveducation.org

[19] https://www.dupont.com/solar-photovoltaic-materials/photovoltaic-backsheet-films.html

[20] *"TRACER, Fact Sheet: Photovoltaics and Wind Power September 2019"*. Christian Doczekal, Güssing Energy Technologies, Austria. www.tracer-h2020.eu

[21] *"Combining wind, solar, batteries and in future even electrolysers, allows hybrid parks to be more cost effective by sharing infrastructure such as roads, grid connections or substations and*

even support the grid stability", Diane Vrielmann. https://group.vattenfall.com/press-and-media/newsroom/2021/hybrid-parks--new-opportunities-with-multi-technology-facilities

[22] *"Vattenfall's largest hybrid energy park is taking shape in the Netherlands"*, Clemens van Gessel. https://group.vattenfall.com/press-and-media/newsroom/2020/vattenfalls-largest-hybrid-energy-park-is-taking-shape-in-the-netherlands

[23] *"Parco Eolico Gravina in Puglia, Relazione tecnico-informativa".* Ing. Alberto Voltolina

[24] *"Technical Documentation Wind Turbine Generator Systems Cypress 158 - 50/60Hz, Technical Description and Data Rev. 07 - Doc-0075288 - EN 2021-06-17"*, General Electric

[25] *"Impianto Fotovoltaico Gravina in Puglia (BA), Relazione tecnico-informativa"*. Ing. Alberto Voltolina

[26] https://www.trinasolar.com/it/product/VERTEX-DEG21C.20

[27] https://en.sungrowpower.com/productDetail/2305

[28] *"Shadow hindrance by wind turbines. Proceedings of the European wind Energy Conference"*. Verkuijlen E, Westra CA. October 1984, Hamburg, Germany

[29] *"Wind turbines, flicker, and photosensitive epilepsy: Characterizing the flashing that may precipitate seizures and optimizing guidelines to prevent them".* Graham Harding, Pamela Harding, Arnold Wilkins.

[30] *"Hinweise zur Ermittlung und Beurteilung der optischen Immissionen von Windenergianlagen" (WEA-Shattenwurf-Hinweise)*

[31] *EMD windPRO 3.6 Environment UserManual*, https://help.emd.dk/knowledgebase/content/windPRO3.6/c6-UK_WindPRO3.6-Environment.pdf

[32] https://it.wikipedia.org/wiki/Eliofania

[33] *"Near shadings 3D scene tutorial*", PVsyst SA - Route de la Maison-Carrée 30 - 1242 Satigny – Switzerland, https://www.pvsyst.com/wp-content/pdf-tutorials/pvsyst-tutorial-v7-grid-connected-2-en.pdf

[34] *"windPRO solar PV User Manual"*, https://help.emd.dk/knowledgebase/content/windPRO3.6/c14-UK_WindPRO3.6-SOLAR_PV.pdf

[35] *"Technical Documentation Wind Turbine Generator Systems Cypress 158 Platform - 50/60 Hz, Technical Description and Data Weights and Dimensions"*, General Electric

[36] https://it.mathworks.com/help/simulink/getting-started-with-simulink.html

[37] https://it.mathworks.com/products/simscape-electrical.html

[38] https://it.mathworks.com/videos/implement-maximum-power-point-tracking-algorithms-using-matlab-and-simulink-108209.html

[39] https://packetdigital.com/power-products/maximum-power-point-tracker/

[40] *"Practical Guide to Implementing Solar Panel MPPT Algorithms"*, Mihnea Rosu-Hamzescu, Sergiu Oprea, Microchip Technology Inc